UNIVERSITY OF SOUTHAMPTON

FACULTY OF MEDICINE

Clinical and Experimental Sciences

EXPRESSION AND ACTIVITY OF WNT1-INDUCIBLE SIGNALLING PROTEIN-1 IN IDIOPATHIC PULMONARY FIBROSIS

by

Lyndsy Jane Ambler

Thesis for the degree of Doctor of Philosophy

November 2016

UNIVERSITY OF SOUTHAMPTON

ABSTRACT

FACULTY OF MEDICINE

Clinical and Experimental Sciences

Thesis for the degree of Doctor of Philosophy

EXPRESSION AND ACTIVITY OF WNT1-INDUCIBLE SIGNALLING PROTEIN-1 IN IDIOPATHIC PULMONARY FIBROSIS

Lyndsy Jane Ambler

Background: Idiopathic pulmonary fibrosis (IPF) is a chronic, progressive interstitial lung disease characterised by excessive extracellular matrix (ECM) deposition and disruption of lung architecture. Wnt1-inducible signalling protein-1 (WISP-1) is a matricellular protein reported to play a role in aberrant epithelial-mesenchymal crosstalk in fibrotic disease. Therefore, it was hypothesised that WISP-1 contributes to pro-fibrotic changes in pulmonary fibroblasts and epithelial cells, and that these effects are mediated by alternatively spliced WISP-1 variants.
Methods: MRC5, A549 and primary parenchymal fibroblasts were stimulated with the pro-fibrotic cytokine TGFβ_1 or the pro-inflammatory cytokine TNFα and mRNA expression of full length (FL) WISP-1 and its splice variants (v2/3/4) was measured. Antibodies were characterised for the detection of WISP-1 protein. Expression constructs for FL WISP-1 and v2, v3 and v4 were made in pcDNA3. HEK293T cells were transfected with WISP-1 constructs and cell conditioned medium (CM) tested on A549 and MRC5 cells. A549 cells were stably transfected with FL WISP-1. Time lapse microscopy, gene expression and cell proliferation analyses were performed.
Results: TNFα induced WISP-1 mRNA expression in pulmonary epithelial (A549) and fibroblast (MRC5) cell lines. TGFβ_1 induced epithelial to mesenchymal transition (EMT) and WISP-1 mRNA expression in A549 cells, and suppressed WISP-1 in MRC5 cells. In primary IPF fibroblasts, higher levels of WISP-1 mRNA were detected compared to control lung fibroblasts. Expression of WISP-1 mRNA in response to TGFβ_1 and TNFα was variable between donors. WISP-1 variant specific qPCR assays showed differences in expression levels between donors, reflecting the overall WISP-1 expression. FL WISP-1 was detected in cell lysates from some IPF and control parenchymal fibroblast donors. When expressed in HEK293T cells, FL WISP-1 and v2, v3 and v4 could be detected in cell lysates. FL WISP-1 and v2 were also detected as secreted proteins. When CM from the different recombinant WISP-1 expressing HEK293T cells were applied to A549 or MRC5 cells, distinct responses were observed. FL WISP-1 CM increased endogenous FL WISP-1 expression in A549 cells, but the WISP-1 variants were without effect. In contrast, WISP-1v4 CM strongly induced FL WISP-1 and WISP-1v4 in MRC5 fibroblasts while WISP-1v2 and v3 only induced their own expression and FL WISP-1 had no effect. FL and variant WISP-1 CM did not stimulate ECM production by MRC5 cells, or EMT in A549 cells.
Conclusions: WISP-1 is expressed in parenchymal fibroblasts and exists as several alternatively spliced forms. WISP-1 is overexpressed in IPF fibroblasts but is not uniformly increased following pro-fibrotic or pro-inflammatory stimulation

in primary fibroblasts. WISP-1 expression is increased following induction of EMT in A549 cells however overexpression of WISP-1 did not induce EMT. The differential responses of epithelial cells and fibroblasts to CM from recombinant HEK293T cells expressing different WISP-1 variants suggests that further work is required to dissect the regulation and function of WISP-1 in relation to lung fibrosis.

Contents

List of Tables

List of Figures

DECLARATION OF AUTHORSHIP

I, Lyndsy Jane Ambler, declare that this thesis entitled 'Expression and Activity of Wnt1-Inducible Signalling Protein-1 in Idiopathic Pulmonary Fibrosis' and the work presented in it are my own, and have been generated by me as the result of my own original research.

I confirm that:

1. This work was done wholly or mainly while in candidature for a research degree at this University;
2. Where any part of this thesis has previously been submitted for a degree or any other qualification at this University or any other institution, this has been clearly stated;
3. Where I have consulted the published work of others, this is always clearly attributed;
4. Where I have quoted from the work of others, the source is always given. With the exception of such quotations, this thesis is entirely my own work;
5. I have acknowledged all main sources of help;
6. Where the thesis is based on work done by myself jointly with others, I have made clear exactly what was done by others and what I have contributed myself;
7. None of this work has been published before submission

Signed: .....

Date: .....

Acknowledgements

This thesis would not have been possible without the help and support of many people. First, I would like to thank my supervisors Donna and Jane. Without their guidance and support (and at times shared frustration), this project would not have been possible. I would also like to thank Dr Kate O'Reilly for sharing her clinical perspective of IPF, and my funders, BBSRC and UCB, without whom this research could not have been carried out.

Thanks to everyone in Brooke lab for all their help/willingness to listen to me complain over the last four years, it is much appreciated. Thanks to Nat and Graham for keeping the lab running, and special thanks to David for all his help trying to figure WISP-1 out.

Outside of the lab, the support of my friends has been invaluable. Thanks go to my housemates Kate, Natt and Ali for cheering me up at the end of a rubbish day, and to Leanne, Dannielle and Caroline for looking after me when I most needed it. I would also like to thank my friends at home for not asking how the PhD is going, I promise you will never have to hear about cells ever again. Finally, I would like to thank my family, particularly my mum and gran, for all their love and support. I would not have got through it without you.

Abbreviations

AEI, AEII	Alveolar epithelial type I or II cell
Akt	Protein kinase B
ANOVA	Analysis of variance
AP-1	Activator protein 1
APS	Ammonium persulphate
ASK1	Apoptosis signal regulating kinase 1
ATII	Alveolar type II cell
BAL(F)	Bronchoalveolar lavage (fluid)
BLAST	Basic Local Alignment Search Tool
BMP	Bone morphogenetic protein
BSA	Bovine serum albumin
cAMP	Cyclic adenosine monophosphate
CCN	CYR61, CTGF, NOV
cDNA	Complementary deoxyribose nucleic acid
COPD	Chronic obstructive pulmonary disease
CREB	cAMP response element binding protein
CT	C-terminal (cysteine knot) domain
CTGF	Connective Tissue Growth Factor
CXCLx	C-X-C motif chemokine ligand x
CYR61	Cysteine rich protein 61
DLCO	Diffusing capacity of the lung for carbon monoxide
DMEM	Dulbecco's Modified Eagles Medium
DNA	Deoxyribose nucleic acid
ECM	Extracellular matrix
ELISA	Enzyme linked immunosorbent assay
EMT	Epithelial to mesenchymal transition
ERK	Extracellular signal regulated kinase, MAPK

ET-1	Endothelin-1
FAK	Focal adhesion kinase
FBS	Foetal bovine serum
FEV1	Forced expiratory volume in 1 second
FGF	Fibroblast growth factor
FN-1	Fibronectin
FVC	Forced vital capacity
Fzd	Frizzled
GSK3B	Glycogen synthase kinase 3beta
hBMSC	Human bone marrow stromal cells
HBSS	Hank's buffered saline solution
HDGF	Hepatoma derived growth factor
HP	Hypersensitivity pneumonitis
HRCT	High resolution computed tomography
HRP	Horseradish peroxidase
HSPG	Heparin sulphate proteoglycan
ICAM	Intracellular adhesion molecule
IGF	Insulin like growth factor
IGFBP	Insulin-like growth factor binding protein domain
IL	Interleukin
ILD	Interstitial lung disease
IPF	Idiopathic pulmonary fibrosis
JNK	c-Jun N-terminal kinase
LEF	Lymphoid enhancer factor
LOX	Lysyl oxidase
LRP	Low density lipoprotein receptor related protein
MAPK	Mitogen activated protein kinase
MEK	MAPK kinase
miR	micro RNA

MMP	Matrix metalloproteinase
MW	Molecular weight
NCBI	National Centre for Biotechnology Information
NEAA	Non-essential amino acids
NFkB	Nuclear factor kappa B
NICE	National Institute for Health and Care Excellence
NOV	Neuroblastoma overexpressed
NSIP	Non-specific interstitial pneumonia
OASF	Osteoarthritic synovial fibroblasts
PAGE	Polyacrylamide gel electrophoresis
PBS	Phosphate buffered saline
PDGF	Platelet derived growth factor
PI3K	Phosphoinositide 3 kinase
PKC	Protein kinase C
qPCR	Quantitative polymerase chain reaction
rhWISP-1	Recombinant human WISP-1
RNA	Ribose nucleic acid
RT	Reverse transcription
SDS	Sodium dodecyl sulphate
shRNA	Short hairpin RNA
siRNA	Short interfering RNA
SMA	Smooth muscle actin
SMC	Smooth muscle cell
SPC	Surfactant protein C
TBS	Thrombospondin domain
TBS(T)	Tris buffered saline (tween)
TCF	T cell factor
TGF	Transforming growth factor
TIMP	Tissue inhibitor of matrix metalloproteinase

TNF	Tumour necrosis factor
UIP	Usual interstitial pneumonia
VCAM	Vascular cell adhesion molecule
VEGF	Vascular endothelial growth factor
VWC	Von Willebrand domain
WISP-1	Wnt1-inducible signalling protein-1
WISP-1v	WISP-1 variant

Chapter 1: Introduction

1.1 Idiopathic pulmonary fibrosis

Idiopathic pulmonary fibrosis (IPF) is an interstitial lung disease (ILD) where patients suffer from respiratory failure due to disruption of the normal lung architecture. Defined by the American (ATS), European (ERS), Japanese (JRS) and Latin American (ALAT) Thoracic/Respiratory societies as a specific form of chronic, progressive fibrosing interstitial pneumonia of unknown cause (1), IPF is thought to develop as a result of damage to alveolar epithelial cells leading to persistent activation of profibrogenic pathways and increased deposition of extracellular matrix (ECM) proteins. The mechanisms behind this are not fully understood.

1.1.1 Incidence and prognosis

The annual incidence of IPF in the UK has been estimated at around 6000 cases with a higher predominance in men. IPF is also more likely to occur in older adults. The prognosis of IPF is variable with a mean survival of 2.5-3.5 years following diagnosis (2). Some patients slowly progress over a number of years whilst others experience an acute respiratory decline of unknown cause, termed an acute exacerbation (1). The reasons behind this inherent variability in the natural history of the disease are unclear.

1.1.2 Symptoms and diagnosis

Patients with IPF present with cough, bibasilar inspiratory crackles and finger clubbing (1). The histopathological hallmark of IPF is a heterogeneous appearance with areas of fibrosis containing dense collagen, subepithelial fibroblastic foci and honeycomb changes alternating with areas of normal lung (1). Diagnosis requires the presence of these characteristic features, known as usual interstitial pneumonia (UIP), on a high-resolution computed tomography (HRCT) scan or biopsy following exclusion of other known causes of ILD (1). An example of UIP pattern is shown in Figure 1.

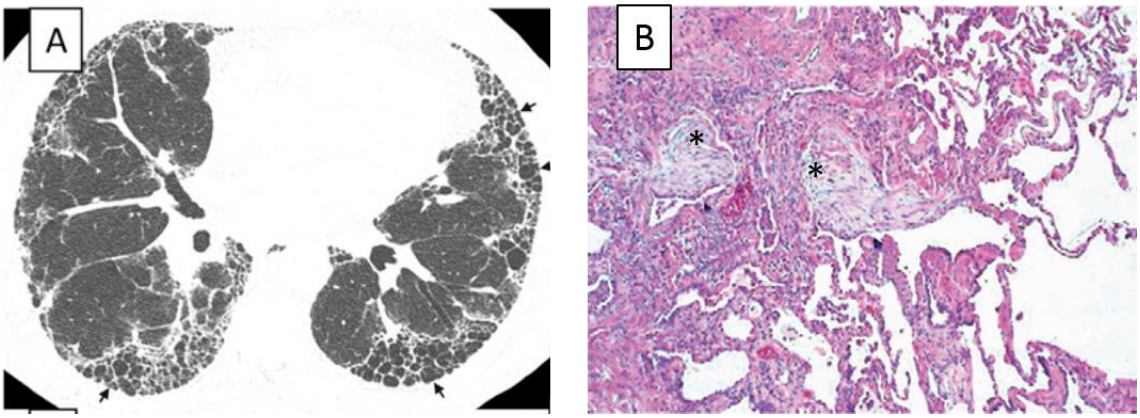

Figure 1. UIP pattern on HRCT and histology. (A) HRCT image showing UIP pattern demonstrates the presence of reticular abnormalities and honeycombing with basal, peripheral predominance (arrows).
Reprinted with permission of the American Thoracic Society. Copyright © 2017 American Thoracic Society. Raghu G, Collard HR, Egan JJ et al. (2011). An Official ATS/ERS/JRS/ALAT Statement: Idiopathic Pulmonary Fibrosis: Evidence-based Guidelines for Diagnosis and Management. American Journal of Respiratory and Critical Care Medicine. Vol 183 pp. 788–824. The American Journal of Respiratory and Critical Care Medicine is an official journal of the American Thoracic Society.
(B) Histology image showing UIP pattern demonstrates areas of dense fibrosis with regions of acellular collagen and fibroblastic foci (*) as well as areas of relatively normal lung tissue. Taken from (2) – permissions in Appendix 1.

1.1.3 Risk factors

Several potential risk factors have been linked with IPF, both environmental and genetic. For example, being a smoker or having previously smoked has been shown to increase the risk of developing IPF (3). Exposures to metal and wood dusts as well as occupations such as hairdressing and farming have also been linked (1). A role for viral infection in IPF development has been suggested but both positive and negative associations have been reported (4, 5).

Another possible risk for factor for IPF is microaspiration, or the inhalation of oropharyngeal or gastric contents into the larynx and lower respiratory tract (6). Abnormally clinically silent gastroesophageal reflux (GER) has been associated with IPF (7) and is a presumed risk factor for microaspiration. However, GER is

common in the normal population and in other lung diseases, and there are no direct clinical data to show that microaspiration causes pulmonary fibrosis (6).

Genetic risk factors

There is evidence of genetics playing a role in IPF. Cases of familial IPF, where two or more members of the same family are affected, have been observed. These patients tend to be younger at diagnosis than sporadic IPF patients but show no differences clinically or histologically (8). Mutations in the genes encoding surfactant protein A2 have been linked with familial IPF (9). Surfactant protein C (SPC) mutations have also been associated with familial disease (10) but not sporadic disease (11).

Shortening of telomeres is another factor implicated in IPF. Mutations in genes encoding telomerase components have been identified in both familial (12) and sporadic cases of IPF (13). These mutations were associated with telomere shortening, a feature observed in cases of familial and sporadic IPF compared with controls for both patients with and without telomerase mutations (14).

Also common to both familial and sporadic cases of IPF, a polymorphism in the promoter of the MUC5B gene (encoding a major component of mucin in the airways) has been associated with IPF (15) but not with lung fibrosis in systemic sclerosis or sarcoidosis (16). Interestingly, the allele which confers the susceptibility risk appears to be protective in terms of survival (17).

1.1.4 Treatment of IPF

Traditionally therapy for IPF has consisted of various different agents taken alone or in combination, including the use of corticosteroids and other immunosuppressive agents. However these have failed to effectively treat the disease. A trial investigating the use of triple therapy (prednisone + azathioprine + N-acetylcysteine) found no evidence of physiological and clinical benefit to the patient and an increased risk of death and hospitalisation (18). In the UK the current NICE guidelines for management of IPF state that azathioprine, prednisone and other immunosuppressive agents should not be used to treat IPF (19). These guidelines also state that N-acetylcysteine may be used but that benefit obtained is uncertain.

Other recent clinical trials have produced more positive results. Nintedanib, a small molecule inhibitor of the receptor tyrosine kinases platelet derived growth factor (PDGF) receptor, fibroblast growth factor (FGF) receptor and vascular endothelial growth factor (VEGF) receptor, was found to reduce the decline in forced vital capacity (FVC) in IPF patients (20). Pirfenidone, a synthetic molecule shown to regulate $TGF\beta_1$, fibroblast proliferation and collagen synthesis in vitro (21), has been demonstrated to reduce the decline in FVC in IPF patients and improve progression-free survival (22). Use of pirfenidone or nintedanib is now recommended for use in IPF if FVC is between 50 and 80% of the predicted value (23, 24) but should be stopped if FVC declines by more than 10% in 12 months.

1.1.5 The normal lung

In IPF and other ILDs it is primarily the interstitial region of the lung that is affected i.e. the tissue and airspaces surrounding the alveoli (25). The alveoli are air sacs situated at the end of the terminal bronchioles in the lung, and are where gas exchange takes place. The alveolar epithelium is composed of two types of cell, shown in Figure 2. Type I alveolar epithelial cells (AEI) are thin squamous cells that constitute 95% of the alveolar epithelium (26). Type I cells are attached to the basement membrane via the basal cell membrane and form the barrier for diffusion of gases between air and the capillaries (27). Type II alveolar epithelial cells (AEII) are cuboidal, secretory cells that produce and secrete the lipid and protein components of surfactant, important for compliance and reducing surface tension. These cells are able to transdifferentiate into type I cells to replace lost type I cells (28).

Interstitial fibroblasts secrete the ECM scaffold for the alveolus (26) (29). In the normal lung these cells synthesise a small amount of matrix. Following an appropriate stimulus, they can differentiate towards a myofibroblast phenotype characterised by α-smooth muscle actin (α-SMA) expression and increased synthesis of ECM components (see section 1.1.6.2). Interstitial fibroblasts typically express the glycoprotein Thy-1 however this expression has been reported to be lost in IPF (30). Also present in the alveoli are macrophages. These phagocytic cells are responsible for the ingestion of pathogens and toxic or allergic agents (31). Alveolar macrophages secrete cytokines and chemokines to initiate inflammatory responses and attract effector immune cells (32).

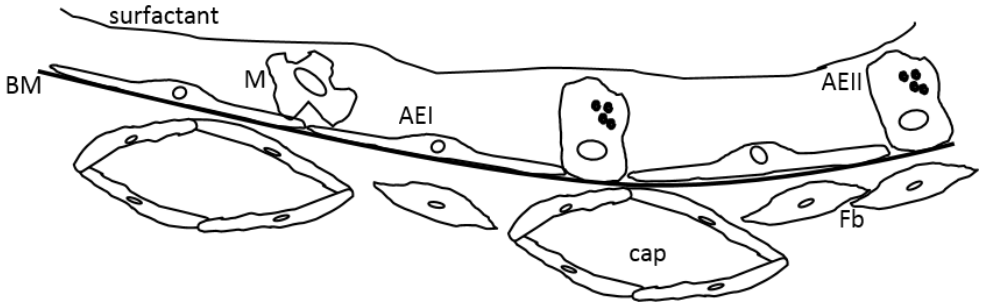

Figure 2. Normal structure of the alveolus. Type I (AEI) and type II (AEII) alveolar epithelial cells are anchored to the basement membrane (BM), in close proximity to fibroblasts (Fb) and pulmonary capillaries (cap) in the underlying interstitial space. The alveolar space contains alveolar macrophages (M) and a layer of surfactant.

1.1.6 IPF pathogenesis

In the majority of interstitial lung diseases inflammation plays an important role in the development and/or persistence of fibrosis (2). Certain inflammatory mediators have been implicated in pulmonary fibrosis including interleukin-1β (IL-1β). Overexpression of IL-1β in rat lung was shown to induce acute lung injury leading to progressive fibrotic changes including the deposition of extracellular matrix components (33), similar to the more commonly studied bleomycin mouse model. In both an IL-1β and a bleomycin model of lung fibrosis, fibrotic changes observed were found to be mediated by another proinflammatory cytokine, IL-17A. In this same study (34), increased levels of IL-1β and IL-17A were detected in bronchoalveolar lavage (BAL) fluid from IPF patients compared with normal volunteers. Increased levels of IL-1β in BAL fluid from IPF patients was also reported in a second study alongside increased IL-1β in serum in IPF (35). IL-13 is a third pro-inflammatory cytokine which has been suggested to play a role in IPF, with higher levels being detected in IPF BAL fluid compared to that from patients with non-specific interstitial pneumonia (NSIP) and to normal controls (36). In the same study, IL-13 levels in the BAL fluid were inversely correlated with the lung function measures DLCO (% predicted) and forced vital capacity (FVC, % predicted) for both IPF and NSIP patients. Increased expression of IL-13Rα2 has been

reported in the IPF lung compared to controls (37). However, IPF patients demonstrate a poor response to anti-inflammatory therapies and evidence suggests that other mechanisms are responsible for driving IPF pathogenesis (Figure 3).

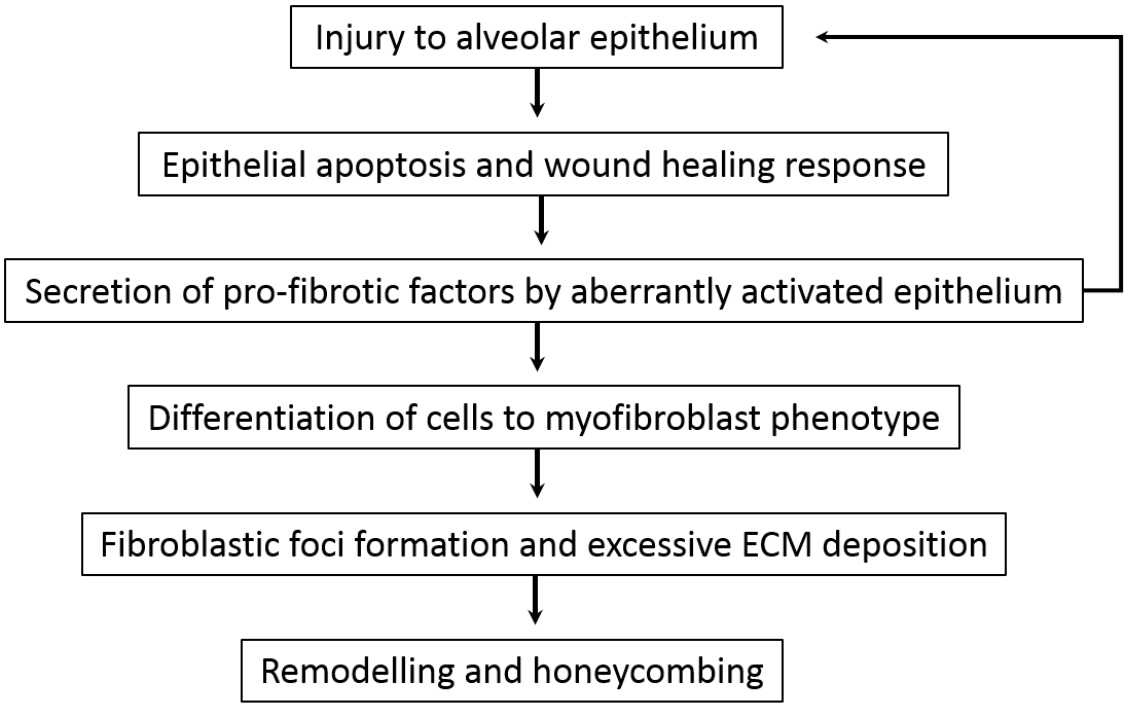

Figure 3. Outline of the current thinking regarding IPF pathogenesis. Adapted from (2)

1.1.6.1 Role of the alveolar epithelium

The current model of IPF pathogenesis suggests that abnormal behaviour of injured alveolar epithelial cells results in the formation of fibroblastic foci, excessive deposition of extracellular matrix components, and subsequent degradation of the lung architecture. The epithelium is thought to contribute to these processes in several ways.

Initially, injury (or repetitive microinjuries) cause alveolar epithelial cells to undergo apoptosis increasing the permeability of the epithelium and allowing a provisional matrix to form. In IPF, alveolar epithelial cells are aberrantly activated and migrate and proliferate in an attempt to repair the damage. This is likely mediated by a number of factors, for example hepatoma-derived growth factor (HDGF), which has been shown to stimulate the proliferation of rat alveolar

epithelial cells and the alveolar epithelial cell line A549. Increased expression of HDGF has been detected in the epithelium of the human IPF lung and the bleomycin mouse model of pulmonary fibrosis (38).

Release of pro-fibrotic cytokines and chemokines by activated alveolar epithelial cells, and inflammatory cells recruited to the site of injury, has been demonstrated to mediate the recruitment, proliferation and differentiation of different cell types which contribute to fibrosis. For example, alveolar epithelial cells in the IPF lung have been shown to strongly express the chemokine CXCL12 (39). In response to CXCL12, fibrocytes (circulating fibroblast progenitor cells) have been shown to traffic to the lung with greater numbers detected in bleomycin-treated compared to saline-treated mice (40). In this same study, use of an anti-CXCL12 antibody reduced the total collagen content in the lungs of bleomycin treated mice suggesting that recruited fibrocytes may contribute to collagen deposition in the fibrotic lung.

Platelet-derived growth factor (PDGF) is another mediator thought to contribute to fibrosis in IPF. PDGF mRNA expression has been reported in the IPF lung where none was detected in control samples (41). In IPF tissue, this expression was mainly detected in epithelial cells and alveolar macrophages. A study investigating the effect of PDGF on human lung fibroblasts found that it acts as a potent mitogen inducing the proliferation of these cells (42). It was also reported that PDGF acts as a chemoattractant for fibrocytes in pulmonary fibrosis (43). PDGF is one of the targets of the now approved drug nintedanib.

Another mediator expressed by epithelial cells and reported to exert fibrotic effects in the IPF lung is the glycoprotein osteopontin. Increased levels of osteopontin have been detected in total RNA from IPF lungs and in BAL fluid from IPF patients (44). The expression of osteopontin in the IPF lung was localised to the alveolar epithelium. This study also investigated the effects of osteopontin on different cell types. Induction of MMP7 in A549 cells and their increased migration and proliferation was observed following osteopontin stimulation. Osteopontin also induced migration and proliferation of human lung fibroblasts, as well as inducing the expression of type 1 collagen in these cells. Stimulated fibroblasts also showed a reduction in the expression of MMP1 which degrades fibrillar collagen, and an increase in the expression of the MMP1 inhibitor TIMP-1

(tissue inhibitor of metalloproteinase-1). Increased serum levels of osteopontin in IPF compared to non-IPF ILD has also been reported (45).

Endothelin-1 (ET-1) is another pro-fibrotic mediator reported to contribute to IPF pathogenesis. In a bleomycin rat model of pulmonary fibrosis, ET-1 expression was found to be increased in bleomycin compared to saline treated mice (46). This expression was localised to fibrotic lesions and increased before the induction of collagen. In IPF, levels of ET-1 are greater compared to controls in plasma (47), as well as at the mRNA level (48) and in BAL fluid (49). In lung tissue ET-1 expression was observed in small vessel endothelial cells (47). ET-1 has been demonstrated to effect matrix synthesis and degradation. For example, in normal skin fibroblasts ET-1 stimulated the synthesis of type I and III collagens and suppressed the expression of MMP1 (50). More recently, ET-1 was reported to enhance TGFβ_1-mediated endothelial to mesenchymal transition (EndoMT) of murine lung microvascular endothelial cells (51).

Alveolar epithelial cells may also play a role in the pathogenesis of IPF through epithelial to mesenchymal transition (EMT) however, the contribution of EMT to the myofibroblast population in IPF remains unclear (2).

A further way in which the alveolar epithelium may contribute to the pathogenesis of IPF is through the loss of alveolar type I cells. It has been proposed (2, 52) that the changes in the composition of the extracellular matrix in the fibrotic lung may affect the transdifferentiation of alveolar type II cells into type I potentially limiting alveolar re-epithelialisation.

Bronchiolisation of the alveolar epithelium has also been reported in the literature. Studies have reported increased expression of markers typically associated with airway epithelium in IPF for example, that of basal-cell specific keratins K5 and K14 (53). Epithelial cell hyperplasia at the bronchoalveolar junction has been reported in IPF tissue (54). Honeycombing, a key feature of UIP, is typically found in the bronchiolar region (55) and the epithelium lining honeycomb cysts has been reported to be bronchiolar-like (54-57) suggesting a distal airway origin (57).

1.1.6.2 Myofibroblasts

A key aspect of IPF pathogenesis is considered to be the fibroblastic focus, usually observed as isolated lesions in the tissue which may form an interconnected fibrotic reticulum (58). An example of a fibroblast focus is shown in Figure 4. Image taken from (60) showing a fibroblastic focus (arrows) Fibroblastic foci contain fibroblasts and myofibroblasts, contractile cells usually characterised by α-SMA expression. These cells are a normal part of the wound healing process but in fibrotic diseases they persist instead of undergoing apoptosis following successful wound healing. This is in comparison to the increased epithelial cell apoptosis observed in the same microenvironment. The reason(s) for this 'apoptosis paradox' in IPF are unknown however prostaglandin E_2 has been demonstrated to increase the sensitivity of fibroblasts to FasL-induced apoptosis, and to protect type II alveolar epithelial cells from FasL-induced apoptosis, and is reported to be decreased in the IPF lung (59).

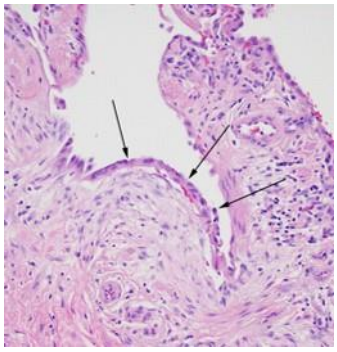

Figure 4. Image taken from (60) showing a fibroblastic focus (arrows).
Reprinted with permission of the American Thoracic Society. Copyright © 2017 American Thoracic Society. Visscher DW and Myers JL (2006). Histologic Spectrum of Idiopathic Interstitial Pneumonias. Proceedings of the American Thoracic Society. Volume 4 pp. 322–329. Proceedings of the American Thoracic Society is an official journal of the American Thoracic Society.

Myofibroblasts are considered to be the cell type responsible for the excessive extracellular matrix deposition observed in IPF. Increased amounts of total collagen have been detected in the fibrotic lung, and in areas of more established fibrosis a shift in collagen composition has been observed with only type I

collagen detected in scar tissue (61). Increased amounts of enzymes involved in collagen cross-linking, lysyl oxidase (LOX) and lysyl oxidase-like 2 (LOXL2), have been detected at increased levels in bronchoalveolar lavage fluid and tissue from IPF patients compared to controls (62, 63). Increased collagen cross-linking due to higher levels of these enzymes may contribute to decreased compliance in the IPF lung by increasing collagen stabilisation and therefore lung stiffness.

Increased expression of several other ECM molecules in lung fibrosis has been reported. For example, increased levels of the glycoprotein fibronectin were detected in BAL fluid in a bleomycin-induced pulmonary fibrosis model (64). In this same study, elevated levels of the ECM component hyaluronan were also detected. In another bleomycin study, fibroblasts from hyaluronan-overexpressing mice were found to be more invasive, and deletion of hyaluronan impeded the development of fibrosis (65). The authors also reported that IPF donor-derived fibroblasts were more invasive than control cells and that this phenotype could be abrogated by siRNA knockdown of hyaluronan. Decorin, another ECM component implicated in lung fibrosis, was reported to be expressed at higher levels in fibrotic compared to control fibroblasts (66). Interestingly, this proteoglycan has been shown to abrogate TGFβ_1-induced α-SMA expression in mouse lungs when both proteins were overexpressed at the same time (67). This could suggest that increased expression of decorin by fibrotic fibroblasts may be an attempt to dampen the effect of TGFβ in fibrosis.

The origin of myofibroblasts is a topic that has been debated in the literature with evidence suggesting that epithelial cells, endothelial cells, fibrocytes and pericytes may each contribute to this population in fibrosis alongside stimulated resident fibroblasts and smooth muscle cells.

Several markers are commonly used to demonstrate epithelial to mesenchymal transition (EMT) such as induction of the mesenchymal markers α-smooth muscle actin (α-SMA), vimentin, desmin and type 1 collagen, and loss of the epithelial markers zona occludens 1 (ZO-1), aquaporin 5, and e-cadherin (68, 69). Co-localisation of some of these markers has been reported in IPF tissue (SPC, and N-cadherin) (70), and increased expression of mesenchymal markers such as α-SMA have been reported in isolated type II alveolar epithelial cells from IPF patients (71). Fate-mapping studies in the bleomcycin model of pulmonary fibrosis have

reported conflicting results. Tanjore et al. (72) reported that differentiated epithelial cells constituted approximately one third of the sorted fibroblast population present after bleomycin administration. However, Rock et al. (73) have since reported that in their study EMT did not contribute to the myofibroblast population. In fibroblasts isolated from IPF tissue, Larsson et al. (74) reported that TGFβ driven EMT was one source of myofibroblasts but that the expression of their EMT panel was not increased in IPF compared to control cells. The ability of $TGF\beta_1$ to induce EMT has been well established in the literature (see 1.1.6.3).

As mentioned above, EndoMT of murine lung microvascular endothelial cells has been reported in the literature (51). EndoMT was also reported in the bleomycin model of fibrosis (75). In this study the authors found expression of α-SMA and type I collagen in labelled endothelial cells after bleomycin induction of fibrosis. They also reported TGFβ-stimulated loss of endothelial marker expression in a microvascular endothelial cell line.

Fibrocytes are a mesenchymal progenitor cells that have been shown to spontaneously differentiate towards a myofibroblast phenotype in the bleomycin model of fibrosis (40). Allergen exposure has been demonstrated to induce the accumulation of α-SMA expressing fibrocyte-like cells in asthmatic airways (76). In this study, TGFβ stimulation of human fibrocytes was demonstrated to induce the release of fibronectin and collagen III. TGFβ-stimulated expression of the myofibroblast marker α-SMA by fibrocytes has also been reported (Hong 2007).

Pericytes are mesenchymal derived cells that have been identified as a source of myofibroblasts in kidney fibrosis models (77). In the bleomycin model of pulmonary fibrosis, pericyte-like cells were detected in the alveolar interstitium but were not found to express the mesenchymal marker α-SMA (73).

Murine pleural mesothelial cells have been demonstrated to express both mesothelial and mesenchymal markers following treatment with $TGF\beta_1$ (78). In this same study, cells expressing the mesothelial marker WT-1 (Wilms tumour-1) were detected in explanted IPF lung.

1.1.6.3 Transforming growth factor beta 1

The profibrotic cytokine transforming growth factor β 1 ($TGF\beta_1$) has been implicated in the pathogenesis of IPF in a multitude of studies. Increased epithelial expression of TGFβ isoform 1 but not 2 or 3 has been associated with advanced pulmonary fibrosis (79) and altered expression of type I and II TGFβ receptors has been reported in the IPF lung (80). In fibrosis, a major effect of $TGF\beta_1$ is the differentiation of different cell types towards a myofibroblast phenotype.

$TGF\beta_1$ is secreted in a latent form attached to a latency-associated peptide and a TGFβ-binding protein. Latent $TGF\beta_1$ can be activated by integrin αvβ6 (81), an epithelial-expressed integrin increased in pulmonary fibrosis (82). It can also be activated by other integrins, reactive oxygen species, increased tissue stiffness, thrombospondin and some MMPs including those upregulated in IPF such as MMP9 (83-85) (86).

A number of studies have demonstrated a role for TGFβ in cell proliferation. Both inhibitory and stimulatory effects have been demonstrated in fibroblasts. Increased fibroblast proliferation and accumulation was reported in a TGFβ overexpression model of fibrosis in mice (87). In human lung fibroblasts, no increase in proliferation was observed when confluent cells were treated with $TGF\beta_1$ or $TGF\beta_3$ (88). In another study, TGFβ did not stimulate an increase in the proliferation of human embryonic lung fibroblasts (89). However, TGFβ co-treatment enhanced the increased rate of proliferation observed following epidermal growth factor stimulation in this study. The difference in responses reported are perhaps due to different amounts of $TGF\beta_1$ having different effects. A biphasic response has been reported in the literature with low concentrations stimulating and higher concentrations inhibiting proliferation. In a study by Battegay et al. (90), it was demonstrated that a low concentration of $TGF\beta_1$ stimulated fibroblast proliferation however this was not the case when a higher concentration was used. The authors proposed that this was mediated via PDGF as at low concentrations of $TGF\beta_1$ PDGF expression was increased, and at higher concentrations the expression of PDGF receptor subunits was suppressed.

Synthesis and deposition of ECM components and expression of α-SMA are hallmark characteristics of myofibroblasts. The role of $TGF\beta_1$ in inducing differentiation of fibroblasts towards a myofibroblast phenotype is well established. In 1987, Ignotz et al. demonstrated $TGF\beta_1$-stimulated induction of type I collagen and fibronectin mRNA in NRK-49 rat fibroblasts (91). In primary rat fibroblasts, TGFβ was shown to induce α-SMA expression via Smad3 (92). The induction of α-SMA via Smad3 has also been reported in a human fetal lung fibroblast cell line (93). Increased secretion and deposition of collagens by primary human lung fibroblasts was induced by both $TGF\beta_1$ and $TGF\beta_3$ to a similar extent in a study by Eickelberg et al. (88). $TGF\beta_1$ was reported to induce the synthesis of type I, III and V collagen in lung fibroblasts from IPF patients and control donors by Raghu et al. (94). In this study no differences in response were observed between IPF and control cells. In vivo, $TGF\beta_1$ overexpression in rat lung stimulated increased deposition of collagen, elastin and fibronectin as well as increased expression of α-SMA by myofibroblasts (87). In the bleomycin model of pulmonary fibrosis, treatment with antibodies to $TGF\beta_1$ and $TGF\beta_2$ following bleomycin instillation resulted in decreased accumulation of collagen in the lung (95).

The induction of EMT by $TGF\beta_1$ has also been well established in vitro and several studies have reported EMT in alveolar epithelial cells. In rat alveolar type II cells, induction of vimentin, desmin, collagen type I and α-SMA, and suppression of zona occludens, cytokeratins and aquaporin 5 was observed following $TGF\beta_1$ stimulation (68). In a TGFβ overexpression model of fibrosis in mice, Kim et al. (70) reported accumulation of vimentin positive mesenchymal cells derived from beta-gal labelled lung epithelial cells. In vitro, Tanjore et al. (72) reported induction of type I collagen alongside loss of e-cadherin and surfactant protein C expression following TGFβ stimulation of primary murine ATII cells. Jayachandran et al. (96) also reported TGFβ-mediated EMT in murine ATII cells. In this study, TGFβ stimulated EMT was also demonstrated in the human alveolar epithelial cell line A549, a finding that was previously reported by Yang et al. (97).

Other effects of $TGF\beta_1$ on epithelial cells have been reported in the literature. For example, in a study investigating lung epithelial cell apoptosis it was reported that $TGF\beta_1$ enhanced Fas-mediated apoptosis of bronchial epithelial cells (98).

Inhibition of alveolar epithelial cell proliferation by TGFβ has been demonstrated in the murine bleomycin-induced fibrosis model (80). In this study the authors observed decreased alveolar epithelial cell proliferation in vivo concurrent with increased levels of active TGFβ. Isolated alveolar epithelial cells cultured with TGFβ also showed decreased levels of proliferation. In bronchial epithelium, the inhibitory effect of TGFβ was reported to be mediated by the integrins αvβ6 and αvβ8 (99).

1.1.6.4 Matrix metalloproteinases

Increased expression of MMPs is thought to contribute to extracellular matrix remodelling and basement membrane degradation observed in IPF. It has been proposed that the imbalance of MMPs and their inhibitors in the fibrotic lung favours ECM deposition (83). MMP1 (collagenase-1) expression is increased in the IPF lung at the mRNA level (100) (48), and in serum (101) and plasma (102) from IPF patients compared to controls. It has been proposed that its epithelial-only expression may suggest a role in the formation of honeycomb cysts (103). MMP3 expression has been reported in alveolar epithelial cells and alveolar macrophages in IPF (104) and elevated serum MMP3 levels have been correlated with decreased survival (105).

Matrix metalloproteinase 7 (MMP7, matrilysin) is another mediator reported to play a role in IPF pathogenesis. Increased MMP7 mRNA expression has been reported in the IPF lung compared to controls (100, 102, 106, 107) as well as increased staining of MMP7 in the alveolar epithelium of the IPF lung (108). Increased levels of MMP7 have also been reported in the BAL fluid (49, 108), plasma (102) and serum (101) (45) from IPF patients. In the bleomycin model, it was reported that MMP7 knockout mice were protected from bleomycin-induced fibrosis, with a significant reduction hydroxyproline content measured in lungs from knockout mice observed (106). A role for MMP7 in epithelial cell migration has been suggested in airway epithelium. In this study, re-epithelialisation of wounded trachea tissue was reduced by MMP inhibition in human tissue and in MMP7 knockout mice compared to wild type (109).

MMP9 is also increased in IPF and has been associated with rapid progression of disease (86). It has been proposed to play a role in the degradation of the basement membrane as it cleaves type IV collagen, a major component of the

basement membrane. The expression of MMP inhibitors, TIMPs, is reportedly increased in IPF also. TIMP1 expression was localised to interstitial macrophages, TIMP2 to fibroblastic foci, TIMP3 to elastic lamina of vessels and TIMP4 to epithelial and plasma cells (110).

1.1.6.5 Developmental signalling in the fibrotic lung

Aberrant activation of different developmental signalling pathways has been reported in IPF. A role for the Notch signalling pathway in TGFβ_1-mediated EMT of alveolar epithelial cells has been proposed (111). Ectopic expression of Notch in a rat alveolar epithelial cell line resulted in decreased expression of epithelial markers and induction of α-SMA and type 1 collagen. Use of a Notch inhibitor partially blocked the TGFβ_1 induction of α-SMA. In the same study, the expression of Notch and α-SMA was co-localised in lung tissue from bleomycin-treated rat lung and UIP lung.

Expression of the developmental protein Sonic hedgehog (SHH) in the epithelium lining honeycomb cysts has been reported in usual interstitial pneumonia (UIP) lungs in greater amounts than in non-specific interstitial pneumonia (NSIP) (112). It was recently reported that SHH induces differentiation of lung fibroblasts into myofibroblasts (113).

Another developmental protein implicated in IPF pathogenesis is phosphatase and tensin homologue (PTEN). Decreased PTEN expression has been reported in myofibroblasts in the IPF lung (114). In fibroblasts from PTEN knockout mice, increased expression of α-SMA, collagen production and cell proliferation was reported. Inhibition of PTEN in wild type fibroblasts induced α-SMA, and adenoviral overexpression in knockout fibroblasts decreased collagen production, cell proliferation and TGFβ_1-induced α-SMA expression. Finally, the authors reported increased amounts of collagen in bleomycin-treated lung following PTEN inhibition. More recently it was demonstrated that PTEN may limit collagen expression in a connective tissue growth factor (CTGF)-dependent manner (115).

Bone morphogenetic protein (BMP) signalling has also been reported to play a role in IPF. BMP2 is decreased and BMP4 increased in the IPF lung (116). BMP4 stimulation of airway epithelial cells was demonstrated to induce the expression of several mesenchymal markers e.g. fibronectin (Fn-1), tenascin C and N-

cadherin, whilst suppressing the expression of epithelial markers such as E-cadherin and β-catenin (117). BMP4 has also been shown to abrogate the response of adult human lung fibroblasts to TGFβ$_1$ stimulation with reduced induction of type 1 collagen, tenascin C and Fn-1 observed with treatment of BMP4 and TGFβ$_1$ (118). In the same study BMP7 was shown to reduce the TGFβ$_1$-induction of α-SMA and increase in MMP2 activity. Tissue expression of the BMP4 inhibitor gremlin is also increased in the IPF lung and in fibroblasts isolated from IPF patients (119). In this study it was also demonstrated that gremlin expression was induced by TGFβ$_1$ in A549 cells, and that overexpression of gremlin increased sensitivity to TGFβ$_1$.

A role for the Wnt/β-catenin signalling pathway in lung fibrosis has been suggested in a number of studies. β-catenin, a key downstream component of Wnt signalling, is proposed to play a protective role in the mouse lung. Mice with epithelial cells deficient in β-catenin have worse fibrosis (assessed by collagen production) following bleomycin instillation (120). siRNA knockdown of β-catenin in murine lung epithelial cells impaired wound closure in a scratch wound assay and resulted in decreased proliferation of these cells. In normal human lung fibroblasts, overexpression of β-catenin and Wnt ligand Wnt3a enhanced cell proliferation but did not induce the expression of genes associated with fibrosis – collagen type 1, α-SMA and CTGF (121).

Increased mRNA expression of several Wnt signalling pathway components has been reported in IPF compared to control samples (122). Expression of the Wnt ligands Wnt1, 7b and 10b, receptors Frizzed (Fzd) 2 and 3, and intracellular signal transducers β-catenin and lymphoid enhancer factor (LEF) 1 were all increased in IPF tissue. In isolated ATII cells Wnt7b and 10b, Fzd3, LEF1, glycogen synthase kinase-3β (GSK-3β) and β-catenin were increased in IPF. The Wnt co-receptor LRP5 (low density lipoprotein receptor 5) has been implicated in pulmonary fibrosis in the bleomycin mouse model (123). LRP5 knockout mice were less sensitive to bleomycin with reduced amounts of collagen detected and less TGFβ$_1$ (total and active) measured in BAL fluid.

Increased expression of several Wnt target genes has also been reported in IPF. Target genes MMP7, Fn-1 and cyclin D1 were reported to be increased in IPF tissue compared to controls in one study (122). Expression of Wnt target genes

such as MMP7 were also reported to be increased in the IPF lung compared to another ILD, hypersensitivity pneumonitis (HP) (48). Another Wnt1 target gene reported to be increased in IPF tissue is Wnt1-inducible signalling protein-1 (WISP-1) (48, 124, 125). WISP-1 has been reported to induce EMT in alveolar epithelial cells and ECM production by lung fibroblasts (124).

1.2 Wnt1-inducible signalling protein-1

1.2.1 CCN family

WISP-1 is a member of the CCN family of proteins named after the prototypic members cysteine rich angiogenic protein 61 (CYR61), connective tissue growth factor (CTGF) and neuroblastoma overexpressed (NOV). The family consists of six proteins designated CCN1-6. This nomenclature was proposed in 2003 (126) however the original names for each protein are still commonly used in the literature and are listed in table 1. In the current study the designation WISP-1 will be used.

Each CCN family member except WISP-2 has one N-terminal localisation sequence and 4 conserved structural modules each arising from a separate exon (detailed in Figure 5). WISP-2 lacks module IV (CT domain).

Protein	CCN designation	Alternative names
CYR61	CCN1	CTGF-2, IGFBP10, IGFBP-rP4
CTGF	CCN2	IGFBP8, IGFBP-rP2
NOV	CCN3	IGFBP9, IGFBP-rP3
WISP-1	CCN4	Elm-1
WISP-2	CCN5	CTGF-3, CTGF-L, Cop-1, HCIP
WISP-3	CCN6	

Table 1. Nomenclature of the CCN family of proteins

The different domains of the CCN proteins are known as the insulin-like growth factor binding domain (IGFBP, module I), von Willebrand type C domain (VWC, module II), thrombospondin type 1 repeat domain (TBS, module III) and the cysteine knot domain (CT, module IV). Each has sequence homology to the protein or domain for which it is named.

Module I

The IGFBP domain is approximately 32% identical to the N-terminal regions of several 'classic' IGF binding proteins (128). For most CCN proteins, the IGFBP domain contains a motif GCGCCXXC thought to be involved in IGF binding (129). This motif is present in CTGF (GCGCCRVC), which has been demonstrated to bind to IGF1/2 with low affinity compared to the high-affinity IGFBPs (130). IGF binding has not been reported for WISP-1, and has not been confirmed for some of the other family members (131). The amino acid sequence of this motif in WISP-1 is GCECCKMC and is missing one cysteine residue. It has been suggested that this motif is not directly involved in IGF binding but that it is involved in the structure of the IGFBP protein, allowing the correct confirmation for IGF binding (132).

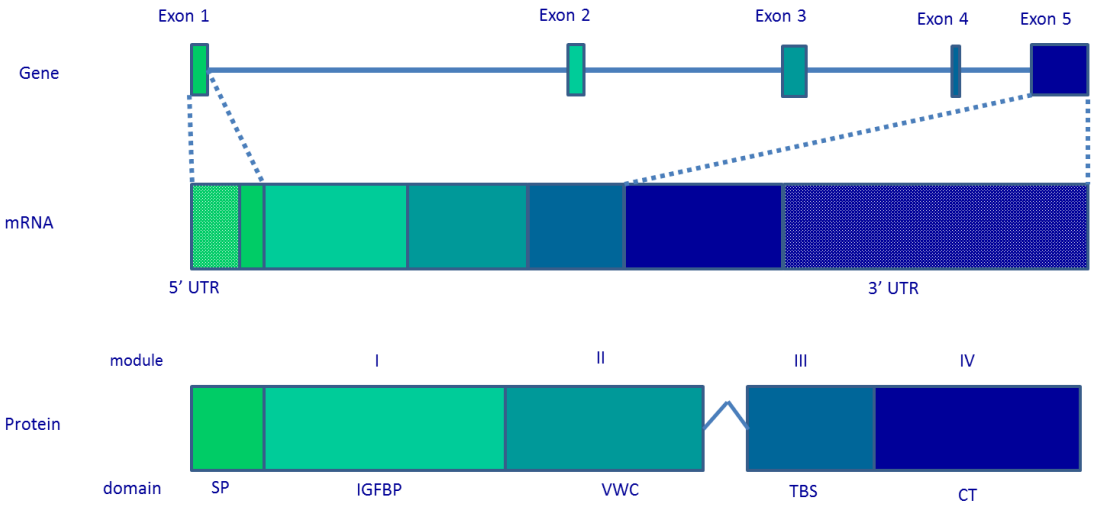

Figure 5. Schematic representation of the CCN family member gene, transcript and protein. Adapted from (127). Each CCN family member gene (except CCN5) contains 5 exons, each encoding for a section of the mature mRNA that in turn codes for an individual protein domain. Exons 1 and 5 also code for the 5' and 3' untranslated regions.

Module II

The VWC domain in the CCN proteins contains one repeat of the VWC motif which is present in multiple copies in other proteins (131), such as mucins, thrombospondins and collagens (128). This repeat has been reported to be involved in regulating cell signalling via the TGFβ/BMP family of proteins (133). Different CCN members have been demonstrated to bind to different members of this family. For example, CTGF was demonstrated to bind to and accentuate the effects of $TGF\beta_1$ (133). In this same study, CTGF was also shown to bind to BMP4. This interaction was found to be stronger and resulted in inhibition of BMP4. Both effects were reported to be due to CTGF binding enhancing or inhibiting $TGF\beta_1$/BMP4 binding to its receptor. CCN protein binding of BMP2 has also been reported in the literature. NOV was reported to bind and inhibit BMP2-induced osteoblast differentiation (134). In contrast, WISP-1 was reported to bind BMP2 and enhance its induction of differentiation in hBMSCs (135).

Other functions attributed to this domain include the modulation of the extracellular matrix, suggested to be mediated by $TGF\beta_1$ (136). A role in oligomerisation has also been suggested for this domain. It has been suggested that the number of repeats of the VWC motif may be linked to the affinity for binding growth factors (136). Therefore, multimers of one CCN protein or complexes with other CCN proteins and other VWC motif-containing proteins may be another way in which the activity of this family of proteins may be regulated. Native WISP-1 was detected in a study by Stephens et al. (137) as a higher order oligomer where the authors suggested that this may increase avidity for receptors in vivo.

Several integrin binding sites are present in this domain and in the other CCN protein domains. The location of these sites are reported in reviews on the CCN family (138, 139) but were not necessarily reported in the original studies that identified their binding to a member of the CCN family. In the VWC domain, binding sites for integrins αVβ3 (140) (141) (142, 143), α11bβ3 (144) and αVβ5 (145) (146) (137). WISP-1 interaction with αVβ1 has also been reported (147) however the location of this site is unknown. This domain is missing from WISP-1 splice variants 2, 3 and 4.

Module III

The TBS domain contains a thrombospondin type 1 repeat (TSR) – a common consensus sequence which is found 187 times in the human genome (131). The TSR binds to many different targets including TGFβ, however this has been shown to require a specific tripeptide RFK (148) not present in the CCN TBS domain. A motif present in the TBS domain, WSXCSXXCG in the CCN proteins, is thought to be involved in the binding of sulphated glycoconjugates (128) however heparin binding has also been demonstrated for short fragments of CTGF consisting of only the cysteine knot domain (149). In WISP-1 the sequence for this motif is WSPCSTSCG.

A binding site for the integrin α6β1 is present in this domain (150). This domain is missing from WISP-1 splice variants 3 and 4. No reported effect of WISP-1 has been attributed to this domain in the literature.

Module IV

The cysteine knot domain is believed to mediate protein-protein interaction/dimerisation (138). Many functions of small growth factors that contain a cysteine knot motif such as TGFβ, are mediated by heparin and HSPGs (151). The proposed heparin binding site in the CT domain of CCN proteins is XBBXBX where B is a basic amino acid and X either an uncharged or hydrophobic amino acid (152). This sequence is not present in the CT domain in WISP-1. CTGF has been demonstrated to bind heparin via its CT domain (149). This binding has been reported to stimulate the adhesion of fibroblasts, myofibroblasts, endothelial cells and epithelial cells to CTGF (153). The CT domain has also been shown to mediate CTGF inhibition of Wnt signalling in Xenopus embryos via LRP-6 (154).

Several integrin binding sites have been reported in the CT domain. Like the VWC domain, the CT domain contains an αVβ3 site, and like the TBS domain, it also contains α6β1 sites (139) (155). The CT domain also contains a binding site for the integrin αMβ2 (156) and α5β1 (157) (158) (135). This domain is missing from WISP-1 splice variant 3.

The CCN family members share approximately 50% of their primary structure (131). Each has a high cysteine content accounting for approximately 10% of the molecule by mass. 38 cysteine residues are conserved in position and number

between the family members and are potentially involved in 17 disulphide bonds across the molecule (136). WISP-2 lacks the CT domain and has 10 less cysteine residues. WISP-3 lacks 4 residues in the VWC domain (131).

Between the VWC and TBS domains a variable linker region is present and is encoded by exon 3 (same exon as VWC domain) (138). This region is susceptible to proteolytic cleavage. This has been demonstrated for CTGF where N-terminal and C-terminal fragments were detected following treatment with MMP-1, -3, -7 and -13, elastase and plasmin (159). Cleavage of regions connecting modules 1 and 2, and modules 3 and 4 has also been reported. Truncated forms of CTGF (approximately 10kDa as opposed to full length at 38kDa) were detected in pig uterine luminal flushings (149), and in conditioned media from mouse connective tissue fibroblasts and human foreskin fibroblasts (160). Full length CTGF was not detected in conditioned media and remained cell-associated in the fibroblast study.

This cleavage of the CCN proteins may represent an additional level of regulation of their activity (136). Another potential level of regulation of protein expression, activity or function is alternative splicing which has been reported for some members of the CCN family (161). Expression of truncated or alternatively spliced proteins may affect interactions with receptors and/or binding proteins and/or alter the confirmation of the protein potentially influencing several aspects of its biology. Despite the potential significance of WISP-1 splice variant expression, there are relatively few studies in the literature that report on their expression or activity. In the few studies available, expression of alternatively spliced variants was detected in both normal and pathological settings (see chapter 4) (127, 162-164).

A recent study investigated the contribution of different protein domains to effects observed through the use of truncated WISP-1 proteins (137). A549 cells were found to adhere to full length and truncated forms of WISP-1, particularly those containing both of the C-terminal protein domains, TBS and CT. This effect was mediated by the integrins $\alpha v\beta 5$, $\alpha v\beta 3$ and $\beta 1$. WISP-1 was shown to induce β-catenin activation and CXCL3 secretion in a rat kidney fibroblast cell line however this effect was not mediated by neutralisation of the integrins studied. This

attribution of an effect of WISP-1 to particular domains highlights the importance of considering the role of variants of WISP-1 when studying its activity.

CTGF is one of the better characterised members of the CCN family and has been implicated in the development of fibrosis by mediating the action of TGFβ (165). In CTGF+TGFβ_2-induced kidney, liver and lung fibrosis models, increased collagen levels and fibrosis scores were reduced by use of an anti-CTGF antibody (166). CTGF expression has been detected in alveolar epithelial cells and interstitial fibroblasts in IPF tissue sections, with greater staining observed in IPF lung compared to controls (167). Increased levels of CTGF have also been reported in BAL fluid from IPF patients (168).

1.2.2 Wnt1-Inducible Signalling Protein-1

WISP-1 has been identified as a WNT target (169) and its increased expression has been demonstrated in IPF (48). Wnt4 does not induce WISP-1 protein expression suggesting that it is a target of the canonical Wnt/β-catenin pathway (169). The canonical Wnt signalling pathway (shown in Figure 6) involves the binding of Wnt proteins (cysteine-rich secreted glycoproteins) to frizzled cell surface receptors. Binding results in GSK-3β inhibition and β-catenin hypophosphorylation. This protein can then translocate to the nucleus. It binds to the lymphoid enhancer-binding factor/T cell factor (LEF/TCF) family of transcription factors and converts them from transcriptional repressors to activators (170). However it has been reported that TCF/LEF sites do not play a major role in the activation of WISP-1 by Wnt1 and that the CRE (cyclic AMP responses element) binding protein is important for this (171). In this study it was also suggested that β-catenin may directly regulate the WISP-1 promoter as it induced the WISP-1 promoter in a dose-dependent manner.

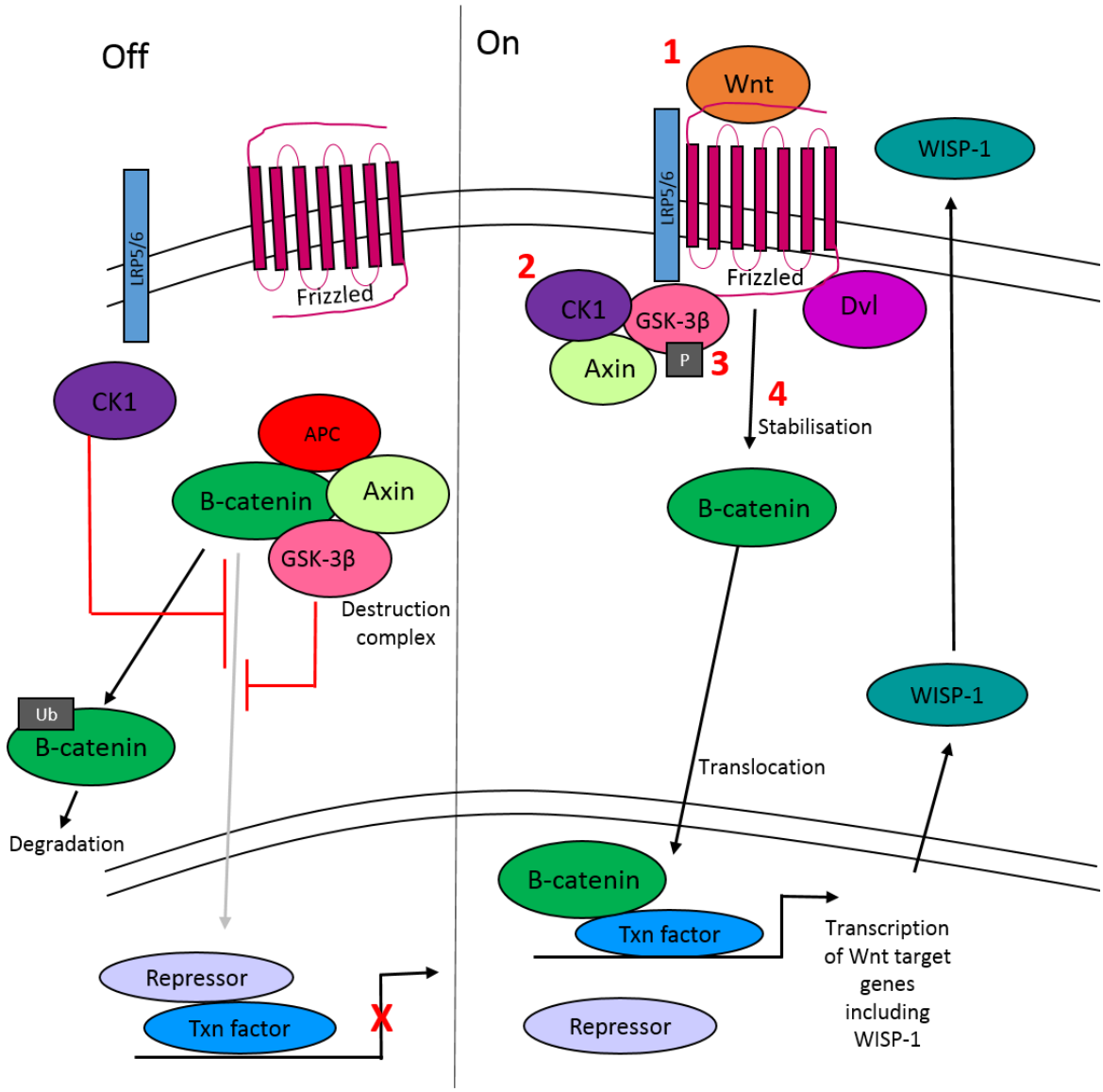

Figure 6. Canonical Wnt signalling pathway. In the off state, the destruction complex (APC/Axin/GSK-3β) and CK1 phosphorylate β-catenin targeting it for proteasomal degradation. In the presence of Wnt signal, the Wnt receptor complex (LRP5/6 and Frizzled) is activated leading to GSK-3β displacement by Dishevelled (Dsh) and subsequent stabilisation of β-catenin. β-catenin is then able to translocate and accumulate in the nucleus where it displaces co-repressors and binds to transcription factors resulting in transcription of Wnt target genes including WISP-1. Numbers 1-4 indicate points at which TNFα and/or TGFβ are thought to interact with this pathway to promote expression of Wnt target genes.

Both the pro-fibrotic cytokine TGFβ$_1$, and the pro-inflammatory cytokine TNFα have been demonstrated to interact with the canonical Wnt signalling to promote expression of Wnt target genes. As highlighted in Figure 6, TNFα has been reported to promote the activation of the Wnt receptor complex [1] (172), and to suppress the mRNA expression of the destruction complex components GSK-3β, Axin and APC [2] (173). Both TNFα and TGFβ are reported to phosphorylate GSK-3β [3] (174, 175), and to increase stabilisation of β-catenin [4] (176, 177).

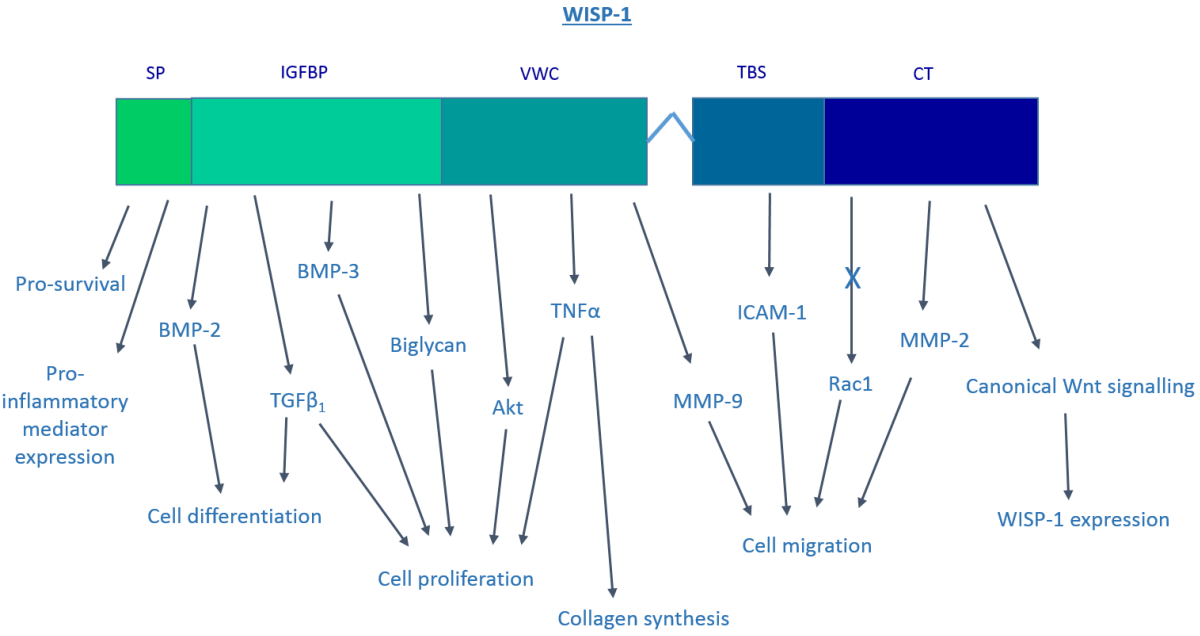

Figure 7. Summary of the roles WISP-1 has been reported to play in different cell types, and the mediators through WISP-1 has been demonstrated to exert these effects. The particular domain(s) through which WISP-1 acts to exert each effect is detailed below where it has been reported in the literature.

WISP-1 has been reported to regulate its own expression in hippocampal neurons (178). Recombinant human WISP-1 (rhWISP-1) treatment increased WISP-1 expression which was enhanced by both Wnt1 and a β-catenin agonist, and was blocked by a β-catenin inhibitor. WISP-1 stimulating its own expression has also been reported in cardiomyocytes and saphenous vein smooth muscle cells (179, 180). As well as stimulating its own expression, a number of roles have been attributed to WISP-1 in the literature, summarised in Figure 7. In particular, WISP-

1 has been implicated in bone development and cancer, and a number of studies have investigated its role in mesenchymal cells, discussed below.

1.2.2.1 WISP-1 in bone development

There are a number of studies in the literature investigating the role of WISP-1 in the development of bone/cartilage. The potential interaction of WISP-1 and biglycan was investigated in relation to osteogenesis (181). In human bone marrow stromal cells (hBMSCs) biglycan overexpression resulted in decreased cell proliferation which was rescued by the addition of recombinant WISP-1. Reduced differentiation of murine BMSCs in biglycan-deficient mice was alleviated by overexpression of full length or an alternatively spliced variant of WISP-1 missing the VWC domain (variant 2, see chapter 4). In a study investigating the regulation of extracellular matrix, WISP-1 induction of TgfβI, Nov, Igfbp5 and Dkk2 was abrogated by knockdown of biglycan in murine embryonic fibroblasts (182).

Other studies have implicated interactions of WISP-1 with other proteins in osteogenesis. For example, a relationship between TGFβ_1 has also been reported (183). In this study rhWISP-1 was shown to increase proliferation and promote differentiation of hBMSCs. When cells were co-treated with TGFβ_1 and WISP-1, WISP-1 limited the increase in proliferation by TGFβ_1, and TGFβ_1 limited the induction of differentiation marker expression by WISP-1. Different effects were observed when WISP-1 was overexpressed in hBMSCs rather than added exogenously and TGFβ_1 co-treatment was required to induce expression of the differentiation marker alkaline phosphastase. In a recent study, overexpression of WISP-1 in hBMSCs was demonstrated to enhance TGFβ_3-induced chondrogenesis (184). siRNA-mediated knockdown of WISP-1 blocked TGFβ_3-induced matrix synthesis and by co-immunoprecipitation, WISP-1 was found to directly bind TGFβ_3.

The effect of WISP-1 on BMP2 activity in osteogenesis has also been studied (135). WISP-1 was reported to enhance the differentiation of hBMSCs induced by BMP2 and its knockdown resulted in decreased expression of the differentiation markers alkaline phosphastase and osteopontin. WISP-1 was shown to directly bind to BMP-2 and to enhance the binding of BMP2 to hBMSCs. This effect was abrogated by the use of an anti-integrin $\alpha_5\beta_1$ antibody. WISP-1 has also been

reported to mediate the effects of BMP3 in mesenchymal stem cells (185). In this study the authors demonstrated BMP3-induced expression of WISP-1 which was required for BMP3-stimulated proliferation of these cells.

A role for WISP-1 mediated by the integrin αvβ5 was reported in osteoarthritic synovial fibroblasts (OASF) (146). WISP-1 was reported to induce the expression of IL-6 in these cells, an effect that was blocked by the use of an anti-integrin αvβ5 antibody, and inhibitors of phosphoinositide 3-kinase (PI3K), protein kinase B (Akt) and nuclear factor kappa-light-chain-enhancer of activated B cells (NFκB). In this study WISP-1 was also found to induce the mRNA expression of MMP2, MMP9, tumour necrosis factor α (TNFα) and IL-1β. The same integrin (αvβ5) has also been reported to mediate the WISP-1 induced expression of vascular cell adhesion molecule 1 (VCAM-1) in OASFs (158). This effect was also blocked by an anti-integrin α6β1 antibody, and by inhibitors of spleen tyrosine kinase (Syk), protein kinase C (PKC), c-Jun N-terminal kinase (JNK) and activator protein 1 (AP-1).

1.2.2.2 WISP-1 in cancer

Several studies demonstrate a role for WISP-1 in cancer. WISP-1 has been shown to induce MMP2 expression in human chondrosarcoma cells as well inducing their migration across a transwell (186). These effects were shown to be mediated by integrin α5β1, focal adhesion kinase (FAK), mitogen activated protein kinase kinase (MEK), mitogen activated protein kinase 1 (ERK), p65 and NFκB through the use of neutralising antibodies, siRNA knockdown and inhibitors. A role for WISP-1 in MMP expression and cell migration has also been reported in osteosarcoma (187). WISP-1 treatment of osteosarcoma cell lines induced the migration of these cells across a transwell and promoted their invasion through matrigel. MMP2 and MMP9 were both induced by WISP-1, as was integrin αvβ3. Knockdown of MMP2 and MMP9 reduced WISP-1 stimulated cell migration, and an antibody against integrin αvβ3 blocked the induction of MMP2 and MMP9 and cell migration induced by WISP-1. This was shown to be mediated by Ras, V-Raf-1 murine leukaemia viral oncogene homologue 1 (Raf-1), MEK, ERK and NFκB.

In oral squamous cell carcinoma cell lines WISP-1 was demonstrated to stimulate cell migration and invasion, and the expression of intracellular adhesion molecule 1 (ICAM-1) (142). These effects were blocked by inhibition of integrin αvβ3,

apoptosis signal regulating kinase 1 (ASK1), JNK/p38 and AP-1. In contrast, WISP-1 has been reported to reduce migration and invasion of lung cancer cell lines through inhibition of Rac (188). WISP-1 overexpression reduced Rac activation and the expression of MMP1. Rac activation was restored by use of antibodies against integrins αvβ5 and α1, and MMP1 expression and migration/invasion of cells was rescued by co-expression of a constitutively active Rac mutant.

WISP-1 has been reported as a pro-survival factor in several studies. In a lung cancer cell line it was shown to protect from DNA damage by reducing cytochrome C release from mitochondria and upregulating the expression of the anti-apoptotic protein Bcl-X_L (189). WISP-1 was not able to protect cells from Fas-ligand activated cell death or protect lung cancer cells lacking p53 expression.

1.2.2.3 WISP-1 and mesenchymal cells

WISP-1 has been shown to bind the proteoglycans decorin and biglycan present in skin fibroblast conditioned media. Interaction of WISP-1 with skin fibroblasts was inhibited by decorin and biglycan in the same study (190)

In human mesenchymal stromal cells, WISP-1 shRNA knockdown was demonstrated to increase cell death implicating WISP-1 as a survival factor in these cells (191). Annexin V staining was increased, as was the expression of multiple apoptosis-responsive genes at the mRNA and protein levels. However in a study investigating Notch signalling in stromal fibroblasts (in relation to melanoma), WISP-1 shRNA knockdown was shown to reduce the increase in apoptotic cell number observed with activation of Notch signalling (192). WISP-1 knockdown also reduced the Notch-induced decrease in proliferation, tumour size and angiogenesis reported.

WISP-1 is upregulated in the post-infarct myocardium (193, 194). TNFα and IL-1β expression was found to precede that of WISP-1 and both TNFα and IL-1β were shown to induce WISP-1 and biglycan expression in neonatal rat ventricular myocytes (193). In this study, WISP-1 induced cardiomyocyte hypertrophy via activation of Akt and increased the proliferation of cardiac fibroblasts and collagen synthesis. TNFα has also been demonstrated to induce WISP-1 expression in primary human cardiac fibroblasts in a CREB-dependent manner via ERK (194). WISP-1 knockdown abrogated TNFα-stimulated cardiac fibroblast

proliferation and collagen synthesis, and recombinant WISP-1 blocked TNFα-induced cell death.

The Akt signalling pathway has also been demonstrated to mediate the effects of WISP-1 on vascular smooth muscle cells (SMCs) (195). WISP-1 overexpression stimulated the proliferation and migration of these cells which was abrogated through the use of Akt and PI3K inhibitors. WISP-1 has also been reported to stimulate the proliferation of bronchial SMCs which was accompanied by induction of p-Akt, PI3K and p-GSK3β (196).

In summary, WISP-1 has been shown to exert several different effects across different cell types and tissues, including the stimulation of cell proliferation, migration, collagen synthesis, and MMP expression. These effects have been reported to be mediated by several different integrins and binding partners and through the activation of different signalling pathways, and several of these processes are of interest in pulmonary fibrosis.

1.2.3 WISP-1 in pulmonary fibrosis

WISP-1 mRNA was reported to be upregulated in IPF lung tissue samples compared to those from patients with hypersensitivity pneumonitis (48). WISP-1 was also one of several Wnt-related genes found to be upregulated in ATII cells from a bleomycin mouse model of pulmonary fibrosis in a microarray study (124). In this study, the authors reported that increased WISP-1 protein was also detected in the bleomycin model. In vitro stimulation with WISP-1 resulted in increased proliferation and migration of ATII cells, as well as changes in gene expression suggestive of EMT, including increased α-SMA and decreased e-cadherin. These cells also had increased expression of MMP7 and osteopontin. Expression of type I collagen, α-SMA and fibronectin was increased in WISP-1-stimulated NIH3T3 cells (a murine fibroblast cell line). Total collagen levels in these cells were also increased following WISP-1 stimulation. Primary human fibroblasts responded similarly with an induction of type I collagen and fibronectin mRNA and increased total collagen after WISP-1 treatment. In vivo a neutralising WISP-1 antibody was shown to attenuate bleomycin-induced fibrosis assessed by a reduction in collagen induction, EMT marker expression, a reduced

decrease in lung compliance and improved survival. WISP-1 expression in human IPF was also measured in this study and was found to be increased in both whole lung (mRNA and protein) and in isolated ATII cells (mRNA) but not in isolated fibroblasts (mRNA).

A study investigating the induction of EMT by mechanical stretch reported that use of an anti-WISP-1 antibody reduced the induction of vimentin and α-SMA, and the reduction in e-cadherin observed following ATII cell stretch (197).

Another study reported that WISP-1 was induced by the pro-fibrotic cytokine $TGF\beta_1$ in primary human lung fibroblasts at the mRNA and protein (cell lysate and supernatant) levels (125). This was found to correlate with decreased miR-92a expression. Fibroblast WISP-1 expression was also measured at the mRNA level and increased expression in IPF fibroblasts compared to controls was reported, in contrast to an earlier study (124). A recent study has reported $TGF\beta_1$ and TNFα stimulated expression of WISP-1 in primary parenchymal fibroblasts from control and IPF donors (198). This induction was reduced at the mRNA level by inhibiting different components of the NFκB signalling pathway. It was also demonstrated that siRNA-mediated knockdown of WISP-1 reduced the expression of IL-6 stimulated by $TGF\beta_1$ or TNFα.

1.3 Hypothesis and objectives

Whilst these studies suggest a role for WISP-1 in the pathogenesis of IPF, they are limited in that the mechanism by which WISP-1 exerts these pro-fibrotic effects is unclear. Literature on the CCN family suggests that these proteins act via one or more of their domains to exert a particular effect. Therefore, the expression and activity of WISP-1 variants missing whole domains is an aspect of WISP-1 biology currently underappreciated in the literature, including in studies investigating the role of WISP-1 in pulmonary fibrosis. Taking this into consideration, the hypotheses for this study are as follows:

- WISP-1 is expressed at higher levels in the IPF lung compared to controls, and is regulated by pro-fibrotic mediators. Expression of individual splice

variants is altered in the IPF lung compared to controls and is also regulated by pro-fibrotic mediators.

- Full length WISP-1 induces the proliferation of fibroblasts and their expression of ECM components, and enhances EMT in epithelial cells. WISP-1 splice variants have a greater or lesser effect on these cell types compared to full length WISP-1.

The first aim of this study is to fully characterise WISP-1 expression, including that of individual splice variants, in primary fibroblasts from IPF and control donors, and in an alveolar epithelial cell line. The second aim is to characterise the effect of full length and variant WISP-1 on these cell types.

Chapter 2: Methods

2.1 Materials

Item	Manufacturer	Code
2-mercaptoethanol	Sigma Aldrich	M7522
Acrylamide	Geneflow	A20072
Agarose	Sigma Aldrich	A9539
Ammonium persulphate	Sigma Aldrich	A3678
Bovine serum albumin fraction V	Sigma Aldrich	A3059
Bromophenol blue	Sigma Aldrich	B8026
Chloroform	Sigma Aldrich	C2432
Citric acid	Sigma Aldrich	C1909
Clarity Western ECL substrate	Biorad	170-5061
Competent E. coli	Promega	L3002
Dimethyl sulphoxide	Sigma Aldrich	D2650
Disodium tetraborate	Sigma Aldrich	221732
Dulbecco's Modified Eagle Medium	Life tech.	110960-044
DNA 100 base pair size marker	Novagen	11300
DNA 1000 base pair size marker	Novagen	11900
DNA-free kit	Life tech.	AM1906
Ethanol	Sigma Aldrich	32221
40% formaldehyde	Sigma Aldrich	F8775
FX20 fixative (sodium thiosulphate)	Fotospeed	FS03140
G418 sulphate	Sigma Aldrich	G8168
Glycerol	Sigma Aldrich	G5150
Glycine	Sigma Aldrich	G8898
Glycogen (from mussels)	Roche	10901393001
Hank's Balanced Salt Solution ($Ca^{-}Mg^{-}$)	Life tech.	14170-138
Heat Inactivated Foetal Bovine Serum	Life tech.	10500-064

Hyperfilm	Amersham	28-9068-36
Human WISP-1 DuoSet	R&D	DY1627
Hydrochloric acid	Sigma Aldrich	07102
Hydrogen peroxide	Fisher Scientific	10386643
Isopropanol	Sigma Aldrich	I9516
KOD polymerase kit	Novagen	710863
LB broth	Sigma Aldrich	L3522
LB agar	Sigma Aldrich	A1296
L-Glutamine	Life tech.	25030-024
Plasmid maxi kit	Qiagen	12162
Methanol	Sigma Aldrich	24229
Methylene blue	Sigma Aldrich	M9140
Milk powder	Marvel	-
Precision Plus protein standards MW marker	Biorad	161-0375
Nancy 520	Sigma Aldrich	01494
Non-Essential Amino Acids	Life tech.	11140-035
pcDNA 3.1 (+)	Life tech.	V790-20
PD5 developer(Phenidone/hydroquinone)	Fotospeed	FS02530
Penicillin-Streptomycin	Life tech.	15140-122
Perfect Probe primers for gene of interest	Primerdesign	PP-hu-600
Perfect Probe primers for housekeeping genes	Primerdesign	HK-PP-hu-600
Phosphate buffered saline	Sigma Aldrich	P4417
PrecisionPLUS- iC mastermix	Primerdesign	Precision-iC
PVDF membrane	Biorad	162-0177
QIAquick gel extraction kit	Qiagen	28704
Reagent diluent	R&D	DY995
Recombinant human IL-13	Peprotech	200-13
Recombinant human IL-1β	Peprotech	200-01B
Recombinant human IL-4	Peprotech	200-04
Recombinant human $TGF\beta_1$	Peprotech	100-21

Recombinant human TNFα	Peprotech	300-01A
Recombinant human WISP-1 (his-tagged, NS0)	R&D	1627-WS-050
Recombinant human WISP-1 (E. coli)	Peprotech	120-18
Restriction enzyme HindIII	Promega	R4044
Restriction enzyme EcoRI	Promega	R4014
Reverse transcription kit	Primerdesign	RT-std
SOC media	Sigma Aldrich	S1797
Sodium azide	Sigma Aldrich	S2002
Sodium chloride	Sigma Aldrich	S9625
Sodium dodecyl sulphate (SDS)	Sigma Aldrich	L6026
Sodium Pyruvate (NaPy)	Life tech.	11360-039
Strata clean resin	Agilent	400714
Sulphuric acid	Sigma Aldrich	00646
SYBR green primers for gene of interest	Primerdesign	SY-hu-600
T4 ligase and buffer	Life tech.	EL0014, B69
TEMED	Sigma Aldrich	T7024
Tetramethylbenzidine solution	EBioscience	00420156
TransIT-LT1 transfection reagent	Mirus Bio	MIR2300
Tris	BDH	10315
Tris-Acetate-EDTA buffer	Geneflow	B90030
TRIzol reagent	Invitrogen	15596018
Trypan blue	Sigma Aldrich	T8154
0.5% Trypsin-EDTA	Life tech.	15400-054
Tween-20	Sigma Aldrich	P2287

Table 2. List of reagents used

2.2 Equipment

Equipment	Manufacturer
Hera Safe KS hood	Heraeus
Hera Safe hood	Heraeus
Hera Cell incubator	Heraeus
Biofuge Fresco 17	Heraeus
Megafuge 16R	Heraeus
Biofuge Fresco	Heraeus
DMIRB Light microscope	Leica
Imager	Amersham
Mistral 3000i centrifuge	MSE
C1000 thermal cycler	Biorad
T100 thermal cycler	Biorad
Multiscan Ascent plate reader	MTX Lab systems
CTR7000 microscope	Leica
Leica Application Suite X software	Leica

Table 3. List of equipment used in this study

2.3 Cell culture

Different cell types required different medium supplements for optimal growth. These are listed below in Table 4.

Cell type	Medium	L-Glutamine	NEAA	Pen/Strep	NaPy	G418
MRC5	DMEM	√	√	√	√	x
Primary fibroblasts	DMEM	√	√	√	√	x
A549	DMEM	√	x	√	x	x
HEK2393T	DMEM	√	√	√	√	x
Stably transfected A549	DMEM	√	x	x	x	√

Table 4. List of media supplements required for each cell type cultured

2.3.1 Establishment of fibroblasts from biopsy

Surgical lung biopsy samples were obtained as part of an ethically approved study: Pathophysiological Mechanisms of Pulmonary Fibrotic Disease (Berkshire LREC No 07/H0607/73).

Surgical lung biopsy samples were placed in a petri dish in culture medium. Any staples present in the sample were removed and the sample was cut into small sections using autoclaved sterile forceps and a scalpel. Small pieces of tissue were scratched into the bottom of wells in a six well plate containing complete DMEM and 10% FBS (2ml/well). After 7 days the medium was changed. Following this, medium was replaced every 2-3 days for approximately 2 weeks and then outgrown fibroblasts were dissociated from the wells using trypsin/EDTA (see below) and placed into a tissue culture flask. Once confluent these cells were detached by trypsinisation, counted (see below) and split 1:3 to increase cell numbers. Once confluent, these cells were detached and counted, and then frozen down for cryogenic storage (see below).

2.3.2 Passaging and seeding of cells

Confluent cells were rinsed twice with HBSS ($Ca^{-}Mg^{-}$) prior to dissociation from the flask by trypsinisation (1ml trypsin-EDTA 0.5% diluted 1:10 with HBSS ($Ca^{-}Mg^{-}$)). MRC5 cells and primary fibroblasts required approximately 5 minutes incubation with trypsin at 37°C, and A549 and HEK293T cells required approximately 2-3 minutes. Trypsin was neutralised by an excess of serum-containing medium (5ml) and cells were removed from flask and placed into a universal tube for centrifugation at 300g for 5 minutes at room temperature. Medium was then removed and the cell pellet resuspended in 1ml medium.

Cell number was counted using a haemocytometer. Cells were diluted 1 in 5 with HBSS and live/dead stain trypan blue (5µl cells + 15µl HBSS + 5µl trypan blue). The stained cell suspension was pipetted onto a haemocytometer (approx. 8µl), and the grid visualised under the microscope (Figure 8). Live cells (trypan blue excluded from cells) were counted in $1mm^2$ squares. Cells on the border of the square were counted on the top and left borders only.

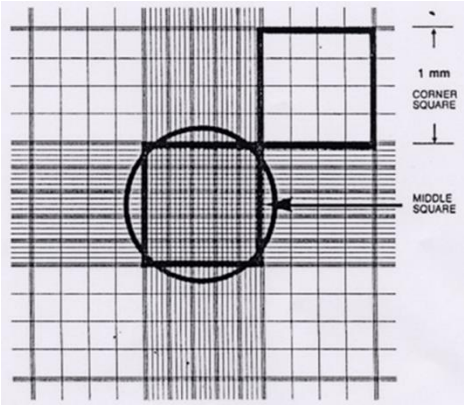

Figure 8. Image of haemocytometer grid under the microscope. From www.phe-culturecollections.org.uk/technical/ccp/cellcounting

Viable cell counts were calculated as follows:

Count = (total number counted/number of squares) x 10^4 x 5

where 10^4 is the area of the square and 5 the dilution of the cells

Number of cells required for seeding was calculated e.g. 6 wells at 6 x 10^4/well equals 3.6 x 10^5 cells. Medium was added to wells (for a 6 well plate 1.5ml media + 0.5ml cell suspension). Cells were diluted to the required concentration and added dropwise to wells.

All cells were maintained in culture through one passage before seeding for an experiment. Experiments were carried out with primary fibroblasts at passage 4-7.

2.3.3 Cell treatments

Cells at approximately 70% confluence were incubated for 24 hours prior to treatment in fresh DMEM (+appropriate supplements) containing either 0.5% or 10% FBS. Treatments were then carried out for length of time and at concentration(s) indicated for each experiment.

At the end of experiments medium was removed from wells, spun to remove cell debris and stored at -80˚. For RNA analysis, cells were harvested directly in Trizol reagent (500µl/ well in a 6 well plate). For protein analysis, cells were scraped in PBS (500µl/ well in a 6 well plate) or lysed directly in sample buffer containing

protease inhibitors (250µl/ well in a 6 well plate) as indicated for each experiment.

2.3.4 Time lapse microscopy

For time lapse experiments, cells were seeded at indicated density and allowed to adhere to the plate for 4-6 hours. Following this, cells were treated (where indicated) then placed inside the time lapse microscope chamber (37˚C, 5% CO_2). One position near the centre of each well was marked using the Leica software and the settings adjusted to take an image at each position every 20 minutes for 72 hours. The time course was started and after 72 hours data were collected and cells were harvested in trizol reagent (HEK293T conditioned medium experiments) or disposed of following disinfection protocol.

2.3.5 Cryogenic storage and regeneration of cell stocks

For cryogenic storage cells were dissociated and counted as described above. They were then diluted to a concentration of 1 x 10^6/ml in complete DMEM containing 10% DMSO. Cells (1ml) were added to labelled cryovials and stored O/N in a -80˚C freezer inside a 'Mr Frosty' container designed to cool cells at a rate of approximately 1˚C/minute to aid preservation. The following day, cells were transferred to racks stored in liquid nitrogen.

To regenerate frozen cell stocks, cells were removed from liquid nitrogen storage and thawed as quickly as possible by the pipetting of pre-warmed medium onto the cells. Cells were then centrifuged at 300g for 5 minutes at room temperature to remove DMSO present in the freezing medium. Cells were resuspended in 1ml medium which was added to an appropriate volume in a T75 flask (12ml total volume). Medium was changed the following day to remove dead cell debris.

2.4 Methylene blue assay

A methylene blue assay was used to determine cell number and whether this was influenced by different treatments.

Cells were seeded into 96 well plates at the following densities: 6000, 3000, 1500, 750, 375 and 187 cells/well. Per condition, each cell density was seeded in

quadruplicate and 4 replicate plates were seeded for each experiment. Cells were given time to adhere (6 hours) and then one plate was fixed – T0 (see below). Where indicated, remaining plates were treated and subsequently fixed at 72 hours.

Cells were fixed as follows: medium was removed from the well and cells washed in 100µl/well HBSS. HBSS was then removed and formal saline **Table 5** added for a minimum of 30 minutes at room temperature (100µl/well). Cells were washed in 100µl/well PBS following the removal of formal saline and then stored at 4˚C in 100µl/well sodium azide in PBS (0.05%) until all plates in the experiment were processed for staining.

At the end of the experiment, all cells were stained with methylene blue in borate (Table 6, Table 7) buffer (100µl/well) for 30 minutes at room temperature. This was removed and plates washed with water before the addition of 100µl/well 1:1 ethanol/0.1M HCl solution (Table 8) to elute the methylene blue from the fixed cells. Absorbance of each well was measured at 630nM using Multiscan Ascent plate reader. Absorbance at 570nm was subtracted to correct for the absorbance of the plastic plate. The average of the four replicates for each timepoint and condition was calculated. T0 values were used to calculate the absorbance value for later time points as a percentage of the T0 value.

Formal saline	
NaCl	9g
40% formaldehyde	100ml
H_2O	900ml

Table 5. Formal saline

10mM Borate buffer	
Disodium tetraborate	3.82g
H_2O	800ml
pH to 8.5	
Make up to 1 litre with H_2O	

Table 6. Borate buffer

1% (w/v) methylene blue in borate buffer	
Methylene blue	5g
10mM borate buffer	500ml
Filter	

Table 7. Methylene blue

Ethanol:HCl	
Ethanol	200ml
0.1M HCl	200ml

Table 8. Ethanol:HCl

2.5 Nucleic acid analysis

2.5.1 RNA isolation

RNA was isolated from cell culture samples via the phenol:chloroform method (199). Cells were lysed in Trizol reagent containing phenol and guanidine isothiocyanate. Chloroform was added (100µl to 500µl trizol reagent) and samples were shaken for approximately 15 seconds then incubated at room temperature for 10 minutes. Samples were then centrifuged at 12000g at 4˚C for 15 minutes. The aqueous phase containing RNA was transferred to a fresh 1.5ml eppendorf tube and glycogen (20µg, 1µl) added as a carrier. An equal volume (to aqueous phase) of ice cold isopropanol was added to each sample to precipitate

RNA. Samples were vortexed and stored overnight at -80˚C. The following day samples were centrifuged at 13000g at 4˚C for 30 minutes to pellet the RNA. Isopropanol was removed and pellets washed in ethanol (equal volume to trizol reagent). Samples were then centrifuged at 7500g at 4˚C for 5 minutes to allow removal of ethanol and pellets were left to air-dry. Samples were then DNase treated to remove contaminating genomic DNA. Using the DNA-free kit (Life technologies), pellets were resuspended in 20µl of DNase stock (1µl DNase + 2µl 10X buffer + 17µl H_2O per sample) and incubated at 37˚C for 1 hour. DNase was neutralised by incubating with DNase inactivation reagent (5µl) at room temperature (included in the kit). Samples were then centrifuged at 13000g at room temperature for 2 minutes to pellet the inactivation reagent. Samples were stored at -80˚C.

2.5.2 RT-qPCR

The concentration of RNA samples was measured using a Nanodrop spectrophotometer and determined by absorbance at 260 and 280nm. Per sample, 1µg of RNA was reverse transcribed using a commercial reverse transcription kit. Reverse transcription was carried out in two stages:

1. Annealing – Mastermix (3µl) consisting of dNTPs, random nonamer and oligodT primers (1µl of each per sample) was added to 1ug of RNA and the volume made up to 15µl with H_2O. Samples were incubated in a heatblock thermocycler at 65˚C for 5 minutes and then snap frozen on ice.
2. Extension – Mastermix (5µl) consisting of reverse transcriptase (RT) (Moloney Murine Leukaemia Virus reverse transcriptase, 0.8µl per sample), 5X buffer (4µl per sample) and H_2O (0.2µl per sample) was added. Samples were then incubated in heatblock thermocycler as follows:
    a. 37˚C for 10 minutes
    b. 42˚C for 60 minutes

Samples were then diluted 1 in 10 to a final volume of 200µl in H_2O and stored at -20˚C. A no RNA control was included for the annealing step and a no RT control for the extension step using the sample with the highest concentration of RNA.

cDNA samples were used for mRNA expression analysis by quantitative real time PCR (qPCR) using the Biorad CFX96 real time system. Assays were carried out using the fluorescent dye SYBR or a sequence –specific probe labelled with a fluorescent probe (Perfect Probe, Primer Design). Primer sequences for each gene analysed and the detection chemistry for each are listed in Table 9.

Reaction volumes are listed in Table 10 and amplification protocols in Figure 9. For SYBR green assays, melt curve analysis was performed following amplification to confirm the specificity of the assay. An example melt curve showing the presence of one PCR product is shown in Figure 10. All samples were assayed in duplicate.

Target	Det.	For	Rev
WISP-1	SYBR	GCATCCCCTACAAGTCTAAGAC	CAGGTTACAGAAGCAGGCATTA
ACTA2	PP	AAGCACAGAGCAAAAGAGGAAT	ATGTCGTCCCAGTTGGTGAT
Probe sequence		CTGACCCTGAAGTACCCGATAGAACATGGCATggtcag	
COL1A1	SYBR	AGACAGTGATTGAATACAAAACCA	GGAGTTTACAGGAAGCAGACA
COL3A1	SYBR	GTCCCGCTGGCATTCCTG	CTCTCCTTTGGCACCATTCTTAC
CTGF	SYBR	CCCAGACCCAACTATGATTAGAG	AGGCGTTGTCATTGGTAACC
UBC/A2	PP	Sequences not disclosed by supplier	
ZEB1	SYBR	TTTGATTGAACACATGCGATTACA	TCTTCAGTAGGAGTAGCGATGA
CDH1	SYBR	CATGAGTGTCCCCCGGTATC	CAGTATCAGCCGCTTTCAGA
IL-6	SYBR	CCTGAACCTTCCAAAGATGGC	TTCACCAGGCAAGTCTCCTCA
MMP2	SYBR	CATACAGGATCATTGGCTACAC	TCACATCGCTCCAGACTTG
MMP7	SYBR	TATTAAAGGCATTCAGAAACTATATGGA	GTGGAGGAACAGTGCTTATCAA
MMP9	SYBR	CTTCCAGTCAAGAGAGAAAGC	CAGGATGTCATAGGTCACGTAG
BMP2	SYBR	GGGCATCCTCTCCACAAAAG	CCACGTCACTGAAGTCCAC
Fn-1	SYBR	GAGAACCAAGACTGAGACGAT	GCTTCTGACATCTGGCTTGA

Table 9. List of primer sequences for gene expression detection by qPCR.

Reagent	Housekeeping genes	Gene of interest
Mastermix	12.5µl	5µl
Primers	1µl	0.5µl
Water	9µl	2µl
cDNA	2.5µl	2.5µl

Table 10. Volumes for qPCR reactions

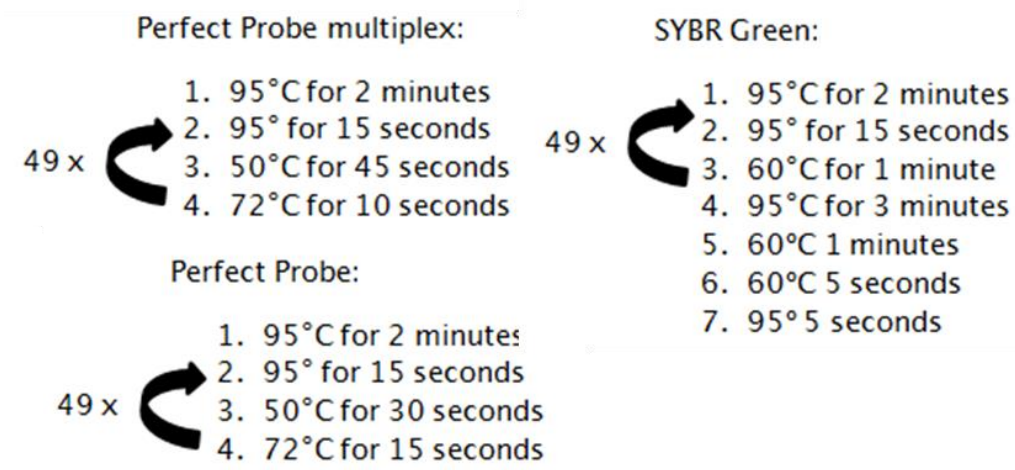

Figure 9. Cycling conditions for qPCR reactions

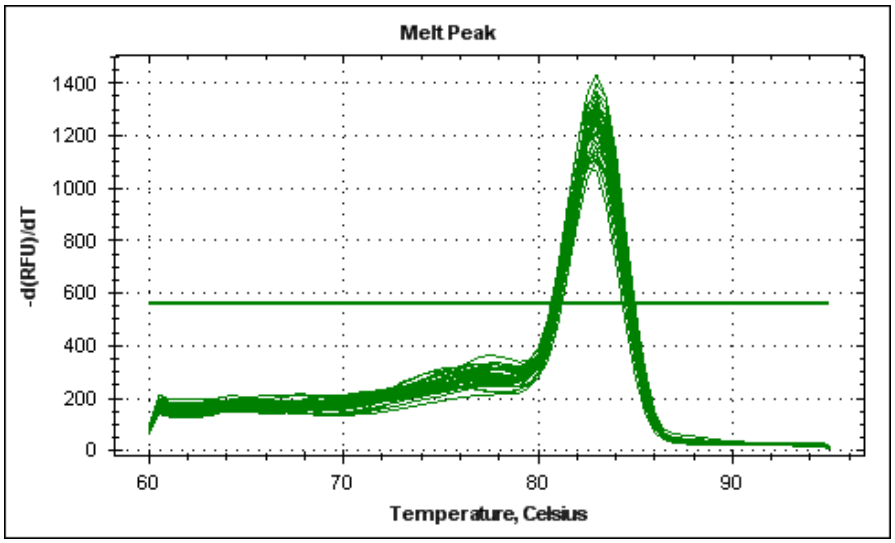

Figure 10. Example melt curve for overall WISP-1 primers

Data were analysed by the $2^{\Delta\Delta}$Ct method. Ct values for gene of interest were averaged and expressed relative to the geometric mean of two housekeeping genes (Ubiquitin C (UBC) and Phospholipase A2 (A2)). These values were then normalised to the expression of one sample as indicated in appropriate figure legends in chapter 3.

2.5.3 Splice variant analysis

Primers were designed to amplify individual splice variants of WISP-1 by qPCR. Sequences are listed in Table 11 and details of design can be found in chapter 4.

Target	For	Rev
FL-WISP-1	GTGTGTGCACAGGTGGTCGG	TATGTGAGGACGACGCCAAGA
WISP-1 v2	TGTGCACATGCTGTGGGTG	CCAATGTTAACGCCCAGTGC
WISP-1 v3	TGTGTGCACGCAGGGAAG	GTCCTGATGGGCTTGGCTT
WISP-1 v4	TGGCCACGGCAGGGAA	TCCTGATGGGCTTGGCTTCT

Table 11. List of primer sequences for splice variant analysis, all using SYBR detection. Purchased from Invitrogen.

2.6 WISP-1 overexpression

2.6.1 Subcloning

Plasmid containing full length WISP-1 DNA (in an unspecified vector) was provided by UCB. The WISP-1 insert was subcloned into the mammalian expression vector pcDNA3.1(+). First, the UCB plasmid was propagated via transformation of *E.coli*. Briefly, plasmid and competent cells (0.5μl plasmid per 25μl bacteria) were mixed then incubated on ice for 30 minutes before a heat shock step at 42˚C for 30 seconds, then placed back on ice for 3-4 minutes. Nutrient rich medium (SOC medium, 125μl per 25μl bacteria) was added and incubated at 37˚C for 10-15 minutes (for ampicillin resistant vectors) or 1 hour (for kanamycin resistant). Bacteria innoculant (100μl) was then spread across the surface of a pre-dried LB

agar plate containing either ampicillin or kanamycin (50μg/ml) and placed in a 37˚C incubator overnight.

The following day a single colony was picked from a kanamycin plate and placed in 10ml LB broth containing kanamycin (50μg/ml) at 37˚C, 100RPM for 7-8 hours. 1ml was then added to fresh LB broth (100ml) containing kanamycin (50μg/ml) and incubated in the same conditions overnight. Bacteria were pelleted by centrifugation at 4˚C, 6000g for 15 minutes) and plasmid purified using Qiagen Plasmid Maxi kit according to manufacturer's instructions. Briefly, pellets were resuspended in a buffer (P1, 10ml) containing Tris-Cl (50mM, pH 8), EDTA (10mM) and RNase A (10μg/ml) then lysed by the addition of lysis buffer (P2, 10ml) containing sodium hydroxide (200mM) and sodium dodecyl sulphate (1%, w/v). Lysis buffer was then neutralised by a pre-chilled buffer (P3, 10ml) containing potassium acetate (3M, pH 5.5) and centrifuged to separate supernatant containing DNA. Supernatant was passed through a QIAGEN-tip (anion-exchange resin) which was then washed twice with a medium salt wash (QC, 1M NaCl, 50mM MOPS (pH 7) 15% isopropanol (v/v)) before elution of DNA with a high salt buffer (QF, 1.25M NaCl, 50mM Tris-Cl (pH 8.5), 15% isopropanol (v/v)). DNA was then precipitated with isopropanol (0.7 volumes), washed with 100% ethanol (100μl) and air-dried before resuspension in a buffer containing Tris-Cl and EDTA (TE buffer, 100mM NaCl, 10mM Tris-Cl (pH 8), 1mM EDTA).

Following plasmid purification, UCB WISP-1 plasmid and expression vectors pcDNA3.1 (+) and (-) were cut with EcoRI and HindIII restriction enzymes. Restriction sites were provided by UCB however the orientation was unknown and so WISP-1 was to be subcloned into both pcDNA 3.1 (+) and (-). Mastermix was made up as shown in Table 12 and samples incubated at 37˚C for 3 hours. Samples were then run a 1.5% agarose gel alongside a 1000 base pair marker (10μl), bands cut out and DNA isolated as described above for splice variant analysis.

	Vol.
DNA	2µl
Buffer 2	5µl
BSA	5µl
HindIII	2µl
EcoRI	2µl
H_2O	34µl

Table 12. Volumes per reaction for restriction enzyme digest

	Vol.
Buffer	1µl
WISP-1 DNA	2µl
Vector	2µl
T4 ligase	0.5µl
H_2O	45µl

Table 13. Volumes per reaction for ligation

	Vol.
pcDNA 3.1 WISP-1	2µl
Buffer 2	2µl
BSA (10X)	2µl
HindIII	0.5µl
EcoRI	0.5µl
H_2o	13µl

Table 14. Reaction volumes for 20µl restriction enzyme digest

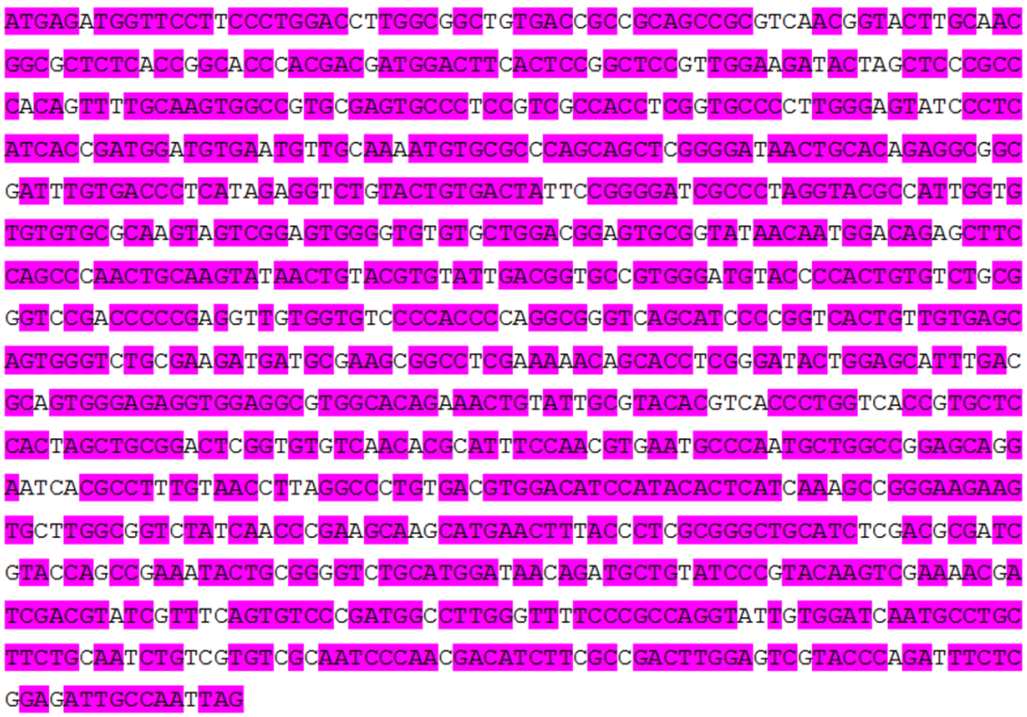

Figure 11. Synthetic UCB full length WISP-1 sequencing. Following its isolation and insertion in to pcDNA3.1, synthetic full length WISP-1 was sequenced to confirm identity and orientation. The pink highlighted sequence corresponds to where the synthetic sequence aligns with the full length WISP-1 reference sequence.

WISP-1 DNA and pcDNA3.1 vectors were ligated using a T4 ligase enzyme. Reaction as detailed in Table 13 were carried out overnight at 4˚C. Following ligation, *E.coli* were transformed as described above and cultured on ampicillin-containing agar plates overnight at 37˚C. Colonies were picked the next day and cultured in 6 well plates (in 3ml). DNA was then isolated from transformed bacteria using a Qiagen Plasmid Mini kit according to manufacturer's protocol. Following DNA purification, pcDNA3.1 WISP-1 was digested with EcoRI and HindIII at 37˚C for 1 hour to check for presence of WISP-1 insert as detailed in Table 14.

The WISP-1 insert was present in both pcDNA 3.1 (+) and (-) samples therefore bacteria transformed with both pcDNA3.1(+) WISP-1 and pcDNA3.1(-) WISP-1 were cultured as described above. DNA was purified using a Plasmid Maxi kit (as described above) and then DNA was then sent out to Source BioScience for sequencing using the Sanger method and the 5' primer listed in Table 15. Sequencing confirmed that the insert is full length WISP-1 that has been edited (to

optimise expression) (Figure 11) and that the appropriate orientation is in the expression vector pcDNA3.1(+). Figure 12 shows the translated sequence aligned with WISP-1 reference sequence.

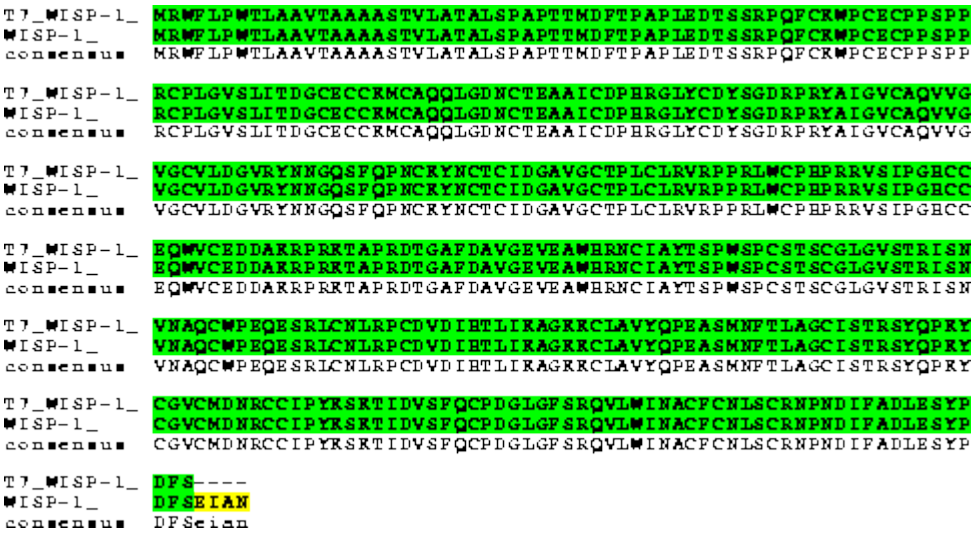

Figure 12. Translated synthetic WISP-1 sequence aligned with reference sequence.

2.6.1.1 Cloning of variants

WISP-1 variants 2, 3 and 4 were cloned from bronchial fibroblast cDNA by Dr David Smart following the protocol outlined above. WISP-1 variants were isolated following amplification with the primers listed in Table 15. Primer sequences for primers used to amplify WISP-1 variants designed to amplify all variants and cloned into pcDNA 3.1 (+). Alignment with the reference sequence for each variant is shown in Figure 13, Figure 14 and Figure 15.

Exons	Forward	Reverse	Company
1-5	ATGAGGTGGTTCCTGCCCTGGA	CAGAAATTGCCAACTAGGCAGG	Invitrogen

Table 15. Primer sequences for primers used to amplify WISP-1 variants. 5' primer lies at start of WISP-1 exon 1 and 3' at end of exon 5.

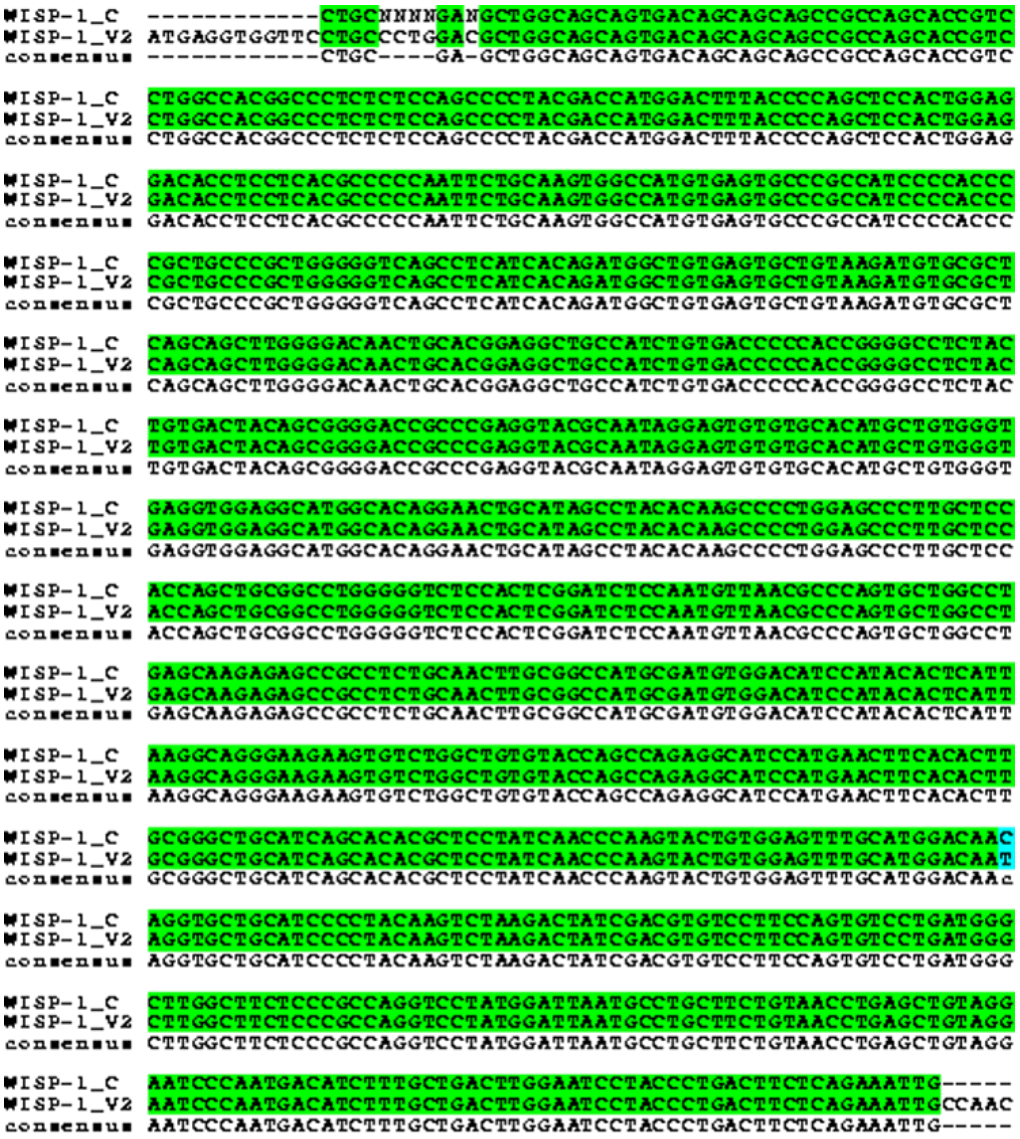

Figure 13. Cloned WISP-1 variant 2 sequence aligned with reference sequence.

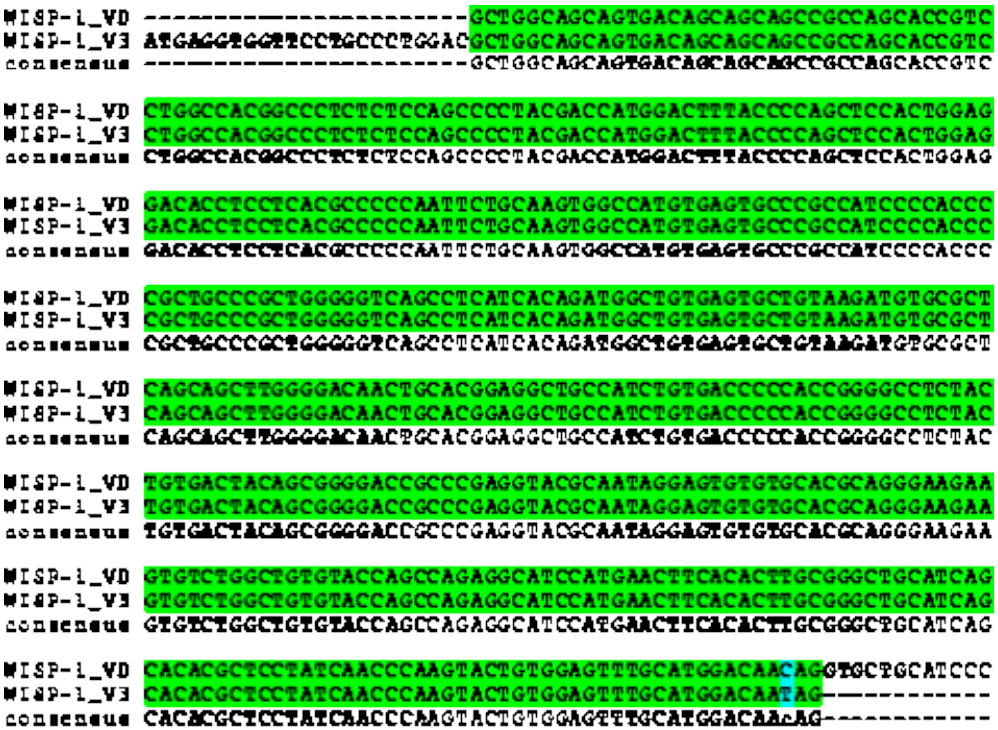

Figure 14. Cloned WISP-1 variant 3 sequence aligned with reference sequence.

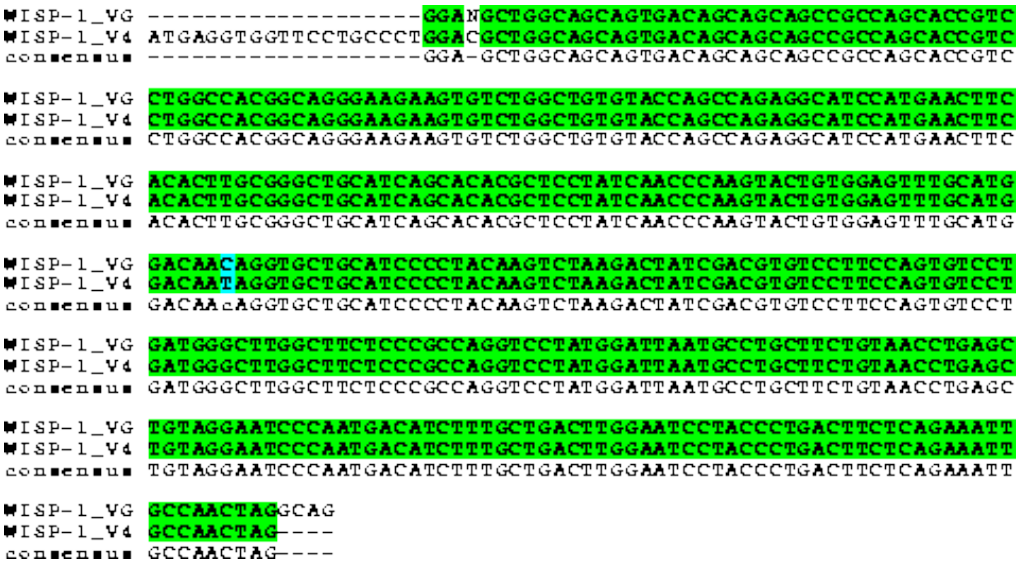

Figure 15. Cloned WISP-1 variant 4 sequence aligned with reference sequence.

2.6.2 Transfection

HEK293T cells were transiently transfected with WISP-1 constructs or empty vector for use in antibody characterisation and to generate conditioned medium. Transfection was carried out using Mirus TransIT-LT1 transfection reagent. Briefly, reagent:DNA complexes were prepared a as detailed in Table 16. These complexes were incubated at room temperature for 30 minutes before being added dropwise to cells. For use in antibody characterisation, cell lysates and supernatants were harvested 48 or 72 hours after transfection as indicated. For conditioned medium experiments, medium was replaced 24 hours after transfection then cell lysates and supernatants were harvested 48 hours later.

Reagent	Vol.
Complete growth medium	2.5ml
Serum-free medium	250µl
DNA (1µg/µl stock)	2.5µl
Trans IT-LT1 reagent	7.5µl

Table 16. Reagent:DNA complex volumes for transfection of cells seeded in 1 well of a six well plate.

Stable transfection

A549 cells were stably transfected with WISP-1 or empty vector to provide additional positive and negative control samples for antibody characterisation, and to provide a source of native WISP-1 protein to allow the study of its function. A549 cells were transfected as described for transient transfection above.

After 48 hours cells were trypsinised as described above and cells transferred to cell culture dishes. A day later cells were placed under high antibiotic selection with G418 at 600µg/ml for 1 week with medium changes every 2 days. Cells were then grown under lower antibiotic selection at 100µg/ml. Once colonies started to form in dishes containing WISP-1 transfected cells, they were marked on the underside of the dish. Wells were formed around individual colonies with cloning rings and vacuum grease to allow for the isolation of individual clones by

trypsinisation (as described above, 50μl per well). Clones were cultured initially in wells in a six well plate then transferred to T25 and T75 flasks as appropriate. Eight WISP-1 clones were isolated and cultured. The two expressing the highest levels of WISP-1 were used as controls for antibody characterisation.

Colonies were not selected for empty vector transfected cells. These were cultured initially under high antibiotic selection (600μg/ml G418 for a week) and then low selection (100μg/ml G418) in cell culture dishes then transferred to T25 and T75 flasks as appropriate.

2.7 Protein analysis

2.7.1 SDS-PAGE and western blotting

For antibody characterisation, recombinant human WISP-1 was added to sample buffer and boiled at 95˚C for 5 minutes in a heat block. Cell culture samples lysed in sample buffer were heated to 95˚C for 5 minutes then left to cool. A positive control of recombinant human WISP-1 in sample buffer (10ng in 20 μl) and a molecular weight marker (10μl) was run alongside all samples.

Supernatant samples were concentrated using strata clean resin where indicated. Strata clean was added 1 in 10 to sample (e.g. 10μl added to 100μl) then vortexed for 15 seconds. Samples were mixed by rotation for 30 minutes at 4˚C then centrifuged at 16000g for 5 minutes. Supernatant was removed and resin resuspended in sample buffer prior to boiling at 95˚C.

Samples were loaded into a 4% stacking gel (Table 19) and run on a 12.5% acrylamide gel (Table 18) in running buffer (Table 20) at 100V for approximately 90 minutes to separate proteins according to their size. Gels were then pre-soaked in transfer buffer (Table 22) before proteins were electrophoretically transferred to a polyvinylidene difluoride (PDVF) membrane at 90V for approximately 2 hours. PDVF membrane was pre-wet with methanol prior to use.

Non-specific binding sites on the membrane were blocked by incubation of the membrane with blocking buffer (5% milk in TBST, Table 21) at room temperature

for 1 hour. Membranes were then incubated overnight in primary antibody (in 5% milk in TBST) at concentrations listed in Table 23 at 4˚C. Following three 5 minute washes in TBST, membranes were incubated with an appropriate secondary HRP-conjugated antibody (in 1% milk in TBST) at room temperature for 1-2 hours (Table 23) and then washed three times in TBST. The protein of interest was then visualised on the membrane by incubating with enhanced chemiluminescent (ECL) substrate (1ml substrate per blot, ratio 1:1 of peroxide and enhancer) for 5 minutes at room temperature.

Sample buffer (5X)	
0.3.125M Tris-HCl pH 6.8	10.41ml; 1.5M
50% glycerol	25ml
25% 2-mercaptoethanol	12.5ml
10% SDS	5g
0.01% bromophenol blue	5mg
dH_2O	Make up to 50ml

Table 17. 5X sample buffer

Separating gel (12.5%) 10ml	
30% (w/v) acrylamide, 0.8% bis	4.2ml
1.5M Tris-HCl, pH8.8	2.5ml
dH_2O	3.2ml
10% (w/v) SDS	100µl
10% APS (0.1g APS/1ml H_2O)	50µl
TEMED	5µl

Table 18. 12.5 % separating polyacrylamide gel for protein separation by size

Stacking gel (4%) 5ml	
30% (w/v) acrylamide, 0.8% bis	0.5ml
0.5M Tris-HCl, pH8.8	1.25ml
dH_2O	3.05ml
10% (w/v) SDS	50µl
0.1% APS (0.1g APS/1ml H_2O)	25µl
TEMED	10µl

Table 19. 5ml 4% stacking gel

Running buffer (10X)	
0.025M Tris	15.5g
0.192M glycine	720g
0.1% (w/v) SDS	250ml 20% SDS
pH to 8.3 with HCl	
dH_2O	Make upto 5 litres

Table 20. 10X running buffer, diluted 1:10 with dH_2O before use

Tris buffered saline (TBS, 10X)	
Tris	24.2g
NaCl	80g
dH_2O	Make upto 1 litre
pH to 7.6 with HCl	
TBST	
1X TBS (1:10 in dH_2O)	1 litre
0.1% (v/v) Tween-20	1ml

Table 21. 10X TBS and TBST

Membranes were then exposed in the dark to autoradiography film for length of time indicated in appropriate figure legends. Film was then developed in developer solution (diluted 1:10 in dH_2O) and then placed in fixative solution (diluted 1:4 in dH_2O) for 1 minute before rinsing in water. Alternatively, membranes were exposed and imaged using a chemiluminescence imager.

Transfer buffer (10X)	
0.025 Tris	151.5g
0.192M glycine	720g
dH_2O	Make upto 5 litres
For 1X: 700ml dH_2O + 200ml methanol + 100ml 10X	

Table 22. Transfer buffer

Target	Source	Purification	Concentration	Company
WISP-1	Mouse monoclonal	Protein A or G purified	2μg/ml	R&D MAB16271
WISP-1	Goat polyclonal	Biotinylated; antigen affinity purified	0.1μg/ml	R&D BAF1627
WISP-1	Goat polyclonal	Antigen affinity purified	0.1μg/ml	R&D AF1627
WISP-1 C-terminal	Rabbit polyclonal	Immunogen affinity purified Sequence: ADLESYPDFSEIAN	0.1μg/ml	Abcam ab178547
Anti-goat (2°)	Rabbit Polyclonal	Immunoglobins, mainly IgG, isolated from goat serum	1 in 1000	DAKO P0449
Anti-rabbit (2°)	Swine Polyclonal	Immunoglobins, mainly IgG, isolated from rabbit serum	1 in 1000	DAKO P0217
Anti-mouse (2°)	Rabbit Polyclonal	Immunoglobins, mainly IgG, isolated from mouse serum	1 in 1000	DAKO P0260

Table 23. List of antibodies used for western blotting

2.7.2 Enzyme linked immunosorbent assay

WISP-1 levels in cell culture supernatants were determined by ELISA using a WISP-1 Duoset ELISA kit. All steps were carried out at room temperature. Flat bottom 96 well plates were coated with anti-WISP-1 capture antibody (MAB16271, 2μg/ml in PBS) overnight (100μl/well). Following washing (3x) in ELISA wash buffer (0.05% Tween-20 in PBS), plates were blocked for 1-2 hours with R&D reagent diluent (diluted 1:10 in H2O) and then washed again (3x). Cell culture supernatants (100μl/well) were added to wells in duplicate alongside recombinant WISP-1 standards (100μl/well). Standards were diluted 2-fold from 2000pg/ml to 31.25pg/ml in reagent diluent. A blank control of reagent diluent was also included. Plates were incubated for 2 hours, washed (3x), then incubated with biotinylated anti-WISP-1 antibody (50ng/ml in reagent diluent, BAF1627 listed in Table 23) for 2 hours (100μl/well). Streptavidin-HRP (diluted 1:200 in reagent diluent) was added to wells for 20 minutes (100μl/well) following washing (3x). Plates were then washed (3x) for a final time and then incubated with TMB (tetramethylbenzidine):H_2O_2 solution for approximately 20-30 minutes (100μl/well). The reaction was stopped by addition of 1M sulphuric acid once a colour difference between the lowest standard and blank control was observed (50μl/well).

As above for WISP-1, IL-6 levels in cell culture supernatants were measured using an R&D Duoset ELISA kit according to the manufacturer's protocol (DY206).

Absorbance was measured at 450nm using a plate reader. Absorbance at 570nm was subtracted to correct for the absorbance of the plastic plate. Blank O.D. values were subtracted from all standards and samples then a standard curve was generated from the known standards and used to determine the WISP-1 concentration in cell culture supernatant samples. An example standard curve generated is shown in Figure 16 alongside WISP-1 levels in WISP-1 transfected HEK293T cells demonstrating that this sample can be used as a positive control.

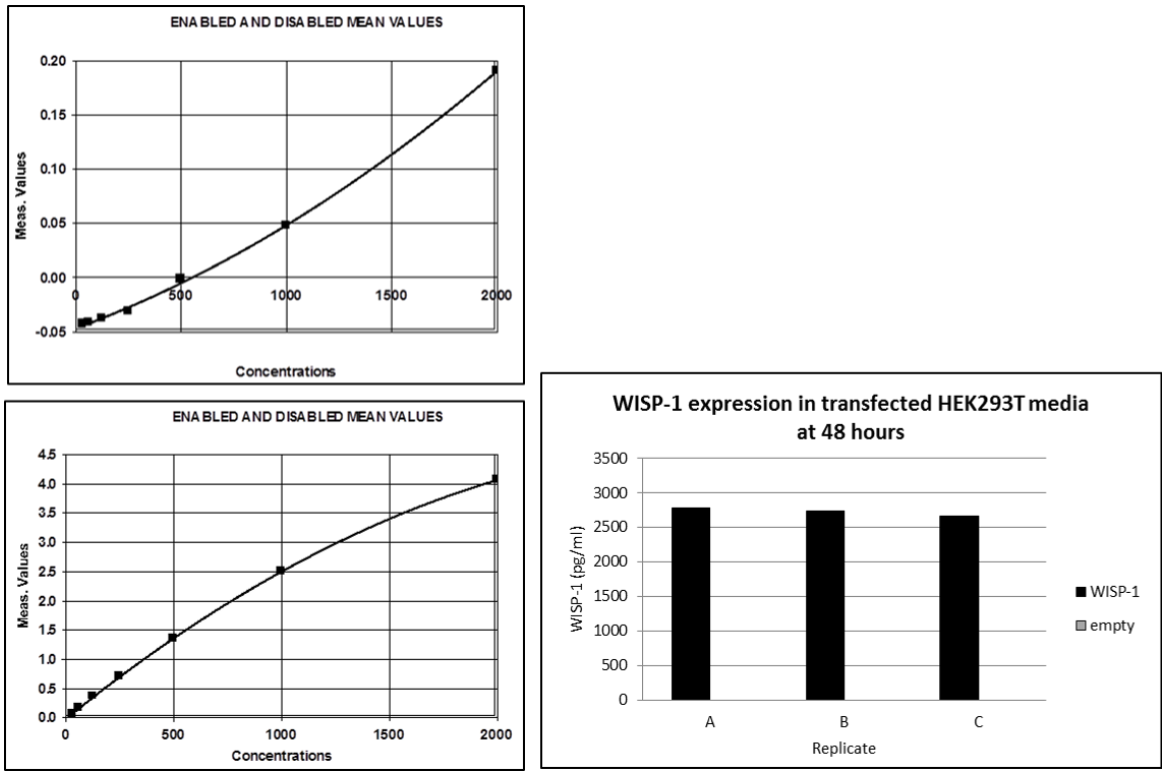

Figure 16. WISP-1 ELISA. An example of a WISP-1 ELISA standard curve using BSA in PBS (top) or R&D reagent as diluent (bottom), and WISP-1 levels detected in transiently transfected HEK293T cells (right).

2.8 Statistics

Normality testing was carried out in SigmaPlot 12.5 using the Shapiro-Wilk test to determine whether parametric or non-parametric statistical test should be used for analysis. Where requested by examiners, results from normality testing can be found in Appendix 2.

Tests of statistical significance were carried out in GraphPad Prism 6 where graphs were generated. Different statistical tests were carried out depending on the normality of the data set and the comparison being made as follows.

- For normally distributed data, multiple comparisons were carried out using either a one-way ANOVA (MRC5 data) or a two way ANOVA (with Bonferroni correction, A549 data). The difference in one variable between two groups was measured using a two-tailed t-test (IPF v healthy).

- For data not normally distributed, various non-parametric statistical tests were carried out to perform multiple comparisons:
    - Wilcoxon test was used to determine statistical difference between two paired groups of data
    - Mann Whitney test was used to determine statistical difference between two non-paired groups of data
    - Friedman test was used to determine statistical difference between multiple paired groups of data

Number of experiments, n, is indicated in the figure legend for each graph.

- For cell line data n=3 is 3 separate experiments.
- For primary fibroblast data n=3 is 3 separate experiments, each using a different donor.

Chapter 3: Characterisation of WISP-1 expression in pulmonary fibroblasts and epithelial cells

3.1 Introduction

Altered expression of Wnt1-inducible signalling protein-1 (WISP-1) has been reported in various studies focusing on the pathogenesis of different lung diseases. In an asthma study by Sharma et al. (200), a single nucleotide polymorphism in the WISP-1 gene was associated with lower FEV_1 and reduced FVC in asthmatic children. The authors also reported differential WISP-1 gene expression between two different stages of human fetal lung development, pseudoglandular and canalicular.

Upregulated WISP-1 mRNA expression was reported in 83% of non-small cell lung cancer samples compared to matched normal tissues (201). Immunohistochemical staining of these tissues showed that WISP-1 protein was also increased in the cancer tissue and suggested that WISP-1 was expressed in the cytoplasm of epithelial cells in the tumour samples.

Zemans et al. (202) reported increased WISP-1 expression in a human lung epithelial cell line following neutrophil transmigration or stimulation with neutrophil elastase. In the same study, increased WISP-1 expression was detected in whole lung extracts (mRNA) and bronchoalveolar lavage (BAL) fluid in a murine model of acute lung injury.

In studies focusing on the pathogenesis of IPF, increased WISP-1 expression has been reported in more than one cohort. Selman et al. (2006) observed upregulated WISP-1 mRNA expression in whole lung tissue from IPF donors compared to tissue from donors with the related ILD hypersensitivity pneumonitis (HP) (48).

In a bleomycin mouse model of pulmonary fibrosis, increased expression of WISP-1 mRNA and protein was reported in bleomycin-treated mice compared to saline-

treated (124). This was also observed in ATII cells isolated from these mice. The authors reported that this was not the case in fibroblasts isolated from these mice. This same study also looked at WISP-1expression in human IPF. Increased levels of WISP-1 mRNA were detected in total lung homogenates from IPF patients compared to controls as well increased WISP-1 mRNA expression in ATII cells isolated from IPF lung tissue. No differential expression of WISP-1 mRNA between IPF and control fibroblasts was observed in the small number of donors tested. WISP-1 expression in IPF tissue was also compared with that in samples from donors with the related ILD non-specific interstitial pneumonia (NSIP) and with chronic obstructive pulmonary disease (COPD), and was found to be upregulated in IPF only.

An important consideration when investigating fibrosis is the phenotype of the cells being studied. The differentiation of fibroblasts towards a myofibroblast phenotype is a process known to occur in IPF (203) and the induction of this process by the pro-fibrotic cytokine TGFβ_1 has been well established (87, 92, 93). The ability of TGFβ_1 to stimulate epithelial to mesenchymal transition is also well established (68, 70, 72, 96, 97, 204). The aforementioned literature relates to WISP-1 expression in unstimulated fibroblasts. Considering the pro-fibrotic environment in the IPF lung, it may be pertinent to investigate the expression of WISP-1 in fibroblasts and epithelial cells following their stimulation with TGFβ_1. The relationship between WISP-1 and pro-inflammatory cytokines such as TNFα is also of interest. The role of inflammation in the pathogenesis of IPF remains unclear. However, increased expression of several pro-inflammatory cytokines has been reported in the IPF lung (34, 205, 206) and increased expression of WISP-1 in fibroblasts following pro-inflammatory stimulation has also been reported (193, 194).

Hypotheses and objectives

Various observations indicate that WISP-1 expression may be dysregulated in lung disease. In IPF, it has been proposed that increased WISP-1 expression by alveolar epithelial cells contributes to disease progression by acting in both an autocrine and paracrine manner. However, the exact of contribution of different cell types

to the increased level of WISP-1 observed in the IPF lung is unknown. Considering that WISP-1 is thought to act extracellularly, its increased expression in the fibrotic lung could be due to increased expression by either fibroblasts or epithelial cells, or both cell types however this has not been extensively investigated in the literature. The influence of pro-fibrotic and pro-inflammatory stimuli on WISP-1 expression in the fibrotic lung also remains unclear. Therefore the hypotheses for this study are as follows:

1) Expression of WISP-1 is greater in fibroblasts derived from IPF compared to healthy donors.
2) Induction of a myofibroblast phenotype in lung fibroblasts will correlate with increased WISP-1 expression.
3) TNFα will stimulate increased WISP1 expression in lung fibroblasts.
4) Induction of epithelial to mesenchymal transition in A549 epithelial cells will correlate with increased WISP-1 expression

The following objectives will be completed in order to test the above hypotheses:

1) To optimise conditions for measurement of WISP-1 mRNA in MRC5 cells at baseline, after induction of a myofibroblast phenotype with $TGF\beta_1$ or after treatment with TNFα
2) To measure WISP1 mRNA expression in primary parenchymal fibroblasts from IPF and control donors, both unstimulated and when stimulated with $TGF\beta_1$ or TNFα
3) To measure WISP-1 expression in A549 cells following induction of EMT by $TGF\beta_1$ and TNFα
4) To measure WISP-1 protein expression in primary parenchymal fibroblast and A549 cell lysates and supernatants

3.2 Results

3.2.1 WISP-1 mRNA expression in MRC5 fibroblasts

In order to investigate WISP-1 mRNA expression in fibroblasts, cells were cultured under various different conditions and WISP-1 mRNA levels were measured by qPCR. Initial pilot experiments were carried out using the fetal human lung fibroblast cell line MRC5 to determine appropriate conditions for future experiments.

WISP-1 mRNA expression was measured in MRC5 cells over time in both 0.5% FBS containing medium and 10% FBS containing medium. As Figure 17 shows, WISP-1 mRNA increased over time up to 72 hours in both levels of FBS. WISP-1 expression was lower overall in 10% FBS medium suggesting that a factor present in FBS may be suppressing the expression of WISP-1 in these cells. In the same experiment, WISP-1 mRNA expression was measured following TGFβ_1 treatment in order to test the hypothesis that WISP-1 mRNA expression increases with induction of a myofibroblast phenotype. MRC5 cells were treated ± TGFβ_1 in 0.5% FBS medium for up to 96 hours.

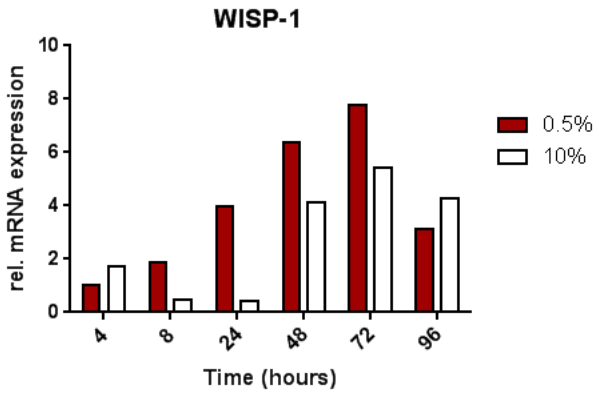

Figure 17. WISP-1 mRNA expression in MRC5 cells over time. MRC5 cells were grown to 70% confluence before medium was replaced with 0.5% (red bars) or 10% (white bars) FBS medium. Medium was replaced again after 24 hours (t0) and cells harvested in trizol for RNA extraction at indicated time points. mRNA expression was measured by qRT-PCR. Data are expressed relative to 0.5% FBS medium at 4 hours. n=1.

Expression of α-SMA was used as a marker to indicate differentiation towards a myofibroblast phenotype as reported in the literature (207). α-SMA was induced by TGFβ$_1$ at 48, 72 and 96 hours (Figure 18, top left). Induction of collagen 3 (COL3A1, top right) and connective tissue growth factor (CTGF, bottom left) also confirmed that the cells responded to TGFβ$_1$. TGFβ$_1$ treated cells showed reduced WISP-1 mRNA expression compared to untreated at 8, 24, 48 and 72 hours (bottom right) suggesting that TGFβ$_1$ suppresses WISP-1 mRNA expression in these cells.

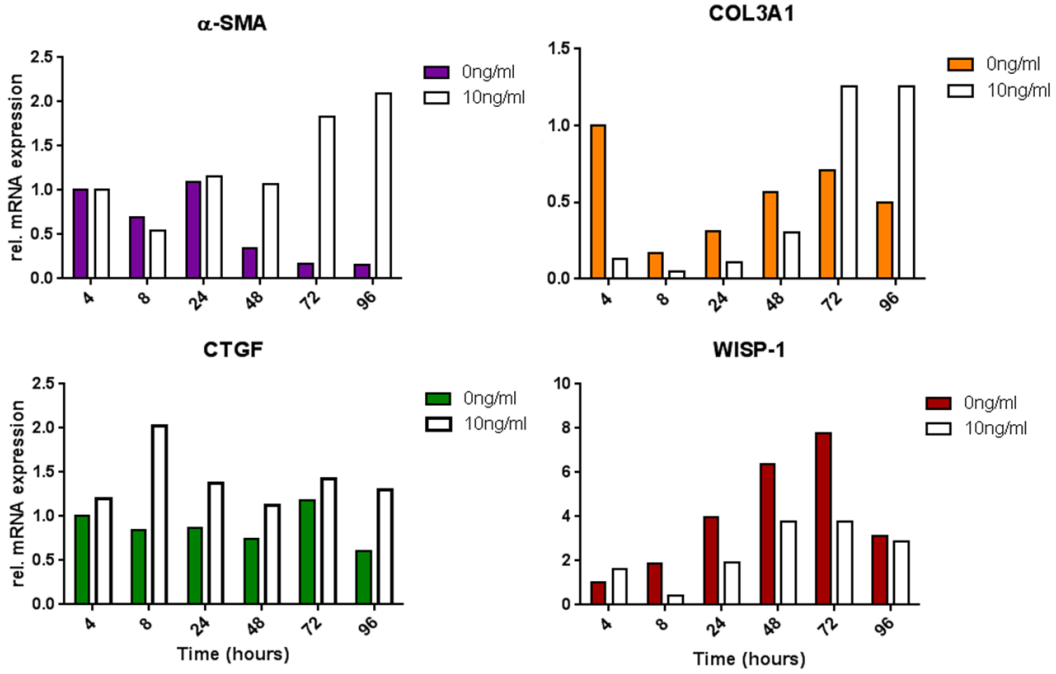

Figure 18. The effect of TGFβ$_1$ treatment on α-SMA, COL3A1, CTGF and WISP-1 mRNA expression in MRC5 cells over time. MRC5 cells were grown to 70% confluence before medium was replaced with 0.5% FBS medium for 24 hours. Cells were then treated ± 10ng/ml TGFβ$_1$ and harvested in trizol for RNA extraction at indicated time points. mRNA expression was measured by qRT-PCR. Data are expressed relative to untreated sample at 4 hours. n=1.

Based on previous studies, 10ng/ml is a higher dose than usually required for TGFβ$_1$ to exert a pro-fibrotic effect (207). MRC5 cells were therefore treated with different doses of TGFβ$_1$ to see whether a lower dose would stimulate WISP-1

expression as hypothesised. A time point of 48 hours was selected for this experiment based on the timecourse data showing an effect of TGFβ$_1$ on both α-SMA and WISP-1 mRNA expression at 48 hours (Figure 18). TGFβ$_1$ induced α-SMA expression at a dose of 2.5, 5 and 10ng/ml (Figure 19, left panel). This was significant at 5ng/ml (p=≤0.01) with a mean induction of approximately 40 times that of untreated MRC5 cells. As seen in the previous experiment, WISP-1 mRNA was suppressed by TGFβ$_1$ treatment (Figure 19, right panel). This was statistically significant at all doses (p=≤0.01) with WISP-1 levels reduced to approximately 25% that of unstimulated cells at 5ng/ml. In summary, WISP-1 mRNA expression was not induced by stimulation with the pro-fibrotic cytokine TGFβ$_1$ in MRC5 cells, contrary to the hypothesis for this study.

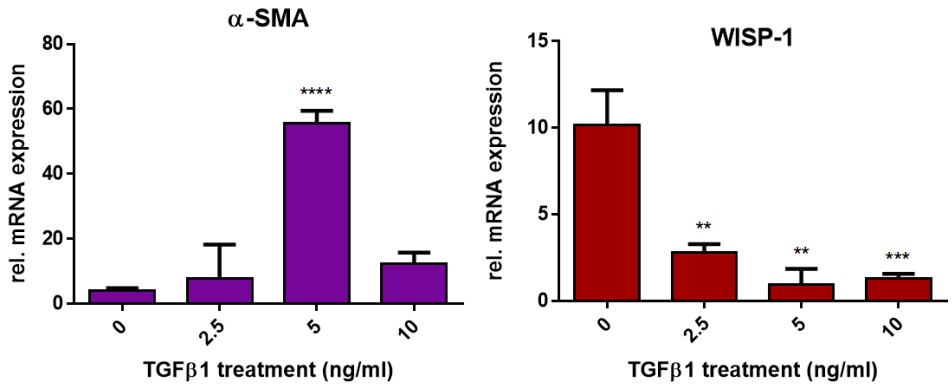

Figure 19. α-SMA and WISP-1 mRNA expression in MRC5 cells following TGFβ$_1$ treatment. MRC5 cells were grown to 70% confluence before medium was replaced with 0.5% FBS medium for 24 hours. Cells were then treated with indicated dose of TGFβ$_1$ and harvested in trizol for RNA extraction after 48 hours. mRNA expression was measured by qRT-PCR. Data are expressed relative to the untreated sample and are presented as mean ± SD. n=5. Statistical significance was tested using one way ANOVA with Bonferroni correction. *p=≤0.05, **p=≤0.01, ***p=≤0.001, p=≤0.0001 compared to untreated.

The effect of pro-inflammatory cytokines on WISP-1 expression was investigated as such stimuli have been reported to stimulate WISP-1 expression in fibroblasts (193). MRC5 cells were treated with the pro-inflammatory cytokines TNFα, IL-1β,

IL-13 and IL-4 and WISP-1 mRNA expression was measured. As Figure 20 (left panel) shows, WISP-1 mRNA was induced by approximately 2.5-fold by TNFα treatment (p=≤0.05). A small increase in WISP-1 mRNA expression was observed with IL-1β treatment also. Stimulation with the Th2 cytokines IL-13 and IL-4 did not alter WISP-1 mRNA expression in this study.

To investigate whether the TNFα/IL-1β-stimulated expression of WISP-1 could be abrogated by $TGF\beta_1$, cells were treated either with TNFα or IL-1β alone (10ng/ml), or in combination with $TGF\beta_1$ at a dose of 5ng/ml. This dose was selected because 5ng/ml $TGF\beta_1$ produced the biggest induction of α-SMA and suppression of WISP-1 mRNA in an earlier experiment (Figure 19). As Figure 20 (right panel) shows, co-treatment of MRC5 cells with TNFα or IL-1β with $TGF\beta_1$ abrogated the induction of WISP-1 mRNA by TNFα by approximately 75% (p=≤0.01), and by IL-1β by approximately 50% (p=≤0.05).

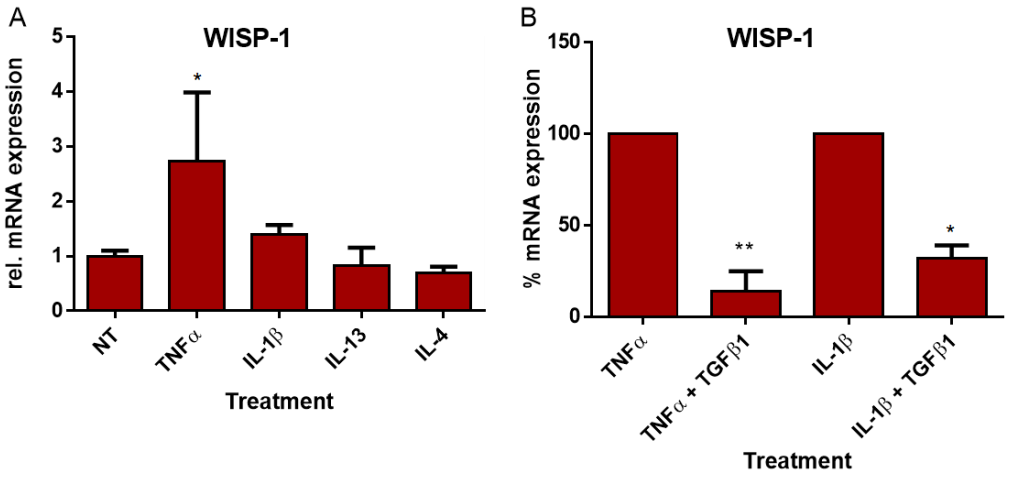

Figure 20. The effect of pro-inflammatory cytokine treatment on WISP-1 expression in MRC5 cells. MRC5 cells were grown to 70% confluence before medium was replaced with 0.5% FBS medium for 24 hours. Following 72 hour treatment with indicated cytokine(s) at a dose of 10ng/ml (except $TGF\beta_1$ at 5ng/ml), cells were harvested in trizol for RNA extraction and mRNA expression measured by RT-qPCR. (A) Data are expressed relative to untreated sample, n=3. (B) Data are expressed as a percentage of TNFα or IL-1β treatment alone, n=3, mean ± SD. Statistical significance was tested by one way ANOVA (A) or two-tailed t-test (B), *p=≤0.05, **p=≤0.01.

3.2.2 WISP-1 mRNA expression in primary parenchymal fibroblasts

Experiments were carried out in MRC5 cells to determine optimal conditions for the measurement of WISP-1 expression. However, based on the results obtained, it was decided that different conditions would also be tested in primary parenchymal fibroblasts in order to fully characterise that expression of WISP-1 in these cells. Data in this section of the thesis are presented as box plots to show the variability of the data.

In order to test the hypothesis that expression of WISP-1 mRNA is greater in IPF fibroblasts compared to control fibroblasts, WISP-1 mRNA expression was measured in untreated fibroblasts at 48 and 72 hours. As the top panel in Figure 21 shows, expression of WISP-1 mRNA showed greater variation between IPF (red) compared to control fibroblasts (white) at both 48 and 72 hours. WISP-1 mRNA expression was higher in IPF fibroblasts as hypothesised, and this was statistically significant at 72 hours ($p=\leq 0.05$).

As with MRC5 cells, the effect of the pro-fibrotic cytokine $TGF\beta_1$ on mRNA expression was also investigated in primary parenchymal fibroblasts. First, the induction of a myofibroblast phenotype in these cells by $TGF\beta_1$ was measured over time. IPF and control fibroblasts were treated ± $TGF\beta_1$ (10ng/ml) for 24, 48, 72 or 96 hours in 0.5% FBS or 10% FBS containing medium, and α-SMA and WISP-1 mRNA levels were measured (Figure 22).

IPF fibroblasts were stimulated by $TGF\beta_1$ to differentiate towards a myofibroblast phenotype, demonstrated by the induction of α-SMA (Figure 22, top panel) seen at 24, 48, 72, and 96 hours in 0.5% FBS medium (top left), which was statistically significant at 48 hours ($p=\leq 0.05$). In 10% FBS medium α-SMA expression was significantly induced at 48, 72 and 96 hours compared to t0 ($p=\leq 0.05$) (top right). As with IPF fibroblasts, α-SMA mRNA expression was induced by $TGF\beta_1$ at 24, 48, 72 and 96 hours in both 0.5% FBS and 10% FBS medium in control donor derived fibroblasts but only reached significance at 96hrs in 0.5% FBS medium ($p=\leq 0.05$) and 48hrs in 10% FBS medium ($p=\leq 0.01$) (Figure 22, bottom panel).

As observed with MRC5 cells, WISP-1 mRNA was not induced by $TGF\beta_1$ in IPF fibroblasts (Figure 23, top panel). In both 0.5% FBS (left) and 10% FBS medium (right), WISP-1 mRNA increased over time. This was statistically significant at 72

hours (p=≤0.05) in 0.5% FBS medium, and at 72 (p=≤0.05) and 96 (p=≤0.01) hours in 10% FBS medium. Levels of WISP-1 were lower at 48 and 72 hours in TGFβ_1-treated fibroblasts compared with untreated in 0.5% FBS medium, and at 24, 72 and 96 hours in 10% FBS medium however this was not statistically significant. WISP-1 expression overall was lower in control fibroblasts than in IPF fibroblasts (Figure 22, bottom panel).

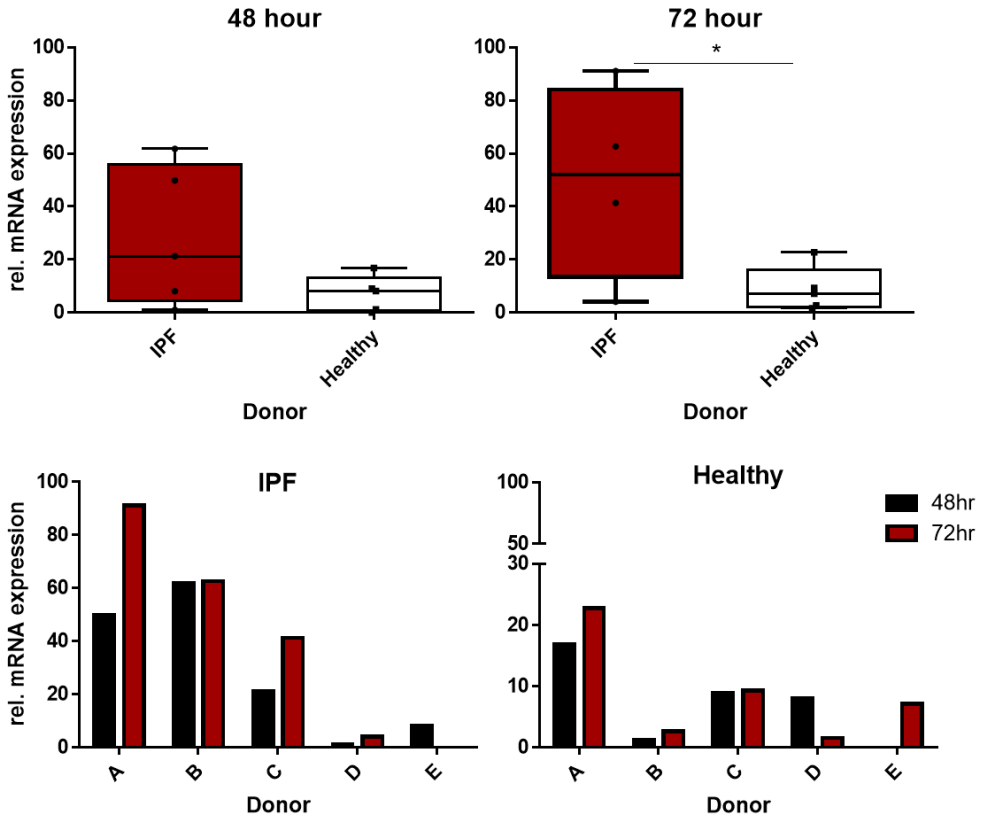

Figure 21. WISP-1 expression in primary parenchymal fibroblasts at 48 and 72 hours. Fibroblasts from IPF and control donors were grown to 70% confluence before medium was replaced with 0.5% FBS medium for 24 hours. Medium was replaced again and cells were harvested after 48 or 72 hours in trizol for RNA extraction. WISP-1 expression was measured by RT-qPCR and data are expressed relative to the lowest expressing IPF donor at each time point, n=5 IPF donors, n=5 control donors. Statistical significance was tested using two-tailed t-test. *p=≤0.05. Normality testing for these samples is shown in Appendix 2.

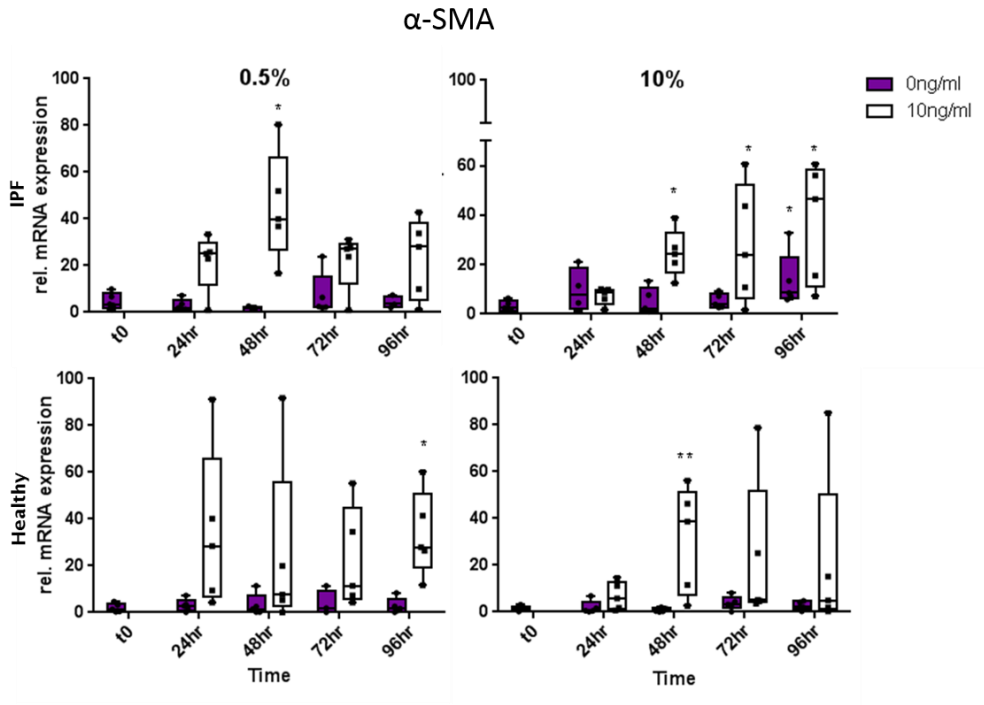

Figure 22. The effect of TGFβ$_1$ treatment on α-SMA expression in IPF and control fibroblasts over time. IPF and control fibroblasts were grown to 70% confluence then medium was replaced with 0.5% FBS or 10% FBS containing medium for 24 hours. Cells were treated ± 10ng/ml TGFβ$_1$ for indicated length of time and cells were harvested in trizol for RNA extraction. α-SMA expression was measured by qRT-PCR. Data are expressed relative to the lowest expressing donor at t0 in 0.5% FBS medium. n=4 IPF donors, 4 control donors. Wilcoxon statistical test was used to measure statistical difference between ± TGFβ$_1$ and 0.5%/10% FBS at each time point. Friedman statistical test was used to measure statistical difference between t0 and other timepoints. *p=≤0.05, **p=≤0.01 compared to t0.

Dose response experiments were also carried out in IPF and control fibroblasts to determine whether a lower dose of TGFβ$_1$ would stimulate WISP-1 expression and whether a higher dose would substantially suppress WISP-1 expression. Figure 24 shows the mRNA expression level of α-SMA (left panel) and WISP-1 (right panel) following 48 hour treatment of primary fibroblasts with indicated doses of TGFβ$_1$.

In IPF fibroblasts, a dose-dependent increase in α-SMA expression was seen in 0.5% FBS medium (purple bars, top panel). In 10% FBS medium (white bars), α-SMA mRNA expression was induced from 2.5ng/ml. At 5ng/ml, α-SMA was induced

significantly by TGFβ$_1$ compared to no treatment in both serum conditions (p=≤0.05). In control fibroblasts (Figure 24, bottom panel), TGFβ$_1$ induced α-SMA expression from 2.5ng/ml (left). This was significant in 0.5% FBS medium at 10 and 25ng/ml, and in 10% FBS medium at 2.5 and 5ng/ml (p=≤0.01). α-SMA levels were lower in control fibroblasts compared with IPF donor derived cells overall, and this was statistically significant in unstimulated cells (top panel).

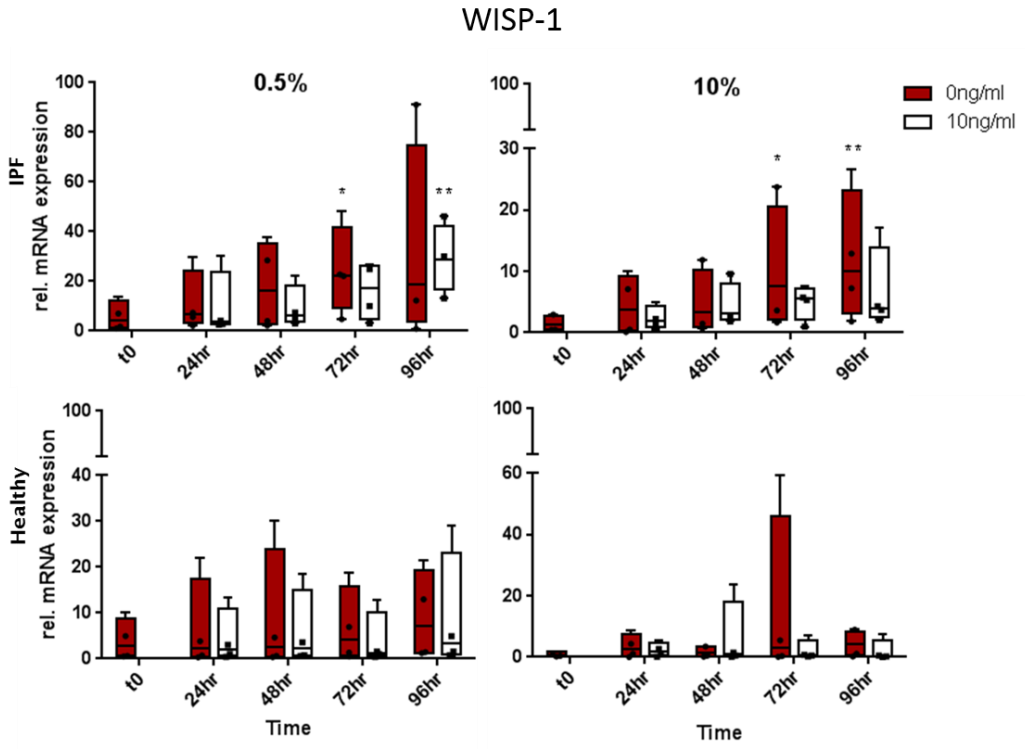

Figure 23. The effect of TGFβ$_1$ treatment on WISP-1 expression in IPF and control fibroblasts over time. IPF and control fibroblasts were grown to 70% confluence then medium was replaced with 0.5% FBS or 10% FBS containing medium for 24 hours. Cells were treated ± 10ng/ml TGFβ$_1$ for indicated length of time and cells were harvested in trizol for RNA extraction. WISP-1 expression was measured by qRT-PCR. Data are expressed relative to the lowest expressing donor at t0 in 0.5% FBS medium. n=4 IPF donors, 4 control donors. Wilcoxon statistical test was used to measure statistical difference between ± TGFβ$_1$ and 0.5%/10% FBS at each time point. Friedman statistical test was used to measure statistical difference between t0 and other timepoints. *p=≤0.05, **p=≤0.01 compared to t0

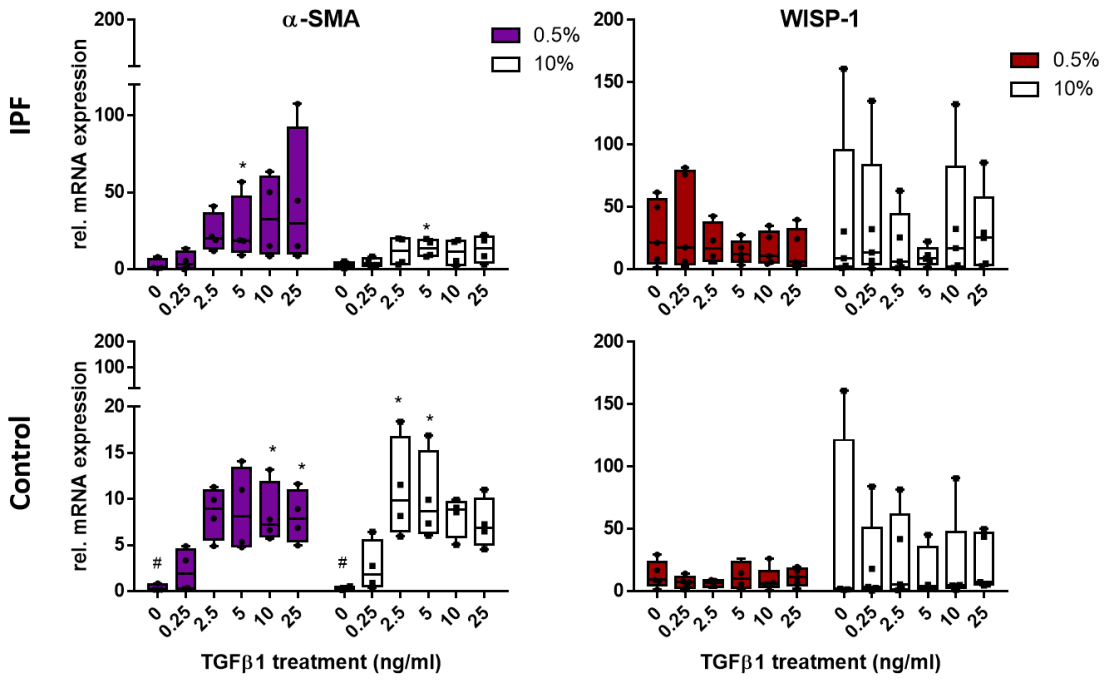

Figure 24. α-SMA and WISP-1 expression in IPF and control fibroblasts following $TGF\beta_1$ treatment. IPF (top) and control (bottom) fibroblasts were grown to 70% confluence then medium was replaced with 0.5% or 10% FBS medium for 24 hours. Cells were treated with indicated dose of $TGF\beta_1$ for 48 hours. Cells were harvested in trizol for RNA extraction and mRNA expression was measured by qRT-PCR. Data are expressed relative to the expression in the lowest-expressing untreated donor in 0.5% FBS medium. n=5 IPF donors, 5 control donors. Friedman statistical test was used to determine statistical difference between untreated and treated samples. Mann Whitney test was used to determine statistical difference between IPF and control donors at each dose. *p=≤0.05 dose compared to untreated in same medium.

WISP-1 mRNA expression showed variation between experiments/donors in both 0.5% FBS and 10% FBS medium in both IPF and control donor derived fibroblasts. There was a trend for $TGF\beta_1$ suppression of WISP-1 up to 5ng/ml of $TGF\beta_1$ in IPF fibroblasts. At higher doses, levels were similar to that of untreated cells, particularly in 10% FBS medium. To try and determine whether the variability observed was due to experimental differences or differences in expression between donors, this experiment was repeated in one IPF and one control donor. Figure 25 shows the WISP-1 mRNA expression in these cells in both experiments.

The pattern of expression was similar in both experiments for the IPF and control donor suggesting that the variability observed may due to inter-donor variation.

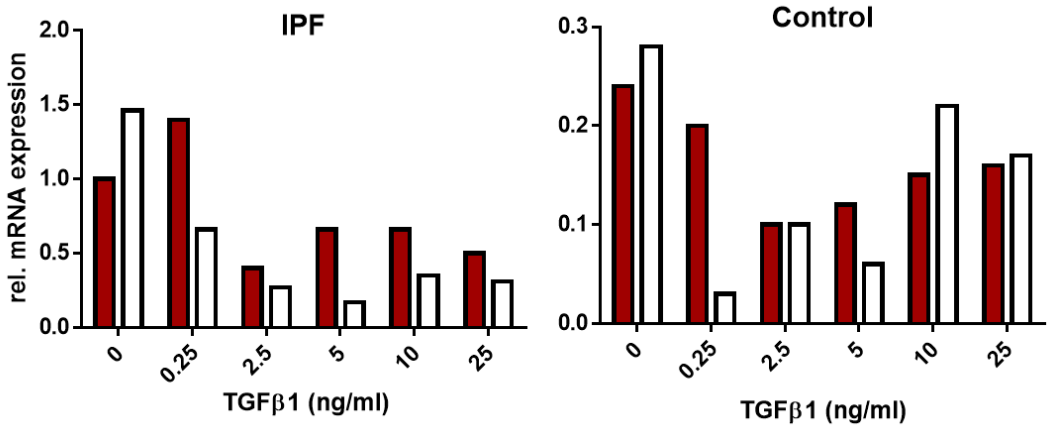

Figure 25. WISP-1 expression in IPF and control fibroblasts following $TGF\beta_1$ treatment. Fibroblasts from one IPF and one control donor were grown to 70% confluence then medium was replaced with 0.5% medium for 24 hours. Cells were treated with indicated dose of $TGF\beta_1$ for 48 hours. Cells were harvested in trizol for RNA extraction and mRNA expression was measured by qRT-PCR. Experiment was repeated with same two donors. Experiment one – red bars, experiment 2 – white bars. Data are expressed relative to the expression in the IPF donor from experiment 1.

Figure 26 shows the WISP-1 mRNA expression of individual donors in the same experiment. IPF donors A and B responded to $TGF\beta_1$ similarly in terms of WISP-1 mRNA expression with suppression observed in 0.5% FBS medium (panel A and B). Donor C fibroblasts expressed less WISP-1 mRNA than A and B when untreated, and WISP-1 expression was suppressed by $TGF\beta_1$ in a dose-dependent manner in 0.5% FBS medium in this donor (panel C). WISP-1 expression was induced by $TGF\beta_1$ in donor C in 10% FBS medium (panel H). Fibroblasts from IPF donor D expressed the lowest amount of WISP-1 mRNA when untreated (panels D and I). These fibroblasts were also the only IPF donor to exhibit a dose-dependent increase of WISP-1 mRNA expression following stimulation with $TGF\beta_1$. Donor E showed a different expression pattern with WISP-1 transcription stimulated by a

mid-dose of TGFβ_1 (5ng/ml) and suppressed by higher doses in 0.5% FBS medium (panel E).

Overall the WISP-1 expression by control parenchymal fibroblasts was lower than in IPF fibroblasts in 0.5% FBS medium (Figure 26). As with the IPF donors, there was variability in response to TGFβ_1 treatment. WISP-1 mRNA expression in control donors A AND peaked at a dose of 10ng/ml in 0.5% FBS medium (panels K and L). In 10% FBS medium, WISP-1 expression decreased in control donor A (panel P) and increased in donor B (panel Q). Donor C showed some increase in levels of WISP-1 following treatment in 10% FBS containing medium (panel R). Donors D and E both expressed variable levels of WISP-1 in both 0.5% FBS and 10% FBS containing medium (panels N, O, S and T).

Figure 26. The effect of TGFβ_1 on WISP-1 expression in individual fibroblast donors. Fibroblasts were grown to 70% confluence then medium was replaced with medium containing either 0.5% FBS or 10% FBS for 24 hours. Cells were treated with indicated dose of TGFβ_1 for 48 hours then harvested in trizol for RNA extraction. mRNA expression was measured by qRT-PCR. Each graph shows the expression of one donor and data are expressed relative to the expression of one donor when untreated: IPF = donor D, control = donor L

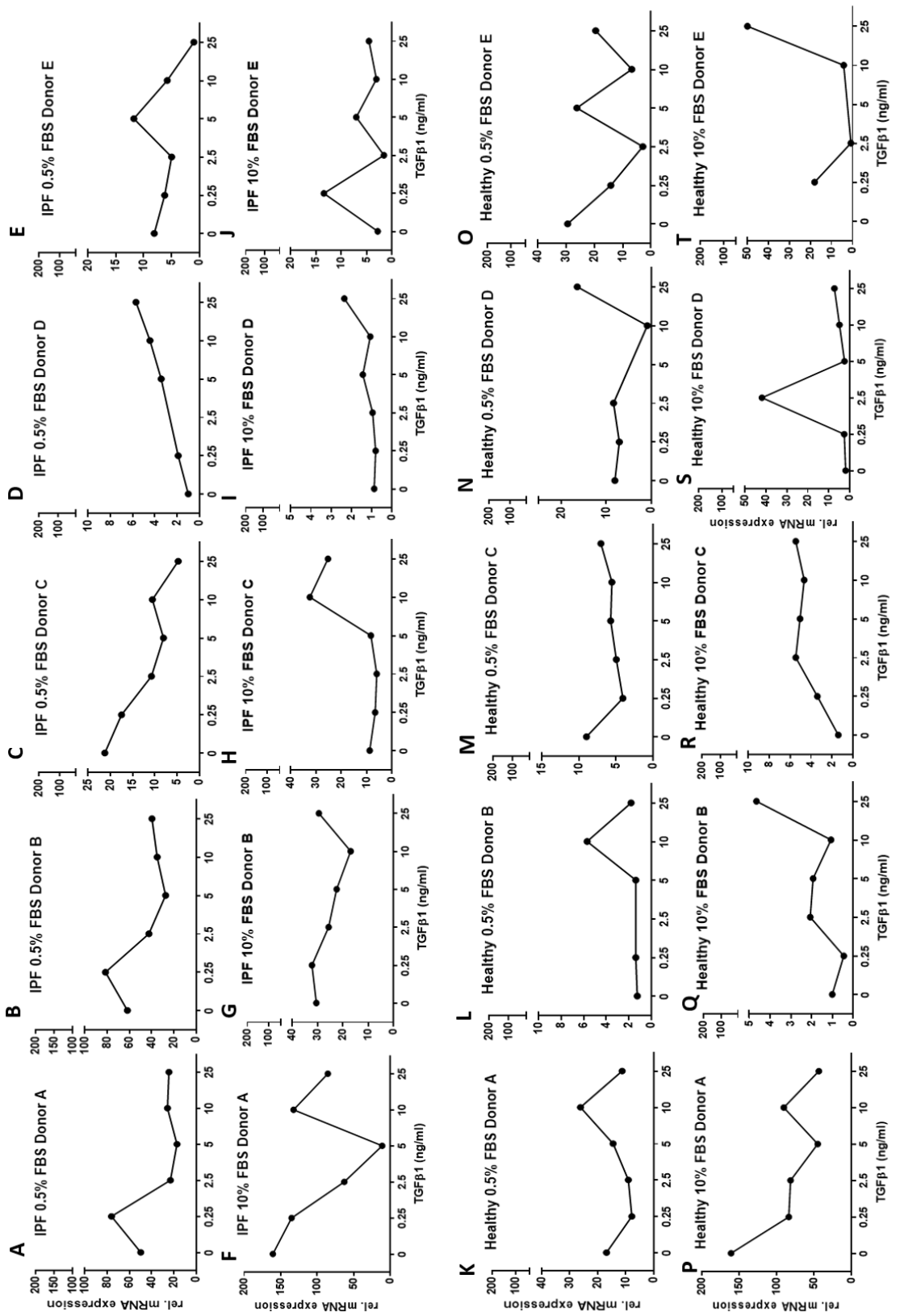
A
IPF 0.5% FBS Donor A
B
IPF 0.5% FBS Donor B
C
IPF 0.5% FBS Donor C
D
IPF 0.5% FBS Donor D
E
IPF 0.5% FBS Donor E
F
IPF 10% FBS Donor A
G
IPF 10% FBS Donor B
H
IPF 10% FBS Donor C
I
IPF 10% FBS Donor D
J
IPF 10% FBS Donor E
K
Healthy 0.5% FBS Donor A
L
Healthy 0.5% FBS Donor B
M
Healthy 0.5% FBS Donor C
N
Healthy 0.5% FBS Donor D
O
Healthy 0.5% FBS Donor E
P
Healthy 10% FBS Donor A
Q
Healthy 10% FBS Donor B
R
Healthy 10% FBS Donor C
S
Healthy 10% FBS Donor D
T
Healthy 10% FBS Donor E
rel. mRNA expression
TGFβ1 (ng/ml)

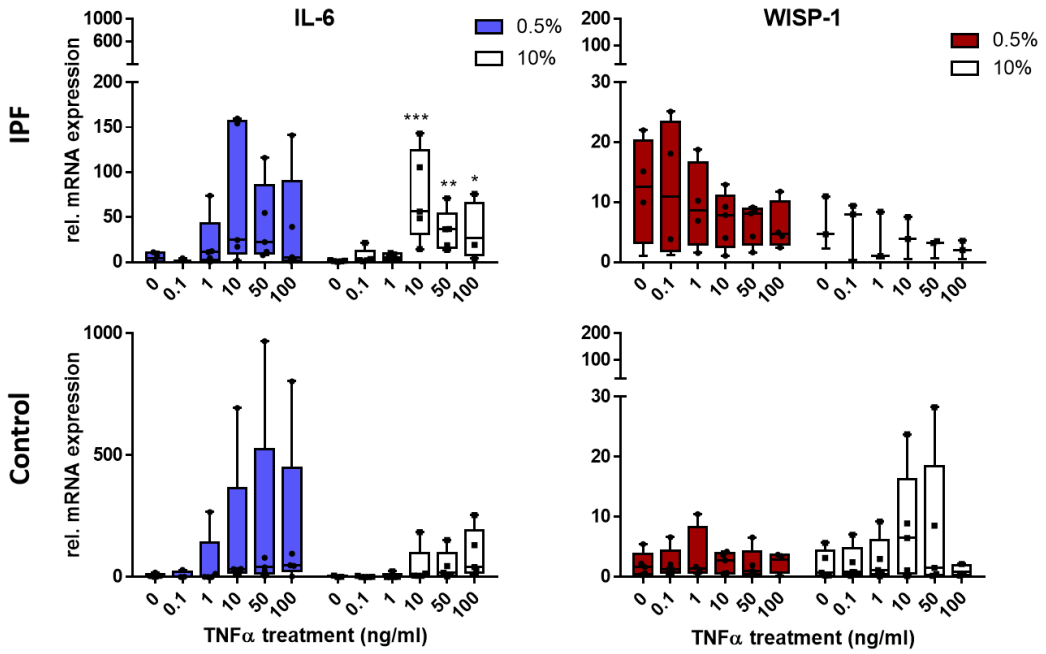

Figure 27. IL-6 and WISP-1 expression in IPF and control fibroblasts following TNFα treatment. IPF (top panel) and control (bottom panel) fibroblasts were grown to 70% confluence then medium was replaced with 0.5% FBS or 10% FBS medium for 24 hours. Cells were treated with indicated dose of TNFα for 72 hours. Cells were harvested in trizol for RNA extraction and mRNA expression was measured by qRT-PCR. Data are expressed relative to the expression in lowest expressing untreated donor in 0.5% FBS medium. n=5 IPF donors in 0.5% FBS medium, 3 IPF donors in 10% FBS medium, 5 control donors in both levels of FBS. Friedman statistical test was used to determine statistical difference between untreated and treated samples.. Mann Whitney test was used to determine statistical difference between IPF and control donors at each dose. *p=≤0.05, **p=≤0.01, ***p=≤0.001 dose compared to untreated in same medium.

Following the lack of clear WISP-1 mRNA induction after differentiation towards a myofibroblast phenotype, WISP-1 expression was measured in fibroblasts stimulated with TNFα. Primary fibroblasts were treated for 72 hours (as with MRC5 cells) with different doses of TNFα, and IL-6 expression was measured to indicate whether the cells responded to TNFα treatment as TNFα has been demonstrated to stimulate IL-6 expression (208).

In IPF fibroblasts (Figure 27, top panel), there was a trend for TNFα stimulated IL-6 expression (left panel) from 1ng/ml up to 50ng/ml in 0.5% FBS medium. IL-6 was also induced by TNFα in 10% FBS medium and this was statistically significant at 10 ($p=\leq 0.001$), 50 ($p=\leq 0.01$) and 100ng/ml ($p=\leq 0.05$). WISP-1 expression (right) was higher overall in 0.5% FBS medium with a trend for WISP-1 suppression by higher doses of TNFα. In 10% FBS medium no clear effect of TNFα treatment was observed.

In control fibroblasts (Figure 27, bottom panel), TNFα induced IL-6 mRNA expression (left) from 1ng/ml in 0.5% FBS medium, and from 10ng/ml in 10% FBS medium. Expression of IL-6 in IPF and control fibroblasts was similar in both levels of FBS when unstimulated. However, the induction of IL-6 by TNFα was greater in control donor-derived parenchymal fibroblasts than IPF donor-derived. WISP-1 expression in control fibroblasts (right panel) was similar in both 0.5% FBS and 10% FBS medium at low doses of TNFα.

3.2.3 WISP-1 mRNA expression in bronchial fibroblasts

Expression of WISP-1 mRNA in primary parenchymal fibroblasts did not increase as hypothesised following pro-fibrotic and pro-inflammatory cytokine treatment. Therefore the expression of WISP-1 mRNA in primary bronchial fibroblasts from healthy donors was measured to see whether a similar pattern would be observed. cDNA used was from experiments carried out by Dr David Smart ($TGF\beta_1$) and Dr Jessica Donaldson (TNFα).

$TGF\beta_1$ induced the expression of α-SMA mRNA in healthy bronchial fibroblasts, as observed with MRC5 cells and both control and IPF parenchymal fibroblasts (Figure 28, left panel). This induction was statistically significant at both 1 and 10ng/ml $TGF\beta_1$ ($p=\leq 0.01$). However, no change in WISP-1 mRNA levels was detected in these cells (right panel). WISP-1 mRNA expression was also measured in TNFα-stimulated bronchial fibroblasts. As Figure 29 shows, treatment with TNFα did not stimulate expression of WISP-1 mRNA.

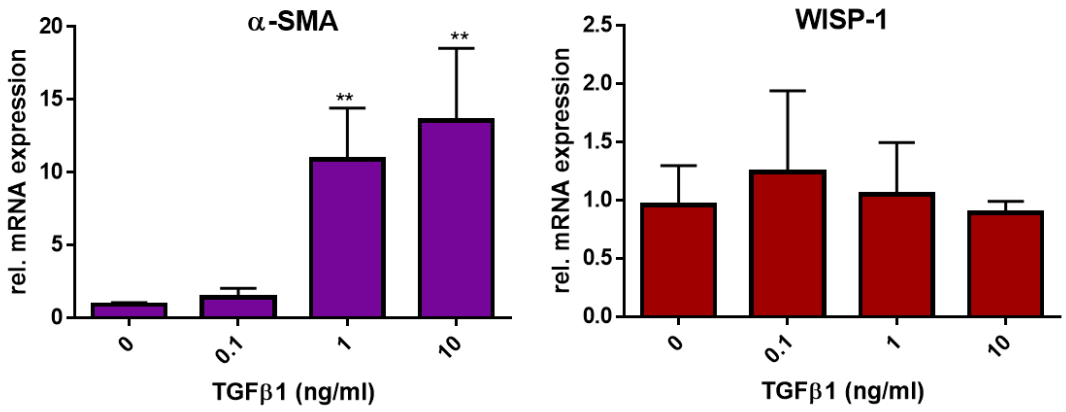

Figure 28. α-SMA and WISP-1 expression in healthy bronchial fibroblasts following $TGF\beta_1$ treatment. Fibroblasts were treated with indicated dose of $TGF\beta_1$ for 24 hours in 10% FBS containing medium. Cells were harvested in trizol for RNA extraction and mRNA expression was measured by qRT-PCR. Data are expressed relative to the expression in one untreated sample. n=3, mean ± SD. Statistical significance was tested by one-way ANOVA, **p=≤0.01.

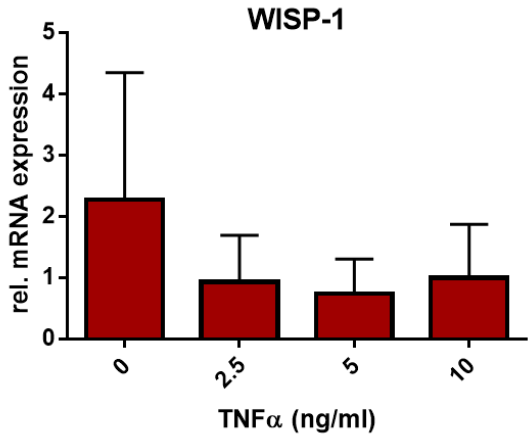

Figure 29. WISP-1 expression in healthy bronchial fibroblasts following TNFα treatment. Fibroblasts were grown to 70% confluence then medium was replaced with 0% FBS containing medium for 24hrs then treated with indicated dose of TNFα for 24 hours in this medium. Cells were harvested in trizol for RNA extraction and mRNA expression was measured by qRT-PCR. Data are expressed relative to the expression in one untreated sample, n=3, mean ± SD

Fibroblast summary

In MRC5 cells there was a trend for WISP-1 mRNA expression to increase over time (Figure 17). It is suppressed by TGFβ_1 treatment (Figure 19) and possibly by a factor present in FBS (Figure 17). TNFα stimulation induces WISP-1 mRNA expression in these cells (Figure 20).

In primary parenchymal fibroblasts, WISP-1 mRNA expression increases over time (Figure 23). When unstimulated, IPF fibroblasts express higher levels of WISP-1 compared to control cells (Figure 21). The observed variability in WISP-1 expression observed may be due to experimental differences or inter-donor variation. This was also observed in the response of these cells to pro-fibrotic and pro-inflammatory stimuli with some donors showing induction and some repression of WISP-1 mRNA following treatment (Figure 25, Figure 26 and Figure 27). α-SMA and IL-6 mRNA induction in these samples indicates that this is not due to a lack of response to stimuli in some donors.

In the small number of donors studied, WISP-1 mRNA expression was variable in bronchial fibroblast samples and was not regulated by TGFβ_1 or TNFα in these cells (Figure 28 and Figure 29).

3.2.4 Expression of WISP-1 mRNA in alveolar epithelial cells

Dose response experiments were carried out in the alveolar epithelial cell line A549 using TGFβ_1 and TNFα. TGFβ_1 is known to induce the expression of epithelial to mesenchymal transition (EMT) markers in these cells (97), a process which may be involved in the aberrant wound healing and excessive extracellular matrix (ECM) deposition taking place in the fibrotic lung. TNFα has been demonstrated to enhance the induction of EMT by TGFβ_1 in A549 cells (204). Experimental conditions were decided based on those used for fibroblast studies above.

First, alpha-smooth muscle actin (α-SMA), zinc finger E-box-binding homeobox-1 (ZEB1), collagen 1 (COL1A1) and E-cadherin (CDH1) mRNA levels were measured in TGFβ_1 stimulated cells to confirm the induction EMT (Figure 30). There was significant induction of α-SMA (top left) in 0.5% FBS containing medium by TGFβ_1

at the doses of 2.5ng/ml (p=≤0.05) and 5ng/ml (p=≤0.05). ZEB1 mRNA was also induced by TGFβ$_1$ at 10ng/ml in 10% FBS containing medium (top right, p=≤0.05). Induction of COL1A1 was observed from TGFβ$_1$ dose 2.5ng/ml upwards (bottom left). In 10% FBS containing medium this was significant at 5ng/ml (p=≤0.001), 10ng/ml (p=≤0.01) and 25ng/ml (p=≤0.0001). TGFβ$_1$ treatment suppressed the mRNA expression of CDH1 from 2.5ng/ml upwards (bottom right). This was significant in 0.5% FBS containing medium at 2.5ng/ml (p=≤0.05), 5ng/ml (p=≤0.0001), 10ng/ml (p=≤0.0001) and 25ng/ml (p=≤0.0001), and in 10% FBS containing medium (all doses, p=≤0.0001).

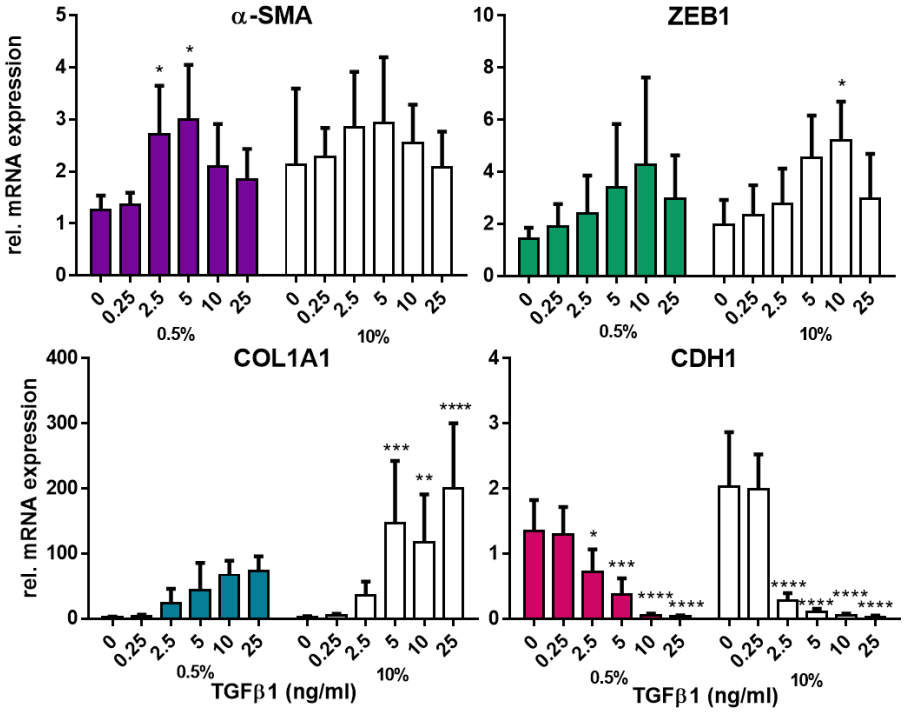

Figure 30. The effect of TGFβ$_1$ treatment on α-SMA, ZEB1, COL1A1 and CDH1 expression in A549 cells. A549 cells were grown to 70% confluence then medium was replaced with either 0.5% or 10% FBS containing medium for 24 hours. Cells were then treated with indicated dose of TGFβ$_1$ for 48 hours and harvested in trizol for RNA extraction. mRNA expression was measured by qRT-PCR. Data are expressed relative to one untreated sample in 0.5% FBS containing medium and are presented as mean ± SD. n=5-6. Statistical significance was tested by two-way ANOVA. * indicates significantly different compared to untreated sample. * p=<0.05, ** p=<0.01, *** p=<0.001, ****p=<0.0001. Ct values for α-SMA were approximately 25-26 in unstimulated cells.

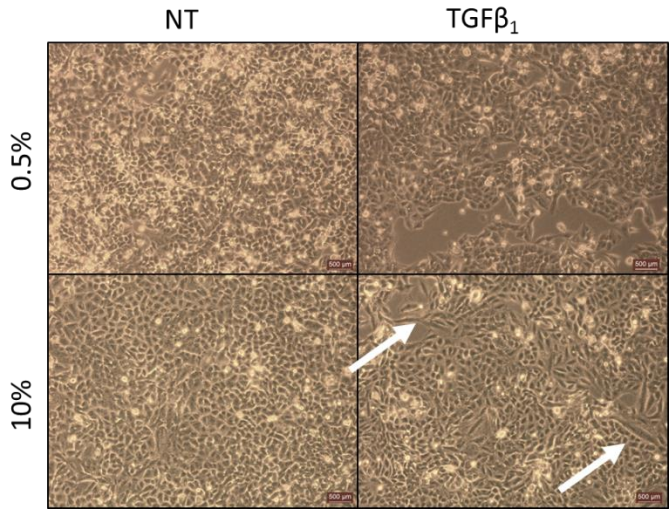

Figure 31. The induction of EMT in A549 cells by TGFβ1. A549 cells were grown to 70% confluence then medium was replaced with either 0.5% or 10% FBS containing medium for 24 hours. Cells were then treated with 5ng/ml of TGFβ1 for 48 hours. Images are representative of 6 separate experiments, and were taken at 5x magnification.

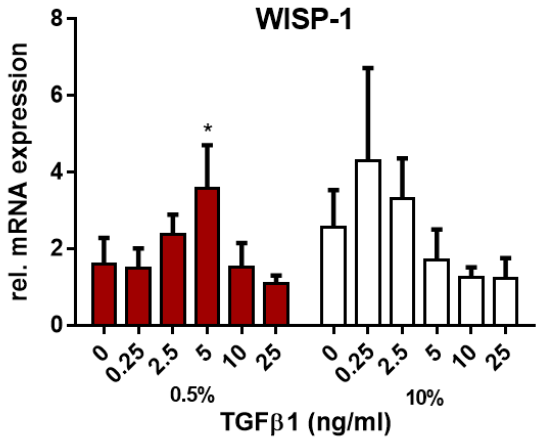

Figure 32. The effect of TGFβ1 treatment on WISP-1 expression in A549 cells. A549 cells were grown to 70% confluence then medium was replaced with either 0.5% or 10% FBS containing medium for 24 hours. Cells were then treated with indicated dose of TGFβ1 for 48 hours and harvested in trizol for RNA extraction. mRNA expression was measured by qRT-PCR. Data are expressed relative to one untreated sample in 0.5% FBS containing medium and are presented as mean ± SD. n=5-6. Statistical significance was tested by two-way ANOVA. * indicates significantly different compared to untreated sample. * p=<0.05.

The increase in α-SMA, ZEB1 and COL1A1, and suppression of CDH1 indicates that EMT-like changes were induced in A549 cells by TGFβ$_1$. This change in cell phenotype can also be seen in images of these cells taken after TGFβ$_1$ treatment (Figure 31). The morphology of some of the A549 cells has changed to a more mesenchymal appearance, highlighted by the white arrows.

Figure 32 shows the expression of WISP-1 mRNA in these cells. WISP-1 was induced by mid-doses of TGFβ$_1$ in 0.5% FBS containing medium (red bars). This was significant at 5ng/ml (p=≤0.05). At higher doses (10 and 25 ng/ml), WISP-1 expression was similar to that of untreated cells.

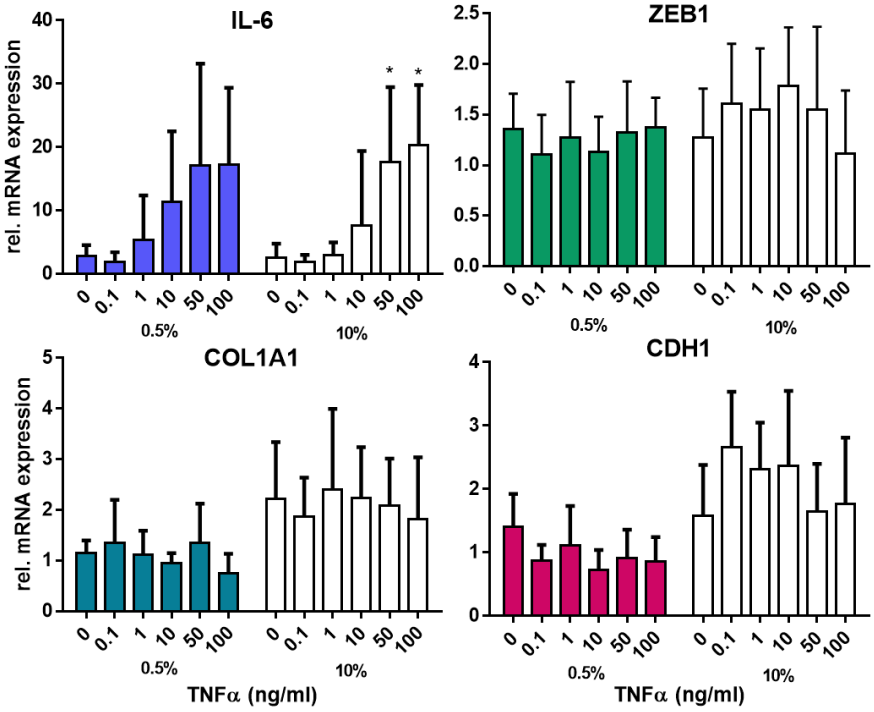

Figure 33. The effect of TNFα treatment on IL-6, ZEB1, COL1A1 and CDH1 expression in A549 cells. A549 cells were grown to 70% confluence then medium was replaced with either 0.5% or 10% FBS containing medium for 24 hours. Cells were then treated with indicated dose of TNFα for 72 hours and harvested in trizol for RNA extraction. mRNA expression was measured by qRT-PCR. Data are expressed relative to one untreated sample in 0.5% FBS containing medium and are presented as mean ± SD. n=3-5. Statistical significance was tested by two-way ANOVA. * indicates significantly different compared to untreated sample. *p=<0.05.

Next, the effect of TNFα on A549 cells was investigated. A549 cells were treated with TNFα at a dose of 0, 0.1, 1, 10, 50 or 100ng/ml for 72 hours in 0.5% or 10% FBS containing medium. Interleukin-6 (IL-6), ZEB1, COL1A1 and CDH1 expression were measured (data shown in Figure 33). There was a trend for IL-6 expression to be induced by TNFα from 1ng/ml upwards in both 0.5% and 10% FBS containing medium (top left). This was significant in 10% FBS containing medium at the higher doses of 50ng/ml (p=≤0.05) and 100ng/ml (p=≤0.01). TNFα did not induce expression of ZEB1 (top right) or COL1A1 (bottom left), and did not suppress E-cadherin (bottom right).

These results suggest that the A549 cells responded to TNFα (IL-6 was induced) but that EMT was not induced by TNFα. This is reflected in the images taken of these cells following TNFα treatment as the cell morphology appears the same as untreated A549 cells (Figure 34). In these experiments, the was a trend for WISP-1 induction by TNFα from 0.1ng/ml in 0.5% FBS containing medium (Figure 35, red bars). In 10% FBS containing medium WISP-1 expression was significantly induced at 0.1ng/ml (p=≤0.01) and 100ng/ml (p=≤0.05) TNFα.

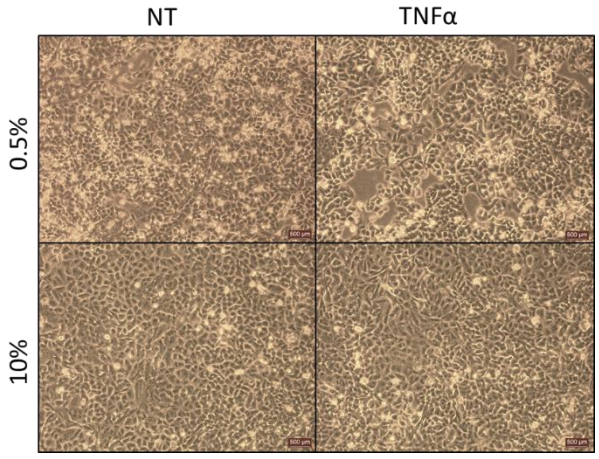

Figure 34. The effect of TNFα treatment on A549 cells. A549 cells were grown to 70% confluence then medium was replaced with either 0.5% or 10% FBS containing medium for 24 hours. Cells were then treated with 10ng/ml of TNFα for 72 hours. Images are representative of 6 separate experiments, and were taken at 5x magnification.

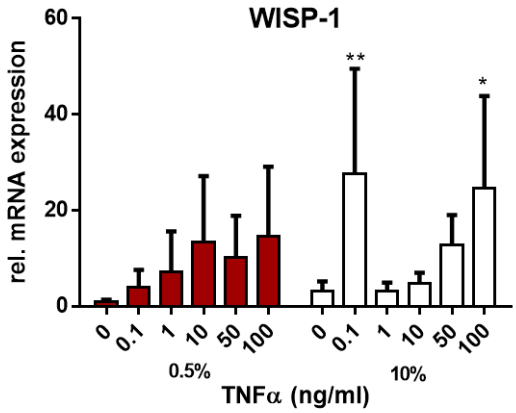

Figure 35. The effect of TNFα treatment on WISP-1 expression in A549 cells. A549 cells were grown to 70% confluence then medium was replaced with either 0.5% or 10% FBS containing medium for 24 hours. Cells were then treated with indicated dose of TNFα for 72 hours and harvested in trizol for RNA extraction. mRNA expression was measured by qRT-PCR. Data are expressed relative to one untreated sample in 0.5% FBS containing medium and are presented as mean ± SD. n=3-5. Statistical significance was tested by two-way ANOVA. * indicates significantly different compared to untreated sample. * p=<0.05, ** p=<0.01.

$TGF\beta_1$ significantly stimulated EMT of A549 cells (Figure 30) however WISP-1 mRNA induction in these cells, whilst statistically significant at 5ng/ml in 0.5% FBS containing medium (Figure 32), was only 2-fold that of untreated cells. Fold induction of WISP-1 mRNA expression by TNFα was greater, for example approximately 15-fold that of untreated at 10ng/ml TNFα in 0.5% FBS containing medium (Figure 35) but EMT was not stimulated by TNFα (lack of effect on ZEB1, COL1A1 and CDH1 expression (Figure 33)). Therefore, the effect of co-treatment of A549 cells with both TNFα and $TGF\beta_1$ was measured to determine whether TNFα enhanced $TGF\beta_1$ induction of EMT and WISP-1 expression.

Expression of α-SMA and IL-6 (Figure 36, top panel) was measured to confirm that A549 cells were able to respond to $TGF\beta_1$ and TNFα respectively. α-SMA was induced approximately 3-fold by $TGF\beta_1$ treatment in 0.5% FBS containing medium ($p=\leq 0.0001$). It was also significantly induced by $TGF\beta_1$ in 10% FBS containing medium ($p=\leq 0.01$). TNFα alone induced IL-6 mRNA in 0.5% and 10% FBS

containing medium. This induction was greater when cells were co-treated with TNFα and TGFβ$_1$, and this enhanced effect in co-treated cells was statistically significant in 0.5% FBS containing medium (p=≤0.01). In 10% FBS containing medium, co-treatment significantly induced expression of IL-6 relative to that in unstimulated cells (p=≤0.01).

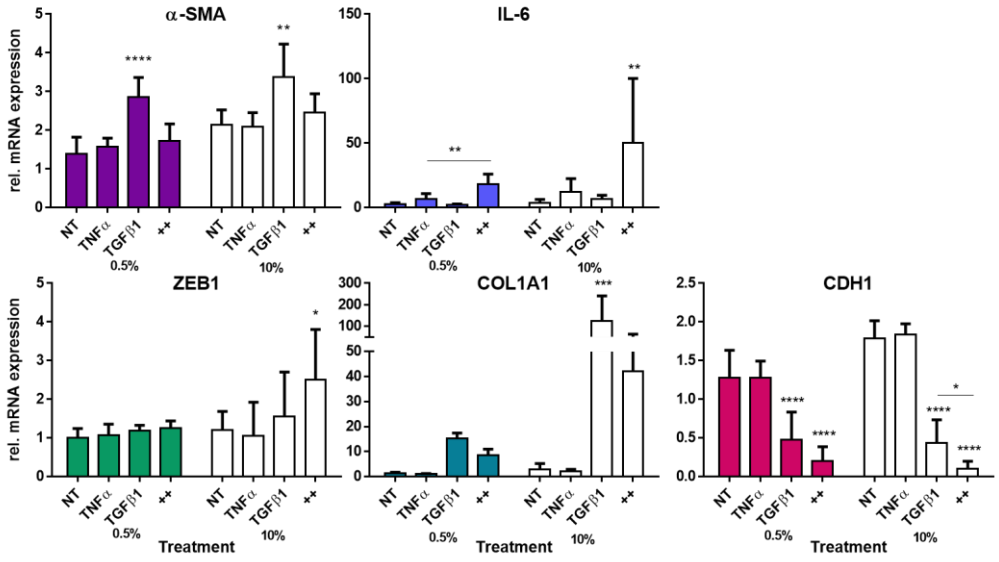

Figure 36. The effect of TNFα and TGFβ$_1$ co-treatment on mRNA expression in A549 cells. A549 cells were grown to 70% confluence then medium was replaced with either 0.5% or 10% FBS containing medium for 24 hours as indicated. Cells were then treated with TNFα (10ng/ml), TGFβ$_1$ (5ng/ml) or TNFα and TGFβ$_1$ for 72 hours. Cells were harvested in trizol for RNA extraction and α-SMA, IL-6, ZEB1, COL1A1 and CDH1 expression was measured by qRT-PCR. Data are expressed relative to one untreated sample in 0.5% FBS containing medium and are presented as mean ± SD. n=4-6. Statistical significance was tested by two-way ANOVA. * indicates significantly different compared to untreated sample.IL-6 * indicates significance between TNFα treated and co-treated, CDH1 * indicates significance between TGFβ1 treated and co-treated. * p=<0.05, ** p=<0.01, *** p=<0.001, ****p=<0.0001.

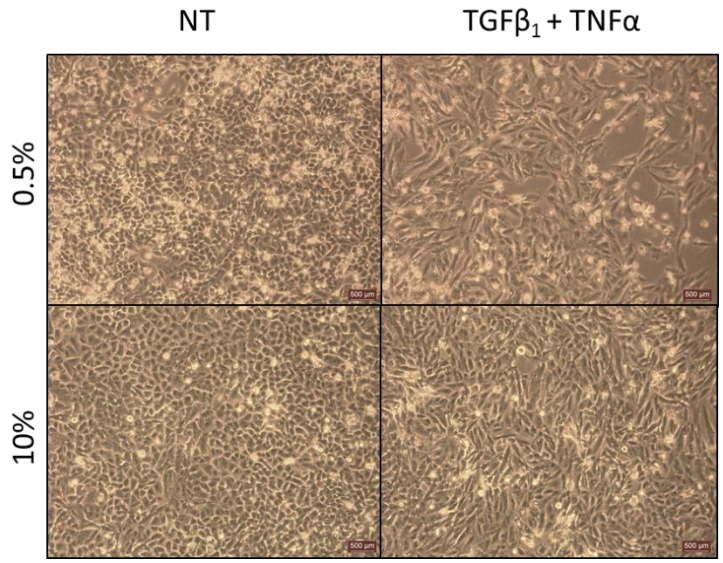

Figure 37. Induction of EMT in A549 cells. A549 cells were grown to 70% confluence then medium was replaced with either 0.5% or 10% FBS containing medium for 24 hours. Cells were then treated with 10ng/ml of TNFα and 5ng/ml of $TGF\beta_1$ for 72 hours. Images are representative of 6 separate experiments, and were taken at 5x magnification.

A549 cells treated with TNFα or $TGF\beta_1$ alone, or in combination showed no change in ZEB1 mRNA expression in 0.5% FBS containing medium (Figure 36, bottom left, green bars). In 10% FBS containing medium, ZEB1 was induced approximately 2.5-fold by TNFα and $TGF\beta_1$ co-treatment ($p=\leq 0.05$). $TGF\beta_1$ alone stimulated COL1A1 mRNA expression in 10% FBS containing medium approximately 40-fold ($p=\leq 0.01$) respectively (bottom centre). Co-treatment with TNFα also induced COL1A1 expression compared with untreated cells, however this was to a lesser extent than $TGF\beta_1$ treatment alone. Significant suppression of CDH1 was observed (bottom right) in 0.5% and 10% FBS containing medium with $TGF\beta_1$ alone ($p=\leq 0.0001$). CDH1 mRNA levels were further reduced following co-treatment with TNFα ($p=\leq 0.0001$). In 10% FBS containing medium, co-treatment significantly repressed CDH1 expression compared to that in $TGF\beta_1$ alone ($p=\leq 0.05$).

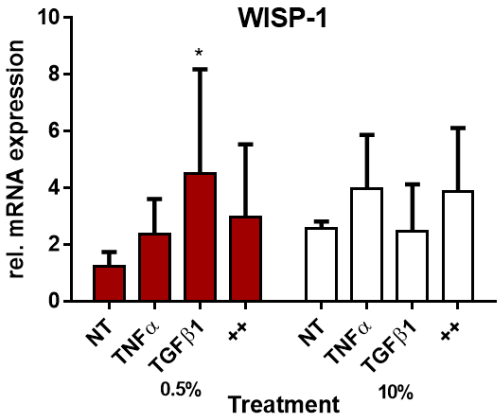

Figure 38. The effect of TNFα and TGFβ$_1$ co-treatment on WISP-1 expression in A549 cells. A549 cells were grown to 70% confluence then medium was replaced with either 0.5% or 10% FBS containing medium for 24 hours as indicated. Cells were then treated with TNFα (10ng/ml), TGFβ$_1$ (5ng/ml) or TNFα and TGFβ$_1$ for 72 hours. Cells were harvested in trizol for RNA extraction and WISP-1 expression was measured by qRT-PCR. Data are expressed relative to one untreated sample in 0.5% FBS containing medium and are presented as mean ± SD. n=5-6. Statistical significance was tested by two-way ANOVA. * indicates significantly different compared to untreated sample. *p=<0.05

These data indicated that co-treatment of A549 cells with TNFα and TGFβ$_1$ enhanced the effect on mRNA expression observed with TGFβ$_1$ treatment alone. Images taken of these cells show that the morphology of the majority of the cells in both 0.5% and 10% FBS containing medium changed with co-treatment to that more typical of a fibroblastic cell (Figure 37). Co-treatment stimulated WISP-1 expression in A549 cells however this was not statistically significant (Figure 38). This increase in WISP-1 expression was greater than that observed for TNFα treatment alone, and less than that for TGFβ$_1$ alone (approximately 4-fold, p=≤0.05) in 0.5% FBS containing medium. In 10% FBS containing medium, TNFα alone stimulated WISP-1 expression approximately 1.5-fold and TGFβ$_1$ alone did not induce WISP-1 above the level of untreated cells.

3.2.5 WISP-1 protein expression

3.2.5.1 WISP-1 protein expression in primary parenchymal fibroblasts

Fibroblast lysates from five control and five IPF donors were probed for WISP-1 expression by western blotting using an R&D polyclonal antibody (non-biotinylated). Commercial his-tagged recombinant human WISP-1 (R&D) was run alongside cell lysate samples as a positive control. As shown in Figure 39, full length WISP-1 was not detected in control fibroblast lysates cultured in 0.5% FBS containing medium (left hand panels). In 10% FBS containing medium (right hand panels), full length WISP-1 was detected at around 50kDa in 3 donors at 48 hours and 2 donors at 72 hours.

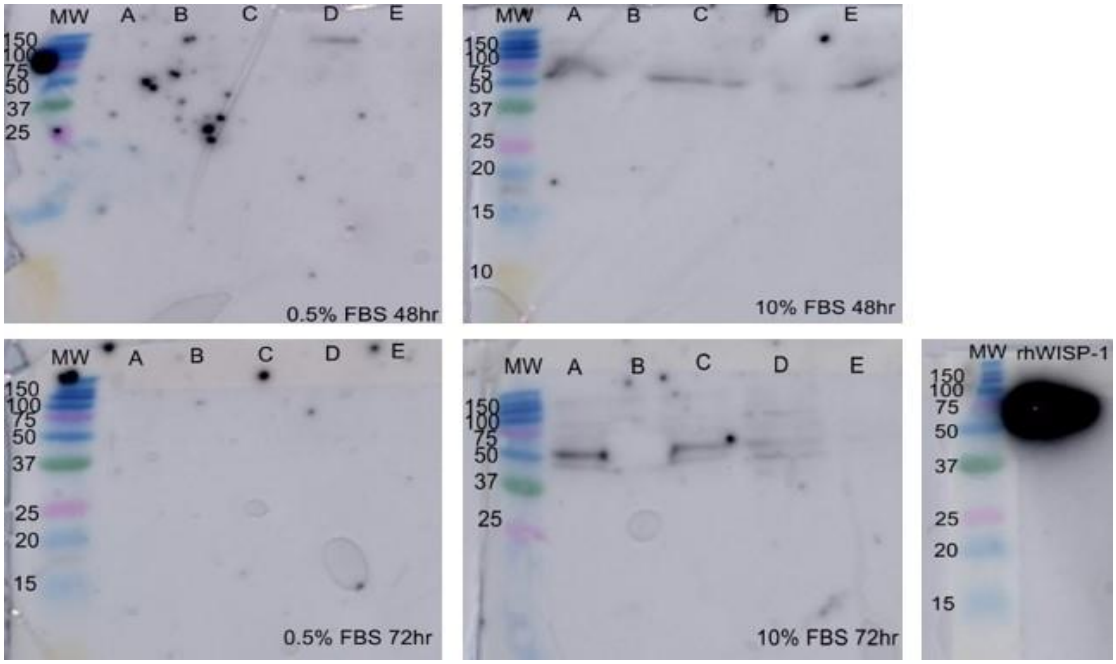

Figure 39. Detection of WISP-1 protein in lysates from control parenchymal lung fibroblasts. Fibroblasts were grown to 70% confluence then medium was replaced with 0.5% FBS or 10% FBS containing medium for 48 or 72 hours. Cells were scraped in sample buffer and lysates were run on a 12.5% SDS-PAGE gel before detection using a polyclonal antibody against WISP-1 (R&D, 10ng/μl). rhWISP-1 was also run as a positive control. A-E refers to donor.

Similarly, in IPF lysates no bands were present in 0.5% FBS containing medium (Figure 40). WISP-1 was detected in 10% FBS medium in 4 of 5 donors at 48 hours and 72 hours. Further bands at a higher molecular weight around 100-150kDa were also detected in these samples, potentially corresponding to multimers of WISP-1. There was also a band present in some lanes, including the MW marker lane, below 20kDa in the 48 hour blots. Recombinant WISP-1 was detected at around 50kDa as expected.

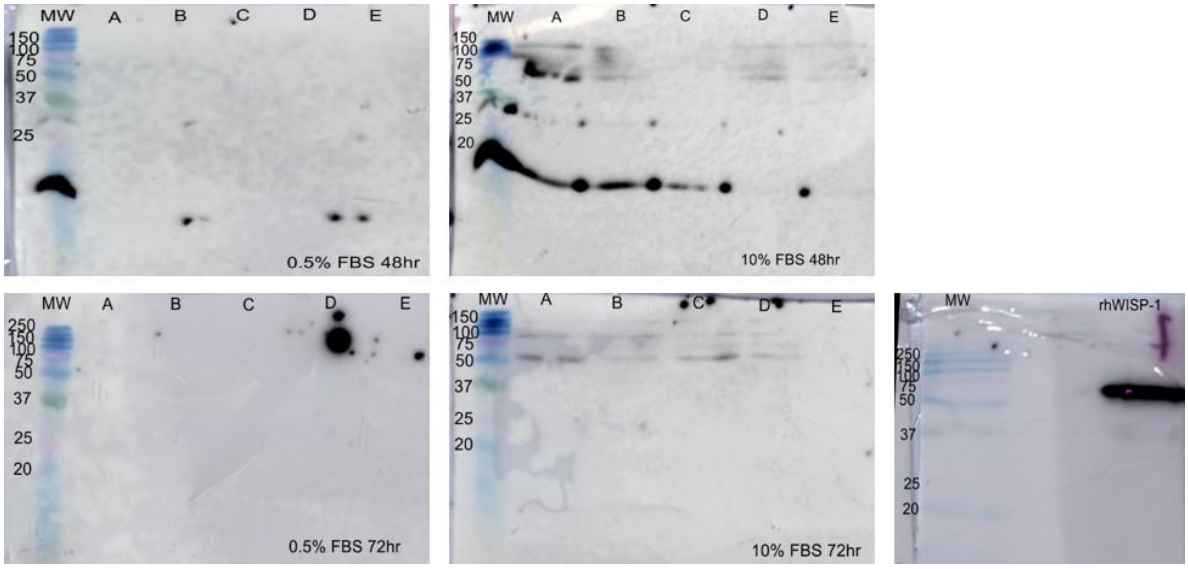

Figure 40. Detection of WISP-1 protein in lysates from IPF parenchymal lung fibroblasts. Fibroblasts were grown to 70% confluence then medium was replaced with 0.5% FBS or 10% FBS medium for 48 or 72 hours. Cells were scraped in sample buffer and lysates were run on a 12.5% SDS-PAGE gel before detection using a polyclonal antibody against WISP-1 (R&D, 10ng/μl). rhWISP-1 was also run as a positive control. A-E refers to donor.

3.2.5.2 WISP-1 protein expression in A549 cells

Expression of WISP-1 in A549 cells treated with TGFβ_1 was measured using the same antibody as above (Figure 41). A band between 37 and 50kDa was detected in all lanes containing lysates from cells cultured in 10% FBS containing medium but not in samples cultured in 0.5% FBS containing medium. In one experiment

there was no dose effect of TGFβ_1 (left-hand blot) however there appeared to be a dose-dependent increase in WISP-1 in the second experiment (right-hand blot). At the highest dose of TGFβ_1 there was also a band present at around 100-150kDa.

Lysates from TNFα-treated A549 cells were also probed for WISP-1 (Figure 42). Again, WISP-1 was only detected in cells treated in 10% FBS containing medium between 37 and 50kDa, and there appeared to be a dose dependent increase of WISP-1, particularly in the second experiment (right-hand blot). In lysates from cells treated with higher concentrations of TNFα bands were also present at around 100kDa, possibly corresponding to multimers of WISP-1.

The lack of bands present in cell lysates cultured in 0.5% FBS containing medium may suggest that a factor present in FBS stimulates WISP-1 translation, or that WISP-1 is present in FBS and is binding to the cell surface. To determine whether WISP-1 in FBS binds to the cell surface A549 cells were treated with either TNFα, TGFβ_1, both cytokines or not treated (as previously) in 0.5% FBS containing medium. After 72 hours the medium in each well was replaced with 10% FBS medium for 1 hour before cells were lysed in sample buffer. A 1 hour incubation with 10% FBS containing medium was selected as this is not a long enough period for translation to occur. No WISP-1 was detected in cells treated with TGFβ_1, TNFα + TGFβ_1 or untreated cells (Figure 43). This could suggest that the WISP-1 previously detected was expressed by the cell and not from the culture medium. However, two bands were detected at around 37 and 50kDa in the TNFα treated sample.

To determine whether TNFα stimulates WISP-1 binding to the cell surface, A549 cells were treated with TNFα in 10% FBS containing medium for 24 hours before the addition of recombinant human WISP-1 for a further 24 hours (Figure 44, left hand blot). A band was present above 50kDa, and a second, fainter band at 37kDa. The larger band likely corresponds to the recombinant WISP-1 added to the cells as this is at the correct molecular weight and is not present in the lanes where no rhWISP-1 was added. The fainter band was also not present in the lanes where on rhWISP-1 was added suggesting that this is not non-specific, and that TNFα may stimulate WISP-1 binding to the cell. TNFα did not stimulate the expression of WISP-1 by A549 cells as observed previously (Figure 42). Commercial recombinant WISP-1 added to medium was detected at a similar level

to that added to TNFα-treated cells (right hand blot). In both DMEM ± rhWISP-1 and FBS lanes, higher bands were detected above 100kDa but no lower bands were present where rhWISP-1 was not added.

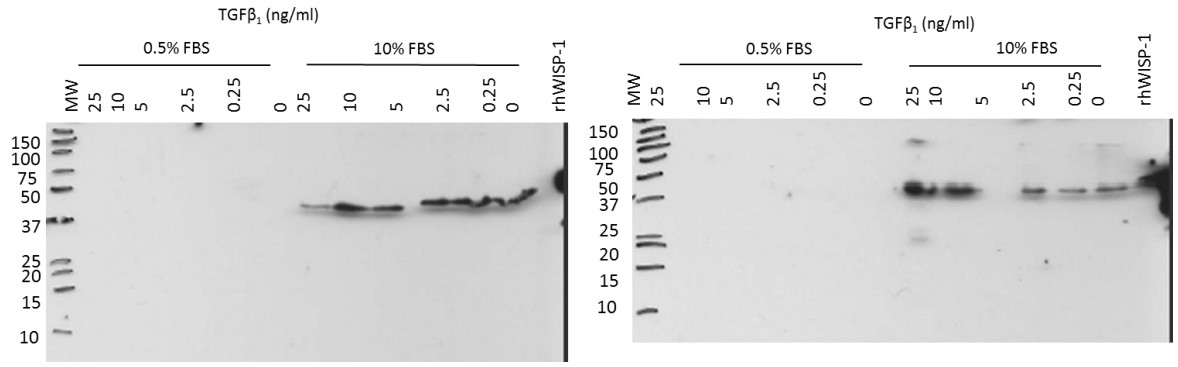

Figure 41. Expression of WISP-1 in lysates of TGFβ1 treated A549 cells were grown to 70% confluence then medium was replaced with either 0.5% or 10% FBS containing medium for 24 hours. Cells were then treated with indicated dose of TGFβ1 for 48 hours and harvested in sample buffer. Samples were run on a 12.5% SDS-PAGE gel and probed with a polyclonal antibody. rhWISP-1 (R&D) run as a positive control.

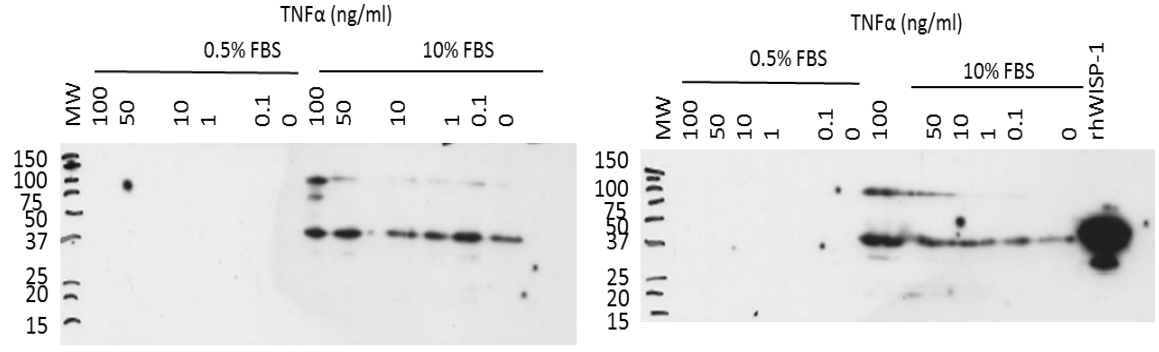

Figure 42. Expression of WISP-1 in lysates from TNFα treated A549 cells were grown to 70% confluence then medium was replaced with either 0.5% or 10% FBS containing medium for 24 hours. Cells were then treated with indicated dose of TNFα for 72 hours and harvested in sample buffer. Samples were run on a 12.5% SDS-PAGE gel and probed with a polyclonal antibody. rhWISP-1 (R&D) run as a positive control.

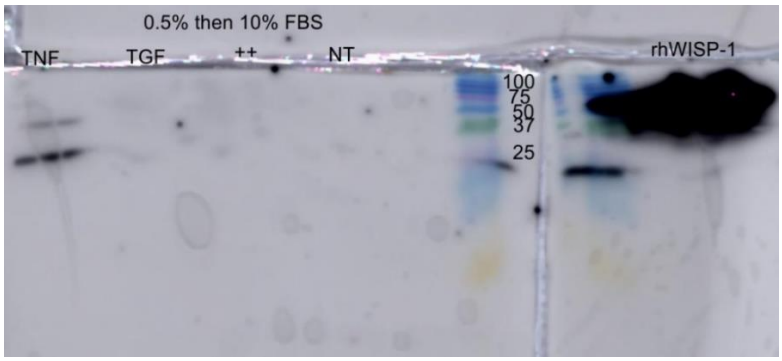

Figure 43. Expression of WISP-1 in A549 lysates treated with TNFα and TGFβ$_1$. A549 cells were grown to 70% confluence then medium was replaced with either 0.5% FBS containing medium for 24 hours. Cells were then treated with TNFα (10ng/ml), TGFβ$_1$ (5ng/ml) or TNFα and TGFβ$_1$ for 72 hours then medium was replaced with 10% FBS containing medium for 1 hour. Cells were then harvested directly in sample buffer. Samples were run on a 12.5% SDS-PAGE gel and probed with a polyclonal antibody. rhWISP-1 (R&D) run as a positive control.

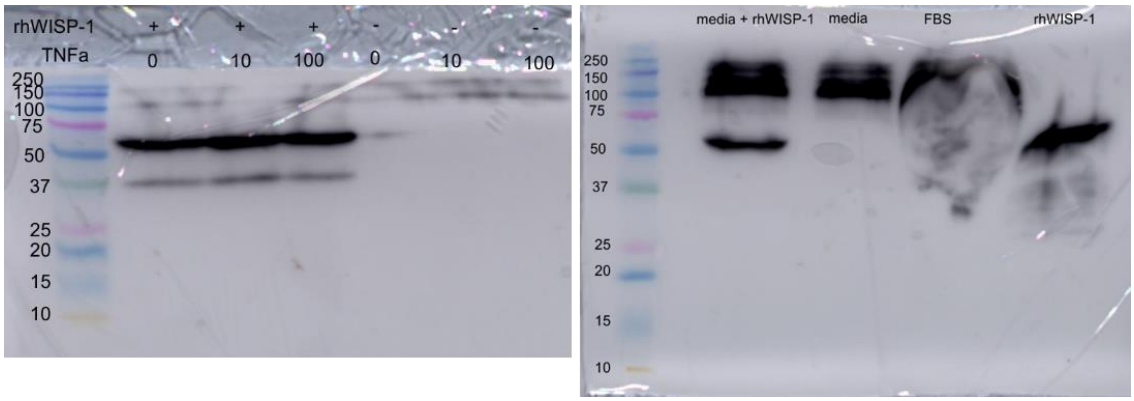

Figure 44. Expression of WISP-1 in A549 lysates treated with TNFα ± WISP-1(left) and WISP-1 detected in complete DMEM ± rhWISP-1 and FBS (right). A549 cells were grown to 70% confluence then treated in 10% FBS containing medium with TNFα (0,10 or 100 ng/ml) for 24 hours. Cells were then treated ± 1ug WISP-1 for 24 hours and harvested in sample buffer. DMEM ± rhWISP-1 and FBS diluted 1 in 2 with sample buffer. Samples were run on a 12.5% SDS-PAGE gel and probed with either a polyclonal antibody against WISP-1. rhWISP-1 (non-biotinylated, R&D) run as a positive control.

3.2.5.3 Expression in cell culture supernatants

Levels of secreted WISP-1 in supernatants from primary parenchymal fibroblasts and A549 cells were measured by ELISA. Samples assayed included those from each condition tested. The level of WISP-1 in all supernatant samples was below the level of detection for the assay (data not shown). Medium from WISP-1 transfected HEK293T cells was run alongside as a positive control (data not shown).

3.3 Discussion

Studies in the literature have identified increased expression of WISP-1 in the IPF lung however the contribution of different cell types, and the influence of pro-fibrotic and pro-inflammatory factors on this increased expression is unclear. Therefore the aim of this study was to characterise the mRNA and protein expression of WISP-1 in primary parenchymal fibroblasts and an alveolar epithelial cell line.

WISP-1 mRNA expression in fibroblasts

Overall, WISP-1 mRNA expression in unstimulated IPF fibroblasts was higher than in control donor-derived fibroblasts at 48 and 72 hours. This is in agreement with one published study (125) however an earlier study by the same group reported no differences between disease and control (124). This is perhaps in part due to inter-donor variation in levels of WISP-1 mRNA expression. Of the donors included in the current study, fibroblasts from three IPF donors had relatively high mRNA expression compared to the other two. In the control fibroblasts, WISP-1 was expressed at relatively high levels in one donor. The other four donors expressed low levels similar to that in the lowest two IPF donors.

WISP-1 mRNA levels were also measured at different time points. Generally, WISP-1 mRNA levels increased over time in unstimulated fibroblasts however in three of

four IPF donors WISP-1mRNA expression peaked at 72 hours and decreased by 96 hours.

Response to TGFβ_1

Variation in WISP-1 mRNA expression was also observed in response to treatment with TGFβ_1 in both time course and dose response experiments. The differences in WISP-1 mRNA expression observed may be due to variation between experiments or between fibroblast donors. A repeat of the TGFβ_1 dose response experiment was carried out in one IPF and one control donor in order to determine the contribution of experimental variation to the differences in WISP-1 expression observed. A similar pattern of expression was seen in both experiments for both donors. This suggests that inter-donor variation was responsible for differences observed however this experiment was not repeated with any further donors.

Responsiveness of fibroblasts to TGFβ1 treatment was confirmed by α-SMA induction in both IPF and control donors, as was observed in MRC5 fibroblasts. There was a trend for WISP-1 expression to be suppressed by TGFβ_1 however this was not statistically significant.

In these experiments, the aim was to measure WISP-1 mRNA expression following the induction of a myofibroblast phenotype in these cells. Induction of WISP-1 expression might therefore have suggested that WISP-1 contributes to the phenotypic changes observed in the cell as it differentiates, or that it is perhaps involved in the maintenance the myofibroblast phenotype. A lack of clear induction as was observed in the current study may suggest that WISP-1 is not involved in the differentiation process in these cells. However, WISP-1 could play a role in other cellular processes, for example their proliferation or migration, as has been reported for other cell types (120, 186, 189, 191, 192).

A possible explanation for the results obtained may be that TGFβ_1 does not regulate WISP-1 expression in these cells. Evidence from the literature suggests that WISP-1 expression can be regulated by TGFβ_1 in different cell types. In the current study, A549 WISP-1 mRNA expression was stimulated by TGFβ_1 at a dose of 5ng/ml after 48 hours in 0.5% FBS containing medium. In non-lung cells, 2nM TGFβ_1 was demonstrated to stimulate an 8-fold induction of WISP-1 mRNA expression after 6 hours in murine osteoblasts (209).

WISP-1 expression has also been reported to be regulated by TGFβ$_1$ in primary human lung fibroblasts in studies that have published since the current study began. Berschneider et al. (125) reported a modest induction of WISP-1 at the mRNA level (approximately 2-fold) in a small number of donors following stimulation with TGFβ$_1$. The experimental conditions in this study differ from those used in the current study - a dose of 2ng/ml TGFβ$_1$ was used and cells were stimulated for 24 hours. The fibroblasts used were from control donors only and a small number of different donors were used.

Another study reported TGFβ$_1$-stimulated WISP-1 expression by primary lung fibroblasts from both control and IPF donors (198). The authors reported a 3-fold induction of WISP-1 mRNA expression following a 24 hour treatment with 2ng/ml TGFβ$_1$ in fibroblasts from 3-6 control donors. The authors also reported a 6-fold induction of WISP-1 mRNA expression following a 24 hour treatment with 2ng/ml TGFβ$_1$ in fibroblasts from 3 IPF donors. Again, the experimental conditions in this study are different to those in the current study and a small number of different fibroblast lines were used from IPF donors.

In this same study the authors also performed analysis of the WISP-1 promoter and identified potential binding sites for the transcription factors TCF, LCF, SMADs and NFκB. The presence of TCF/LEF binding sites in the WISP-1 promoter was previously reported in a study investigating the regulation of WISP-1 by β-catenin (171). The authors also identified a binding site for CREB which they reported to be more important than the TCF/LEF binding sites in the transcriptional activation of WISP-1 by β-catenin. A search of the WISP-1 promoter using SABiosciences Champion ChIP transcription factor search portal shows potential binding sites for a number of other transcription factors including ATF-2, c-Jun, NFAT and HOXA9 (http://www.sabiosciences.com/chipqpcrsearch.php?gene=WISP1&factor=Over+200+TF&species_id=0&ninfo=n&ngene=n&nfactor=y).

The presence of these binding sites coupled with the known crosstalk between the Wnt/β-catenin and TGFβ$_1$ signalling pathways (210-212) make it unsurprising that transcriptional regulation of the Wnt target WISP-1 by TGFβ$_1$ has been reported in the literature. However, from the data presented in the current study it is unclear whether WISP-1 is transcriptionally regulated in the cells used. A way to confirm this could be to block TGFβ$_1$ signalling in these cells and measure

WISP-1 expression. This could be done by preventing TGFβ_1 binding to its receptor or by blocking its downstream signalling.

Response to TNFα

In this study, the response of lung fibroblasts to pro-inflammatory stimuli was also characterised. As with TGFβ_1 stimulation, differences were observed both between MRC5 cells and primary fibroblasts and between primary fibroblast donors. All primary fibroblasts were responsive to TNFα treatment as demonstrated by induction of IL-6 mRNA however TNFα did not stimulate WISP-1 mRNA expression in these cells.

TNFα induction of WISP-1 has been reported in other cell types and tissues. For example, in a model of the post-infarct myocardium TNFα and IL-1β were found to preceed expression of WISP-1 in vivo and to stimulate its expression in rat myocytes in vitro (193). In human cardiac fibroblasts TNFα was shown to upregulate WISP-1 mRNA and protein expression at a dose of 10ng/ml (194). In this study it was demonstrated that TNFα acted to stimulate WISP-1 expression via the transcription factor CREB.

TNFα stimulated expression of WISP-1 was recently demonstrated in primary control parenchymal fibroblasts by Klee et al. (198). At a dose of 10ng/ml TNFα, a 4-5-fold induction of WISP-1 mRNA was observed at 8, 24 and 48 hours (n=3-4). This dose of TNFα also stimulated a small increase in WISP- 1 levels detected in the supernatant. In IPF donor derived fibroblasts TNFα stimulated a 3-fold induction of WISP-1 mRNA (n=3). In this study the authors proposed that this induction was via NFκB the use of inhibitors of different components of NFκB signalling blocked WISP-1 induction.

The data presented in the current study suggest that TNFα does not stimulate WISP-1 mRNA expression in primary parenchymal lung fibroblasts. A potential reason for the difference in response observed to those published could be due to the different experimental conditions e.g. levels of serum, dose or length of treatment.

The primary fibroblasts used in this study are assumed to be parenchymal as they were isolated from tissue from IPF patients undergoing VATS biopsy for

diagnosis. However, there is a chance that these cells are more representative of bronchial fibroblasts. Therefore the expression of WISP-1 in TGFβ_1 and TNFα treated bronchial fibroblasts was measured. The conditions in these experiments vary to those used for parenchymal fibroblasts however the level of WISP-1 expression was similar. Overall, no clear effect of either treatment on WISP-1 mRNA was observed. This is likely due to the variation in response between donors. For both treatments, two of the three donors showed a similar pattern of WISP-1 expression whilst the third was different.

Use of MRC5 cells

MRC5 cells are a lung fibroblast cell line isolated from fetal human lung at 14 weeks (213). The primary fibroblasts used in this study were isolated from lung tissue from older adults with IPF, or similarly aged controls. Therefore differences in the response of the two types of fibroblasts perhaps should be expected. However, evidence from several studies in the literature suggest that developmental signalling pathways are recapitulated in IPF therefore MRC5 cells could be a useful model for investigating fibrotic processes. Of relevance to this particular study, WISP-1 expression has been demonstrated to be increased during the pseudoglandular stage of human lung development (200) which is the same stage at which MRC5 cells were isolated. The suitability of MRC5 cells as a model for fibrotic fibroblasts is undermined by the different responses to both TGFβ_1 and TNFα stimulation observed in the current study.

WISP-1 mRNA expression in A549 cells

WISP-1 mRNA expression was measured in A549 cells following the induction of epithelial to mesenchymal transition as WISP-1 was reported to stimulate this process in murine alveolar type II cells (124). Induction of epithelial to mesenchymal transition of A549 cells by TGFβ_1 was confirmed by increased expression of the transcriptional repressor ZEB1 and decreased expression of its target, the epithelial cell marker E-cadherin. Increased expression of the myofibroblast marker α-SMA was also observed in these cells, as well as increased levels of collagen 1 mRNA. These markers are amongst those commonly used to demonstrate this differentiation process (214). The transition of these cells towards a mesenchymal phenotype was also evident in photographs of the cells

taken following treatment showing increased number of cells with a spindle-like morphology.

In the current study, no induction of EMT was observed when A549 cells were treated with TNFα alone. Induction of EMT by TNFα has been reported in several studies, particularly in those investigating EMT in cancer. For example, Soria et al. (215) reported TNFα-induced morphological changes in a breast cancer cell line alongside reduced expression of E-cadherin and increased expression of vimentin. TNFα-induced EMT has also been implicated in wound healing. Yan et al. (216) reported increased vimentin expression, decreased E-cadherin expression and morphological changes in TNFα treated primary skin keratinocytes. However, in a study investigating the induction of EMT by TNFα in A549 cells, no change in cell morphology or expression of e-cadherin (CDH1) mRNA was observed, consistent with the current study (204).

A549 cells co-treated with TNFα and TGFβ$_1$ had a greater level E-cadherin mRNA suppression compared to cells treated with TGFβ$_1$ alone. Whilst TNFα and TGFβ$_1$ have been demonstrated to have opposing effects on the induction of type I collagen with TGFβ$_1$ stimulating gene transcription (91) and TNFα suppressing it (217), enhancement of TGFβ$_1$-induced EMT by TNFα has also been reported in the literature. In a study investigating airway remodelling using the airway epithelial cell line BEAS-2B (218), morphological changes and increased vimentin expression in TGFβ$_1$ treated cells were enhanced following co-treatment with TNFα. A similar effect has also been reported in A549 cells (204). In this study the authors reported that suppression of e-cadherin mRNA and changes in cell morphology was greater in co-treated cells compared to TGFβ$_1$ treated cells, consistent with the current study.

WISP-1 mRNA levels increased in a bell-shaped fashion in response to TGFβ$_1$ treatment (Figure 32). WISP-1 mRNA expression was also induced by TNFα (Figure 35). This induction suggests that WISP-1 may play a role in the epithelial to mesenchymal transition process as has been suggested by published studies using murine ATII cells. Heise et al. (197) reported a 2-fold increase in WISP-1 mRNA expression following mechanical stretch-induced EMT. The authors also observed a decreased level of EMT caused by mechanical stretch when a WISP-1 blocking antibody was used, demonstrated by a lack on induction of vimentin and

α-SMA, and a lack of E-cadherin suppression in these cells. In a second study, Konigshoff et al. (124) reported altered expression of several EMT markers including α-SMA, vimentin, occludin and E-cadherin following treatment with 1μg/ml recombinant WISP-1. In a recent study, WISP-1 was linked with EMT in oesophageal squamous cell carcinoma (219). The authors associated WISP-1 expression with an EMT-like phenotype in radiotherapy resistant cells and demonstrated that WISP-1 expression was negatively linked to patient survival.

A549 cells as a model for type II alveolar epithelial cells

Primary ATII cells require a large amount of tissue for their isolation and lung tissue is not readily available in such quantities. Once isolated, the continuous culture of primary ATII cells on plastic results in the loss of ATII cell characteristics such as increased expression of caveolin-1 and decreased expression of surfactant protein C (220). Therefore a model for ATII cells is required.

A549 cells are an alveolar epithelial cell line originally isolated from lung carcinoma tissue (221). Early studies reported that they expressed abundant lamellar bodies containing dipalmitoyl phosphatidylcholine (DPPC), the main lipid component in pulmonary surfactant (221, 222) however a more recent study reported that A549 cells contained significantly less phospholipid than primary ATII cells due to lower numbers of lamellar bodies (223). Whilst A549 cells may not be an ideal model of ATII cells, the aim of this study was to characterise WISP-1 expression following the induction of EMT, a process which has been previously characterised in this cell line (97, 204). In addition, A549 cells have relatively simple culture requirements and were readily available at the time of this study.

WISP-1 protein expression

Unstimulated parenchymal fibroblast lysates were probed for WISP-1 expression by western blotting. Interestingly, WISP-1 was only detected in cells cultured in 10% FBS containing medium as was observed with A549 cells suggesting that a factor present in FBS may stimulate the expression of WISP-1, its translation, or its secretion from the cell.

In 10% FBS containing medium, a band corresponding to the correct size for full length WISP-1 was present in 3 of 5 control fibroblast donors at 48 hours and 2 of

5 at 72 hours. This was the case for 4 of 5 IPF fibroblast donors at both time points. The donors for which WISP-1 protein was detected do not correspond to the highest WISP-1 expressing fibroblast donors at the mRNA for both control and IPF cells.

In IPF fibroblast lysates bands were present at a higher molecular weight than the 37-50kDa full length WISP-1 band. These bands were around 100kDa, similar to the higher MW band present in A549 cell lysates. The detection of multiple bands alongside that considered to the major canonical form of WISP-1 (full length) has been reported for other members of the CCN family (224). In this review it was suggested that such bands may correspond to multimers of the CCN protein, or protein-complexes containing the CCN protein, that are resistant to commonly used denaturing agents. Pre-adsorbing the WISP-1 antibody with recombinant protein would demonstrate whether or not these higher MW bands correspond to complexes containing WISP-1.

In A549 cells, comparable levels of WISP-1 were detected at the mRNA level 0.5% FBS and 10% FBS containing medium suggesting that a factor in FBS is not stimulating the expression of WISP-1 in these cells. Alternatively, the presence of WISP-1 in 10% FBS containing medium lysates could be WISP-1 from the FBS that is bound to the cell surface. Subsequently, cells were treated in 0.5% FBS containing medium then switched to 10% FBS medium for a short period of time at the end of the experiment. WISP-1 was only detected in the TNFα-stimulated sample suggesting that the WISP-1 detected previously was not from the FBS. Another possibility is that the short length of time that 10% FBS containing medium was added to the cells was not long enough for WISP-1 present in the FBS to bind to the cell surface. A third potential explanation for the lack of WISP-1 detected in 0.5% FBS containing medium samples could be that lower levels of WISP-1 or a factor stimulating its expression were present in the particular batch of FBS used in comparison to the earlier experiment.

The presence of a band in the TNFα-stimulated lysates in this experiment could suggest that TNFα stimulated WISP-1 binding to the cell surface. This was also suggested by the presence of a band at 37kDa in cells treated with TNFα + WISP-1 in the subsequent experiment. However, no effect was observed where WISP-1 was not exogenously added. This could possibly be explained by batch-to-batch

variation in FBS or the difference in the length of this experiment compared to earlier experiments.

Other possible explanations for the lack of WISP-1 detected in cell lysates cultured in 0.5% FBS containing medium could be that a factor in FBS stimulates the translation of WISP-1 mRNA to protein. An experiment carried out in which cells are cultured in 10% FBS containing medium with and without a protein translation inhibitor could demonstrate whether this is the case. Detection of WISP-1 protein in cells cultured with such an inhibitor would suggest that the WISP-1 being measured was not newly synthesised within the cell. Alternatively, a factor in FBS could stimulate the release of WISP-1 from the cell rather than stimulating its translation. Use of an antibiotic to disrupt protein secretion could provide an insight into whether this accounts for the lack of WISP-1 in 0.5% FBS medium lysates.

Secretion of WISP-1

The lack of detectable WISP-1 in cell culture supernatants from both primary parenchymal fibroblast and A549 cells suggests that either the levels of secreted WISP-1 are not high enough to be detected by this assay or that WISP-1 is not secreted by the cells studied. WISP-1 detection using the same ELISA kit as used here has been reported in the literature. For example, Berschneider et al. (125) reported detection of increased WISP-1 in supernatants from TGFβ_1-stimulated primary human lung fibroblasts. The amount of WISP-1 detected in some samples in this study are below the level of detection for this assay suggesting that the authors may have had to concentrate the supernatants. In a more recent study in primary lung fibroblasts, supernatants were concentrated to allow detection of WISP-1 (198). This assay has also been reported to detect secreted WISP-1 without concentration of supernatant in oesophageal carcinoma cells (225).

An alternative method to determine whether or not WISP-1 protein is present in the supernatant could be to pull out the proteins from the medium using a resin such as strata clean. This could then be probed by western blotting using the antibody used to detect WISP-1 in cell lysates. Should none be detected it may mean that either WISP-1 is not secreted from these cells or that it is secreted from the cell where it becomes associated with the cell surface.

A further possible explanation for the lack of WISP-1 detected in cell culture supernatants may be that secreted WISP-1 binds to a soluble receptor or a binding partner in the supernatant which blocks the epitope for one of the antibodies used in the assay as has been reported for WISP-1 binding to decorin and biglycan in skin fibroblast conditioned medium (190). Alternatively, WISP-1 could be secreted from the cell where it then becomes associated with the matrix or cell surface and is therefore not detected in the supernatant. It has been reported that this is the case for Cyr61 (CCN1). In a study by Yang et al. (226), Cyr61 was shown to bind to both the cell surface and the extracellular matrix once secreted from the cells.

Though the CCN family of proteins are typically thought to be secreted there is evidence to suggest that this may always be the case (224). For example, Steffen et al. (160) found that full length CTGF was primarily detected in human foreskin fibroblast lysates and not in the cell culture medium from these cells. In MRC5 cells, TGFβ_1-induced CTGF has been detected by mass spectrometry in cell lysates but not in corresponding supernatants (Leanne Wickens, personal communication). WISP-1 was also not detected in these samples.

There are several methods that could be employed to determine the localisation of WISP-1. A549 cells could be stained for WISP-1 using a reliable antibody. A tagged WISP-1 protein could be added either to A549 cells in culture or to a decellularised matrix to see whether there is any binding to the cell surface or to the matrix. This could be detected by staining for the tag rather than for WISP-1.

The role of post-translational modifications in the regulation of interactions between CCN proteins and different binding partners is an aspect of CCN biology yet to be fully elucidated. This could impact on both the structure and function of WISP-1 and therefore its detection. Another important aspect of WISP-1 biology to be considered when trying to detect its expression is alternative splicing. Several alternatively spliced variants of WISP-1 have been reported in the literature (see chapter 4), each missing one or more whole exons. Each exon codes for a protein domain therefore a variant missing one exon would be missing one full protein domain when translated. The epitopes of several antibodies tested are unknown meaning that an alternatively spliced variant would not be detected if the epitopes for the antibody lie within the missing domain.

3.3.1 Conclusions

As hypothesised, higher levels of WISP-1 mRNA were detected in IPF fibroblasts compared to control when unstimulated. In primary parenchymal fibroblasts, there was a trend for $TGF\beta_1$ to suppress WISP-1 mRNA expression similar to that observed in MRC5 cells. WISP-1 expression was not clearly regulated by $TNF\alpha$ in primary fibroblasts, unlike in MRC5 cells.

In A549 cells, WISP-1 mRNA expression was induced by both $TGF\beta_1$ and $TNF\alpha$ treatments alone. Treatment with both cytokines did not stimulate WISP-1 mRNA expression further. This could suggest that WISP-1 plays a role in the transition from an epithelial to a mesenchymal phenotype in these cells, perhaps being involved in the induction of some of the phenotypic changes or in this persistence of the phenotype.

WISP-1 protein expression was detected in primary parenchymal fibroblast and A549 cell lysates using a polyclonal antibody from R&D. WISP-1 protein was only detected in lysates cultured in 10% FBS containing medium suggesting that perhaps a factor present in FBS stimulates WISP-1 translation or secretion. WISP-1 was not detected in corresponding supernatants from primary parenchymal fibroblast and A549 cells.

The problems encountered in detecting WISP-1 protein likely reflect the complex biology of the CCN family of proteins, therefore this should be considered in future studies. For example, expression of alternatively spliced variants could potentially influence several aspects of WISP-1 biology yet this is not widely recognised in the literature in studies investigating its expression and activity.

Chapter 4: Characterisation of WISP-1 splice variant expression

4.1 Introduction

The human WISP-1 gene consists of five exons separated by four introns. Each WISP-1 protein domain (as well as the signal peptide) arises from one of the five exons. Expression of alternatively spliced variants has been reported in the literature for several of the CCN family members as well as other variants being documented in genomic databases. For WISP-1, five variants (including full length) are reported (Figure 45).

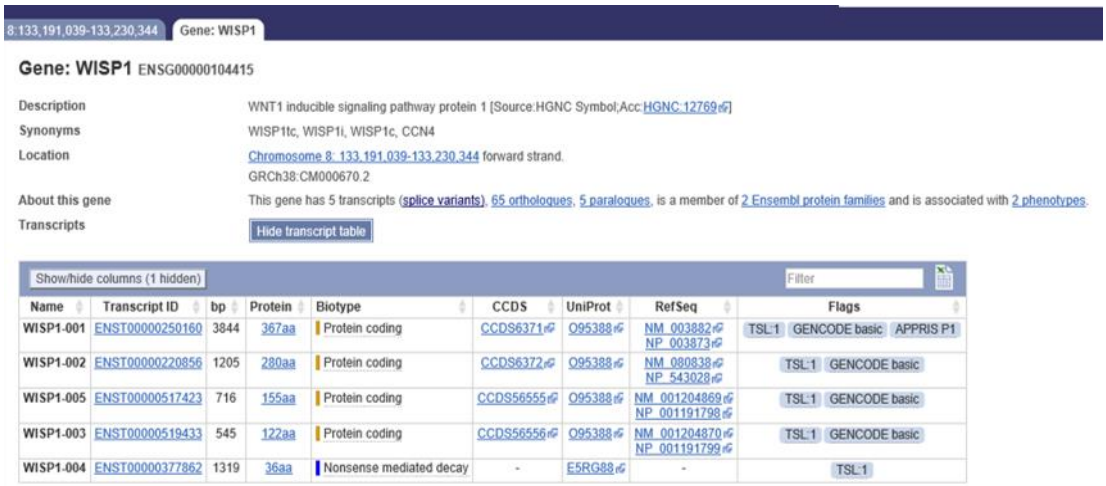
8:133,191,039-133,230,344 Gene: WISP1

Gene: WISP1 ENSG00000104415

Description	WNT1 inducible signaling pathway protein 1 [Source:HGNC Symbol;Acc:HGNC:12769]
Synonyms	WISP1tc, WISP1i, WISP1c, CCN4
Location	Chromosome 8: 133,191,039-133,230,344 forward strand. GRCh38:CM000670.2
About this gene	This gene has 5 transcripts (splice variants), 65 orthologues, 5 paralogues, is a member of 2 Ensembl protein families and is associated with 2 phenotypes.
Transcripts	Hide transcript table

Show/hide columns (1 hidden) Filter

Name	Transcript ID	bp	Protein	Biotype	CCDS	UniProt	RefSeq	Flags
WISP1-001	ENST00000250160	3844	367aa	Protein coding	CCDS6371	O95388	NM_003882 NP_003873	TSL:1 GENCODE basic APPRIS P1
WISP1-002	ENST00000220856	1205	280aa	Protein coding	CCDS6372	O95388	NM_080838 NP_543028	TSL:1 GENCODE basic
WISP1-005	ENST00000517423	716	155aa	Protein coding	CCDS56555	O95388	NM_001204869 NP_001191798	TSL:1 GENCODE basic
WISP1-003	ENST00000519433	545	122aa	Protein coding	CCDS56556	O95388	NM_001204870 NP_001191799	TSL:1 GENCODE basic
WISP1-004	ENST00000377862	1319	36aa	Nonsense mediated decay	-	E5RG88	-	TSL:1

Figure 45. Screenshot of Ensembl database listing for human WISP-1 gene showing the 5 transcript variants. WISP1-001 – full length, WISP1-002 – variant 2, WISP1-005 – variant 3, WISP1-003 – variant 4, WISP1-004 – variant 5 (227)

WISP-1 variant 2

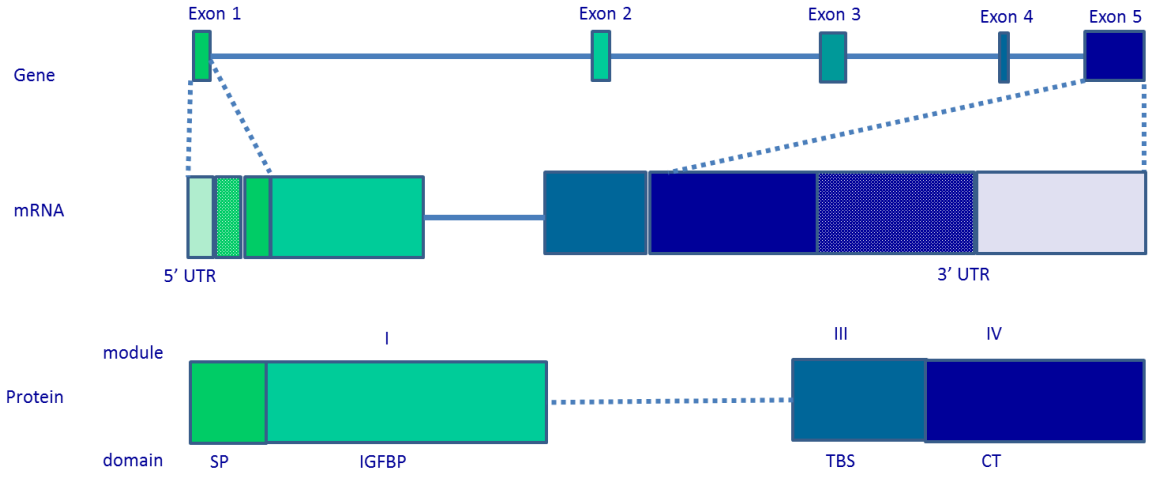

Figure 46. Representation of human WISP-1 variant 2 gene, transcript and protein domains. Adapted from (228)

WISP-1v2 (shown in Figure 46) is the first most commonly reported alternatively spliced variant of WISP-1in the literature. This transcript is missing exon three which encodes the VWC domain in the wild type mRNA. WISP-1v2 transcript is 1205 base pairs and the protein 280 amino acids long.

Expression of this variant has been reported in different pathological circumstances. Tanaka et al. (163) reported expression of WISP-1v2 in scirrhous carcinoma tissues of the stomach but not in adjacent normal mucosa. The authors also reported that when overexpressed WISP-1v2 enhanced the invasive phenotype of gastric carcinoma cells, an effect not observed with overexpression of full length WISP-1. In a later study (162), the same authors reported expression of WISP-1v2 in the liver. WISP-1v2 was found to be expressed in cholangiocarcinoma tissue but not in adjacent uninvolved liver tissue. This expression was associated with increased invasion of tumour cells and poor prognosis.

Cervello et al. (164) reported WISP-1v2 expression in 2 different hepatocellular carcinoma cell lines. Their results suggested that WISP-1v2 expression was not related to the grade of cell differentiation and was independent of activated Wnt/β-catenin signalling. In a study looking at various different cell types, Yanagita et al. (127) measured the expression of WISP-1v2 in various different cell

types. They reported WISP-1v2 expression in chondrosarcoma-derived chondrocytic cells and human osteoblastic cells but not in several other cell lines tested including HeLa and HEK293.

Expression of WISP-1v2 has also been reported in a non-pathological setting. Inkson et al. (183) detected WISP-1v2 in human bone marrow stromal cells (HBMCs). In this study, WISP-1v2 was reported to induce proliferation when overexpressed as was observed with overexpression of full length WISP-1.

WISP-1 variant 3

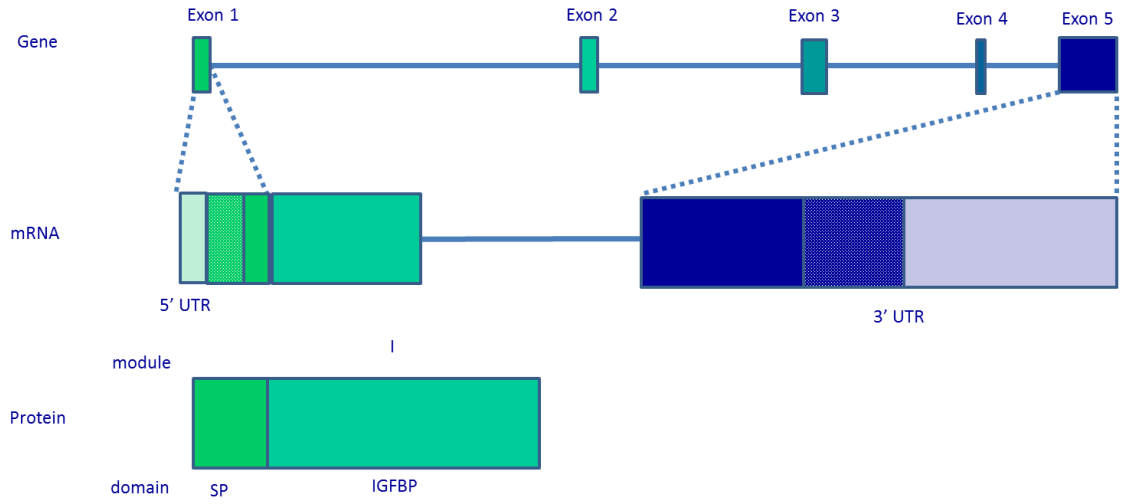

Figure 47. Representation of human WISP-1 variant 3 gene, transcript and protein domains. Adapted from (228)

Another alternatively spliced variant of WISP-1, WISP-1v3 (shown in Figure 47), is missing exons three and four. The joining of exons two and five creates a frameshift resulting in premature termination of translation (164). WISP-1v3 protein therefore only contains the signal peptide and IGFBP domain. WISP-1v3 transcript is 716 base pairs and the protein 155 amino acids long.

Expression of this variant has also been described in the literature. Cervello et al. (164) reported WISP-1v3 expression in 2 of 4 human hepatocellular carcinoma cell lines tested along with full length WISP-1 and WISP-1v2. Similarly, Yanagita et al. (127) reported WISP-1v3 expression in chondrosarcoma-derived chondrocytic cells

and not in several other cell lines including HeLa and HEK293. However, unlike WISP-v2, WISP-1v3 was not detected in human osteoblastic cells.

WISP-1 variant 4

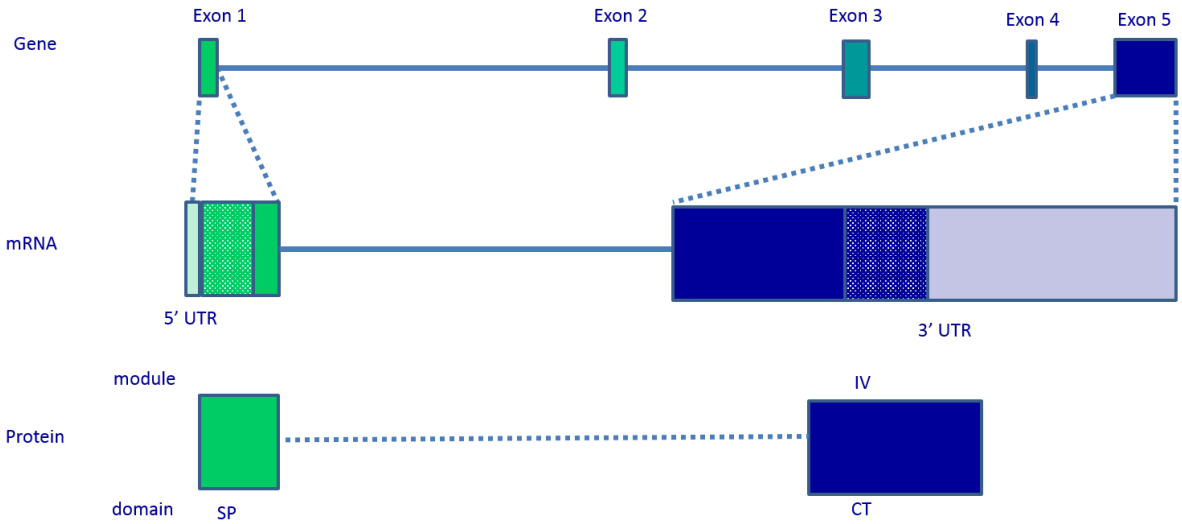

Figure 48. Representation of human WISP-1 variant 4 gene, transcript and protein domains. Adapted from (228)

WISP-1 variant 4 (WISP-1v4) is predicted to be a protein-coding splice variant of WISP-1 (Figure 48). Expression of this variant has not been reported in the scientific literature. It is missing part of the 5'UTR (exon one), exons two, three and four, and part of the 3'UTR (exon five). This translates to a protein containing the signal peptide and cysteine knot domain. WISP-1v4 transcript is 545 base pairs and the protein is 122 amino acids long.

A fifth variant of WISP-1 documented in genomic databases (WISP-1v5) is predicted to undergo nonsense-mediated decay (227). Expression of this transcript has not been reported in the literature.

The large number of interacting proteins and different effects attributed to the various CCN proteins in different tissues has given rise to the school of thought that any particular function of a CCN protein can be attributed to one individual domain or multiple domains acting in concert (136).

Figure 49. Primers for WISP-1 detection by qPCR. WISP-1 exon sequence. Highlighted region indicates primers and arrows indicate direction. Grey font indicates untranslated region.

This has been demonstrated recently for WISP-1 in a study aiming to elucidate how WISP-1 mediates its downstream effects by integrins (137). The authors reported that WISP-1-mediated adhesion of A549 cells was regulated by the C-terminal domains of WISP-1 and that this was integrin-driven. Activation of β-catenin signalling in, and CXCL3 secretion by NRK-49F cells observed following WISP-1 stimulation was also attributed to the C-terminal domains of the protein. However, this second aspect of function was not mediated by the integrins studied, highlighting both the potential importance of differential variant expression and that two effects mediated by the same domain(s) may act via different mechanisms e.g. through interaction with different binding partners.

The expression of WISP-1 splice variants in different tissues is not well characterised and the expression in control and fibrotic lung does not appear to have been reported in the scientific literature to date. WISP-1 mRNA data presented in chapters 3 and 4 relates to the expression of all WISP-1 variants

amplified by the primer set used. As shown in Figure 49, the binding sites for this primer set both lie in exon 5 allowing all 4 protein-coding variants to be amplified. Changes in the expression of any one particular variant are not detected by this method.

Hypotheses and objectives

The potential importance of missing domains in CCN proteins including WISP-1 has been recognised in the literature however this expression of different variants has not been investigated in control or fibrotic lung. Considering this, the hypotheses for this study are as follows:

1) Expression of WISP-1 splice variant transcripts is altered in the IPF donor-derived lung fibroblasts compared to control cells
2) Expression of WISP-1 splice variant transcripts is altered following fibroblast to myofibroblast differentiation in primary parenchymal lung fibroblasts
3) Expression of WISP-1 splice variant transcripts is altered following the induction of epithelial to mesenchymal transition in the alveolar epithelial cell line A549

In order to investigate these hypotheses, the aims of this study are to:

1) Set up assays to identify and quantify individual transcript variants
2) Analyse the expression of different transcript variants in:
    i. alveolar epithelial cells at baseline and following induction of epithelial to mesenchymal transition
    ii. fibroblasts at baseline and following differentiation into a myofibroblast phenotype

4.2 Results

4.2.1 Assay for the detection of WISP-1 splice variants

In order to quantify the relative amounts of each splice variant in a given sample, primers were designed to bind to allow amplification of one variant only. To distinguish between individual variants of WISP-1, one of the primer pair must cross an exon boundary:

- Variant 2 is missing exon 3 → exon 2-4 boundary
- Variant 3 is missing exons 3 and 4 → exon 2-5 boundary
- Variant 4 is missing exons 2, 3 and 4 → exon 1-5 boundary
- Each alternatively spliced variant is missing exon 3 therefore primers across the exon 2-3 boundary should only allow amplification of full length WISP-1

Primers were designed for each variant using NCBI Primer-BLAST. Each forward primer crosses the appropriate exon boundary for the variant as shown in figures 50-53. A test qPCR was carried out for each primer set and melt curves run to check primers (Figure 54).

Figure 50. Primers for amplification of full length WISP-1 only. 5' primer crosses exon 2-3 boundary. Each paragraph represents one exon.

Figure 51. Primers for amplification of WISP-1 variant 2 only. 5' primer crosses exon 2-4 boundary. Each paragraph represents one exon.

Figure 52. Primers for amplification of WISP-1 variant 3 only. 5' primer crosses exon 2-5 boundary. Each paragraph represents one exon.

Figure 53. Primers for amplification of WISP-1 variant 4 only. 5' primer crosses exon 1-5 boundary. Each paragraph represents one exon.

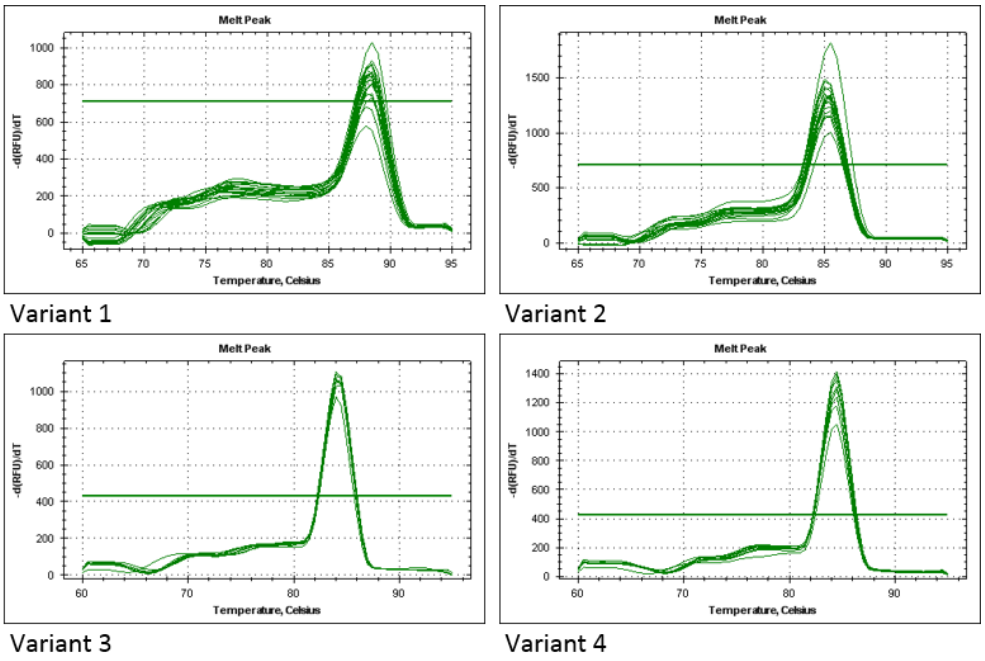

Figure 54. Melt peak for each primer set detailed in figures 48-51.

4.2.2 Expression of WISP-1 splice variants in A549 cells

WISP-1 splice variant expression was measured in A549 cells using cDNA samples from experiments carried out in chapter 3. The expression of each variant was measured by qPCR using the primers designed above. Data are presented here relative to the untreated value from each individual experiment to observe the response to stimuli rather than variation between experiments (or donors/experiments for primary parenchymal fibroblasts). For all samples tested, the Ct values for full length WISP-1 expression were above 30 cycles and therefore data is not shown.

The expression of WISP-1 splice variants in TGFβ_1-stimulated A549 cells is shown in Figure 55. When expressed relative to the untreated value from each individual experiment, total WISP-1 mRNA express was increased by TGFβ_1 in a bell-shaped response in 0.5% FBS containing medium, however this was not statistically significant. In 10% FBS containing medium total WISP-1 mRNA were lower in cells

treated with the higher doses of TGFβ$_1$, 10 and 25ng/ml.. WISP-1 variant 3 expression was suppressed by TGFβ$_1$ in 10% FBS containing medium however this was not statistically significant. A greater effect was observed on variant 4 mRNA expression in these cells. There was a trend for induction of WISP-1 variant 4 by TGFβ$_1$ in a bell-shaped response in both 0.5% and 10% FBS containing medium however this was not statistically significant.

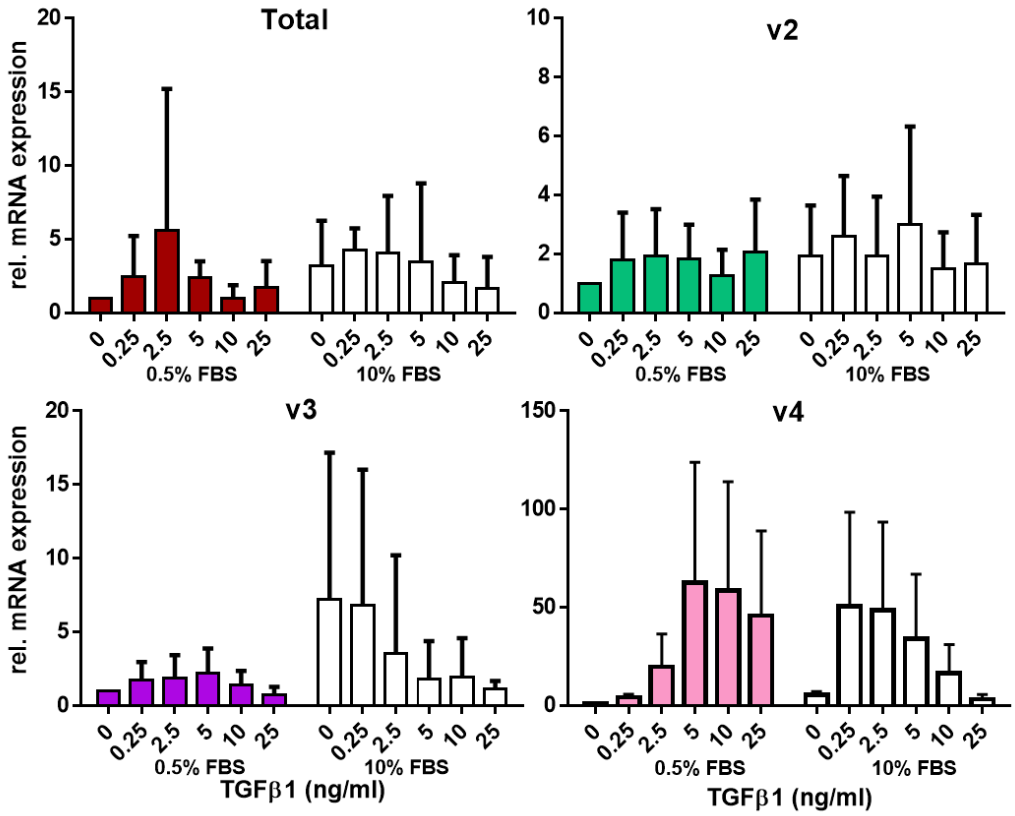

Figure 55. Expression of WISP-1 splice variants in A549 cells following TGFβ$_1$ stimulation. Experiment carried out as in **Figure 32**. Data are expressed relative to untreated sample in 0.5% FBS containing media within each experiment and are presented as mean ± SD. Total n=5-6 , variant 2 n=5-6, variant 3 n=4-6, variant 4 n=5-6. Statistical significance was tested by two-way ANOVA with Bonferroni correction. Ct values were between 28 and 30, 22 and 26, and 26 and 28 for variants 2, 3 and 4 respectively in unstimulated cells.

WISP-1 variant expression in TNFα treated A549 cells in shown in Figure 56. There was a trend for total WISP-1 and WISP-1 variant 2 to be induced in a dose-dependent fashion by TNFα in 0.5% FBS containing medium however this was not statistically significant. A small increase in WISP-1 variants 3 and 4 was observed with 10, 50 and 100ng/ml TNFα in 0.5% FBS containing medium however this was not significant. In 10% FBS containing medium expression of WISP-1 variants 2, 3 and 4 was increased at the lower doses of TNFα (0.1 and 1 ng/ml) however this was not statistically significant.

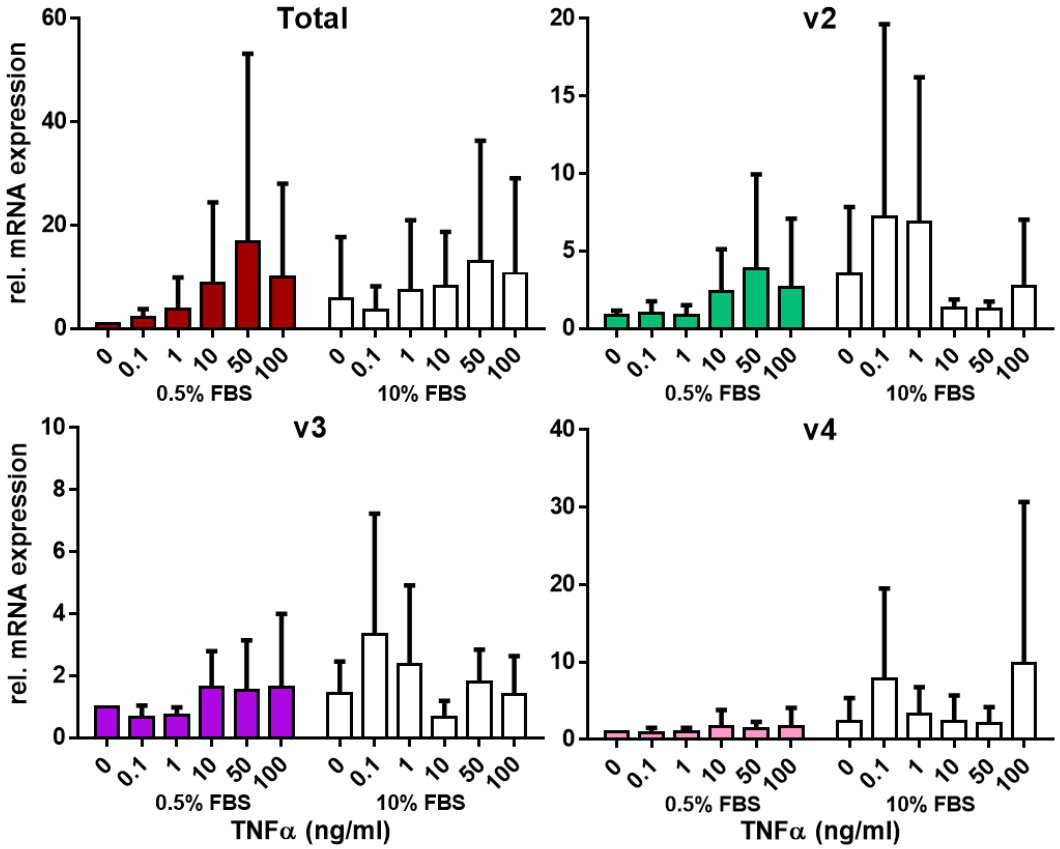

Figure 56. Expression of WISP-1 splice variants in A549 cells following TNFα stimulation. Experiment carried out as in **Figure 35**. Data are expressed relative to untreated sample in 0.5% FBS containing media within each experiment and are presented as mean ± SD. Total n=4-6, variant 2 n=5-6, variant 3 n=4-6, variant 4 n=5-6. Statistical significance was tested by two-way ANOVA with Bonferroni correction.

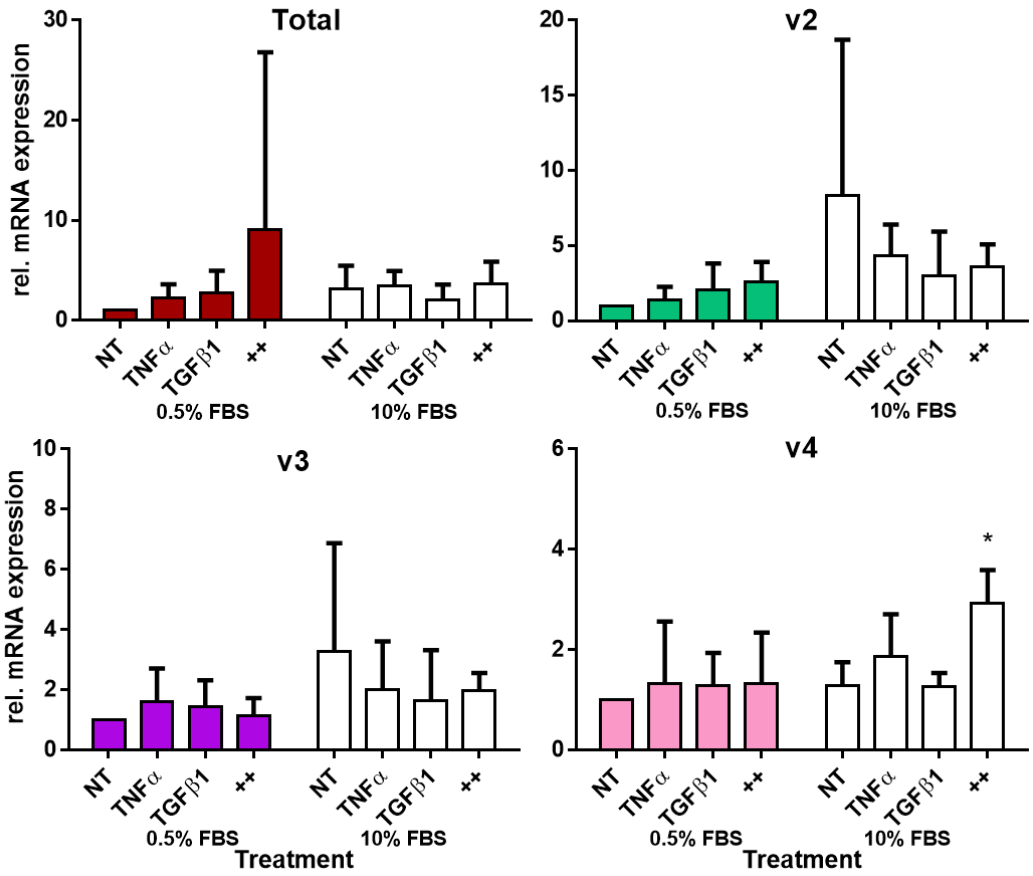

Figure 57. Expression of WISP-1 splice variants in A549 cells following TNFα and TGFβ$_1$ stimulation. Experiment carried out as in **Figure 38**. Data are expressed relative to untreated sample in 0.5% FBS containing media within each experiment and are presented as mean ± SD. Total n=5-6, variant 2 n=5-6, variant 3 n=4-6, variant 4 n=5-6. Statistical significance was tested by two-way ANOVA with Bonferroni correction. * indicates significantly different to untreated samples, x indicates significantly different compared to TGFβ$_1$ alone. * p=<0.05

In cells co-treated with TGFβ$_1$ and TNFα, total WISP-1 mRNA expression was increased compared to TNFα or TGFβ$_1$ alone in 0.5% containing medium however this was not statistically significant (Figure 57). WISP-1 variant 2 expression was decreased in 10% FBS containing medium compared to unstimulated cells however this was not statistically significant. Little effect of treatment was observed on WISP-1 variant 3 mRNA expression in 0.5% FBS containing medium. In 10% FBS containing medium, the expression of WISP-1 variant 3 was lower in all

treated cells compared to unstimulated however this was not statistically significant. No effect of treatment was observed on WISP-1 variant 4 expression in 0.5% FBS containing medium however in 10% FBS containing medium WISP-1 variant 4 mRNA expression was stimulated by co-treatment with TNFα and $TGF\beta_1$. This increase was statistically significant compared to both unstimulated cells and $TGF\beta_1$ treated cells ($p=\leq 0.05$).

4.2.3 Expression of WISP-1 in primary parenchymal fibroblasts

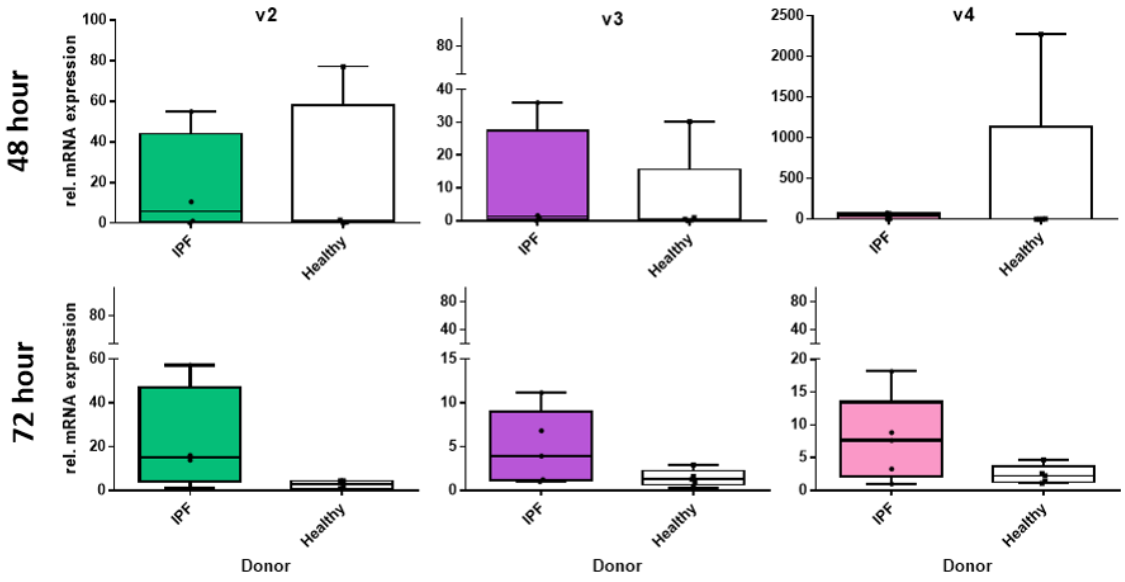

Figure 58. Relative expression of WISP-1 variants 2, 3 and 4 in unstimulated parenchymal fibroblasts from IPF and control donors. Expressed relative to the expression of one IPF donor at each time point. Top panel – 48 hours, Bottom panel – 72 hours. Variant 2 n=4 IPF and 4 control, variant 3 n=4 IPF (48hr), 5 IPF (72hr) and 5 control, variant 4 n=4 IPF (48hr), 5 IPF (72hr) and 5 control. Normality testing for these samples is shown in Appendix 2.

WISP-1 splice variant expression was measured in primary parenchymal fibroblasts using cDNA samples from fibroblast experiments in chapter 3. Figure 58 shows the expression of WISP-1 variants 2, 3 and 4 in unstimulated fibroblasts. At 48 hours, expression of each variant was highly variable between

donors, both in fibroblasts from IPF and control donors. At 72 hours, expression was of each variant was variable in IPF donors. Expression in control donors was less variable and appeared to be lower than that in IPF cells however this was not statistically significant. No WISP-1v2 was detected in one control donor.

Expression of WISP-1 variants 2, 3 and 4 was also measured in primary parenchymal fibroblasts stimulated with TGFβ_1 and TNFα. As with A549 variant expression, these data are presented relative each donor expressed relative to its own expression when untreated in 0.5% FBS containing medium, to allow an effect of treatment to be observed rather than variability between experiments/donors.

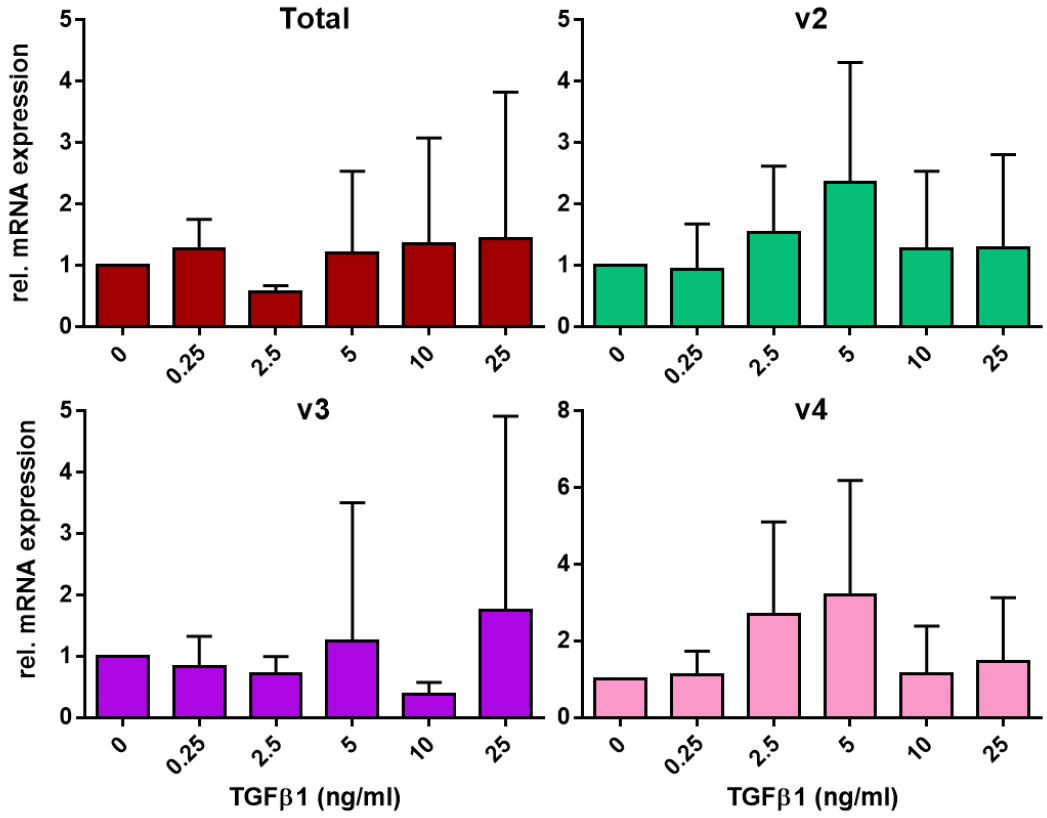

Figure 59. Expression of WISP-1 splice variants in IPF fibroblasts following TGFβ_1 stimulation 0.5% FBS medium. Experiment carried out as in **Figure 24**. Data are expressed relative to untreated sample for each individual donor in 0.5% FBS containing media and are presented as mean ± SD. Total WISP-1 n=4-5, variant WISP-1 n=3-4. Friedman statistical test was used to determine statistical difference between untreated and treated samples.

In IPF donor-derived fibroblasts (Figure 59) WISP-1 variants 2 and 4 were stimulated by TGFβ$_1$ in a bell-shaped response however this was not statistically significant. WISP-1v3 mRNA expression appeared to be suppressed by TGFβ$_1$ at 10ng/ml but this was not statistically significant. In control donor-derived fibroblasts there was a trend for total WISP-1 mRNA induction by TGFβ$_1$ (Figure 60). Little effect of treatment on WISP-1v2 expression was observed in these cells. The mean expression of WISP-1v3 was increased at 2.5 and 10ng/ml TGFβ$_1$ however this was not significant. WISP-1v4 was increased at 2.5ng/ml TGFβ$_1$. Again, this was not statistically significant.

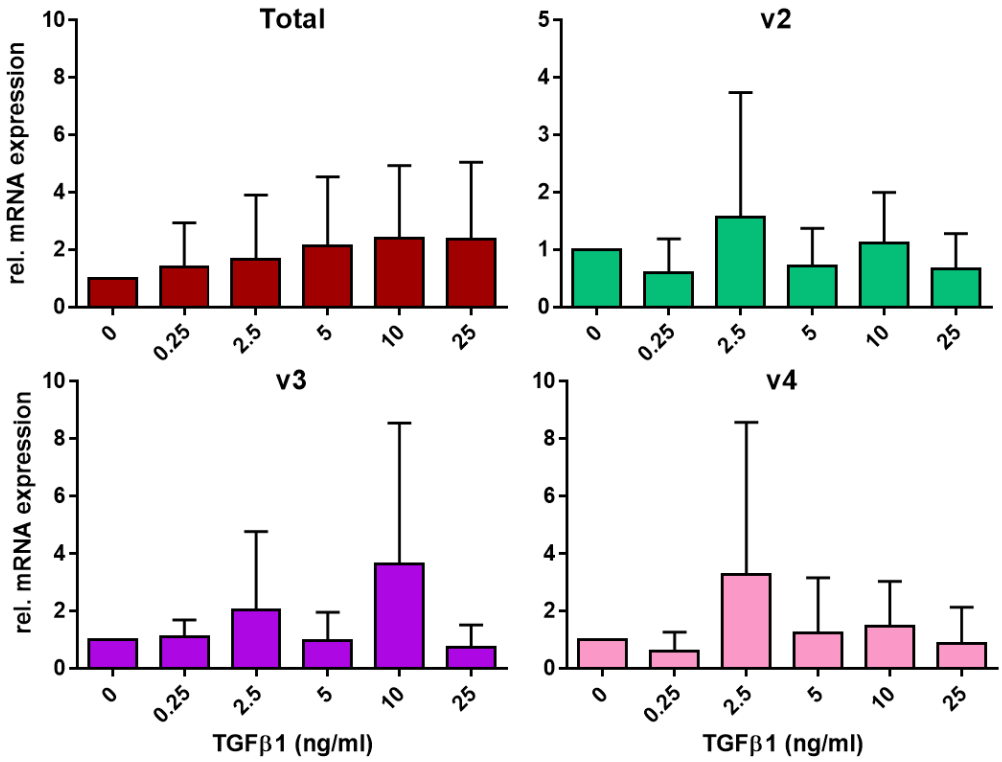

Figure 60. Expression of WISP-1 splice variants in control fibroblasts following TGFβ1 stimulation 0.5% FBS medium. Data are expressed relative to untreated sample for each individual donor in 0.5% FBS containing media and are presented as mean ± SD. Total WISP-1 n=4-5, variant 2 n=3-4, variant 3 n=3-5, variant 4 n=4-5. Friedman statistical test was used to determine statistical difference between untreated and treated samples. Mann Whitney U test was used to determine statistical difference between IPF (Figure 59) and control fibroblasts at each dose for each variant.

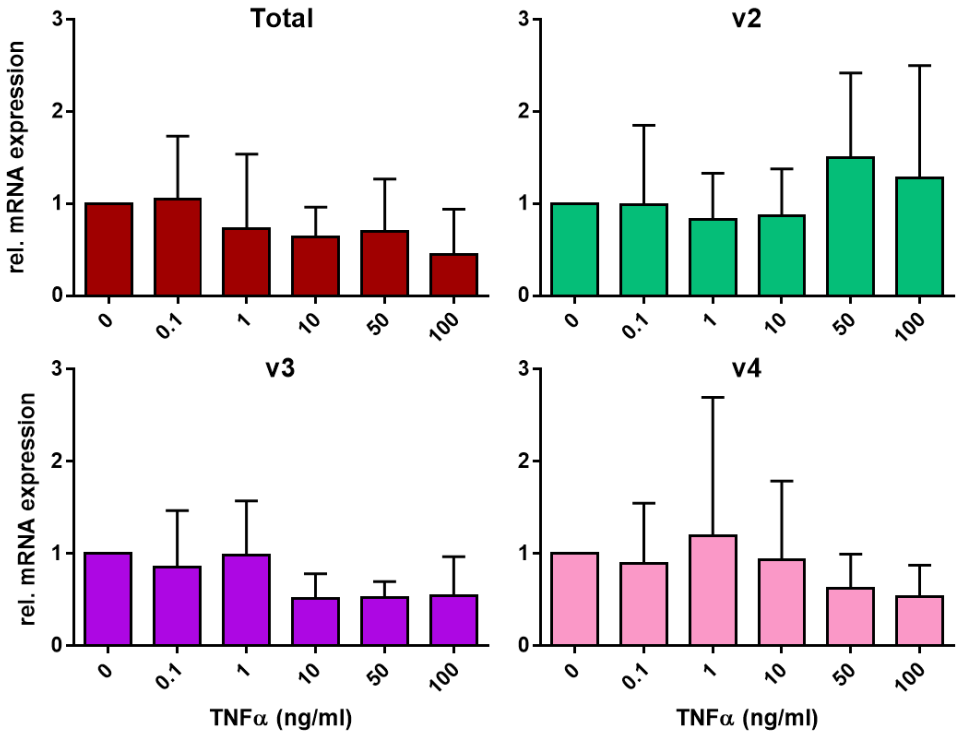

Figure 61. Expression of WISP-1 splice variants in IPF fibroblasts following TNFα stimulation 0.5% FBS medium. Experiment carried out as in **Figure 27**. Data are expressed relative to untreated sample for each individual donor in 0.5% FBS containing media and are presented as mean ± SD. Total WISP-1 n=4-5, variant 2 n=3-4, variant 3 n=3-5. Friedman statistical test was used to determine statistical difference between untreated and treated samples.

The expression of WISP-1 variants in TNFα-stimulated IPF fibroblasts is shown in Figure 61. There was a trend for total WISP-1, and WISP-1 variants 3 and 4 to be decreased with the higher doses of TNFα. Mean variant 2 expression was increased in these conditions however this was not significant. In control donor-derived fibroblasts, little effect of TNFα treatment was observed (Figure 62). In these cells the mean expression of WISP-1v3 was increased with 1ng/ml TNFα but this was not statistically significant.

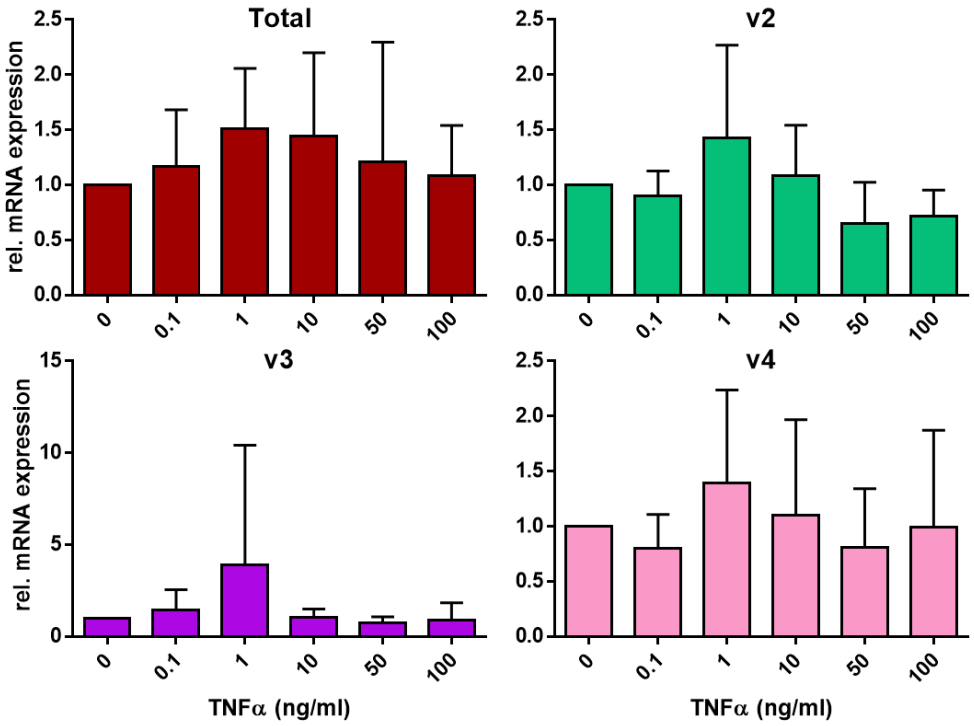

Figure 62. Expression of WISP-1 splice variants in control fibroblasts following TNFα stimulation 0.5% FBS medium. Experiment carried out as in **Figure 27**. Data are expressed relative to untreated sample for each individual donor in 0.5% FBS containing media and are presented as mean ± SD. Total WISP-1 n=4-5, variant 2 n=3-4, variant 3 n=4-5, variant 4 n=4-5. Friedman statistical test was used to determine statistical difference between untreated and treated samples. Mann Whitney U test was used to determine statistical difference between IPF (Figure 61) and control fibroblasts at each dose for each variant.

Summary

In A549 cells, there was a trend for a bell-shaped induction of WISP-1 variant 4 by $TGF\beta_1$. In TNFα treated cells there was a small, dose-dependent increase in the expression of the three WISP-1 splice variants however this was not statistically significant. Co-treatment of A549 cells with $TGF\beta_1$ and TNFα stimulated a significant increase in WISP-1 variant 4 expression in 10% FBS containing medium compared to both unstimulated cells and cells treated with $TGF\beta_1$ alone.

The expression of WISP-1 splice variants was variable between experiments, particularly in IPF fibroblasts, possibly reflecting inter-donor variation in WISP-1

expression. In unstimulated cells at 72 hours, the expression of each variant was higher in IPF fibroblasts was higher than that in control cells however this was not statistically significant. There was a trend for WISP-1 variant 2 and 4 induction in TGFβ_1-stimulated IPF fibroblasts, and increased variant 4 in control fibroblast. Little effect of TNFα treatment on WISP-1 splice variant expression was observed.

4.3 Discussion

The CCN family of proteins contain an N-terminal secretory signal peptide and four functional domains. Each functional domain is encoded by a separate exon. The effects of the different CCN proteins have in many instances been attributed to one domain therefore the loss of one or more domains through alternative splicing of exons is likely to impact on the function of the CCN protein. The varied binding partners/interactions detailed for WISP-1 and the other CCN proteins (see chapter 1) highlights both the complexity of CCN biology, and the potential impact of differential splice variant expression. Of particular interest/relevance for the current study of WISP-1 in lung fibrosis are the reported binding sites for TGFβ/BMP, various integrins and HSPGs present in specific CCN protein domains.

A549 variant expression

In the current study, some changes in the expression of each WISP-1 variant were detected in A549 cells. There was a trend for TGFβ_1 stimulated expression of WISP-1 variant 4 in a bell-shaped response and this was significantly enhanced by co-treatment with TNFα in 10% FBS containing medium, as has been reported for EMT markers in these cells, chapter 3 and (204). In these samples, there was altered mRNA expression of different genes suggestive of EMT (chapter 3) which may suggest a role for this variant in the epithelial to mesenchymal transition process in these cells.

WISP-1 variant 4 contains only the CT (cysteine knot) domain out of the four functional WISP-1 domains. This domain is thought to be responsible for protein-protein interactions involving the CCN proteins, and dimerisation/multimerisation of the CCN proteins (138). Domains containing a cysteine knot motif such as that

found in the CCN CT domain are thought to be responsible for binding to heparin and heparin sulphate proteoglycans (HSPGs) in other proteins (151). Whilst WISP-1 does not contain the proposed heparin binding site present in some of the other CCN proteins, it has been reported to bind to the HSPGs decorin and biglycan (190).

Increased expression and subsequent binding of WISP-1 variant 4 to such molecules would limit the availability of said molecules for full length or variant 2 WISP-1 to bind to. This would not affect WISP-1 variant 3 due to its lack of CT domain. This could potentially affect the activity of WISP-1 in different ways. For example, it may be the case that WISP-1 binding to HSPGs in the ECM prevents WISP-1 binding to a receptor and therefore limits the effect of WISP-1 on a particular cell type. Decreased binding of full length WISP-1 (or variant 2) to said HSPGs caused by limited availability of these molecules would therefore leave WISP-1 free to bind to a receptor. Alternatively, binding of WISP-1 to HSPGs (or other molecules) may anchor WISP-1 in the ECM where it can interact with other binding partners to enhance or dampen their activity. Decreased binding would therefore reduce the effect of WISP-1 on the activity of its binding partner(s). Whether such an effect of WISP-1 variant 4 would be pro- or anti-fibrotic would be dependent on the effect of full length WISP-1 or variant 2 that is being blocked. However, in the current study WISP-1 variant 4 expression was increased in cells undergoing EMT-like changes suggesting that this variant could be involved in inducing some of the changes observed in these cells.

Primary fibroblast expression

Expression of WISP-1 variants 2, 3 and 4 was variable either between experiments or donors however at 72 hours expression was greater in IPF fibroblasts, as was observed for the overall WISP-1 expression in chapter 3.

In IPF fibroblasts, there was a trend for expression of WISP-1v2 to be stimulated by TGFβ_1 in a bell-shaped response, an effect that was not observed in control donor-derived cells. WISP-1 variant 2 is the most well characterised of the WISP-1 splice variants however studies investigating this variant are limited. Its expression has mainly been reported in pathological settings (127, 162-164) where it was been linked to increased invasiveness of tumour cells (162, 163). In normal hBMSCs, overexpression of WISP-1v2 had a similar effect to that of full

length WISP-1 (183). The expression of this variant or others has not been reported in IPF.

WISP-1v2 is missing the VWC domain, the domain which is thought to be responsible for binding to members of TGFβ/BMP family of proteins. WISP-1 has been demonstrated to directly bind to BMP2 in a study investigating its role in osteogenesis (135). Interestingly, the effect of WISP-1 reported in this study was the enhancement of BMP2 activity rather than a direct effect of WISP-1. This was neutralised by blocking the integrin α5β1, the binding site for which is thought to be in the CT domain of WISP-1 and other CCN proteins (138) suggesting that both domains are required for WISP-1 to exert this effect.

Increased expression of WISP-1 variant 2 stimulated by $TGF\beta_1$ in IPF fibroblasts might suggest a pro-fibrotic effect of this variant compared to full length WISP-1. Based on the VWC domain being the putative site for interaction of the CCN proteins with TGFβ and BMPs as has been demonstrated for CTGF (133), it could be speculated that increased expression of WISP-1 variant 2 results in less binding of TGFβ to WISP-1 and therefore less TGFβ anchored in the matrix. Of course should WISP-1 binding to TGFβ through this domain enhance its effects in some way as has been demonstrated for BMP2 (135), and for CTGF binding to TGFβ (133), it may be the case that expression of WISP-1 variant 2 would have an anti-fibrotic effect. Interestingly, in a study investigating osteogenesis $TGF\beta_1$ was able to partially reduce the induction of cell proliferation by WISP-1 variant 2 but not full length WISP-1 suggesting an indirect interaction requiring an additional factor(s) can occur between these two molecules (183).

Other considerations and potential implications

In the current study, full length WISP-1 was not detected within the limits of the assay used in the A549 and primary parenchymal fibroblast cDNA samples tested. This suggests that either very little full length WISP-1 is expressed by these particular cell types or that the primer set used was not suitable for the detection of this transcript. Melt curve analysis (Figure 54) shows that one product was amplified by this primer set however this would have to be sequenced to confirm that it aligns with the full length WISP-1 reference sequence. Considering the detection of bands at the appropriate MW for full length WISP-1 in both primary parenchymal fibroblast and A549 cell lysates in chapter 3, it may be the case that

the assay used here is unsuitable. Alternatively, the WISP-1 protein previously detected may be WISP-1 that was not newly synthesised but stored inside the cell.

The data presented in the current study relate to the expression of alternatively spliced variants of WISP-1. Though not reported for WISP-1 in the literature, other variants of CCN proteins have been detected such as the proteolytic cleaved CTGF fragments present in uterine secretory fluids (149, 229). In the current study, the mRNA levels of WISP-1 splice variants is reported therefore this method would not be suitable for the detection and/or quantitation of WISP-1 fragments that are the result of proteolytic cleavage at susceptible sites.

Any conclusions drawn from the presented data are limited in that this data relates the transcript levels of the WISP-1 variants. There is no indication here as to whether any of these transcripts is translated into protein, and whether they would subsequently be secreted from the cell and become cell- or matrix-associated following secretion. This family of proteins are typically thought to be secreted however there is some evidence to suggest that the CCN proteins may serve nuclear functions. WISP-2 was localised to the cytoplasm and nucleus in human breast tissue (230) and the authors reported that WISP-2 acts as transcriptional repressor through its recruitment to the TGFβRII promoter. This could suggest that these proteins are not secreted from the cell, or alternatively, that they are endocytosed upon receptor binding (139).

The antibody used to detect WISP-1 in lysates from primary parenchymal fibroblasts and A549 cells (chapter 3) did not detect any bands at a lower MW than that expected for full length WISP-1, either because they were not expressed in these cells or because the antibody is unable to detect these variants. The antibody was raised against recombinant WISP-1 containing the four functional domains. This suggests that it should be able to detect each alternatively spliced variant however the number of epitopes for the antibody would likely be reduced where there are missing domains of WISP-1.

Modelling of the structural domains of the CCN family of proteins by Holbourn et al. (136), suggested that the linker/hinge region between the VWC and TBS domains, and the short inter-domain linkers, allow flexibility within the molecule. How this might be affected by missing domain(s) is unclear, and whilst this would

not affect the detection the variants by western blotting, it would affect the detection of native WISP-1 in cell supernatants by ELISA.

4.3.1 Conclusions

Evidence in the literature suggests that WISP-1 exerts its effects through interactions with other proteins that are mediated via one or more its domains acting in concert, highlighting the potential impact of differential splice variation expression.

In A549 cells, the largest effect observed was the induction of WISP-1 variant 4 stimulated by TGFβ_1, and enhanced by co-treatment with TNFα. In primary parenchymal fibroblasts, TGFβ_1 stimulated WISP-1 variant 2 and 4 in IPF cells, and variant 4 in control cells. In unstimulated cells, the expression of each variant was greater in IPF fibroblasts.

The characterisation of WISP-1 splice variants in A549 cells and primary parenchymal fibroblasts has not previously been published to the authors knowledge. This data relates to mRNA expression of WISP-1 variants and whether or not these transcripts are translated and subsequently secreted is unknown therefore there is a need to characterise available antibodies for their ability to detect WISP-1 variants.

Chapter 5: Effect of WISP-1 splice variants

5.1 Introduction

A number of roles have been attributed to WISP-1 in both development and disease, several of relevance to fibrosis. For example, WISP-1 was demonstrated to stimulate the migration of vascular smooth muscle cells in a scratch wound assay (195). In this study, the authors also demonstrated increase cell proliferation following overexpression of WISP-1, an effect that has also been reported for bronchial smooth muscle cells using recombinant human WISP-1 (196). Venkatachalam et al. (194) also reported an effect of WISP-1 on cell proliferation. In this study, WISP-1 was shown to mediate TNFα-stimulated cardiac fibroblast proliferation and collagen synthesis, as demonstrated by knockdown of WISP-1. Induction of MMP9 following stimulation with recombinant WISP-1 has been reported in osteosarcoma cells (187) and synovial fibroblasts (146). In the second study, WISP-1 was found to induce the expression of IL-6. Klee et al. (198) reported that IL-6 induction stimulated by $TGF\beta_1$ or TNFα was mediated by WISP-1. Knockdown of WISP-1 using siRNA resulted in reduced lung fibroblast proliferation following $TGF\beta_1$ or TNFα stimulation.

In a study investigating the role of WISP-1 in pulmonary fibrosis, recombinant WISP-1 was used to demonstrate WISP-1-induced primary murine type II alveolar epithelial cell proliferation, and A549 cell proliferation (124). The authors also reported that WISP-1 stimulated the migration of murine type II alveolar epithelial cells and their expression of MMP7 and MMP9. WISP-1 was also demonstrated to induce mesenchymal cell marker expression and suppress the expression of epithelial cell markers, suggesting that WISP-1 can induce EMT in these cells. In this study, WISP-1 did not stimulate the proliferation of primary fibroblasts but was demonstrated to induce the expression of type I collagen and fibronectin in both cell types and in the murine fibroblast cell line NIH3T3.

Most of these studies investigated the effect of full length WISP-1 via stimulation of cells with recombinant human WISP-1, or through its siRNA/shRNA-mediated knockdown. However, none of these studies investigated the effect of different variants of WISP-1, nor their expression in the cells studied. Studies that have

investigated the effect of different variants of WISP-1 or their expression are limited to a small number, despite the potential for differential effects exerted by different variants. It is therefore unclear whether available antibodies are able to detect WISP-1 variants.

Hypotheses and objectives

Recognising the above, the hypotheses for this study are as follows:

1) Full length WISP-1 stimulates the differentiation of fibroblasts towards a myofibroblast phenotype.
2) Full length WISP-1 stimulates EMT and proliferation of alveolar epithelial cells.
3) These effects are not observed for WISP-1 variants, or are observed to a lesser extent.

In order to investigate these hypotheses, the aims of this study are as follows:

1) Characterise available antibodies for WISP-1 detection by western blotting
2) Confirm the expression of different WISP-1 variants following transfection of expression constructs into HEK293T cells
3) Generate conditioned medium from transfected HEK293T cells for each WISP-1 variant and empty vector
4) Culture MRC5 and A549 cells with conditioned medium from transfected HEK293T cells or recombinant WISP-1 and
    a. observe changes in morphology
    b. measure changes in gene expression
    c. assess cell proliferation
5) Transfect A549 cells with WISP-1 variants to generate stably expressing cells to observe the effect(s) of the different variants on cell phenotype

5.2 Results

5.2.1 Antibody characterisation and expression of WISP-1 variants

To be able to investigate the effect of WISP-1 variants using either conditioned medium or overexpression, confirmation of expression was first required. A polyclonal antibody from R&D was previously used to detect WISP-1 in primary parenchymal fibroblast and A549 cell lysates (chapter 3). However, the reliability of reagents for the CCN family of proteins has been questioned in the literature (224). Therefore the ability of other available antibodies to detect WISP-1 was characterised. The epitope(s) for some of these antibodies is unknown therefore their ability to detect full length WISP-1 was characterised initially. Details of these antibodies, provided by the manufacturer, can be found in Table 23.

Recombinant human WISP-1 was diluted to varying concentrations in sample buffer, blotted and then probed with different WISP-1 antibodies. Initially, rh-WISP-1 from Peprotech was used, and as this was reconstituted in PBS containing 0.2% BSA, a PBS/BSA control was included in these assays. Figure 63 shows Peprotech rhWISP-1 detection by two antibodies from R&D. The monoclonal antibody was unable to detect rhWISP-1 (left). WISP-1 was also not detected when a higher concentration of this antibody was used (data not shown). The biotinylated antibody detected rhWISP-1 at around 37kDa (right) consistent with the predicted MW of WISP-1 (40kDa). Several other bands were detected at both higher and lower MW in lanes containing the highest quantities of rhWISP-1. A band at 37kDa was also detected in the BSA lane, possibly suggesting that BSA may contain WISP-1 as a contaminating protein, or that biotin binds to a molecule present in BSA.

Due to the presence of this band in the BSA lane, his-tagged, NS0-derived rhWISP-1 from R&D was used in subsequent assays as its diluent (PBS) did not contain BSA. This rhWISP-1 has a histidine tag and its predicted MW following SDS-PAGE is 62kDa, according to the manufacturer (R&D) (231). The ability of two further polyclonal antibodies to detect full length WISP-1 was assessed (Figure 64). One antibody against the C-terminal portion of WISP-1 purchased from Abcam was able to detect rhWISP-1 at the highest concentrations used (left). The second antibody, a non-biotinylated version of the polyclonal antibody from R&D, was tested as an alternative to the biotinylated antibody due to possible binding to

BSA. This antibody detected WISP-1 at all concentrations used. As with the biotinylated antibody, additional bands were also detected. These bands are only present in the lanes containing the highest concentrations of WISP-1and therefore represent a small component of the total WISP-1 detected. The higher molecular weight bands may correspond to multimers of WISP-1 that are not suspeceptible to SDS mediated degradation. The lower molecular weight bands could correspond to fragments of WISP-1 generated during lyophilisation, reconstitution or storage. Pre-adsorption of the antibody with recombinant protein would provide confirmation that these bands represent multimers/fragments of WISP-1.

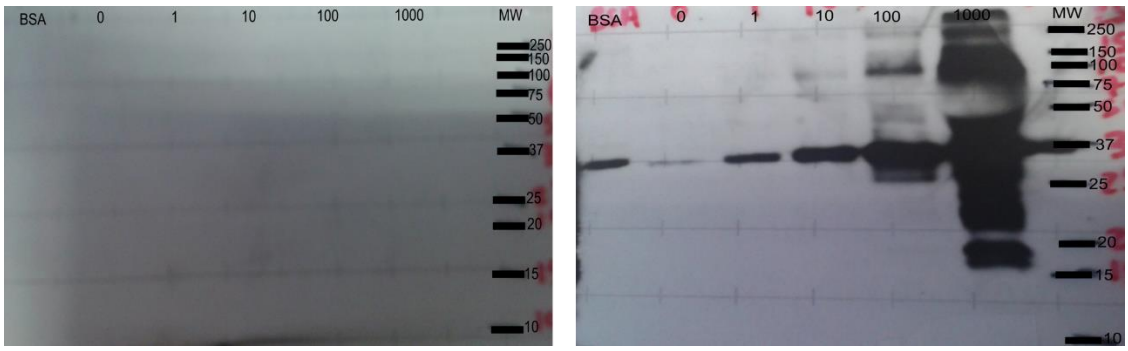

Figure 63. Detection of recombinant human WISP-1 by western blotting. rhWISP-1 (Peprotech) was diluted in sample buffer to indicated concentrations (ng/ml) and was run on a 12.5% SDS-PAGE gel then probed with monoclonal (left) and biotinylated polyclonal (right) antibodies. BSA lane ran as control for rhWISP-1 diluent.

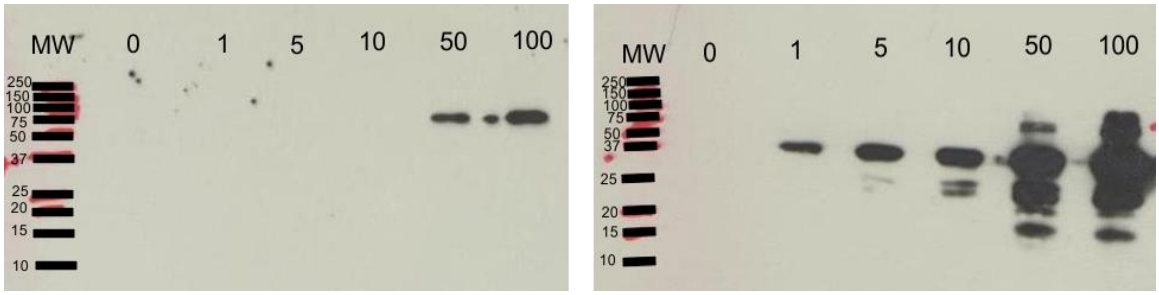

Figure 64. Detection of recombinant human WISP-1 by western blotting. rhWISP-1 (his-tagged, R&D) was diluted in sample buffer to indicated concentrations (x ng/ml) and was run on a 12.5% SDS-PAGE gel then probed with polyclonal antibodies from Abcam (left) and R&D (right).

Next, the ability of these two antibodies to detect HEK293T cell-derived recombinant WISP-1 was tested. HEK293T cells were transiently transfected with pcDNA3.1+ WISP-1, pcDNA3.1+ GFP, or empty vector for 48 hours (2.6.2). Cells were harvested directly in sample buffer and lysates run alongside rhWISP-1 from R&D (Figure 65). The Abcam antibody did not detect HEK293T-derived WISP-1 (left). The non-biotinylated R&D polyclonal antibody detected both rhWISP-1 and WISP-1 from transfected HEK293T cells (right). Several bands were detected in the WISP-1 transfected HEK293T lysate lane, possibly suggesting multimers of WISP-1, or complexes of WISP-1 with another protein.

The specificity of the non-biotinylated polyclonal R&D antibody was further tested by pre-adsorption of the antibody with rhWISP-1 (from R&D) as described in chapter 2. As shown in Figure 66, HEK293T-derived WISP-1 was detected between 37 and 50kDa. Further bands at a higher MW were also present in this lane as observed previously. rhWISP-1 was also detected on this blot between 37 and 50kDa, as previously. When the antibody was pre-adsorbed overnight with rhWISP-1, none of these bands were detected. This suggests that the higher MW bands detected do correspond to complexes containing WISP-1.

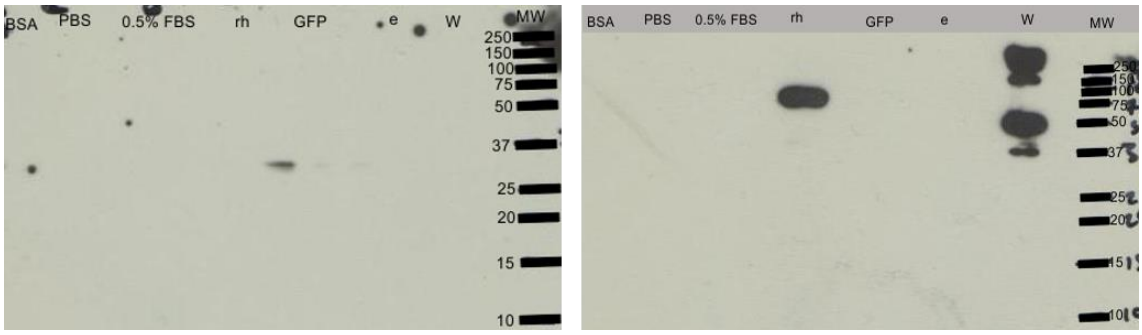

Figure 65. Detection of recombinant WISP-1 by western blotting. HEK293T cells were transiently transfected with pcDNA3.1+ WISP-1 (W), pcDNA3.1+ GFP (GFP) or pcDNA3.1+ empty vector (e). Cells were harvested after 48 hours in sample buffer and lysates run on a 12.5% SDS-PAGE then probed with polyclonal antibodies from Abcam (left) and R&D (right). rhWISP-1 (rh, his-tagged, R&D, 10ng/μl) run as positive control and medium, PBS and BSA as negative controls.

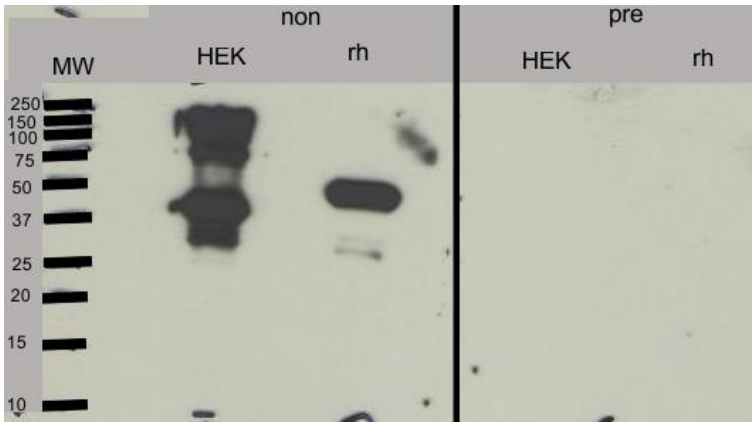

Figure 66. Detection of recombinant WISP-1 by western blotting. HEK293T cells were transiently transfected with pcDNA3.1+ WISP-1 and cells harvested in sample buffer after 48 hours. Lysate (HEK) was run alongside rhWISP-1 (rh, his-tagged, R&D, 10ng) on a 12.5% SDS-PAGE gel and probed with a polyclonal antibody from R&D (non) or the same antibody pre-adsorbed O/N with rhWISP-1 (pre, his-tagged, R&D), final antibody concentration, 0.2µg/ml.

The non-biotinylated antibody from R&D was found to reliably detect recombinant full length WISP-1. Therefore the ability of this antibody to detect WISP-1 variants was tested. HEK293T cells were transiently transfected with expression constructs for full length WISP-1 (UCB), variants 2, 3 and 4, or empty vector. The full length WISP-1 construct was sub-cloned from a vector provided by UCB. Constructs for variants 2, 3 and 4 were kindly cloned from bronchial fibroblast cDNA by Dr David Smart, as detailed in chapter 2. A control of non-transfected cells was also included. Medium was replaced after 24 hours to remove reagent:DNA complexes. After 48 hours, cells and supernatants were collected. Supernatant from several wells was pooled and aliquoted for use in conditioned medium experiments. The molecular weight of each variant was predicted using the Swiss Institute of Bioinformatics ExPASy ProtParam tool (http://web.expasy.org/protparam/) and is shown in Table 24.

As Figure 67 shows, full length WISP-1 was detected as previously at around 40kDa in both HEK293T lysates and supernatant. Several other bands were detected in the lysates both at a higher and lower MW than the full length WISP-1 band. These bands were lost when the antibody was pre-adsorbed with recombinant protein suggesting that correspond to WISP-1. The larger band

(marked by arrow) may correspond to multimers of WISP-1 or complexes of WISP-1 and other proteins. The smaller bands (marker by arrow) may correspond to cleaved fragments of WISP-1.

Variant	Predicted MW (kDa)
Full length	40.3
Variant 2	30.7
Variant 3	16.8
Variant 4	13.5

Table 24. The predicted molecular weight for each WISP-1 variant calculated based on its amino acid sequence.

In variant 2 transfected cells, a strong band was detected below 37kDa. This band was also observed in the corresponding cell-free supernatant sample, and likely corresponds to WISP-1 variant 2 which has a predicted molecular weight of 30.7kDa. Fainter bands were also detected in the variant 2 transfected lysates, both above and below the strongest band. The larger band is a similar molecular weight to full length WISP-1, and was also observed in all other lanes. This band was not detected following antibody pre-adsorption possibly suggesting that it corresponds to full length WISP-1 naturally expressed by HEK293T cells. The smaller bands may correspond to a cleaved fragment of WISP-1.

A strong band around 20kDa was detected in variant 3 transfected cells, likely corresponding to WISP-1 variant 3 which has a predicted molecular weight of 16.8kDa. No variant 3 was detected in the supernatant from variant 3 transfected cells however a faint band was present at around 37kDa. This band was not lost following pre-adsorption of the antibody suggesting that it is non-specific.

Two faint bands were present at a molecular weight lower than the 20kDa marker in variant 4 transfected lysates. These bands likely correspond to WISP-1 variant 4 as its predicted molecular weight is 13.5kDa. No similar-sized bands were detected in the corresponding supernatant sample.

In empty vector (e) transfected cells, not transfected (NT) cells and fresh medium (media), no bands were detected aside from the faint band at around 40kDa which may correspond to the expression of full length WISP-1 by HEK293T cells.

This result suggests that full length WISP-1 (UCB) and variant 2 are expressed by transfected HEK293T cells and subsequently secreted into the supernatant. Variants 3 and 4 were also detected in the transfected cell lysates however no bands were present in the corresponding supernatant samples. For variant 4, this could be due to a lack of epitope for the antibody to bind to rather than a lack of WISP-1 variant 4 as suggested by the weak detection in the cell lysate.

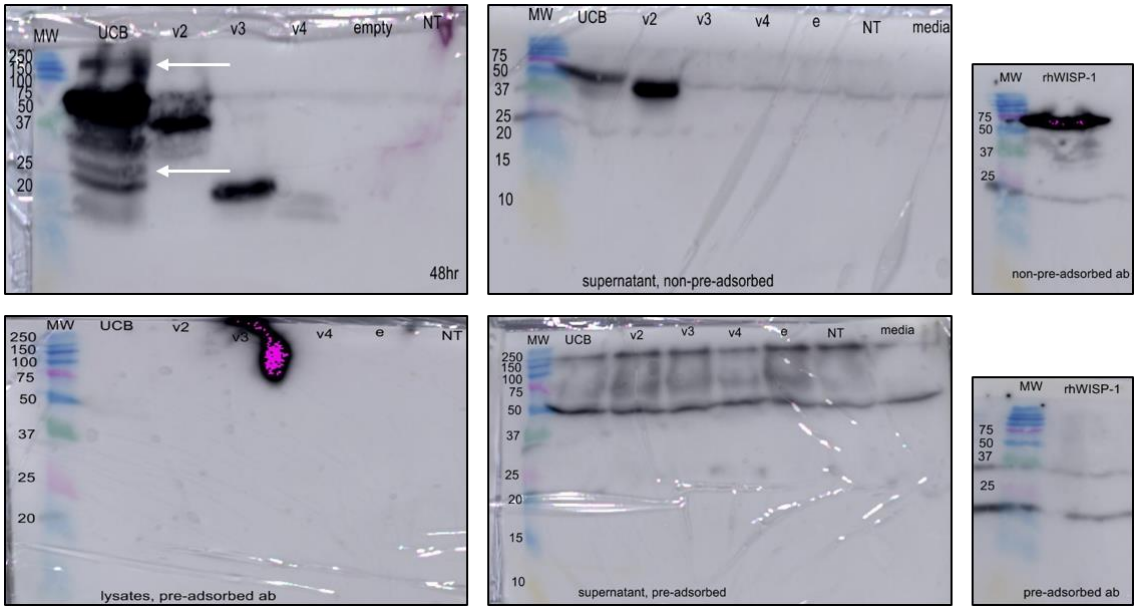

Figure 67. Detection of WISP-1 variants by western blotting. HEK293T cells were transiently transfected with expression constructs for either full length WISP-1 (UCB), WISP-1v2, v3, v4 or empty vector. Cell lysates (top panel) and supernatants (bottom panel) were harvested after 48 hours. Protein in supernatants was concentrated using strata clean resin. Samples were run alongside conditioned medium from non-transfected HEK293T cells (NT), fresh medium, and rhWISP-1 (his-tagged, R&D, 10ng) on a 12.5% SDS-PAGE gel, and probed with a polyclonal antibody from R&D or the same antibody pre-adsorbed O/N with rhWISP-1 (pre, his-tagged, R&D), final antibody concentration, 0.2µg/ml.

5.2.2 Effect of transfected HEK293T conditioned medium

Following the confirmation that each variant was expressed in the transfected HEK293T cells, this conditioned medium was incubated with A549 and MRC5 cells to observe the effect of each variant of WISP-1 on cell phenotype. All conditioned medium was diluted 1 in 2 with fresh complete DMEM prior to use. Cells were also stimulated with commercial recombinant NS0-derived his-tagged WISP-1 (R&D) and either TGFβ_1 (MRC5 cells) or TGFβ_1 + TNFα (A549 cells) as a positive control.

Timelapse microscopy was used to observe any changes in cell morphology induced by culture with transfected HEK293T conditioned medium or recombinant WISP-1. A549 cell images at T0, 24, 48 and 72 hours are shown in Figure 68. A549 cells in all conditions had a typical cobblestone appearance and with the presence of a few larger cells in each well. There was no suggestion of differentiation towards a mesenchymal phenotype induced by full length WISP-1, or any of the variants. There was little difference in the movement of the cells between wells. There appeared to be increased numbers of cells in wells incubated with variant 2 and variant 4 conditioned medium, and less with full length (UCB) conditioned medium compared with empty vector. Images of MRC5 cells cultured with conditioned medium or recombinant WISP-1 are shown in Figure 69. As with A549 cells, there was no obvious change in the morphology of these cells induced by full length WISP-1, WISP-1 variant 2, 3 or 4, or recombinant WISP-1. All cells displayed a typical fibroblast-like spindle morphology. There was no suggestion of increased migration or proliferation of these cells in any condition tested.

To determine whether any WISP-1 variant influenced cell proliferation, cells were seeded into wells in 96-well plates and allowed to adhere. After 6 hours, one plate was washed and fixed and the remaining plates cultured with HEK293T conditioned medium, commercial recombinant WISP-1 for 72 hours. Cell number was determined using a methylene blue assay (232). The effect of WISP-1 variant 3 and 4 conditioned medium was not assessed in this experiment due to there being an insufficient amount of medium.

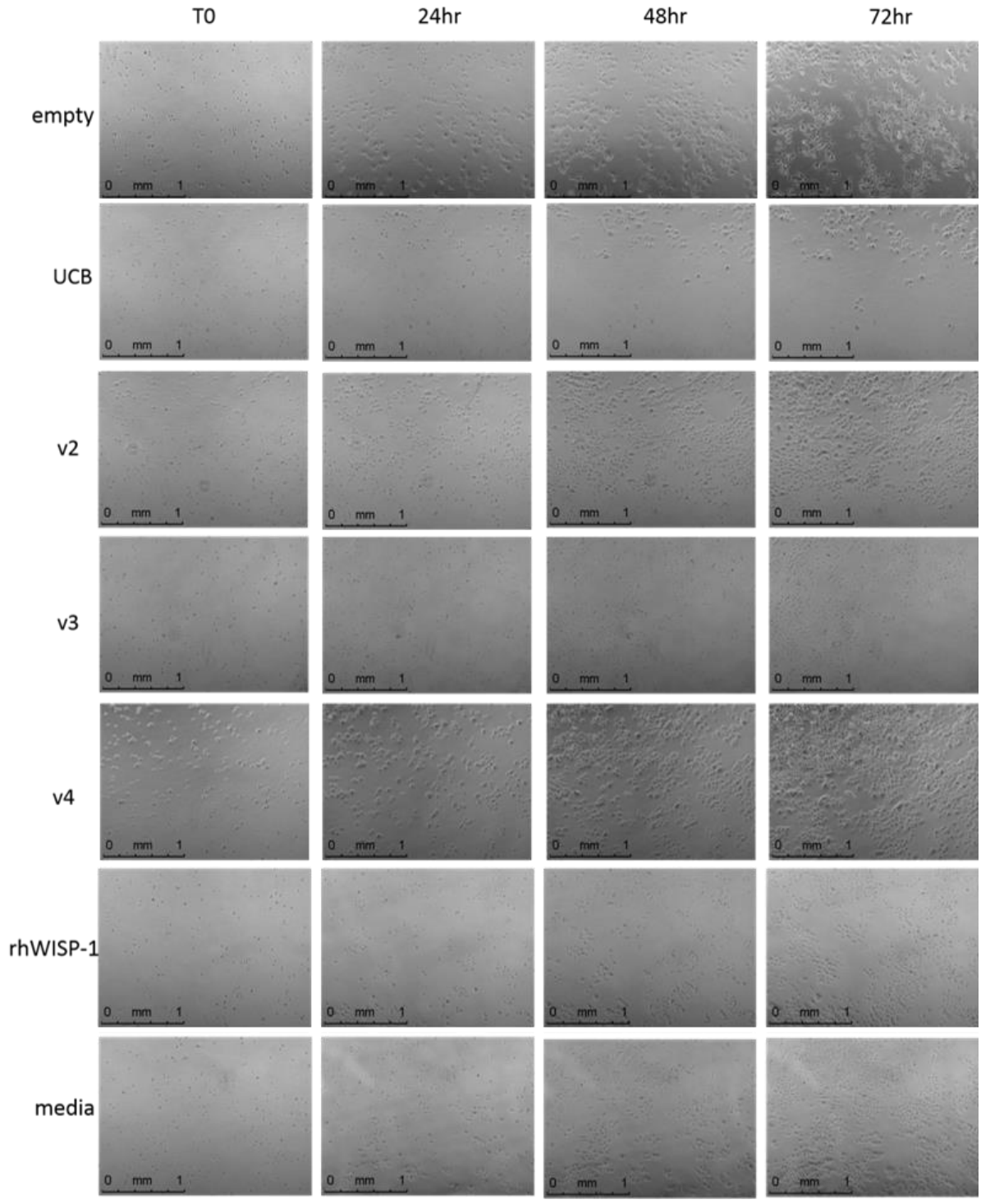

Figure 68. Timelapse images of A549 cells cultured with transfected HEK293T conditioned medium. A549 cells were seeded into wells in a 12 well plate at 30,000 cells/well. After 6 hours, cells were treated as indicated and incubated inside the timelapse microscope chamber for 72 hours. One image per well was captured every 20 minutes at 10X magnification.

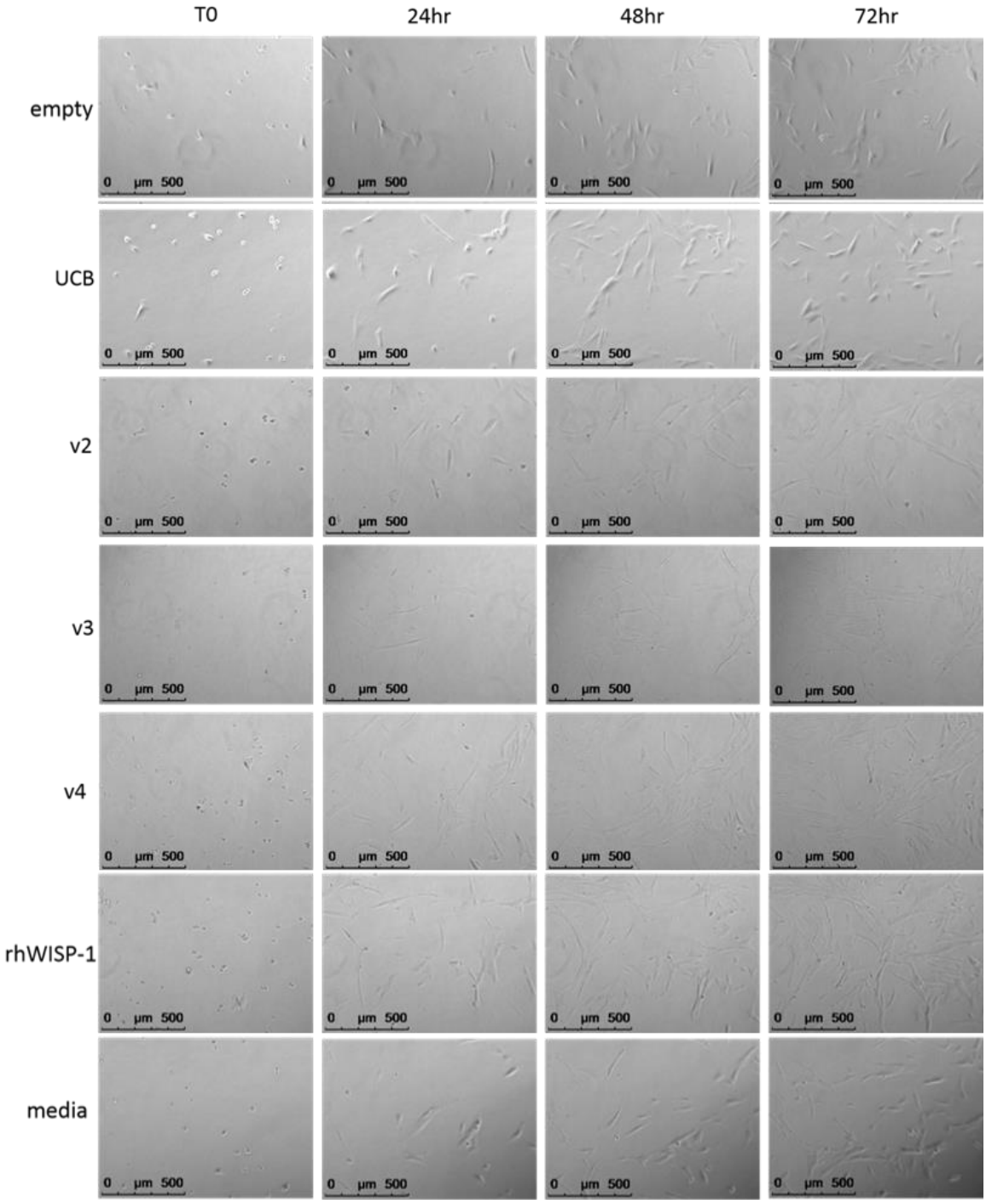

Figure 69. Timelapse images of MRC5 cells cultured with transfected HEK293T conditioned medium. MRC5 cells were seeded into wells in a 12 well plate at 30,000 cells/well. After 6 hours, cells were treated as indicated, and incubated inside the timelapse microscope chamber for 72 hours. One image per well was captured every 20 minutes at 10X magnification.

As Figure 70 shows, A549 cell number did not significantly increase suggesting that these cells were in the lag phase of growth. No differences were observed between different conditions. MRC5 cell number was also assessed. Empty vector and WISP-1 variant 2 conditioned medium, and fresh medium did not stimulate an increase in MRC5 cells number. Full length WISP-1 conditioned medium cultured MRC5 cell number increased at 72 hours (p=<0.001 compared to T0). This was also statistically significant compared to empty vector and variant 2 (p=<0.01). Commercial recombinant WISP-1 stimulated an increase in the proliferation of MRC5 cells at 72 hours compared to T0 (p=<0.01).

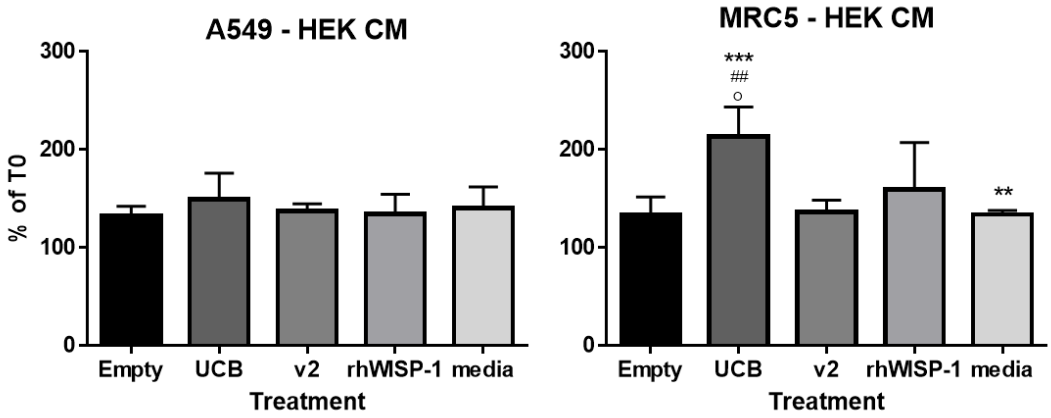

Figure 70. A549 and MRC5 cell number following culture with transfected HEK293T conditioned medium or rhWISP-1. Cells were seeded in triplicate and allowed to adhere. At T0, one plate of cells was fixed and the other cells were treated as indicated for 72 hours. Cell number was assessed by methylene blue absorbance and is expressed as a percentage of the absorbance at T0. n=3independent experiments, mean ± SD. Statistical significance was tested by two way ANOVA. * compared to T0, # v compared to empty vector at same timepoint, ˚ compared to v2 at same timepoint, · compared to media at same timepoint.

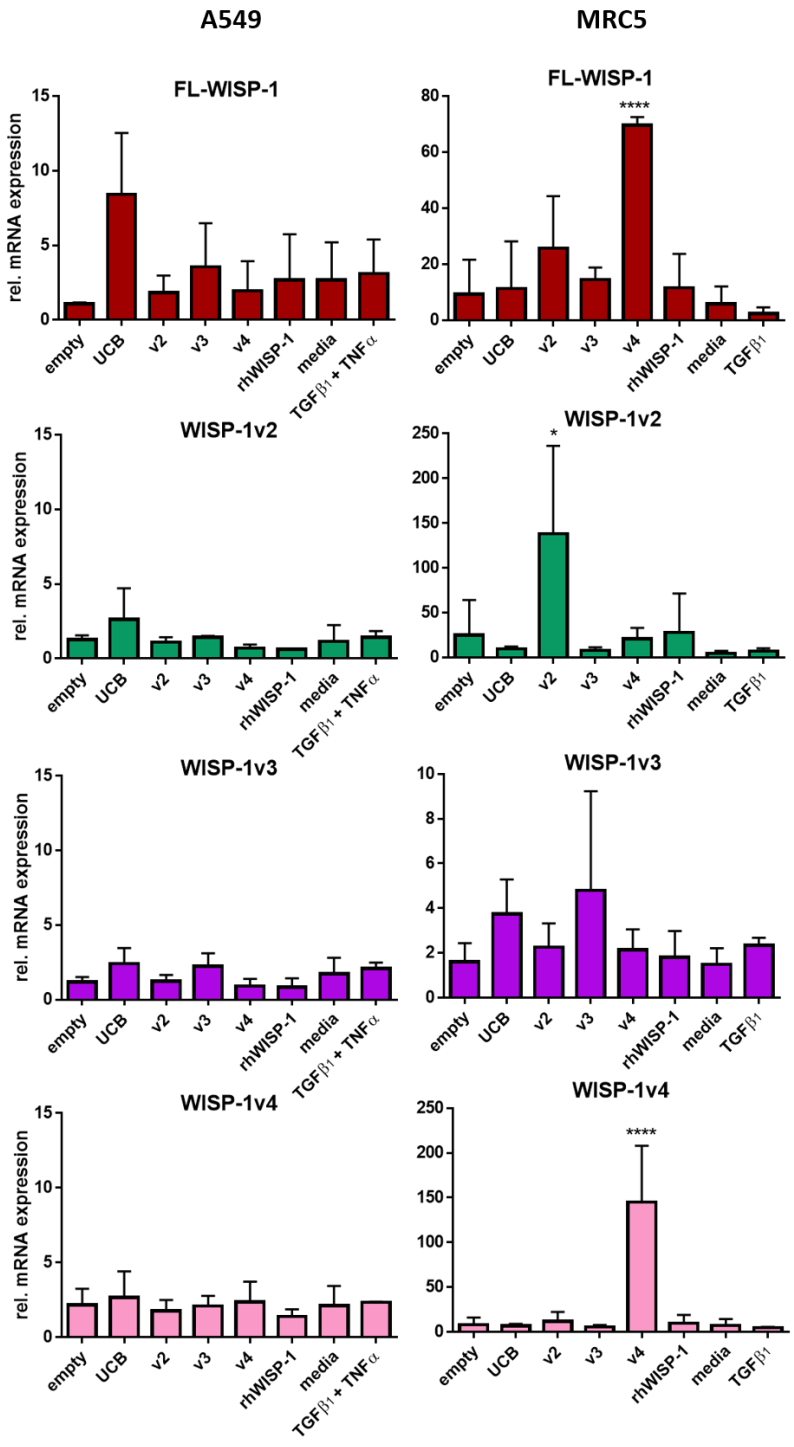

Figure 71. WISP-1 expression in A549 and MRC5 cells cultured with transfected HEK293T conditioned medium. Cells were seeded into wells at 30,000 cells/well. After 6 hours, cells were treated as indicated. After 72 hours, cells were harvested for RNA extraction and mRNA expression was measured by qRT-PCR. Data are expressed relative to empty vector conditioned medium and are presented as mean ± SD. n=3 A549, n=3-4 MRC5. Statistical significance was tested by one-way ANOVA. * p=<0.05, ****p=<0.00001, compared to empty vector.

Changes in the expression of various genes of interest was also measured in these cells. First, the expression of full length and variant WISP-1 was measured to determine whether WISP-1 induced its own expression. As Figure 71 shows, full length WISP-1 expression was increased in cells cultured with full length conditioned medium (UCB) only in A549 cells (left panel). This was approximately an 8-fold increase compared to empty vector (not statistically significant). Commercial recombinant WISP-1 and TGFβ_1 + TNFα did not induce or suppress full length WISP-1 expression compared to medium alone. Little effect of any condition on WISP-1 variant 2, 3 and 4 expression was observed in these cells.

A greater effect on WISP-1 mRNA expression was observed in MRC5 cells (right panel). Full length WISP-1 was induced by variant 4 conditioned medium. This was approximately 7.5-fold that of empty vector conditioned medium and was statistically significant ($p=<0.00001$). Expression of full length WISP-1 was also increased by variant 2 conditioned medium however this was not statistically significant. Full length WISP-1 was not induced by full length WISP-1 conditioned medium (UCB) or recombinant WISP-1. Levels of full length WISP-1 were lower in TGFβ_1-stimulated cells as was previously observed for overall WISP-1 mRNA expression in these cells (chapter 3). Expression of WISP-1 variant 2 was induced in MRC5 cells by culture with variant 2 conditioned medium only. This was approximately 5.5-fold greater than empty vector and was statistically significant ($p=<0.05$). There was a trend for WISP-1 variant 3 to be induced by full length (UCB) and variant 3 conditioned medium (mean induction 2.5 and 3-fold respectively) however this was not statistically significant. Levels of variant 3 were similar to empty vector in all other conditions. The expression of WISP-1 variant 4 was strongly induced by variant 4 conditioned medium. This was approximately an 18-fold induction compared to empty vector and was statistically significant ($p=<0.0001$). This effect suggests that either WISP-1 variant 4 was secreted into the supernatant but was not detected by the antibody used, or that expression of WISP-1 variant 4 stimulated the express/release of another factor into the supernatant that subsequently stimulated WISP-1 variant 4 expression in MRC5 cells.

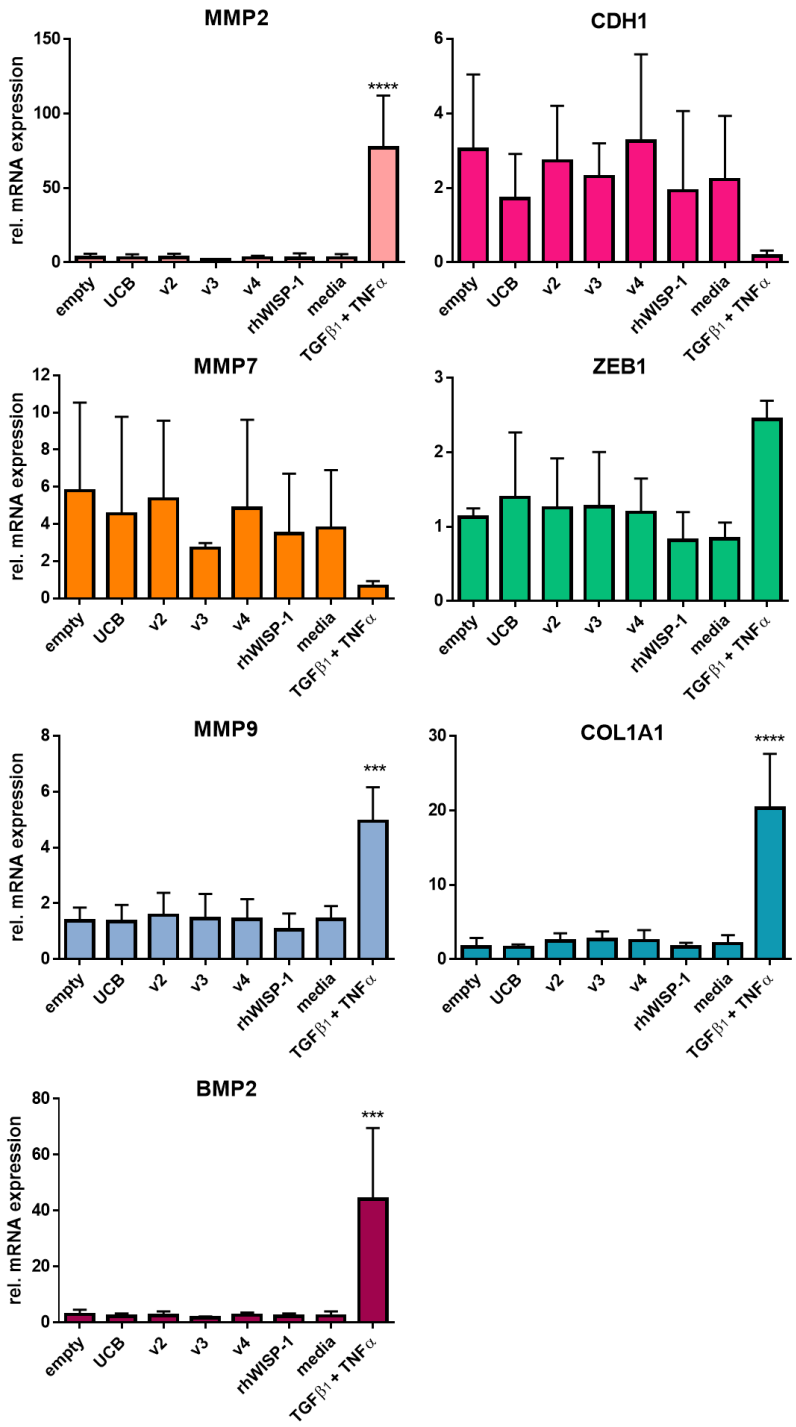

Figure 72. The effect of transfected HEK293T conditioned medium on A549 cell gene expression. Cells were seeded at 30,000 cells/well. After 6 hours, cells were treated as indicated. After 72 hours, cells were harvested for RNA extraction. mRNA expression was measured by qRT-PCR. Data are expressed relative to empty vector and are presented as mean ± SD. n=3. Statistical significance was tested by one-way ANOVA. *** p=<0.001, ****p=<0.00001, compared to medium alone.

The ability of the WISP-1 variants to induce EMT was tested using A549 cells, using TGFβ_1 and TNFα treatment as a positive control (Figure 72). HEK293T conditioned medium alone did not alter the expression of any of the genes measured. No significant effect of any WISP-1 variant was observed on gene expression in these cells. Treatment with commercial recombinant WISP-1 did not change the expression of any genes measured.

TGFβ_1 + TNFα stimulated a change in the expression of each gene measured. MMP7 was suppressed in this condition by approximately 6-fold compared to medium alone. Expression of MMP2, MMP9 and BMP2 was induced approximately 27-fold ($p=<0.0001$), 3.5-fold ($p=<0.001$) and 19-fold ($p=<0.001$) respectively, compared to medium alone. The expression of epithelial to mesenchymal gene was also altered as was observed previously (chapter 3). ZEB1 and COL1A1 were induced approximately 3 and 10-fold respectively. This induction was statistically significant for COL1A1 ($p=<0.0001$). Expression of CDH1 suppressed approximately 10-fold compared to medium alone however this was not statistically significant.

The expression of markers of myofibroblast differentiation was also measured in MRC5 cells exposed to WISP-1 variants using TGFβ_1 as a positive control (Figure 73). HEK293T conditioned medium alone did not alter the expression of any of the genes measured. Expression of α-SMA (ACTA2) and collagen 3 (COL3A1) tended to be suppressed by each variant of WISP-1 compared to empty vector conditioned medium. No other effect of WISP-1 conditioned medium was observed.

TGFβ_1 treatment stimulated an induction in the expression of several genes compared to medium alone. IL-6, MMP2 and α-SMA were induced approximately 3-fold. This was statistically significant for MMP2 ($p=<0.0001$). Collagen 1 (COL1A1) and fibronectin (FN1) were induced to a greater extent, by approximately 4 ($p=<0.0001$) and 6-fold ($p=<0.05$).

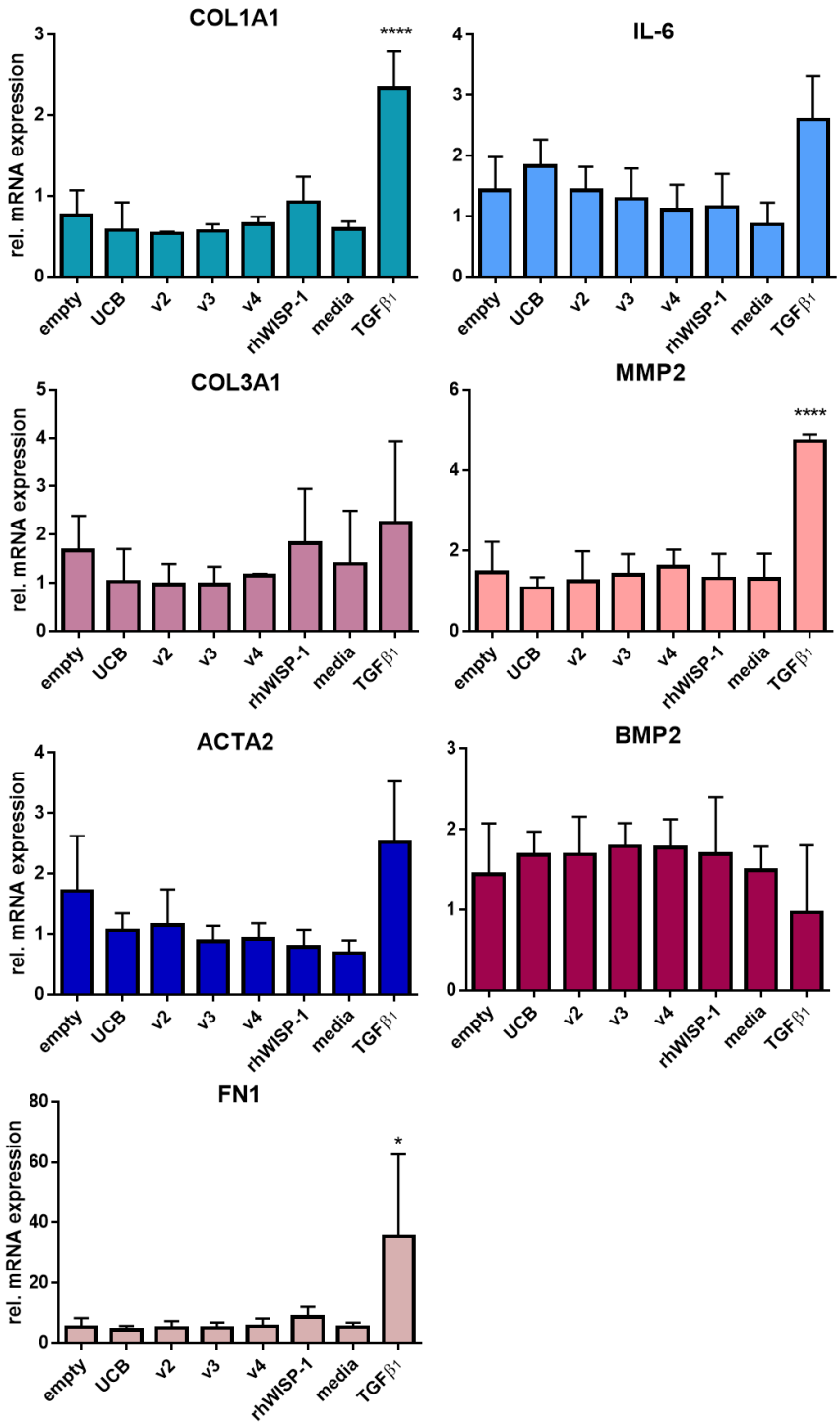

Figure 73. The effect of transfected HEK293T conditioned medium on MRC5 cell gene expression. Cells were seeded at 30,000 cells/well. After 6 hours, cells were treated as indicated. After 72 hours, cells were harvested for RNA extraction. mRNA expression was measured by qRT-PCR. Data are expressed relative to empty vector and are presented as mean ± SD. n=3-4. Statistical significance was tested by one-way ANOVA. * p=<0.05, ****p=<0.0001, compared to medium alone.

Summary of HEK293T conditioned medium experiments

The ability of several antibodies to detect full length WISP-1 was characterised. A polyclonal antibody from R&D was able to detect both commercial and HEK293T-derived full length WISP-1, as well as WISP-1 variants 2, 3 and 4 when overexpressed in HEK293T cells.

HEK293T cells were successfully transfected with expression constructs for full length WISP-1 (UCB) and WISP-1 variants 2, 3 and 4 as confirmed by western blotting. Full length WISP-1 and WISP-1 variant 2 were detected in the supernatant of transfected cells. No WISP-1 variant 3 or 4 was detected in the supernatant using this antibody.

No effect on the morphology or proliferation of A549 cells was observed following culture with WISP-1 transfected HEK293T conditioned medium or commercial recombinant WISP-1. Full length conditioned medium stimulated the mRNA expression of full length WISP-1 however no effect of full length WISP-1 or variant WISP-1 was observed on EMT marker expression.

No effect on the morphology of MRC5 cells was observed with culture with WISP-1 transfected HEK293T conditioned medium however full length WISP-1 and commercial recombinant WISP- 1 stimulated an increase in MRC5 cell proliferation. WISP-1 variant 2, 3 and 4 each induced their own expression. Variant 4 also significantly induced the expression of full length WISP-1. Little of effect of WISP-1 variants on the expression of myofibroblast differentiation markers was observed. There was a trend for decreased α-SMA and COL3A1 expression in these cells with WISP-1 (full length and variant) conditioned medium.

5.2.3 Stable overexpression of WISP-1 in A549 cells

In experiments above using HEK293T conditioned medium, a greater effect was observed on MRC5 cells. In order to model epithelial-mesenchymal cross-talk to further characterise the effect of WISP-1 on fibroblasts, A549 cells were stably transfected with WISP-1 with the aim of using these cells in a fibroblast-epithelial co-culture model. As detailed in in chapter 2 section 1.6, A549 cells were

transfected with full length WISP-1 (UCB) and placed under antibiotic selection before the isolation of several WISP-1-expressing clones. Expression of WISP-1 by these cells was determined by RT-qPCR, western blotting and ELISA.

As shown in Figure 74, full length WISP-1 was detected in each of the WISP-1 clones at a MW between 37 and 50kDa (top panel). The WISP-1 mRNA expression in each clone is shown in the bottom left panel. Six of eight clones expressed higher levels of WISP-1 compared to empty vector. The two highest expressing clones were G and H at approximately 6 and 8-fold higher than empty vector. Levels of secreted WISP-1 were measured by ELISA in the corresponding supernatants from these two clones (bottom right panel). WISP-1 was detected in empty vector supernatant at approximately 100pg/ml. In WISP-1 transfected cells, secreted WISP-1 levels were higher at 237pg/ml for clone G and 218pg/ml for clone H.

Figure 75 shows images of empty vector and WISP-1 transfected A549 cells captured by timelapse microscopy. A549 cells typically have a cobblestone-like epithelial morphology. During epithelial to mesenchymal transition, A549 cells start to lose their cell-cell contacts and display a more spindle fibroblast-like morphology. In these cultures, the majority of the cells in each well had a typical A549 appearance. A few cells with a ‘fried egg’ appearance were also present in each well. No clear differences in the migration/movement of the cells were observed between empty vector and WISP-1 transfected cells. In the wells containing WISP-1 expressing cells there were some cells with a longer, flatter appearance (circled). Whether these are cells that are dividing is unclear therefore the effect of stable WISP-1 expression on A549 proliferation was measured. It may also suggest WISP-1 expression stimulates a differentiation of these cells towards a more mesenchymal phenotype.

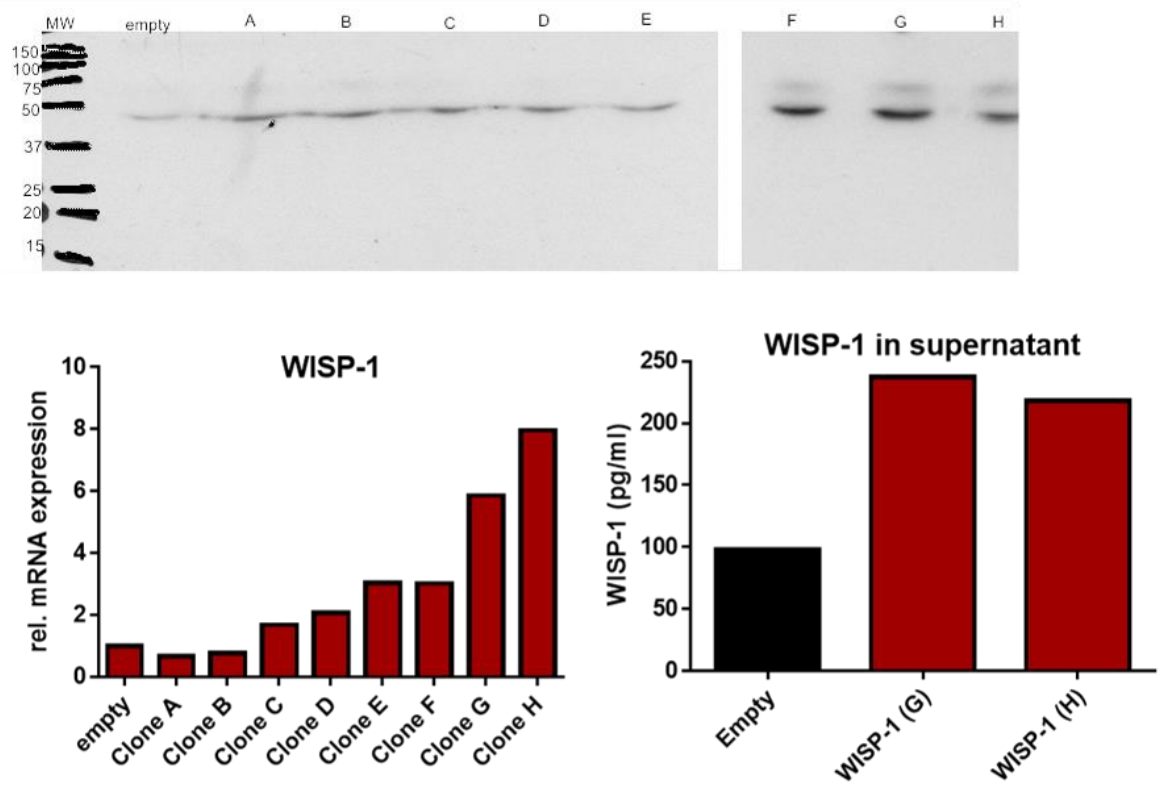

Figure 74. Confirmation of WISP-1 expression in stably transfected A549 cells. A549 cells were transfected with full length WISP-1 construct (UCB) and different clones isolated following antibiotic selection. Cells were cultured for 48 hours then supernatants collected and cells harvested either in sample buffer or trizol. Top: detection of WISP-1 in cell lysates by western blotting. Samples were run alongside rhWISP-1 (R&D, 10n) on a 12.5% SDS-PAGE gel, and probed with a polyclonal antibody from R&D. Bottom left: overall mRNA expression in each isolated clone, measured by qPCR. Bottom right: WISP-1 levels in supernatants from the two highest expressing clones at the mRNA level, clones F and G, and empty vector transfected cells measured by ELISA.

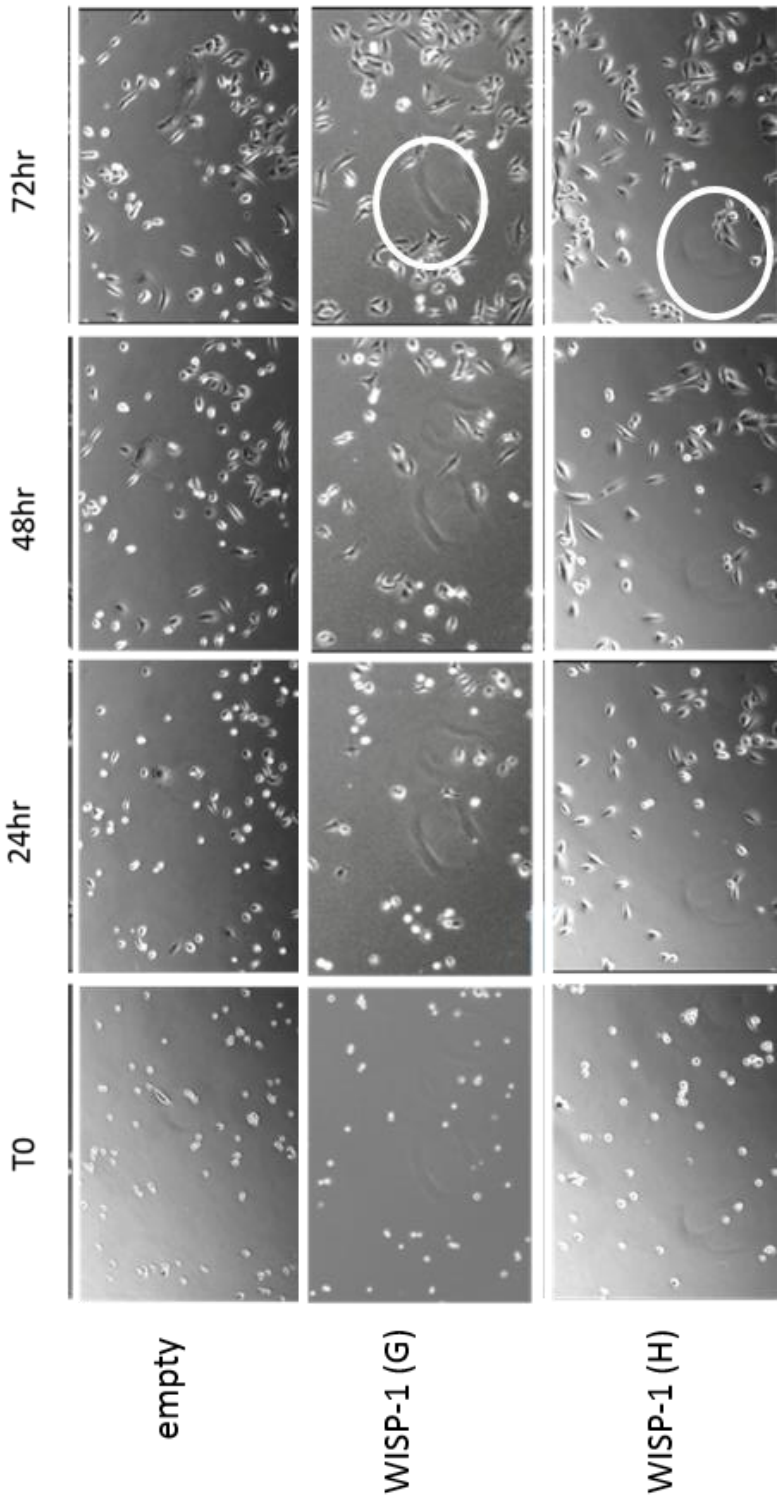

Figure 75. Timelapse images of A549 cells stably transfected with full length WISP-1 (UCB). Empty vector transfected cells, and the two highest expressing WISP-1 clones were seeded and incubated inside the timelapse microscope chamber for 72 hours. One image per well was captured every 20 minutes at 10X magnification.

Figure 76 shows cell number in WISP-1 and empty vector transfected A549 cells. In empty vector transfected cells, cell number was increased by approximately 7 times that of T0 at 72 hours (p=<0.0001). A similar increase was also observed for both WISP-1 expressing clones. Cell number was significantly increased at 72 hours by approximately 8-fold for clone G (p=<0.0001) and 9-fold for clone H (p=<0.0001) however no significant difference between WISP-1 expressing clones and empty vector transfected cells were observed.

The expression of EMT marker genes was measured in cells these to determine whether the elongated cells observed under timelapse microscopy might be co-expressing epithelial and mesenchymal markers (Figure 77). The average expression of COL1A1and MMP9 was significantly increased in WISP-1 transfected cells compared to empty vector cells (top left panel, p=≤0.05 and p=≤0.0001 respectively) however the expression of these and other genes of interest in individual clones did not correlate with the mRNA expression of total WISP-1 (shown in Figure 74, WISP-1 low→high = A→H).

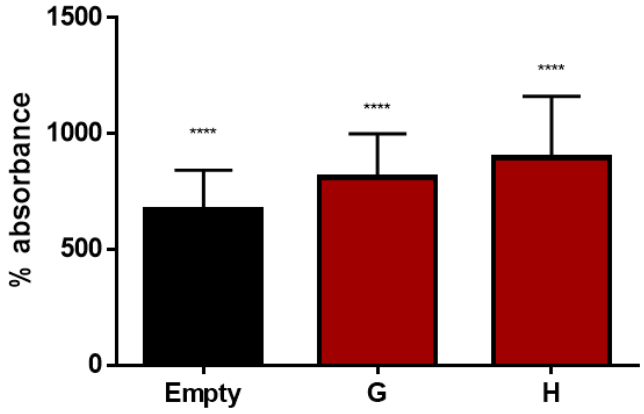

Figure 76. Effect of WISP-1 overexpression on A549 cell number. Empty vector transfected cells, and the two highest expressing WISP-1 clones (G&H) were seeded and allowed to adhere. At T0, one plate of cells was fixed and the others cultured for 72 hours. Cell number was assessed by methylene blue absorbance and is expressed as a percentage of the absorbance at T0. n=3 independent experiments. Statistical significance was tested by two way ANOVA. **** p=<0.0001vs T0

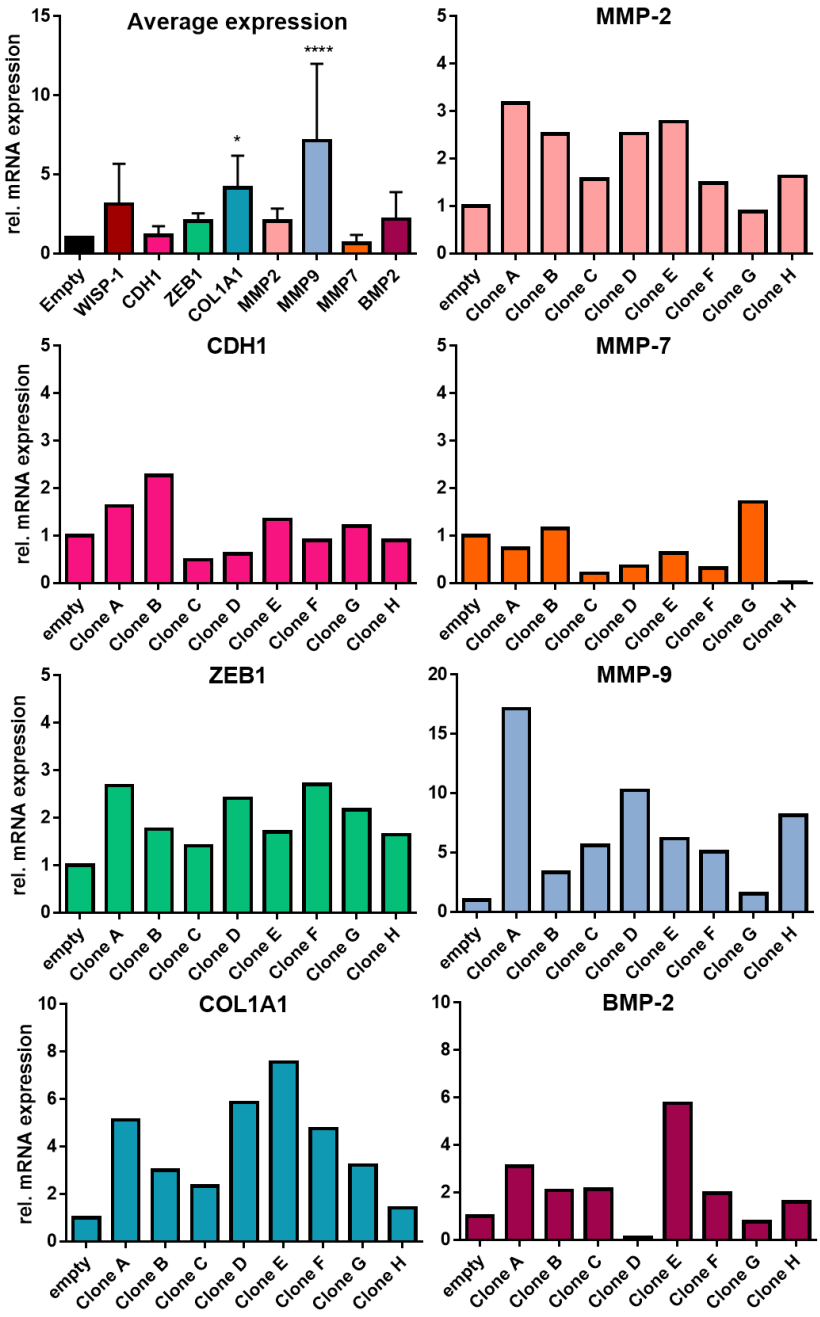

Figure 77. mRNA expression in different WISP-1 expressing clones. A549 cells were transfected with full length WISP-1 construct (UCB) and different clones isolated following antibiotic selection. Cells were cultured for 48 hours then harvested in trizol. mRNA expression was measured by qRT-PCR. For average expression, mean ± SD of all WISP-1 clones (n=8) is shown relative to empty vector expression. Statistical significance was tested by one-way ANOVA. * indicates significantly different compared to empty vector, *p=≤0.05, ****p=≤0.00001. For all other graphs, expression in each clone is shown relative to that in empty vector sample. Clone A→H = low→high WISP-1, n=1.

5.3 Discussion

There are various ways in which the effect of WISP-1 on different cell types could be investigated. The majority of studies in the literature have used recombinant WISP-1 to investigate the effects of this protein. In the current study the use of recombinant protein is limited for two reasons. First, different effects of exogenously added and endogenously expressed full length WISP-1 have been reported, suggesting perhaps that recombinant WISP-1 is not subject to appropriate post-translational modifications (183). Second, only full length recombinant WISP-1 is commercially available meaning that WISP-1 variants 2, 3 and 4 would have to be expressed and purified in-house. Reports in the literature suggest that purification of CCN proteins is difficult with studies reporting production of low yields and insoluble protein. Holbourn et al. (233) reported successful purification of each CCN family member following a screening process to determine optimal conditions for refolding. However, in the current study expression constructs were used for each of the WISP-1 variants in order to assess their effects.

Antibody characterisation

The ability of several antibodies to detect WISP-1 by western blotting was characterised so that any effects observed could be attributed to WISP-1. The monoclonal antibody tested was unable to detect recombinant WISP-1 at the concentrations of antibody used. The amount of recombinant WISP-1 used in this assay was detected by each of the other antibodies tested. A possible explanation for the lack of WISP-1 detection could be that the antibody recognises a conformational epitope not present in the denatured sample. The other antibodies tested were all polyclonal and therefore are more likely to be able to detect an epitope present in the sample. The biotinylated polyclonal antibody was able to detect recombinant protein at all concentrations of WISP-1 used. There was also a band present in the control BSA lane in this assay, suggesting that the antibody or biotin bound to a protein present in the BSA, possibly WISP-1. The third antibody tested was a polyclonal antibody from Abcam raised against a synthetic peptide corresponding to human WISP-1 C-terminus, amino acids 354-367. This was able to detect recombinant human WISP-1 but was unable to detect WISP-1 in transfected cell lysates. This could be due to a smaller amount of WISP-

1 being present in the transfected cell lysate compared to the recombinant protein as rhWISP-1 was only detected by this antibody in lanes containing the highest amounts of protein. The fourth antibody tested was a non-biotinylated version of the R&D polyclonal antibody previously tested. This antibody was able to detect both commercial rhWISP-1 and HEK293T-derived WISP-1 at all concentrations tested and was therefore selected for further characterisation over the biotinylated antibody. Pre-adsorption with recombinant protein gave confidence in the specificity of this antibody and it was subsequently characterised for its ability to detect different variants of WISP-1.

HEK293T cells were selected for transfection with WISP-1 expression constructs as they are transformed with the SV40 large T-antigen and are competent to replicate vectors carrying the SV40 origin of replication. Full length WISP-1, variant 2, variant 3 and variant 4 were detected in cell lysates, and full length WISP-1 and variant 2 was detected in supernatants. No WISP-1 variant 3 or variant 4 was detected in the supernatant in this assay. This could suggest that these variants are either not secreted or are associated with the cell surface following secretion from the cell. However, for WISP-1 variant 4 in particular, it may be that a low amount was secreted but not detected by this antibody. A small amount was detected in the corresponding lysate, suggestive of either low expression or poor detection by the antibody used. The antigen for this antibody is the four structural domains of WISP-1 however the epitope(s) is unknown. To determine whether variant 4 is present in the supernatant of these transfected HEK293T cells, an alternative antibody could be used such as the C-terminal antibody from Abcam, characterised in chapter 3. Variant 3 was clearly detected in the cell lysate suggesting that this variant was not present in the supernatant. The use of the C-terminal antibody would not be helpful to confirm this as this variant does not contain the cysteine knot domain due to a frameshift.

A further possible method for determining the secretion of WISP-1 variants into the cell culture supernatant is by ELISA. Whether or not the different WISP-1 variants can be detected by the antibodies in the ELISA assay is unknown. The antigen for both capture and detection antibodies is the four structural domains of WISP-1. When tested, the standard curve was poor and so the detection of WISP-1 in the supernatant samples was not determined.

HEK293T conditioned medium

Both MRC5 cells and A549 cells were cultured with transfected HEK293T conditioned medium for 72 hours, and the cell morphology, proliferation and gene expression assessed in order to test the hypotheses for this study. Induction of epithelial to mesenchymal transition in A549 cells can be easily identified by changes in cell morphology from a cobblestone appearance to spindle-like cells with less cell-cell contacts. Therefore, increased numbers of cells with a spindle-like morphology were expected in A549 cells cultured with full length WISP-1 conditioned medium compared to empty vector. No obvious changes in cell morphology were observed with this medium, or any other condition in this experiment. Similarly, no changes in the morphology of MRC5 cells were observed with any conditioned medium or recombinant WISP-1.

In these images, there appeared to be an increased number of A549 cells in wells cultured with either WISP-1 variant 2 or 4 conditioned medium. This may be due to an increased number of cells in that particular field of view or due to an increase in proliferation mediated by the WISP-1 variants. In the literature, reports of WISP-1-mediated cellular proliferation have used full length WISP-1, either recombinant or overexpressed, and have not identified which domain(s) is responsible for the effect observed. Studies on other CCN proteins have suggested that it is the C-terminal half of the protein that is responsible for mediating effects on proliferation. Grotendorst et al. (234) reported that this was the case for CTGF-stimulated fibroblast proliferation. More recently, the anti-proliferative effect of NOV was attributed to the CT domain of this protein (235). Making the assumption that this domain is solely responsible for WISP-1-mediated cell proliferation, no differences in proliferative would be expected between full length WISP-1, variant 2 and variant 4. WISP-1 variant 3 is missing the cysteine knot domain therefore no effect on cell proliferation would be expected.

WISP-1 has previously been shown to stimulate A549 cell proliferation (124) therefore increased cell number with both full length WISP-1 and variant 2 would be expected. This was not observed in the methylene blue assay used. Only a small increase in cell number was seen over time for these cells in all conditions suggesting that they were not in the log phase of growth, making a pro- or anti-proliferative effect difficult to see.

This assay was also used to determine whether WISP-1 influenced the proliferation of MRC5 fibroblasts. Cells cultured with full length WISP-1 conditioned medium or recombinant WISP-1 showed an increase in cell number at 72 hours, which was significantly greater than the cell number in empty vector conditioned medium or medium alone. No effect was observed with WISP-1 variant 2. These results could suggest that WISP-1 induces the proliferation of MRC5 cells. In the literature, WISP-1 has been reported to mediate the proliferative effects of other proteins. For example, WISP-1 mediated cardiac fibroblast proliferation stimlulated by TNFα (194), and primary lung fibroblast proliferation stimulated by IL-6 (198), but was reported to have no direct effect on the proliferation of primary lung fibroblasts in another study (124). The lack of induction with WISP-1 variant 2 could suggest that the VWC domain is involved in mediating this effect in contrast to published studies investigating the role of other CCN proteins in proliferation, discussed above.

Expression of several genes was measured in A549 and MRC5 cells following culture with transfected HEK293T conditioned medium or recombinant WISP-1. Interestingly, WISP-1 induced its own expression in both cell types. Medium was replaced 24 hours after transfection to remove DNA:transfection reagent complexes suggesting that this induction was not due to tranfection of A549 or MRC5 cells with the expression constructs.

The greatest effect observed was in MRC5 cells with WISP-1 variant 4 conditioned medium. WISP-1 variant 4 contains only the CT domain of the protein which contains a cysteine knot motif and is thought to be involved in mediating protein-protein interactions (138). Interaction of this variant with another molecule would limit the availability of this molecule to interact with full length WISP-1 therefore WISP-1 variant 4 may act as a negative regulator of WISP-1 activity that is mediated through one or more of its other domains and that requires the presence of an additional factor(s). Therefore it would be interesting to determine whether the effect of WISP-1 is enhanced by the presence of additional factors, for example, HSPGs as WISP-1 has been reported to bind to decorin and biglycan (190), which is likely mediated through this domain as has been demonstrated for other cysteine knot motif-containing proteins (151).

The requirement of additional factors for WISP-1 to exert an effect is also suggested by the lack of effect of WISP-1 variants on EMT marker and ECM expression. In MRC5 cells there was a trend for COL3A1 and ACTA2 expression to be decreased in all WISP-1 conditioned medium conditions. It would therefore be interesting to see whether WISP-1 would significantly suppress the expression of these genes following their stimulation by a TGFβ_1. The concentration of WISP-1 present in the conditioned medium used in these experiments was not determined therefore the lack of effect observed may also be due to the expression being too low to have an effect. However, commercial recombinant WISP-1 (NS0-derived, his-tagged, R&D) also had little effect on the expression of the transcripts measured but was used at a concentration reported to be sufficient to exert such effects in the literature (124).

Generally, more of an effect of WISP-1 transfected HEK293T conditioned medium was observed on MRC5 cells. This could suggest that WISP-1 does not influence changes in the proliferation, morphology or gene expression of A549 cells, or that the quantity of WISP-1 present in the conditioned medium was not sufficient to elicit such effects. A lack of expression of required co-factors by A549 cells could therefore contribute to the lack of effect of WISP-1 observed in these cells. A549 cells have been demonstrated to express the integrins αVβ1, αVβ3 and αVβ5 (236) which have been demonstrated to mediate the effects of WISP-1 in different studies (137, 142, 143, 146, 147), but do not express the integrin subunit α5 (237) which has also been demonstrated to mediate the effects of WISP-1 (135, 238). It may also be the case that WISP-1 induces other changes in these cells that were not measured in the current study.

As with any methods, there are limitations to using conditioned medium as a source of WISP-1 protein. This medium was incubated with HEK293T cells for 48 hours prior to being pooled, aliquoted and frozen and subsequently used as culture medium for A549 and MRC5 cells. Therefore there is likely to be depletion of some components in the medium. To try and compensate for this, conditioned medium was diluted 1 in 2 with fresh complete DMEM prior to being added to experimental cells. This of course diluted the amount of WISP-1 present in the medium. The secreted protein may have also be affected by the thawing of the culture medium.

Another possible limitation of these experiments is the time point selected. A 72 hour incubation was selected to allow cells time to proliferate in the methylene blue assay. However, it may be that some changes in gene expression occurred at an earlier time and were missed by the 72 hour time point. It could also be the case that WISP-1 induced the expression of another factor that was not measured, either in the HEK293T cells or in the experimental cells. This factor could then in turn influence the cell morphology, proliferation or gene expression. Neutralising antibodies against different WISP-1 variants could help to determine whether any effect observed was due to the WISP-1 variant or another factor expressed by the cell/present in the conditioned medium.

Stable WISP-1 expression

A549 cells were stably transfected with full length WISP-1 and expression was confirmed by qPCR and western blot, and secretion of WISP-1 by ELISA. Several different clones were isolated and cultured, each expressing varying amounts of WISP-1. As with A549 cells cultured with transfected HEK293T conditioned medium, cells were observed over time to observe any changes in cell morphology. Whilst most cells had a typical cobblestone appearance there were some elongated cells present in WISP-1 wells therefore EMT marker gene was assessed. The average mRNA expression of some EMT markers was altered in WISP-1 expressing cells compared to empty vector transfected cells however this did not correlate with either high or low expression of WISP-1 in individual clones. Cell number was also assessed in these cells after 72 hours of culture as with A549/MRC5 cells cultured with WISP-1 transfected HEK293T conditioned medium. In each condition, cell number was significantly increased at 72 hours however no differences were observed a between the WISP-1 clones and empty vector transfected cells.

The amount of WISP-1 detected in the supernatant of WISP-1 expressing A549 cells was low compared to that detected in transiently transfected HEK293T cells in an earlier experiment (approximately 200pg/ml v 2.5ng/ml, chapter 2). This may be the reason for the lack of effect observed in the current study. It could also be the case that WISP-1 secreted by the cells becomes bound to the cells surface and was therefore not detected in the supernatant. Or as discussed

above, it may be that certain co-factors are required for WISP-1 to exert its effects as has been suggested by different studies in the literature (135, 183).

WISP-1 overexpression is a useful tool for investigating the role of this protein in relation to fibrosis. However, these cells may stop expressing WISP-1 whilst maintaining their antibiotic resistance. These cells would then be able to outcompete WISP-1 expressing cells, leaving a population of cells with low or no expression of WISP-1. Therefore, continued monitoring of WISP-1 expression by these cells would be required.

Further work

The methods used in this study provide useful tools for investigating the of WISP-1. There are a number of aspects to WISP-1 function that have been reported in the literature that were not investigated in the current study, for example migration. In addition to measuring these effects, there are several other ways in which the available tools could be utilised to further characterise WISP-1 function in relation to fibrosis.

The effect of WISP-1 on primary fibroblasts was not investigated in the current study and it would be particularly interesting to determine whether or not fibrotic and normal fibroblasts respond differently to a particular variant using transfected HEK293T conditioned medium. Co-culture of overexpressing A549 cells with fibroblasts would provide a way to investigate autocrine and paracrine effects of epithelial-derived WISP-1 as proposed by Konigshoff et al. (124). Fibroblasts overexpressing WISP-1 would also be a useful tool to investigate the effects of WISP-1 in these cells, particularly if WISP-1 mediates effects within the cell.

In the current study, only full length WISP-1 was overexpressed in A549 cells. Generation of cells that stably express the alternatively spliced variants would allow any effect observed with full length WISP-1 to be attributed to a particular domain(s). Use of neutralising antibodies against individual domains of WISP-1 would complement this approach. Identification of the specific domain(s) responsible for a particular effect of WISP-1 could help to identify the mechanism via which WISP-1 exerts this effect. Addition of other factors (such as TGFβ_1) or

use of antibodies against other proteins (such as integrins) to WISP-1 expressing cells would also help to further determine how WISP-1 functions in these cells.

5.3.1 Conclusions

HEK293T cells were successfully transfected with expression constructs for full length WISP-1, and variants 2, 3 and 4. Conditioned medium from these cells did not induce changes in the morphology of A549 cells or their proliferation. No changes in the expression of EMT marker and other genes of interst were measured in these cells. A similar lack of effect was observed with the highest expressing stable WISP-1 clones. Transfected HEK293T conditioned medium did not induced changes in the morphology of MRC5 cells. Increased expression of WISP-1 variants was observed but no changes indicative of differentiation towards a more fibrotic phenotype were measured. Full length WISP-1 stimluated proliferation of MRC5 cells.

Aside WISP-1 inducing its own expression, little effect on the cell phenotype was observed with either method used. This could suggest that expression of WISP-1 alone is not sufficient for an effect to be observed, and that any future experiments should take this into consideration.

Chapter 6: Discussion

6.1 Discussion

Idiopathic pulmonary fibrosis is a chronic, progressive interstitial lung disease with limited treatment options and poor prognosis. The aetiology of IPF is unclear however the failure of immunosuppressive agents to effectively treat the disease prompted a change in the thinking around IPF pathogenesis (18). Evidence suggests that aberrant epithelial-mesenchymal crosstalk and dysregulated wound healing responses are responsible for driving the excess extracellular matrix deposition, remodelling and subsequent destruction of the lung architecture observed in IPF (2).

A number of different factors and signalling pathways have been reported to play a role in IPF pathogenesis. Wnt1-inducible signalling protein-1 is one such factor. WISP-1 expression is increased in IPF (48, 124, 125) and it is a target of the canonical Wnt/β-catenin signalling pathway that is overexpressed in IPF (48, 122). It is related to the pro-fibrotic protein CTGF and has been reported to interact with various proteins that are also indicated in IPF pathogenesis such as TGFβ$_1$ (183). These properties combined with its proposed location as a matricellular protein and its modular structure make WISP-1 an interesting target to study in relation to IPF.

The key findings of this study were that WISP-1 expression is increased in fibroblasts isolated from the lung parenchyma of IPF patients, although regulation of WISP-1 expression by TGFβ or TNFα was not a consistent finding, and contrasted with some previous studies (125, 198). Most importantly, in this work, the complexity of WISP-1 expression revealed by demonstration of the production of several alternatively spliced variants of WISP-1 in an alveolar epithelial cell line, A549, and primary parenchymal fibroblasts from IPF and control donors. Furthermore, when expressed as recombinant proteins, these splice variants had differential effects on epithelial cells and fibroblasts, especially in relation to auto-induction of WISP-1 variants.

Lack of consideration of WISP-1 splice variant expression may go some way towards explaining the differences between the current and published studies

relating to the regulation of WISP-1 expression by TGFβ_1 and TNFα. In the current study, no induction of total WISP-1 mRNA was observed following stimulation with these cytokines in contrast with recent studies in parenchymal lung fibroblasts (125, 198). The primers used to detect WISP-1 mRNA in these studies are shown in Figure 78. Both the forward and reverse primers used in the current study (highlighted in pink) lie in WISP-1 exon 5 meaning that full length WISP-1 and variants 2, 3 and 4 were detected. The primers used in the two published studies (highlighted in green) lie in exons 1 (forward) and 2 (reverse). Exon 2 is present in full length WISP-1 and variants 2 and 3 but not variant 4. Therefore, this variant would not be detected using this primer set. When the expression of individual splice variants was measured in the current study, both IPF and control fibroblasts were found to express each variant, therefore previous studies have underestimated the total amount of WISP-1 variant expression in the cells.

WISP-1 is a modular matricellular protein that is thought to exert its effects through interactions with other molecules via its individual domains acting alone or in concert. Under appreciation of the different variants of WISP-1 is common amongst studies investigating the role of WISP-1 in either pathological or non-pathological settings. This is despite the potential impact of differential splice variant expression on WISP-1 activity. Furthermore, WISP-1 can also be subjected to proteolytic cleavage (Figure 79), further increasing the complexity of the regulation of this molecule. Therefore, a variant missing one or more domains would be unable to interact with as many partners as the full length protein, but would have the potential to compete for specific binding sites. Thus, when expressed, WISP-1 splice variants could potentially act as negative regulators of full length WISP-1 activity (e.g. by preventing full length WISP-1 from binding) or as modulators of other growth factors (e.g. by displacing them from the matrix to promote interaction with cellular receptors). Figure 79 shows the reported binding partners for WISP-1 by domain, highlighting the types of interactions that might be affected by differential splice variant expression.

The expression of WISP-1 splice variants following TGFβ_1 and TNFα stimulation was measured in this study. There was a trend for WISP-1 variant 2 expression to be stimulated by TGFβ_1 in IPF but not control fibroblasts. In contrast, WISP-1 variant 3 was stimulated by TGFβ_1 in control but not IPF fibroblasts. Compared to WISP-1 variant 2, variant 3 is missing the C-terminal part of the protein that

contains the thrombospondin and cysteine knot domains, thought to be involved in binding heparin sulphate proteoglycans, and mediating cell attachment and protein-protein interactions. Increased presence of these domains through increased expression of WISP-1 variant 2 by IPF fibroblasts could potentially alter the effect of WISP-1 through increased binding to other matrix proteins, for example, by changing its localisation through increased binding to the cell surface. Increased WISP-1 variant 2 expression could also abrogate an effect of WISP-1 mediated through the VWC domain as shown in Figure 80. Variant 2 stimulated its own expression in MRC5 fibroblasts.

Figure 78. WISP-1 sequence highlighting primers used in the current and published studies. Highlighted in green – primers used in Berschneider et al. 2009 (125) and Klee et al. 2016 (198) to measure mRNA levels of WISP-1. Highlighted in pink – primers used in the current study to measure total WISP-1 mRNA expression.

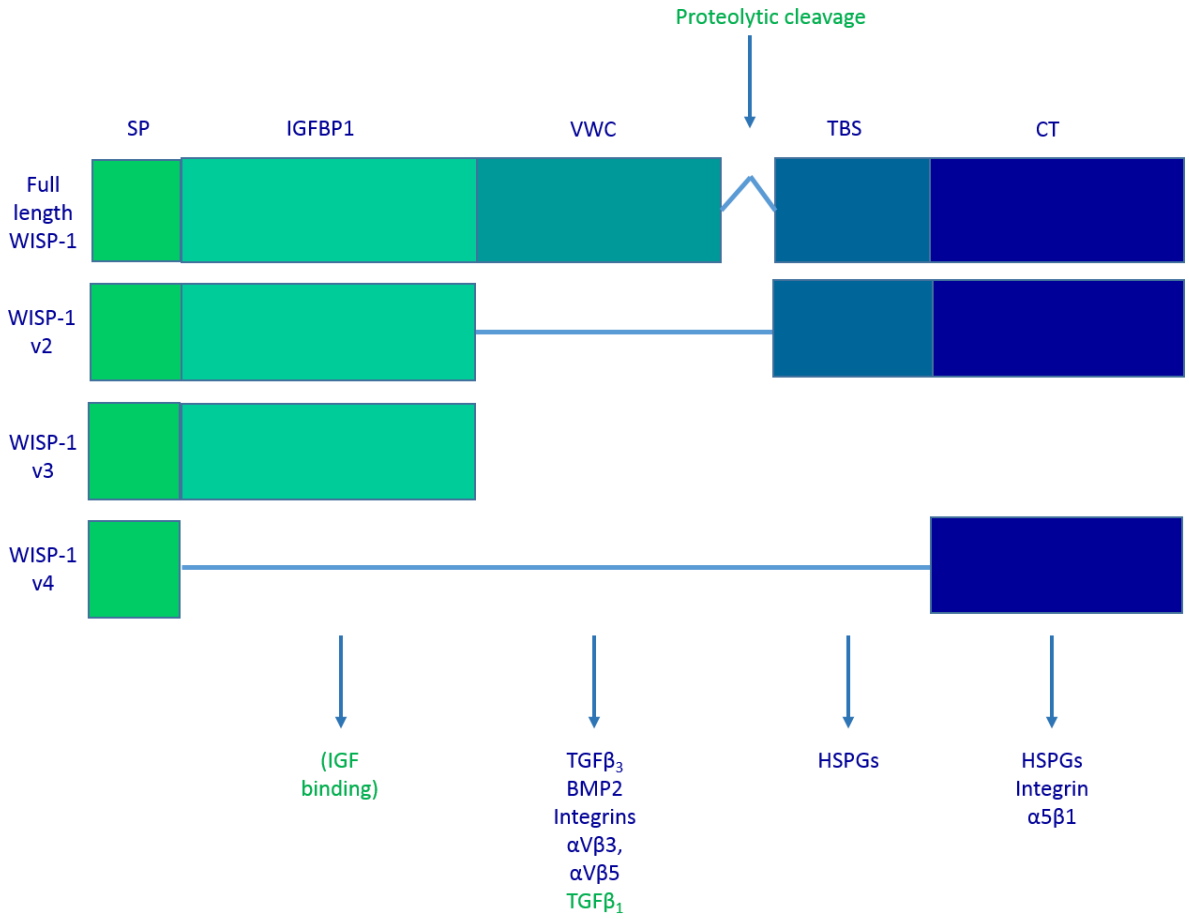

Figure 79. Known binding partners for WISP-1. Shown in blue are the known binding partners for WISP-1 sorted by the domain through which the interaction is thought to occur. WISP-1 has been reported to directly bind TGFβ3 (184) and BMP2 (135). A relationship between WISP-1 and TGFβ1 has been described in more than one study however no direct interaction has been reported to date (shown in green). Integrin binding sites are present in three of the four CCN domains (239). Effects of WISP-1 have been reported to be mediated by integrins αVβ3 (141, 143), αVβ5 (137, 146), α5β1 (135, 158) and αVβ1 (137, 147), the site for which is unknown. WISP-1 has also been reported to bind to the HSPGs decorin and biglycan (190). Reports in the literature suggest that the CCN proteins are susceptible to proteolytic cleavage at the hinge region between the VWC and TBS domains, and between the other domains (159). WISP-1 also contains a putative site for IGF binding (shown in green).

.

In A549 cells, TGFβ_1 stimulated small increases in WISP-1 variants 2 and 3 in 0.5% FBS. WISP-1 variant 4 expression was induced by TGFβ_1 to a greater extent, correlating with the change in EMT marker expression. Making the assumption that WISP-1 binding to another molecule via the cysteine knot domain is required for WISP-1 to exert a particular effect via a different domain(s), increased expression of WISP-1 variant 4 (containing only the cysteine knot domain) could act to negatively regulate this effect of full length WISP-1. In the case of epithelial to mesenchymal-like changes in epithelial cells, this could suggest that full length WISP-1 typically exerts an anti-fibrotic effect that is dampened by the binding of variant 4 instead of full length WISP-1 to molecule X via the cysteine knot domain, shown in Figure 80.

Interestingly, culture of MRC5 fibroblasts with WISP-1 variant 4 conditioned medium stimulated a significant increase in the expression of both this variant and that of full length WISP-1. As culture of A549 cells with full length conditioned medium stimulated full WISP-1 expression, this might suggest a feedback loop between these two variants. A hypothetical scenario in which dysregulation of such a feedback loop might occur in a pro-fibrotic environment could be postulated based on findings in the current study. IPF parenchymal fibroblasts expressed higher levels of WISP-1 variant 4 compared to controls, and there was a trend for TGFβ_1 stimulation of variant 4 expression in these cells. Therefore, in the pro-fibrotic environment, high levels of TGFβ_1 would stimulate fibroblast expression of variant 4. TGFβ_1 would also stimulate epithelial cells expression of WISP-1 variant 4 expression which would then act on fibroblasts to stimulate their expression of variant 4 further, as demonstrated with MRC5 cells. This would lead to there being a relatively high level of WISP-1 variant 4 in the ECM and subsequent change in WISP-1 activity. As shown in Figure 80, this could result in the release of TGFβ_1 from the matrix were it bound to WISP-1 via the VWC domain.

This hypothetical scenario relies on the assumption that increased expression of WISP-1 variant 4 by MRC5 fibroblasts is due to the presence of WISP-1 variant 4 in the conditioned medium. This was not confirmed by western blotting, possibly due to lack of epitope for the antibody as suggested by the weak detection in corresponding cell lysates. An alternative explanation is that WISP-1 variant 4 expression stimulated the expression/secretion of another factor by HEK293T

cells into the supernatant which subsequently stimulated WISP-1 expression by fibroblasts. While this remains unclear, it serves to highlight the complexity of molecules like WISP-1 and hints at the need to properly consider different aspects of WISP-1 biology when investigating its expression and activity.

This is also highlighted by the lack of effect of commercial recombinant WISP-1 on ECM and EMT gene expression despite being mammalian-derived and therefore comparable to HEK293T overexpressed WISP-1 in terms of post-translational modifications. This suggests that another factor either expressed and secreted by WISP-1 transfected HEK293T cells, or by A549/MRC5 cells following WISP-1 stimulation, is required for WISP-1 to exert an effect. This requirement for an additional factor(s) may help to explain differences between the current study and reports in the literature i.e. if expression of a particular molecule is required for WISP-1 to induce a particular effect, perhaps the fibroblasts used in the current study (MRC5s) do not express this molecule but cell types used in other studies do. WISP-1 has been reported in a number of studies to mediate the effects of other proteins such as TGFβ_1 (198) and TNFα (194, 198), and interactions of WISP-1 with other proteins has been reported in the literature. For example, WISP-1 has been shown to have a relationship with TGFβ_1 (183), BMP2 (135) and biglycan (181) in bone development studies, and has been demonstrated to bind to decorin and biglycan in fibroblast conditioned medium (190).

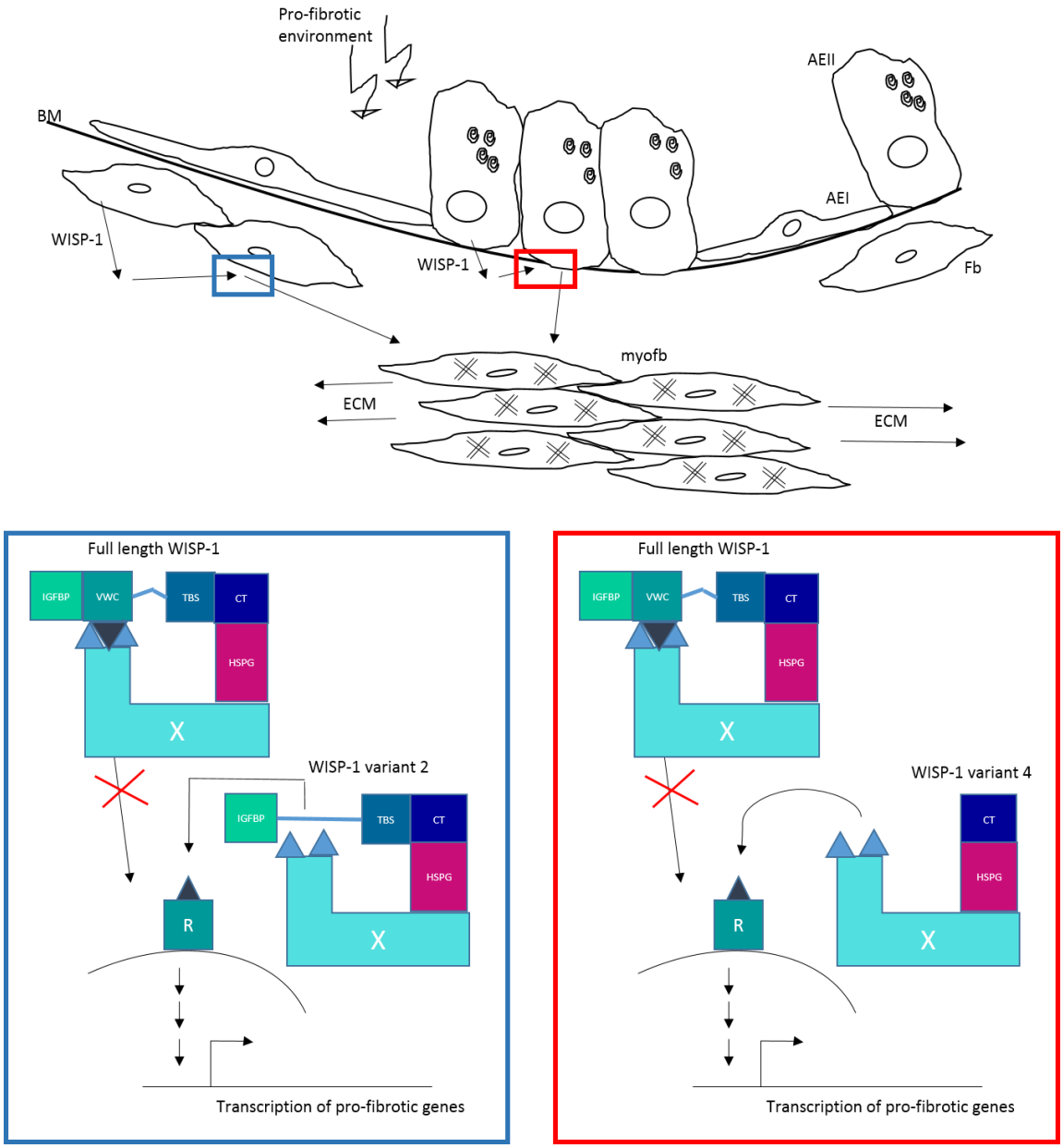

Figure 80. Hypothetical effect of WISP-1 variants in a pro-fibrotic environment. In a pro-fibrotic environment, type II alveolar epithelial cells (AEII) and interstitial fibroblasts (fb) express increased levels of WISP-1 which is secreted from the cell. Through interaction with extracellular matrix (ECM) molecules such as heparin sulphate proteoglycans (HSPG), full length WISP-1 is able to abrogate the effect of a pro-fibrotic molecule (X) thereby limiting epithelial to mesenchymal transition and myofibroblast differentiation stimulated by this molecule. Expression of variant WISP-1 is unable to block the effect of molecule X due its missing domain(s), and also limits the ability of full length WISP-1 to do so by binding to co-factors in the ECM.

6.2 Future work

There are many gaps in the understanding of WISP-1/CCN biology, particularly relating to interactions of WISP-1 with other molecules (including those that may act as a receptor for WISP-1), and the role of WISP-1 variants (alternatively spliced and those resulting from proteolytic cleavage) both in normal and pathological settings. Increased understanding of these aspects would help to delineate the role of WISP-1 in IPF further and provide insight into how WISP-1 might be targeted in disease either to abrogate a pro-fibrotic effect, or enhance an anti-fibrotic effect, were it to be demonstrated that WISP-1 plays such a role in IPF. To this end, the work in this thesis could be advanced in several ways, summarised here:

- All experiments in the current study were carried out using cell monocultures. Co-cultures of fibroblasts and epithelial cells would provide a better system to model epithelial-fibroblast crosstalk. Overexpression of WISP-1 in one of these cell types in a co-culture model would allow the effect of WISP-1 on both cell types to be studied. By expressing WISP-1 in epithelial cells in such a system, differential responses to WISP-1 by IPF and control fibroblasts could be investigated.
- The domains through which WISP-1 exerts any effects observed could be delineated through overexpression of WISP-1 splice variants. Confirmation of the secretion of these variants should be determined, and ideally the variants would be quantified. Whether this would be possible using commercially available reagents is unclear.
- In WISP-1 overexpression studies, the question of whether an effect observed is a direct effect of WISP-1 or is due to another factor influenced by WISP-1 could be investigated by using WISP-1 neutralising antibodies. Domain specific antibodies could also be used to confirm findings from overexpression of splice variants. Another way to determine this could be to purify each of the splice variants and observe whether the same effect is observed as with conditioned medium/overexpression, or to incubate commercial recombinant WISP-1 with HEK293T cells prior to target cells.
- The requirement of additional factors for WISP-1 to exert a particular effect could be studied by stimulating WISP-1 overexpressing cells with different molecules. Of interest would be HSPGs, integrins and the TGFβ/BMP family

of proteins based on reports in the literature relating both to WISP-1 activity and IPF pathogenesis.

- Better understanding of the effects of wisp-1 and its variants may come from transcriptomic or proteomic approaches carried out on transfected cell conditioned medium target cells.

6.3 Final conclusion

The work presented in this thesis has aimed to fully characterise the expression of WISP-1, and its activity in relation to the pathogenesis of IPF. Whilst differences were observed between the current and published studies, several aspects of the current study contribute to the understanding of WISP-1 biology, specifically, the characterisation of WISP-1 splice variant expression, the use of different methods to investigate the effect of WISP-1 (full length and variant), and the characterisation of several antibodies for the detection of WISP-1. This should inform future studies to further the understanding of the role of WISP-1 in IPF with the aim of determining its suitability as a therapeutic target.

List of References

1. Raghu G, Collard HR, Egan JJ, Martinez FJ, Behr J, Brown KK, et al. An official ATS/ERS/JRS/ALAT statement: idiopathic pulmonary fibrosis: evidence-based guidelines for diagnosis and management. Am J Respir Crit Care Med. 2011;183(6):788-824.
2. King TE, Jr., Pardo A, Selman M. Idiopathic pulmonary fibrosis. Lancet (London, England). 2011;378(9807):1949-61.
3. Baumgartner KB, Samet JM, Stidley CA, Colby TV, Waldron JA. Cigarette smoking: a risk factor for idiopathic pulmonary fibrosis. American journal of respiratory and critical care medicine. 1997;155(1):242-8.
4. Egan JJ, Stewart JP, Hasleton PS, Arrand JR, Carroll KB, Woodcock AA. Epstein-Barr virus replication within pulmonary epithelial cells in cryptogenic fibrosing alveolitis. Thorax. 1995;50(12):1234-9.
5. Wangoo A, Shaw RJ, Diss TC, Farrell PJ, du Bois RM, Nicholson AG. Cryptogenic fibrosing alveolitis: lack of association with Epstein-Barr virus infection. Thorax. 1997;52(10):888-91.
6. Lee JS, Collard HR, Raghu G, Sweet MP, Hays SR, Campos GM, et al. Does chronic microaspiration cause idiopathic pulmonary fibrosis? The American journal of medicine. 2010;123(4):304-11.
7. Raghu G, Freudenberger TD, Yang S, Curtis JR, Spada C, Hayes J, et al. High prevalence of abnormal acid gastro-oesophageal reflux in idiopathic pulmonary fibrosis. The European respiratory journal. 2006;27(1):136-42.
8. Marshall RP, Puddicombe A, Cookson WO, Laurent GJ. Adult familial cryptogenic fibrosing alveolitis in the United Kingdom. Thorax. 2000;55(2):143-6.
9. Wang Y, Kuan PJ, Xing C, Cronkhite JT, Torres F, Rosenblatt RL, et al. Genetic defects in surfactant protein A2 are associated with pulmonary fibrosis and lung cancer. American journal of human genetics. 2009;84(1):52-9.
10. Thomas AQ LK, Phillips J, Prince M, Markin C, Speer M, Schwartz DA, Gaddipati R, Marney A, Johnson J, Roberts R, Haines J, Stahlman M, Loyd JE. Heterozygosity for a surfactant protein C gene mutation associated with usual interstitial pneumonitis and cellular nonspecific interstitial pneumonitis in one kindred. Am J Respir Crit Care Med. 2002;165(9):1322-8.
11. Markart P, Ruppert C, Wygrecka M, Schmidt R, Korfei M, Harbach H, et al. Surfactant protein C mutations in sporadic forms of idiopathic interstitial pneumonias. The European respiratory journal. 2007;29(1):134-7.
12. Armanios MY, Chen JJ, Cogan JD, Alder JK, Ingersoll RG, Markin C, et al. Telomerase mutations in families with idiopathic pulmonary fibrosis. The New England journal of medicine. 2007;356(13):1317-26.
13. Tsakiri KD, Cronkhite JT, Kuan PJ, Xing C, Raghu G, Weissler JC, et al. Adult-onset pulmonary fibrosis caused by mutations in telomerase. Proceedings of the National Academy of Sciences of the United States of America. 2007;104(18):7552-7.
14. Cronkhite JT, Xing C, Raghu G, Chin KM, Torres F, Rosenblatt RL, et al. Telomere shortening in familial and sporadic pulmonary fibrosis. American journal of respiratory and critical care medicine. 2008;178(7):729-37.
15. Seibold MA, Wise AL, Speer MC, Steele MP, Brown KK, Loyd JE, et al. A common MUC5B promoter polymorphism and pulmonary fibrosis. The New England journal of medicine. 2011;364(16):1503-12.

16. Stock CJ, Sato H, Fonseca C, Banya WA, Molyneaux PL, Adamali H, et al. Mucin 5B promoter polymorphism is associated with idiopathic pulmonary fibrosis but not with development of lung fibrosis in systemic sclerosis or sarcoidosis. Thorax. 2013;68(5):436-41.
17. Peljto AL, Zhang Y, Fingerlin TE, Ma SF, Garcia JG, Richards TJ, et al. Association between the MUC5B promoter polymorphism and survival in patients with idiopathic pulmonary fibrosis. Jama. 2013;309(21):2232-9.
18. Raghu G, Anstrom KJ, King TE, Jr., Lasky JA, Martinez FJ. Prednisone, azathioprine, and N-acetylcysteine for pulmonary fibrosis. The New England journal of medicine. 2012;366(21):1968-77.
19. NICE. Idiopathic pulmonary fibrosis: The diagnosis and management of suspected idiopathi cpulmonary fibrosis 2013. Available from: https://www.nice.org.uk/guidance/cg163/chapter/1-recommendations#management.
20. Richeldi L, du Bois RM, Raghu G, Azuma A, Brown KK, Costabel U, et al. Efficacy and safety of nintedanib in idiopathic pulmonary fibrosis. The New England journal of medicine. 2014;370(22):2071-82.
21. Noble PW, Albera C, Bradford WZ, Costabel U, Glassberg MK, Kardatzke D, et al. Pirfenidone in patients with idiopathic pulmonary fibrosis (CAPACITY): two randomised trials. Lancet (London, England). 2011;377(9779):1760-9.
22. King TE, Jr., Bradford WZ, Castro-Bernardini S, Fagan EA, Glaspole I, Glassberg MK, et al. A phase 3 trial of pirfenidone in patients with idiopathic pulmonary fibrosis. The New England journal of medicine. 2014;370(22):2083-92.
23. NICE. Pirfenidone for treating idiopathic pulmonary fibrosis 2013. Available from: https://www.nice.org.uk/guidance/ta282.
24. NICE. Nintedanib for treating Idiopathic Pulmonary Fibrosis 2016. Available from: https://www.nice.org.uk/guidance/ta379/chapter/1-Recommendations.
25. Foundation BL. What is pulmonary fibrosis? 2016. Available from: https://www.blf.org.uk/support-for-you/pulmonary-fibrosis/what-is-pulmonary-fibrosis.
26. Crapo JD, Barry BE, Gehr P, Bachofen M, Weibel ER. Cell number and cell characteristics of the normal human lung. The American review of respiratory disease. 1982;126(2):332-7.
27. Weibel ER. On the tricks alveolar epithelial cells play to make a good lung. American journal of respiratory and critical care medicine. 2015;191(5):504-13.
28. Danto SI, Shannon JM, Borok Z, Zabski SM, Crandall ED. Reversible transdifferentiation of alveolar epithelial cells. American journal of respiratory cell and molecular biology. 1995;12(5):497-502.
29. Herzog EL, Brody AR, Colby TV, Mason R, Williams MC. Knowns and unknowns of the alveolus. Proceedings of the American Thoracic Society. 2008;5(7):778-82.
30. Hagood JS, Prabhakaran P, Kumbla P, Salazar L, MacEwen MW, Barker TH, et al. Loss of fibroblast Thy-1 expression correlates with lung fibrogenesis. The American journal of pathology. 2005;167(2):365-79.
31. Sibille Y, Reynolds HY. Macrophages and polymorphonuclear neutrophils in lung defense and injury. The American review of respiratory disease. 1990;141(2):471-501.
32. Rubins JB. Alveolar macrophages: wielding the double-edged sword of inflammation. American journal of respiratory and critical care medicine. 2003;167(2):103-4.
33. Kolb M, Margetts PJ, Anthony DC, Pitossi F, Gauldie J. Transient expression of IL-1beta induces acute lung injury and chronic repair leading to pulmonary fibrosis. The Journal of clinical investigation. 2001;107(12):1529-36.
34. Wilson MS, Madala SK, Ramalingam TR, Gochuico BR, Rosas IO, Cheever AW, et al. Bleomycin and IL-1beta-mediated pulmonary fibrosis is IL-17A dependent. The Journal of experimental medicine. 2010;207(3):535-52.

35. Barlo NP, van Moorsel CH, Korthagen NM, Heron M, Rijkers GT, Ruven HJ, et al. Genetic variability in the IL1RN gene and the balance between interleukin (IL)-1 receptor agonist and IL-1beta in idiopathic pulmonary fibrosis. Clinical and experimental immunology. 2011;166(3):346-51.
36. Park A, Jang. IL-13 and its receptors in IIP. 2009.
37. Karo-Atar D, Bordowitz A, Wand O, Pasmanik-Chor M, Fernandez IE, Itan M, et al. A protective role for IL-13 receptor alpha 1 in bleomycin-induced pulmonary injury and repair. Mucosal immunology. 2016;9(1):240-53.
38. Mori M, Morishita H, Nakamura H, Matsuoka H, Yoshida K, Kishima Y, et al. Hepatoma-derived growth factor is involved in lung remodeling by stimulating epithelial growth. American journal of respiratory cell and molecular biology. 2004;30(4):459-69.
39. Andersson-Sjoland A, de Alba CG, Nihlberg K, Becerril C, Ramirez R, Pardo A, et al. Fibrocytes are a potential source of lung fibroblasts in idiopathic pulmonary fibrosis. The international journal of biochemistry & cell biology. 2008;40(10):2129-40.
40. Phillips RJ, Burdick MD, Hong K, Lutz MA, Murray LA, Xue YY, et al. Circulating fibrocytes traffic to the lungs in response to CXCL12 and mediate fibrosis. The Journal of clinical investigation. 2004;114(3):438-46.
41. Antoniades HN, Bravo MA, Avila RE, Galanopoulos T, Neville-Golden J, Maxwell M, et al. Platelet-derived growth factor in idiopathic pulmonary fibrosis. The Journal of clinical investigation. 1990;86(4):1055-64.
42. Clark JG, Madtes DK, Raghu G. Effects of platelet-derived growth factor isoforms on human lung fibroblast proliferation and procollagen gene expression. Experimental lung research. 1993;19(3):327-44.
43. Aono Y, Kishi M, Yokota Y, Azuma M, Kinoshita K, Takezaki A, et al. Role of platelet-derived growth factor/platelet-derived growth factor receptor axis in the trafficking of circulating fibrocytes in pulmonary fibrosis. American journal of respiratory cell and molecular biology. 2014;51(6):793-801.
44. Pardo A, Gibson K, Cisneros J, Richards TJ, Yang Y, Becerril C, et al. Up-regulation and profibrotic role of osteopontin in human idiopathic pulmonary fibrosis. PLoS medicine. 2005;2(9):e251.
45. White ES, Xia M, Murray S, Dyal R, Flaherty CM, Flaherty KR, et al. Plasma Surfactant Protein-D, Matrix Metalloproteinase-7, and Osteopontin Index Distinguishes Idiopathic Pulmonary Fibrosis From Other Idiopathic Interstitial Pneumonias. American journal of respiratory and critical care medicine. 2016.
46. Mutsaers SE, Foster ML, Chambers RC, Laurent GJ, McAnulty RJ. Increased endothelin-1 and its localization during the development of bleomycin-induced pulmonary fibrosis in rats. American journal of respiratory cell and molecular biology. 1998;18(5):611-9.
47. Uguccioni M, Pulsatelli L, Grigolo B, Facchini A, Fasano L, Cinti C, et al. Endothelin-1 in idiopathic pulmonary fibrosis. Journal of clinical pathology. 1995;48(4):330-4.
48. Selman M, Pardo A, Barrera L, Estrada A, Watson SR, Wilson K, et al. Gene expression profiles distinguish idiopathic pulmonary fibrosis from hypersensitivity pneumonitis. American journal of respiratory and critical care medicine. 2006;173(2):188-98.
49. Foster MW, Morrison LD, Todd JL, Snyder LD, Thompson JW, Soderblom EJ, et al. Quantitative proteomics of bronchoalveolar lavage fluid in idiopathic pulmonary fibrosis. Journal of proteome research. 2015;14(2):1238-49.
50. Shi-Wen X, Denton CP, Dashwood MR, Holmes AM, Bou-Gharios G, Pearson JD, et al. Fibroblast matrix gene expression and connective tissue remodeling: role of endothelin-1. The Journal of investigative dermatology. 2001;116(3):417-25.

51. Wermuth PJ, Li Z, Mendoza FA, Jimenez SA. Stimulation of Transforming Growth Factor-beta1-Induced Endothelial-To-Mesenchymal Transition and Tissue Fibrosis by Endothelin-1 (ET-1): A Novel Profibrotic Effect of ET-1. PloS one. 2016;11(9):e0161988.
52. Selman M, Pardo A. Role of epithelial cells in idiopathic pulmonary fibrosis: from innocent targets to serial killers. Proceedings of the American Thoracic Society. 2006;3(4):364-72.
53. Yang IV, Burch LH, Steele MP, Savov JD, Hollingsworth JW, McElvania-Tekippe E, et al. Gene Expression Profiling of Familial and Sporadic Interstitial Pneumonia. American journal of respiratory and critical care medicine. 2007;175(1):45-54.
54. Chilosi M, Poletti V, Murer B, Lestani M, Cancellieri A, Montagna L, et al. Abnormal re-epithelialization and lung remodeling in idiopathic pulmonary fibrosis: the role of deltaN-p63. Laboratory investigation; a journal of technical methods and pathology. 2002;82(10):1335-45.
55. Katzenstein A-LA, Mukhopadhyay S, Myers JL. Diagnosis of usual interstitial pneumonia and distinction from other fibrosing interstitial lung diseases. Human pathology. 2008;39(9):1275-94.
56. Chilosi M, Poletti V, Zamò A, Lestani M, Montagna L, Piccoli P, et al. Aberrant Wnt/β-Catenin Pathway Activation in Idiopathic Pulmonary Fibrosis. The American journal of pathology. 2003;162(5):1495-502.
57. Seibold MA, Smith RW, Urbanek C, Groshong SD, Cosgrove GP, Brown KK, et al. The Idiopathic Pulmonary Fibrosis Honeycomb Cyst Contains A Mucocilary Pseudostratified Epithelium. PloS one. 2013;8(3):e58658.
58. Cool CD, Groshong SD, Rai PR, Henson PM, Stewart JS, Brown KK. Fibroblast foci are not discrete sites of lung injury or repair: the fibroblast reticulum. American journal of respiratory and critical care medicine. 2006;174(6):654-8.
59. Maher TM, Evans IC, Bottoms SE, Mercer PF, Thorley AJ, Nicholson AG, et al. Diminished prostaglandin E2 contributes to the apoptosis paradox in idiopathic pulmonary fibrosis. American journal of respiratory and critical care medicine. 2010;182(1):73-82.
60. Visscher DW, Myers JL. Histologic Spectrum of Idiopathic Interstitial Pneumonias. Proceedings of the American Thoracic Society. 2006;3(4):322-9.
61. Bateman ED, Turner-Warwick M, Adelmann-Grill BC. Immunohistochemical study of collagen types in human foetal lung and fibrotic lung disease. Thorax. 1981;36(9):645-53.
62. Calderwood CJ JM, Hoile L, Havelock T, Maher TM, O'Reilly KMA, Davies DE, editor Secreted lysyl oxidase is elevated in the BALF of patients with IPF. British Thoracic Society Winter Meeting 2012; 2012: Thorax.
63. Barry-Hamilton V, Spangler R, Marshall D, McCauley S, Rodriguez HM, Oyasu M, et al. Allosteric inhibition of lysyl oxidase-like-2 impedes the development of a pathologic microenvironment. Nat Med. 2010;16(9):1009-17.
64. Hernnas J, Nettelbladt O, Bjermer L, Sarnstrand B, Malmstrom A, Hallgren R. Alveolar accumulation of fibronectin and hyaluronan precedes bleomycin-induced pulmonary fibrosis in the rat. The European respiratory journal. 1992;5(4):404-10.
65. Li Y, Jiang D, Liang J, Meltzer EB, Gray A, Miura R, et al. Severe lung fibrosis requires an invasive fibroblast phenotype regulated by hyaluronan and CD44. The Journal of experimental medicine. 2011;208(7):1459-71.
66. Westergren-Thorsson G, Sime P, Jordana M, Gauldie J, Sarnstrand B, Malmstrom A. Lung fibroblast clones from normal and fibrotic subjects differ in hyaluronan and decorin production and rate of proliferation. The international journal of biochemistry & cell biology. 2004;36(8):1573-84.
67. Kolb M, Margetts PJ, Sime PJ, Gauldie J. Proteoglycans decorin and biglycan differentially modulate TGF-beta-mediated fibrotic responses in the lung. American journal of physiology Lung cellular and molecular physiology. 2001;280(6):L1327-34.
68. Willis BC, Liebler JM, Luby-Phelps K, Nicholson AG, Crandall ED, du Bois RM, et al. Induction of epithelial-mesenchymal transition in alveolar epithelial cells by transforming growth factor-

beta1: potential role in idiopathic pulmonary fibrosis. The American journal of pathology. 2005;166(5):1321-32.
69. Chen HH, Zhou XL, Shi YL, Yang J. Roles of p38 MAPK and JNK in TGF-beta1-induced human alveolar epithelial to mesenchymal transition. Archives of medical research. 2013;44(2):93-8.
70. Kim KK, Kugler MC, Wolters PJ, Robillard L, Galvez MG, Brumwell AN, et al. Alveolar epithelial cell mesenchymal transition develops in vivo during pulmonary fibrosis and is regulated by the extracellular matrix. Proceedings of the National Academy of Sciences of the United States of America. 2006;103(35):13180-5.
71. Marmai C, Sutherland RE, Kim KK, Dolganov GM, Fang X, Kim SS, et al. Alveolar epithelial cells express mesenchymal proteins in patients with idiopathic pulmonary fibrosis. American journal of physiology Lung cellular and molecular physiology. 2011;301(1):L71-8.
72. Tanjore H, Xu XC, Polosukhin VV, Degryse AL, Li B, Han W, et al. Contribution of epithelial-derived fibroblasts to bleomycin-induced lung fibrosis. American journal of respiratory and critical care medicine. 2009;180(7):657-65.
73. Rock JR, Barkauskas CE, Cronce MJ, Xue Y, Harris JR, Liang J, et al. Multiple stromal populations contribute to pulmonary fibrosis without evidence for epithelial to mesenchymal transition. Proceedings of the National Academy of Sciences of the United States of America. 2011;108(52):E1475-83.
74. Larsson O, Diebold D, Fan D, Peterson M, Nho RS, Bitterman PB, et al. Fibrotic myofibroblasts manifest genome-wide derangements of translational control. PloS one. 2008;3(9):e3220.
75. Hashimoto N, Phan SH, Imaizumi K, Matsuo M, Nakashima H, Kawabe T, et al. Endothelial-mesenchymal transition in bleomycin-induced pulmonary fibrosis. American journal of respiratory cell and molecular biology. 2010;43(2):161-72.
76. Schmidt M, Sun G, Stacey MA, Mori L, Mattoli S. Identification of circulating fibrocytes as precursors of bronchial myofibroblasts in asthma. Journal of immunology (Baltimore, Md : 1950). 2003;171(1):380-9.
77. Humphreys BD, Lin SL, Kobayashi A, Hudson TE, Nowlin BT, Bonventre JV, et al. Fate tracing reveals the pericyte and not epithelial origin of myofibroblasts in kidney fibrosis. The American journal of pathology. 2010;176(1):85-97.
78. Zolak JS JR, Surolia R, Karki S, Oliva O, Hock T, Guroji P, Diang Q, Liu RM, Bolisetty S, Agarwal A, Thannickal VJ, Antony VB. Pleural mesothelial cell differentiation and invasion in fibrogenic lung injury. Am J Pathol. 2013.
79. Ask K, Bonniaud P, Maass K, Eickelberg O, Margetts PJ, Warburton D, et al. Progressive pulmonary fibrosis is mediated by TGF-beta isoform 1 but not TGF-beta3. The international journal of biochemistry & cell biology. 2008;40(3):484-95.
80. Khalil N, Parekh TV, O'Connor R, Antman N, Kepron W, Yehaulaeshet T, et al. Regulation of the effects of TGF-beta 1 by activation of latent TGF-beta 1 and differential expression of TGF-beta receptors (T beta R-I and T beta R-II) in idiopathic pulmonary fibrosis. Thorax. 2001;56(12):907-15.
81. Munger JS, Huang X, Kawakatsu H, Griffiths MJ, Dalton SL, Wu J, et al. The integrin alpha v beta 6 binds and activates latent TGF beta 1: a mechanism for regulating pulmonary inflammation and fibrosis. Cell. 1999;96(3):319-28.
82. Horan GS, Wood S, Ona V, Li DJ, Lukashev ME, Weinreb PH, et al. Partial inhibition of integrin alpha(v)beta6 prevents pulmonary fibrosis without exacerbating inflammation. American journal of respiratory and critical care medicine. 2008;177(1):56-65.
83. Fernandez IE, Eickelberg O. The impact of TGF-beta on lung fibrosis: from targeting to biomarkers. Proceedings of the American Thoracic Society. 2012;9(3):111-6.

84. Hinz B. Tissue stiffness, latent TGF-beta1 activation, and mechanical signal transduction: implications for the pathogenesis and treatment of fibrosis. Current rheumatology reports. 2009;11(2):120-6.
85. Yu Q, Stamenkovic I. Cell surface-localized matrix metalloproteinase-9 proteolytically activates TGF-beta and promotes tumor invasion and angiogenesis. Genes & development. 2000;14(2):163-76.
86. Selman M, Carrillo G, Estrada A, Mejia M, Becerril C, Cisneros J, et al. Accelerated variant of idiopathic pulmonary fibrosis: clinical behavior and gene expression pattern. PloS one. 2007;2(5):e482.
87. Sime PJ, Xing Z, Graham FL, Csaky KG, Gauldie J. Adenovector-mediated gene transfer of active transforming growth factor-beta1 induces prolonged severe fibrosis in rat lung. The Journal of clinical investigation. 1997;100(4):768-76.
88. Eickelberg O, Kohler E, Reichenberger F, Bertschin S, Woodtli T, Erne P, et al. Extracellular matrix deposition by primary human lung fibroblasts in response to TGF-beta1 and TGF-beta3. The American journal of physiology. 1999;276(5 Pt 1):L814-24.
89. Fine A, Goldstein RH. The effect of transforming growth factor-beta on cell proliferation and collagen formation by lung fibroblasts. The Journal of biological chemistry. 1987;262(8):3897-902.
90. Battegay EJ, Raines EW, Seifert RA, Bowen-Pope DF, Ross R. TGF-beta induces bimodal proliferation of connective tissue cells via complex control of an autocrine PDGF loop. Cell. 1990;63(3):515-24.
91. Ignotz RA, Endo T, Massague J. Regulation of fibronectin and type I collagen mRNA levels by transforming growth factor-beta. The Journal of biological chemistry. 1987;262(14):6443-6.
92. Hu B, Wu Z, Phan SH. Smad3 mediates transforming growth factor-beta-induced alpha-smooth muscle actin expression. American journal of respiratory cell and molecular biology. 2003;29(3 Pt 1):397-404.
93. Gu L, Zhu YJ, Yang X, Guo ZJ, Xu WB, Tian XL. Effect of TGF-beta/Smad signaling pathway on lung myofibroblast differentiation. Acta pharmacologica Sinica. 2007;28(3):382-91.
94. Raghu G, Masta S, Meyers D, Narayanan AS. Collagen synthesis by normal and fibrotic human lung fibroblasts and the effect of transforming growth factor-beta. The American review of respiratory disease. 1989;140(1):95-100.
95. Giri SN, Hyde DM, Hollinger MA. Effect of antibody to transforming growth factor beta on bleomycin induced accumulation of lung collagen in mice. Thorax. 1993;48(10):959-66.
96. Jayachandran A, Konigshoff M, Yu H, Rupniewska E, Hecker M, Klepetko W, et al. SNAI transcription factors mediate epithelial-mesenchymal transition in lung fibrosis. Thorax. 2009;64(12):1053-61.
97. Yang Y, Haitchi HM, Cakebread J, Sammut D, Harvey A, Powell RM, et al. Epigenetic mechanisms silence a disintegrin and metalloprotease 33 expression in bronchial epithelial cells. The Journal of allergy and clinical immunology. 2008;121(6):1393-9, 9.e1-14.
98. Hagimoto N, Kuwano K, Inoshima I, Yoshimi M, Nakamura N, Fujita M, et al. TGF-beta 1 as an enhancer of Fas-mediated apoptosis of lung epithelial cells. Journal of immunology (Baltimore, Md : 1950). 2002;168(12):6470-8.
99. Fjellbirkeland L, Cambier S, Broaddus VC, Hill A, Brunetta P, Dolganov G, et al. Integrin alphavbeta8-mediated activation of transforming growth factor-beta inhibits human airway epithelial proliferation in intact bronchial tissue. The American journal of pathology. 2003;163(2):533-42.
100. Konishi K, Gibson KF, Lindell KO, Richards TJ, Zhang Y, Dhir R, et al. Gene expression profiles of acute exacerbations of idiopathic pulmonary fibrosis. American journal of respiratory and critical care medicine. 2009;180(2):167-75.

101. Morais A, Beltrao M, Sokhatska O, Costa D, Melo N, Mota P, et al. Serum metalloproteinases 1 and 7 in the diagnosis of idiopathic pulmonary fibrosis and other interstitial pneumonias. Respiratory medicine. 2015;109(8):1063-8.
102. Rosas IO, Richards TJ, Konishi K, Zhang Y, Gibson K, Lokshin AE, et al. MMP1 and MMP7 as potential peripheral blood biomarkers in idiopathic pulmonary fibrosis. PLoS medicine. 2008;5(4):e93.
103. Pardo A, Selman M. Role of matrix metaloproteases in idiopathic pulmonary fibrosis. Fibrogenesis & tissue repair. 2012;5(Suppl 1):S9.
104. Yamashita CM, Dolgonos L, Zemans RL, Young SK, Robertson J, Briones N, et al. Matrix metalloproteinase 3 is a mediator of pulmonary fibrosis. The American journal of pathology. 2011;179(4):1733-45.
105. DePianto DJ, Chandriani S, Abbas AR, Jia G, N'Diaye EN, Caplazi P, et al. Heterogeneous gene expression signatures correspond to distinct lung pathologies and biomarkers of disease severity in idiopathic pulmonary fibrosis. Thorax. 2015;70(1):48-56.
106. Zuo F, Kaminski N, Eugui E, Allard J, Yakhini Z, Ben-Dor A, et al. Gene expression analysis reveals matrilysin as a key regulator of pulmonary fibrosis in mice and humans. Proceedings of the National Academy of Sciences of the United States of America. 2002;99(9):6292-7.
107. Bauer Y, Tedrow J, de Bernard S, Birker-Robaczewska M, Gibson KF, Guardela BJ, et al. A novel genomic signature with translational significance for human idiopathic pulmonary fibrosis. American journal of respiratory cell and molecular biology. 2015;52(2):217-31.
108. Fujishima S, Shiomi T, Yamashita S, Yogo Y, Nakano Y, Inoue T, et al. Production and activation of matrix metalloproteinase 7 (matrilysin 1) in the lungs of patients with idiopathic pulmonary fibrosis. Archives of pathology & laboratory medicine. 2010;134(8):1136-42.
109. Dunsmore SE, Saarialho-Kere UK, Roby JD, Wilson CL, Matrisian LM, Welgus HG, et al. Matrilysin expression and function in airway epithelium. The Journal of clinical investigation. 1998;102(7):1321-31.
110. Selman M, Ruiz V, Cabrera S, Segura L, Ramirez R, Barrios R, et al. TIMP-1, -2, -3, and -4 in idiopathic pulmonary fibrosis. A prevailing nondegradative lung microenvironment? American journal of physiology Lung cellular and molecular physiology. 2000;279(3):L562-74.
111. Aoyagi-Ikeda K, Maeno T, Matsui H, Ueno M, Hara K, Aoki Y, et al. Notch induces myofibroblast differentiation of alveolar epithelial cells via transforming growth factor-{beta}-Smad3 pathway. American journal of respiratory cell and molecular biology. 2011;45(1):136-44.
112. Coon DR, Roberts DJ, Loscertales M, Kradin R. Differential epithelial expression of SHH and FOXF1 in usual and nonspecific interstitial pneumonia. Experimental and molecular pathology. 2006;80(2):119-23.
113. Hu B, Liu J, Wu Z, Liu T, Ullenbruch MR, Ding L, et al. Reemergence of hedgehog mediates epithelial-mesenchymal crosstalk in pulmonary fibrosis. American journal of respiratory cell and molecular biology. 2015;52(4):418-28.
114. White ES, Atrasz RG, Hu B, Phan SH, Stambolic V, Mak TW, et al. Negative regulation of myofibroblast differentiation by PTEN (Phosphatase and Tensin Homolog Deleted on chromosome 10). American journal of respiratory and critical care medicine. 2006;173(1):112-21.
115. Parapuram SK, Thompson K, Tsang M, Hutchenreuther J, Bekking C, Liu S, et al. Loss of PTEN expression by mouse fibroblasts results in lung fibrosis through a CCN2-dependent mechanism. Matrix biology : journal of the International Society for Matrix Biology. 2015;43:35-41.
116. Selman M, Pardo A, Kaminski N. Idiopathic pulmonary fibrosis: aberrant recapitulation of developmental programs? PLoS medicine. 2008;5(3):e62.
117. Molloy EL, Adams A, Moore JB, Masterson JC, Madrigal-Estebas L, Mahon BP, et al. BMP4 induces an epithelial-mesenchymal transition-like response in adult airway epithelial cells. Growth factors (Chur, Switzerland). 2008;26(1):12-22.

118. Pegorier S, Campbell GA, Kay AB, Lloyd CM. Bone morphogenetic protein (BMP)-4 and BMP-7 regulate differentially transforming growth factor (TGF)-beta1 in normal human lung fibroblasts (NHLF). Respiratory research. 2010;11:85.
119. Koli K, Myllarniemi M, Vuorinen K, Salmenkivi K, Ryynanen MJ, Kinnula VL, et al. Bone morphogenetic protein-4 inhibitor gremlin is overexpressed in idiopathic pulmonary fibrosis. The American journal of pathology. 2006;169(1):61-71.
120. Tanjore H, Degryse AL, Crossno PF, Xu XC, McConaha ME, Jones BR, et al. beta-catenin in the alveolar epithelium protects from lung fibrosis after intratracheal bleomycin. American journal of respiratory and critical care medicine. 2013;187(6):630-9.
121. Lam AP, Flozak AS, Russell S, Wei J, Jain M, Mutlu GM, et al. Nuclear beta-catenin is increased in systemic sclerosis pulmonary fibrosis and promotes lung fibroblast migration and proliferation. American journal of respiratory cell and molecular biology. 2011;45(5):915-22.
122. Konigshoff M, Balsara N, Pfaff EM, Kramer M, Chrobak I, Seeger W, et al. Functional Wnt signaling is increased in idiopathic pulmonary fibrosis. PloS one. 2008;3(5):e2142.
123. Lam AP, Herazo-Maya JD, Sennello JA, Flozak AS, Russell S, Mutlu GM, et al. Wnt coreceptor Lrp5 is a driver of idiopathic pulmonary fibrosis. American journal of respiratory and critical care medicine. 2014;190(2):185-95.
124. Konigshoff M, Kramer M, Balsara N, Wilhelm J, Amarie OV, Jahn A, et al. WNT1-inducible signaling protein-1 mediates pulmonary fibrosis in mice and is upregulated in humans with idiopathic pulmonary fibrosis. The Journal of clinical investigation. 2009;119(4):772-87.
125. Berschneider B, Ellwanger DC, Baarsma HA, Thiel C, Shimbori C, White ES, et al. miR-92a regulates TGF-beta1-induced WISP1 expression in pulmonary fibrosis. The international journal of biochemistry & cell biology. 2014;53:432-41.
126. Brigstock DR, Goldschmeding R, Katsube KI, Lam SC, Lau LF, Lyons K, et al. Proposal for a unified CCN nomenclature. Molecular pathology : MP. 2003;56(2):127-8.
127. Yanagita T, Kubota S, Kawaki H, Kawata K, Kondo S, Takano-Yamamoto T, et al. Expression and physiological role of CCN4/Wnt-induced secreted protein 1 mRNA splicing variants in chondrocytes. The FEBS journal. 2007;274(7):1655-65.
128. Bork P. The modular architecture of a new family of growth regulators related to connective tissue growth factor. FEBS letters. 1993;327(2):125-30.
129. Brigstock DR. The connective tissue growth factor/cysteine-rich 61/nephroblastoma overexpressed (CCN) family. Endocrine reviews. 1999;20(2):189-206.
130. Kim HS, Nagalla SR, Oh Y, Wilson E, Roberts CT, Rosenfeld RG. Identification of a family of low-affinity insulin-like growth factor binding proteins (IGFBPs): Characterization of connective tissue growth factor as a member of the IGFBP superfamily. Proceedings of the National Academy of Sciences of the United States of America. 1997;94(24):12981-6.
131. Holbourn KP, Acharya KR, Perbal B. The CCN family of proteins: structure-function relationships. Trends in biochemical sciences. 2008;33(10):461-73.
132. Sitar T, Popowicz GM, Siwanowicz I, Huber R, Holak TA. Structural basis for the inhibition of insulin-like growth factors by insulin-like growth factor-binding proteins. Proceedings of the National Academy of Sciences of the United States of America. 2006;103(35):13028-33.
133. Abreu JG, Ketpura NI, Reversade B, De Robertis EM. Connective-tissue growth factor (CTGF) modulates cell signalling by BMP and TGF-beta. Nature cell biology. 2002;4(8):599-604.
134. Minamizato T, Sakamoto K, Liu T, Kokubo H, Katsube K, Perbal B, et al. CCN3/NOV inhibits BMP-2-induced osteoblast differentiation by interacting with BMP and Notch signaling pathways. Biochemical and biophysical research communications. 2007;354(2):567-73.
135. Ono M, Inkson CA, Kilts TM, Young MF. WISP-1/CCN4 regulates osteogenesis by enhancing BMP-2 activity. Journal of bone and mineral research : the official journal of the American Society for Bone and Mineral Research. 2011;26(1):193-208.

136. Holbourn KP, Perbal B, Ravi Acharya K. Proteins on the catwalk: modelling the structural domains of the CCN family of proteins. Journal of cell communication and signaling. 2009;3(1):25-41.
137. Stephens S, Palmer J, Konstantinova I, Pearce A, Jarai G, Day E. A functional analysis of Wnt inducible signalling pathway protein -1 (WISP-1/CCN4). Journal of cell communication and signaling. 2015;9(1):63-72.
138. Lau LF, Lam SC. The CCN family of angiogenic regulators: the integrin connection. Experimental cell research. 1999;248(1):44-57.
139. Jun JI, Lau LF. Taking aim at the extracellular matrix: CCN proteins as emerging therapeutic targets. Nature reviews Drug discovery. 2011;10(12):945-63.
140. Kireeva ML, Lam SC, Lau LF. Adhesion of human umbilical vein endothelial cells to the immediate-early gene product Cyr61 is mediated through integrin alphavbeta3. The Journal of biological chemistry. 1998;273(5):3090-6.
141. Chen Z, Ding X, Jin S, Pitt B, Zhang L, Billiar T, et al. WISP1-αvβ3 integrin signaling positively regulates TLR-triggered inflammation response in sepsis induced lung injury. Scientific reports. 2016;6.
142. Chuang JY, Chang AC, Chiang IP, Tsai MH, Tang CH. Apoptosis signal-regulating kinase 1 is involved in WISP-1-promoted cell motility in human oral squamous cell carcinoma cells. PloS one. 2013;8(10):e78022.
143. Chuang JY, Chen PC, Tsao CW, Chang AC, Lein MY, Lin CC, et al. WISP-1 a novel angiogenic regulator of the CCN family promotes oral squamous cell carcinoma angiogenesis through VEGF-A expression. Oncotarget. 2015;6(6):4239-52.
144. Jedsadayanmata A, Chen CC, Kireeva ML, Lau LF, Lam SC. Activation-dependent adhesion of human platelets to Cyr61 and Fisp12/mouse connective tissue growth factor is mediated through integrin alpha(IIb)beta(3). The Journal of biological chemistry. 1999;274(34):24321-7.
145. Chen CC, Young JL, Monzon RI, Chen N, Todorovic V, Lau LF. Cytotoxicity of TNFalpha is regulated by integrin-mediated matrix signaling. The EMBO journal. 2007;26(5):1257-67.
146. Hou CH, Tang CH, Hsu CJ, Hou SM, Liu JF. CCN4 induces IL-6 production through alphavbeta5 receptor, PI3K, Akt, and NF-kappaB singling pathway in human synovial fibroblasts. Arthritis research & therapy. 2013;15(1):R19.
147. Tai HC, Chang AC, Yu HJ, Huang CY, Tsai YC, Lai YW, et al. Osteoblast-derived WNT-induced secreted protein 1 increases VCAM-1 expression and enhances prostate cancer metastasis by down-regulating miR-126. Oncotarget. 2014;5(17):7589-98.
148. Schultz-Cherry S, Chen H, Mosher DF, Misenheimer TM, Krutzsch HC, Roberts DD, et al. Regulation of transforming growth factor-beta activation by discrete sequences of thrombospondin 1. The Journal of biological chemistry. 1995;270(13):7304-10.
149. Brigstock DR, Steffen CL, Kim GY, Vegunta RK, Diehl JR, Harding PA. Purification and characterization of novel heparin-binding growth factors in uterine secretory fluids. Identification as heparin-regulated Mr 10,000 forms of connective tissue growth factor. The Journal of biological chemistry. 1997;272(32):20275-82.
150. Heng ECK, Huang Y, Black SA, Trackman PC. CCN2, CONNECTIVE TISSUE GROWTH FACTOR, STIMULATES COLLAGEN DEPOSITION BY GINGIVAL FIBROBLASTS VIA MODULE 3 AND α6- AND β1 INTEGRINS. Journal of cellular biochemistry. 2006;98(2):409-20.
151. Rider CC. Heparin/heparan sulphate binding in the TGF-beta cytokine superfamily. Biochemical Society transactions. 2006;34(Pt 3):458-60.
152. Cardin AD, Weintraub HJ. Molecular modeling of protein-glycosaminoglycan interactions. Arteriosclerosis, Thrombosis, and Vascular Biology. 1989;9(1):21-32.
153. Ball DK, Rachfal AW, Kemper SA, Brigstock DR. The heparin-binding 10 kDa fragment of connective tissue growth factor (CTGF) containing module 4 alone stimulates cell adhesion. The Journal of endocrinology. 2003;176(2):R1-7.

154. Mercurio S, Latinkic B, Itasaki N, Krumlauf R, Smith JC. Connective-tissue growth factor modulates WNT signalling and interacts with the WNT receptor complex. Development. 2004;131(9):2137-47.
155. Todorovic V, Chen CC, Hay N, Lau LF. The matrix protein CCN1 (CYR61) induces apoptosis in fibroblasts. The Journal of cell biology. 2005;171(3):559-68.
156. Schober JM, Chen N, Grzeszkiewicz TM, Jovanovic I, Emeson EE, Ugarova TP, et al. Identification of integrin alpha(M)beta(2) as an adhesion receptor on peripheral blood monocytes for Cyr61 (CCN1) and connective tissue growth factor (CCN2): immediate-early gene products expressed in atherosclerotic lesions. Blood. 2002;99(12):4457-65.
157. Gao R, Brigstock DR. A novel integrin α5β1 binding domain in module 4 of connective tissue growth factor (CCN2/CTGF) promotes adhesion and migration of activated pancreatic stellate cells. Gut. 2006;55(6):856-62.
158. Liu JF, Hou SM, Tsai CH, Huang CY, Hsu CJ, Tang CH. CCN4 induces vascular cell adhesion molecule-1 expression in human synovial fibroblasts and promotes monocyte adhesion. Biochimica et biophysica acta. 2013;1833(5):966-75.
159. Hashimoto G, Inoki I, Fujii Y, Aoki T, Ikeda E, Okada Y. Matrix metalloproteinases cleave connective tissue growth factor and reactivate angiogenic activity of vascular endothelial growth factor 165. The Journal of biological chemistry. 2002;277(39):36288-95.
160. Steffen CL, Ball-Mirth DK, Harding PA, Bhattacharyya N, Pillai S, Brigstock DR. Characterization of cell-associated and soluble forms of connective tissue growth factor (CTGF) produced by fibroblast cells in vitro. Growth factors (Chur, Switzerland). 1998;15(3):199-213.
161. Perbal B. Alternative splicing of CCN mRNAs .... it has been upon us. Journal of cell communication and signaling. 2009;3(2):153-7.
162. Tanaka S, Sugimachi K, Kameyama T, Maehara S, Shirabe K, Shimada M, et al. Human WISP1v, a member of the CCN family, is associated with invasive cholangiocarcinoma. Hepatology (Baltimore, Md). 2003;37(5):1122-9.
163. Tanaka S, Sugimachi K, Saeki H, Kinoshita J, Ohga T, Shimada M, et al. A novel variant of WISP1 lacking a Von Willebrand type C module overexpressed in scirrhous gastric carcinoma. Oncogene. 2001;20(39):5525-32.
164. Cervello M, Giannitrapani L, Labbozzetta M, Notarbartolo M, D'Alessandro N, Lampiasi N, et al. Expression of WISPs and of their novel alternative variants in human hepatocellular carcinoma cells. Annals of the New York Academy of Sciences. 2004;1028:432-9.
165. Leask A, Abraham DJ. The role of connective tissue growth factor, a multifunctional matricellular protein, in fibroblast biology. Biochemistry and cell biology = Biochimie et biologie cellulaire. 2003;81(6):355-63.
166. Wang Q, Usinger W, Nichols B, Gray J, Xu L, Seeley TW, et al. Cooperative interaction of CTGF and TGF-beta in animal models of fibrotic disease. Fibrogenesis & tissue repair. 2011;4(1):4.
167. Pan LH, Yamauchi K, Uzuki M, Nakanishi T, Takigawa M, Inoue H, et al. Type II alveolar epithelial cells and interstitial fibroblasts express connective tissue growth factor in IPF. The European respiratory journal. 2001;17(6):1220-7.
168. Allen JT, Knight RA, Bloor CA, Spiteri MA. Enhanced insulin-like growth factor binding protein-related protein 2 (Connective tissue growth factor) expression in patients with idiopathic pulmonary fibrosis and pulmonary sarcoidosis. American journal of respiratory cell and molecular biology. 1999;21(6):693-700.
169. Pennica D, Swanson TA, Welsh JW, Roy MA, Lawrence DA, Lee J, et al. WISP genes are members of the connective tissue growth factor family that are up-regulated in wnt-1-transformed cells and aberrantly expressed in human colon tumors. Proceedings of the National Academy of Sciences of the United States of America. 1998;95(25):14717-22.

170. Luo J, Chen J, Deng ZL, Luo X, Song WX, Sharff KA, et al. Wnt signaling and human diseases: what are the therapeutic implications? Laboratory investigation; a journal of technical methods and pathology. 2007;87(2):97-103.
171. Xu L, Corcoran RB, Welsh JW, Pennica D, Levine AJ. WISP-1 is a Wnt-1- and beta-catenin-responsive oncogene. Genes & development. 2000;14(5):585-95.
172. Gustafson B, Smith U. Cytokines Promote Wnt Signaling and Inflammation and Impair the Normal Differentiation and Lipid Accumulation in 3T3-L1 Preadipocytes. Journal of Biological Chemistry. 2006;281(14):9507-16.
173. Coskun M, Olsen AK, Bzorek M, Holck S, Engel UH, Nielsen OH, et al. Involvement of CDX2 in the cross talk between TNF-α and Wnt signaling pathway in the colon cancer cell line Caco-2. Carcinogenesis. 2014;35(5):1185-92.
174. Oguma K, Oshima H, Aoki M, Uchio R, Naka K, Nakamura S, et al. Activated macrophages promote Wnt signalling through tumour necrosis factor-α in gastric tumour cells. The EMBO journal. 2008;27(12):1671-81.
175. Zhou B, Liu Y, Kahn M, Ann DK, Han A, Wang H, et al. Interactions Between β-Catenin and Transforming Growth Factor-β Signaling Pathways Mediate Epithelial-Mesenchymal Transition and Are Dependent on the Transcriptional Co-activator cAMP-response Element-binding Protein (CREB)-binding Protein (CBP). Journal of Biological Chemistry. 2012;287(10):7026-38.
176. Cawthorn WP, Heyd F, Hegyi K, Sethi JK. Tumour necrosis factor-[alpha] inhibits adipogenesis via a [beta]-catenin//TCF4(TCF7L2)-dependent pathway. Cell Death Differ. 2007;14(7):1361-73.
177. Jian H, Shen X, Liu I, Semenov M, He X, Wang X-F. Smad3-dependent nuclear translocation of β-catenin is required for TGF-β1-induced proliferation of bone marrow-derived adult human mesenchymal stem cells. Genes & development. 2006;20(6):666-74.
178. Wang S, Chong ZZ, Shang YC, Maiese K. WISP1 (CCN4) autoregulates its expression and nuclear trafficking of beta-catenin during oxidant stress with limited effects upon neuronal autophagy. Current neurovascular research. 2012;9(2):91-101.
179. Venkatesan B, Prabhu SD, Venkatachalam K, Mummidi S, Valente AJ, Clark RA, et al. WNT1-Inducible Signaling Pathway Protein-1 Activates Diverse Cell Survival Pathways and Blocks Doxorubicin-induced Cardiomyocyte Death. Cellular signalling. 2010;22(5):809-20.
180. Reddy VS, Valente AJ, Delafontaine P, Chandrasekar B. Interleukin-18/WNT1-inducible signaling pathway protein-1 signaling mediates human saphenous vein smooth muscle cell proliferation. J Cell Physiol. 2011;226(12):3303-15.
181. Inkson CA, Ono M, Bi Y, Kuznetsov SA, Fisher LW, Young MF. The potential functional interaction of biglycan and WISP-1 in controlling differentiation and proliferation of osteogenic cells. Cells, tissues, organs. 2009;189(1-4):153-7.
182. Li Z, Dang J, Chang KY, Rana TM. MicroRNA-mediated regulation of extracellular matrix formation modulates somatic cell reprogramming. RNA (New York, NY). 2014;20(12):1900-15.
183. Inkson CA, Ono M, Kuznetsov SA, Fisher LW, Robey PG, Young MF. TGF-beta1 and WISP-1/CCN-4 can regulate each other's activity to cooperatively control osteoblast function. Journal of cellular biochemistry. 2008;104(5):1865-78.
184. Yoshioka Y, Ono M, Maeda A, Kilts TM, Hara ES, Khattab H, et al. CCN4/WISP-1 positively regulates chondrogenesis by controlling TGF-beta3 function. Bone. 2016;83:162-70.
185. Cernea M, Tang W, Guan H, Yang K. Wisp1 mediates Bmp3-stimulated mesenchymal stem cell proliferation. Journal of molecular endocrinology. 2016;56(1):39-46.
186. Hou CH, Chiang YC, Fong YC, Tang CH. WISP-1 increases MMP-2 expression and cell motility in human chondrosarcoma cells. Biochemical pharmacology. 2011;81(11):1286-95.
187. Wu CL, Tsai HC, Chen ZW, Wu CM, Li TM, Fong YC, et al. Ras activation mediates WISP-1-induced increases in cell motility and matrix metalloproteinase expression in human osteosarcoma. Cellular signalling. 2013;25(12):2812-22.

188. Soon LL, Yie TA, Shvarts A, Levine AJ, Su F, Tchou-Wong KM. Overexpression of WISP-1 down-regulated motility and invasion of lung cancer cells through inhibition of Rac activation. The Journal of biological chemistry. 2003;278(13):11465-70.
189. Su F, Overholtzer M, Besser D, Levine AJ. WISP-1 attenuates p53-mediated apoptosis in response to DNA damage through activation of the Akt kinase. Genes & development. 2002;16(1):46-57.
190. Desnoyers L, Arnott D, Pennica D. WISP-1 binds to decorin and biglycan. The Journal of biological chemistry. 2001;276(50):47599-607.
191. Schlegelmilch K, Keller A, Zehe V, Hondke S, Schilling T, Jakob F, et al. WISP 1 is an important survival factor in human mesenchymal stromal cells. Gene. 2014;551(2):243-54.
192. Shao H, Cai L, Grichnik JM, Livingstone AS, Velazquez OC, Liu ZJ. Activation of Notch1 signaling in stromal fibroblasts inhibits melanoma growth by upregulating WISP-1. Oncogene. 2011;30(42):4316-26.
193. Colston JT, de la Rosa SD, Koehler M, Gonzales K, Mestril R, Freeman GL, et al. Wnt-induced secreted protein-1 is a prohypertrophic and profibrotic growth factor. American journal of physiology Heart and circulatory physiology. 2007;293(3):H1839-46.
194. Venkatachalam K, Venkatesan B, Valente AJ, Melby PC, Nandish S, Reusch JE, et al. WISP1, a pro-mitogenic, pro-survival factor, mediates tumor necrosis factor-alpha (TNF-alpha)-stimulated cardiac fibroblast proliferation but inhibits TNF-alpha-induced cardiomyocyte death. The Journal of biological chemistry. 2009;284(21):14414-27.
195. Lu S, Liu H, Lu L, Wan H, Lin Z, Qian K, et al. WISP1 overexpression promotes proliferation and migration of human vascular smooth muscle cells via AKT signaling pathway. European journal of pharmacology. 2016;788:90-7.
196. Yang M, Du Y, Xu Z, Jiang Y. Functional Effects of WNT1-Inducible Signaling Pathway Protein-1 on Bronchial Smooth Muscle Cell Migration and Proliferation in OVA-Induced Airway Remodeling. Inflammation. 2016;39(1):16-29.
197. Heise RL, Stober V, Cheluvaraju C, Hollingsworth JW, Garantziotis S. Mechanical stretch induces epithelial-mesenchymal transition in alveolar epithelia via hyaluronan activation of innate immunity. The Journal of biological chemistry. 2011;286(20):17435-44.
198. Klee S, Lehmann M, Wagner DE, Baarsma HA, Konigshoff M. WISP1 mediates IL-6-dependent proliferation in primary human lung fibroblasts. Scientific reports. 2016;6:20547.
199. Chomczynski P, Sacchi N. Single-step method of RNA isolation by acid guanidinium thiocyanate-phenol-chloroform extraction. Analytical biochemistry. 1987;162(1):156-9.
200. Sharma S, Tantisira K, Carey V, Murphy AJ, Lasky-Su J, Celedon JC, et al. A role for Wnt signaling genes in the pathogenesis of impaired lung function in asthma. American journal of respiratory and critical care medicine. 2010;181(4):328-36.
201. Chen PP, Li WJ, Wang Y, Zhao S, Li DY, Feng LY, et al. Expression of Cyr61, CTGF, and WISP-1 correlates with clinical features of lung cancer. PloS one. 2007;2(6):e534.
202. Zemans RL, Briones N, Campbell M, McClendon J, Young SK, Suzuki T, et al. Neutrophil transmigration triggers repair of the lung epithelium via beta-catenin signaling. Proceedings of the National Academy of Sciences of the United States of America. 2011;108(38):15990-5.
203. Fireman E, Shahar I, Shoval S, Messer G, Dvash S, Grief J. Morphological and biochemical properties of alveolar fibroblasts in interstitial lung diseases. Lung. 2001;179(2):105-17.
204. Yamauchi Y, Kohyama T, Takizawa H, Kamitani S, Desaki M, Takami K, et al. Tumor necrosis factor-α enhances both epithelial-mesenchymal transition and cell contraction induced in A549 human alveolar epithelial cells by transforming growth factor-β1. Experimental lung research. 2010;36(1):12-24.
205. Piguet PF, Ribaux C, Karpuz V, Grau GE, Kapanci Y. Expression and localization of tumor necrosis factor-alpha and its mRNA in idiopathic pulmonary fibrosis. The American journal of pathology. 1993;143(3):651-5.

206. Park SW, Ahn MH, Jang HK, Jang AS, Kim DJ, Koh ES, et al. Interleukin-13 and its receptors in idiopathic interstitial pneumonia: clinical implications for lung function. Journal of Korean medical science. 2009;24(4):614-20.
207. Desmouliere A, Geinoz A, Gabbiani F, Gabbiani G. Transforming growth factor-beta 1 induces alpha-smooth muscle actin expression in granulation tissue myofibroblasts and in quiescent and growing cultured fibroblasts. The Journal of cell biology. 1993;122(1):103-11.
208. Yoshida S, Katoh T, Tetsuka T, Uno K, Matsui N, Okamoto T. Involvement of thioredoxin in rheumatoid arthritis: its costimulatory roles in the TNF-alpha-induced production of IL-6 and IL-8 from cultured synovial fibroblasts. Journal of immunology (Baltimore, Md : 1950). 1999;163(1):351-8.
209. Parisi MS, Gazzerro E, Rydziel S, Canalis E. Expression and regulation of CCN genes in murine osteoblasts. Bone. 2006;38(5):671-7.
210. Attisano L, Labbe E. TGFbeta and Wnt pathway cross-talk. Cancer metastasis reviews. 2004;23(1-2):53-61.
211. Guo X, Wang XF. Signaling cross-talk between TGF-beta/BMP and other pathways. Cell research. 2009;19(1):71-88.
212. Attisano L, Wrana JL. Signal integration in TGF-β, WNT, and Hippo pathways. F1000Prime Reports. 2013;5.
213. Cultures PHE-ECoAC. MRC-5. Available from: https://www.phe-culturecollections.org.uk/products/celllines/generalcell/detail.jsp?refId=05011802&collection=ecacc_gc.
214. Kalluri R, Weinberg RA. The basics of epithelial-mesenchymal transition. The Journal of clinical investigation. 2009;119(6):1420-8.
215. Soria G, Ofri-Shahak M, Haas I, Yaal-Hahoshen N, Leider-Trejo L, Leibovich-Rivkin T, et al. Inflammatory mediators in breast cancer: coordinated expression of TNFalpha & IL-1beta with CCL2 & CCL5 and effects on epithelial-to-mesenchymal transition. BMC cancer. 2011;11:130.
216. Yan C, Grimm WA, Garner WL, Qin L, Travis T, Tan N, et al. Epithelial to mesenchymal transition in human skin wound healing is induced by tumor necrosis factor-alpha through bone morphogenic protein-2. The American journal of pathology. 2010;176(5):2247-58.
217. Solis-Herruzo JA, Brenner DA, Chojkier M. Tumor necrosis factor alpha inhibits collagen gene transcription and collagen synthesis in cultured human fibroblasts. The Journal of biological chemistry. 1988;263(12):5841-5.
218. Kamitani S, Yamauchi Y, Kawasaki S, Takami K, Takizawa H, Nagase T, et al. Simultaneous stimulation with TGF-beta1 and TNF-alpha induces epithelial mesenchymal transition in bronchial epithelial cells. International archives of allergy and immunology. 2011;155(2):119-28.
219. Zhang H, Luo H, Hu Z, Peng J, Jiang Z, Song T, et al. Targeting WISP1 to sensitize esophageal squamous cell carcinoma to irradiation. Oncotarget. 2015;6(8):6218-34.
220. Fuchs S, Hollins AJ, Laue M, Schaefer UF, Roemer K, Gumbleton M, et al. Differentiation of human alveolar epithelial cells in primary culture: morphological characterization and synthesis of caveolin-1 and surfactant protein-C. Cell and tissue research. 2003;311(1):31-45.
221. Lieber M, Smith B, Szakal A, Nelson-Rees W, Todaro G. A continuous tumor-cell line from a human lung carcinoma with properties of type II alveolar epithelial cells. International journal of cancer. 1976;17(1):62-70.
222. Shapiro DL, Nardone LL, Rooney SA, Motoyama EK, Munoz JL. Phospholipid biosynthesis and secretion by a cell line (A549) which resembles type II aleveolar epithelial cells. Biochimica et biophysica acta. 1978;530(2):197-207.
223. Swain RJ, Kemp SJ, Goldstraw P, Tetley TD, Stevens MM. Assessment of cell line models of primary human cells by Raman spectral phenotyping. Biophysical journal. 2010;98(8):1703-11.
224. Perbal B. CCN proteins: A centralized communication network. Journal of cell communication and signaling. 2013;7(3):169-77.

225. Li WF, Zhang L, Li HY, Zheng SS, Zhao L. WISP-1 contributes to fractionated irradiation-induced radioresistance in esophageal carcinoma cell lines and mice. PloS one. 2014;9(4):e94751.
226. Yang GP, Lau LF. Cyr61, product of a growth factor-inducible immediate early gene, is associated with the extracellular matrix and the cell surface. Cell growth & differentiation : the molecular biology journal of the American Association for Cancer Research. 1991;2(7):351-7.
227. Ensembl. Wnt1-inducible signalling protein-1. Available from: http://www.ensembl.org/Homo_sapiens/Gene/Splice?db=core;g=ENSG00000104415;r=8:133191039-133230344.
228. Berschneider B, Konigshoff M. WNT1 inducible signaling pathway protein 1 (WISP1): a novel mediator linking development and disease. The international journal of biochemistry & cell biology. 2011;43(3):306-9.
229. Ball DK, Surveyor GA, Diehl JR, Steffen CL, Uzumcu M, Mirando MA, et al. Characterization of 16- to 20-kilodalton (kDa) connective tissue growth factors (CTGFs) and demonstration of proteolytic activity for 38-kDa CTGF in pig uterine luminal flushings. Biology of reproduction. 1998;59(4):828-35.
230. Sabbah M, Prunier C, Ferrand N, Megalophonos V, Lambein K, De Wever O, et al. CCN5, a novel transcriptional repressor of the transforming growth factor beta signaling pathway. Molecular and cellular biology. 2011;31(7):1459-69.
231. SYSTEMS RD. Recombinant Human WISP-1/CCN4 Protein, CF [cited 2016]. Available from: https://www.rndsystems.com/products/recombinant-human-wisp-1-ccn4-protein-cf_1627-ws.
232. Oliver MH, Harrison NK, Bishop JE, Cole PJ, Laurent GJ. A rapid and convenient assay for counting cells cultured in microwell plates: application for assessment of growth factors. Journal of cell science. 1989;92 (Pt 3):513-8.
233. Holbourn KP, Acharya KR. Cloning, expression and purification of the CCN family of proteins in Escherichia coli. Biochemical and biophysical research communications. 2011;407(4):837-41.
234. Grotendorst GR, Duncan MR. Individual domains of connective tissue growth factor regulate fibroblast proliferation and myofibroblast differentiation. FASEB journal : official publication of the Federation of American Societies for Experimental Biology. 2005;19(7):729-38.
235. Bleau AM, Planque N, Lazar N, Zambelli D, Ori A, Quan T, et al. Antiproliferative activity of CCN3: involvement of the C-terminal module and post-translational regulation. Journal of cellular biochemistry. 2007;101(6):1475-91.
236. Triantafilou K, Triantafilou M, Takada Y, Fernandez N. Human Parechovirus 1 Utilizes Integrins αvβ3 and αvβ1 as Receptors. Journal of Virology. 2000;74(13):5856-62.
237. Atlas P. Available from: http://www.proteinatlas.org/ENSG00000161638-ITGA5/cell/HPA002642/A549.
238. Liu H, Dong W, Lin Z, Lu J, Wan H, Zhou Z, et al. CCN4 regulates vascular smooth muscle cell migration and proliferation. Molecules and Cells. 2013;36(2):112-8.
239. Lau LF. Cell surface receptors for CCN proteins. Journal of cell communication and signaling. 2016;10(2):121-7.

Appendix 1

Permissions for figures used in this thesis

Figure 1

This Agreement between Lyndsy Ambler ("You") and Elsevier ("Elsevier") consists of your license details and the terms and conditions provided by Elsevier and Copyright Clearance Center.

License Number	4098290551954
License date	Apr 29, 2017
Licensed Content Publisher	Elsevier
Licensed Content Publication	The Lancet
Licensed Content Title	Idiopathic pulmonary fibrosis
Licensed Content Author	Talmadge E King,Annie Pardo,Moisés Selman
Licensed Content Date	3–9 December 2011
Licensed Content Volume	378
Licensed Content Issue	9807
Licensed Content Pages	13
Start Page	1949
End Page	1961
Type of Use	reuse in a thesis/dissertation
Portion	figures/tables/illustrations
Number of figures/tables/illustrations	1
Format	both print and electronic
Are you the author of this Elsevier article?	No
Will you be translating?	No
Order reference number	
Original figure numbers	Figure 1
Title of your thesis/dissertation	Expression and Activity of Wnt1-inducible Signalling Protein-1 in Idiopathic Pulmonary Fibrosis
Expected completion date	May 2017
Estimated size (number of pages)	200
Elsevier VAT number	GB 494 6272 12
Requestor Location	Lyndsy Ambler Flat 8 Welbeck Court 61-63 Welbeck Avenue

	Southampton, SO17 1ST United Kingdom Attn: Lyndsy Ambler
Publisher Tax ID	GB 494 6272 12
Total	0.00 GBP

Appendix 2

Figure 21

Normality Test (Shapiro-Wilk)

Data source: Data 1 in Notebook1.JNB

48hr

IPF Col 1: W-Statistic = 0.914 P = 0.490 Passed

Control Col 2: W-Statistic = 0.926 P = 0.568 Passed

72hr

IPF Col 3: W-Statistic = 0.995 P = 0.982 Passed

Control Col 4: W-Statistic = 0.854 P = 0.208 Passed

Figure 59

Normality Test (Shapiro-Wilk)

Data source: Data 1 in Notebook1.JNB

48hr variant 2

IPF Col 5: W-Statistic = 0.763 P = 0.050 Passed

Control Col 6: W-Statistic = 0.643 P = 0.002 Failed

48hr variant 3

IPF Col 7: W-Statistic = 0.665 P = 0.004 Failed

Control Col 8: W-Statistic = 0.576 P < 0.001 Failed

48hr variant 4

IPF Col 9: W-Statistic = 0.780 P = 0.071 Passed

Control Col 10: W-Statistic = 0.553 P < 0.001 Failed

72hr variant 2

IPF Col 11: W-Statistic = 0.852 P = 0.233 Passed

Control Col 12: W-Statistic = 0.794 P = 0.092 Passed

72hr variant 3

IPF Col 13: W-Statistic = 0.906 P = 0.446 Passed

Control Col 14: W-Statistic = 0.957 P = 0.788 Passed

72hr variant 4

IPF Col 15: W-Statistic = 0.928 P = 0.583 Passed

Control Col 16: W-Statistic = 0.891 P = 0.363 Passed